



TECHNISCHE
UNIVERSITÄT
WIEN

Dissertation

BIOCATALYTIC CASCADE REACTIONS TOWARDS THE PRODUCTION OF VALUABLE FINE CHEMICALS

ausgeführt zum Zwecke der Erlangung des akademischen Grades eines
Doktors der technischen Wissenschaften unter der Leitung von

Prof. Dr. Marko D. Mihovilovic

und **Dr. Florian Rudroff**

Institut für Angewandte Synthesechemie, E163

eingereicht an der Technischen Universität Wien

Fakultät für Technische Chemie

von

Dipl.Ing. Nikolin Oberleitner

e0426252

Morizgasse 4/1/12

A-1060 Wien

Wien, November 2016

*Science and everyday life
cannot and should not be separated.*

ROSALIND FRANKLIN

*Schau ganz tief in die Natur,
und dann verstehst Du alles besser.*

ALBERT EINSTEIN

Front Matter

Table of Contents

Front Matter	i	
Table of Contents	i	
Acknowledgements - Danksagung	vi	
Abstract	viii	
Kurzfassung	ix	
A	Synthetic schemes	10
A I	Chemical syntheses	10
A I.1	Starting material	10
A I.1.1	2-Bromo-4-methylcyclohexanone (16)	10
A I.1.2	4-Methylcyclohex-2-en-1-one (2c)	10
A I.1.3	4-Methylcyclohex-2-en-1-ol (2b)	10
A I.1.4	3-Isobutoxy-2-methylcyclohex-2-enone (19)	10
A I.1.5	2-Methylcyclohex-2-en-1-one (3c)	11
A I.1.6	2-Methylcyclohex-2-en-1-ol (3b)	11
A I.1.7	2-benzylidenecyclohexanone (5c)	11
A I.1.8	2-benzylidenecyclohexanol (5b)	11
A I.1.9	(1 <i>S</i> ,5 <i>R</i>)-2-methyl-5-(prop-1-en-2-yl)cyclohex-2-en-1-yl acetate (22) and (1 <i>R</i> ,5 <i>R</i>)-Carveol (1R-6b)	11
A I.1.10	(1 <i>S</i> ,5 <i>R</i>)-Carveol (1S-6b)	12
A I.1.11	(1 <i>S</i> ,5 <i>S</i>)-Carveol (1S-7b)	12
A I.2	Reference material	12
A I.2.1	<i>R</i> -(-)-Carvone (6c) to <i>trans</i> - 6d and <i>cis</i> - 6d	12
A I.2.2	<i>S</i> -(+)-Carvone (7c) to <i>trans</i> - 7d and <i>cis</i> - 7d	12
A I.2.3	Baeyer-Villiger oxidation (BVOx) of ketones to lactones	13
A I.2.4	Reduction of ketones to alcohols	13
A II	Biocatalytic reactions	14
A II.1	Analytical scale cascades	14
A II.2	Preparative scale cascades	15
A II.2.1	(<i>S</i>)-4-Methyloxepan-2-one ((<i>S</i>)-4-Methylcaprolactone, S-4f)	15
A II.2.2	(3 <i>R</i> ,6 <i>S</i>)-3-Methyl-6-(prop-1-en-2-yl)oxepan-2-one ((3 <i>R</i> ,6 <i>S</i>)-abn-carvolactone, 6e)	15
A II.2.3	(4 <i>S</i> ,7 <i>R</i>)-7-Methyl-4-(prop-1-en-2-yl)oxepan-2-one ((4 <i>S</i> ,7 <i>R</i>)-carvolactone, 7e)	15
B	Introduction	16
B I	Cascade reactions	16
B I.1	Chemocatalytic cascades	16
B I.2	Enzymatic cascades	17
B I.3	Chemo-enzymatic cascades	17
B II	Multistep biocatalysis	18
B II.1	<i>In vitro</i> cascades	18
B II.2	<i>In vivo</i> cascades	20
B II.2.1	Enzyme activity and proximity	20
B II.2.2	Host background	21
B II.2.3	Growth deficiencies	21
B II.2.4	Cell membrane	21
B II.3	Redox enzymes in cascade reactions	23
B II.3.1	Oxygenases	23
B II.3.2	Alcohol dehydrogenases (ADHs)	23

B II.3.3	Enoate reductases (EREDs)	25
B II.3.4	Baeyer-Villiger monooxygenases (BVMOs)	27
B III	Scope of this thesis	30
C	Results and discussion	31
C I	Enzymatic redox cascades by a retrosynthetic approach	31
C I.1	Substrate scope	32
C I.1.1	BVMO reaction types	33
C I.1.1.1	Desymmetrization	33
C I.1.1.2	Kinetic resolution	33
C I.1.1.3	Regiodivergent transformations	35
C I.2	The enzymatic toolbox	37
C I.2.1	Three-step cascade and its substrate scope	37
C I.2.1.1	Substrate accessibility	37
C I.2.2	ADHs	38
C I.2.3	EREDs	40
C I.2.4	BVMO	41
C I.3	Summary	42
C II	<i>In vitro</i> characterization of enzymatic redox cascades	43
C II.1	<i>In vitro</i> cascade starting from cyclohex-2-en-1-ol (1b)	44
C II.2	<i>In vitro</i> cascade starting from 4-methylcyclohex-2-en-1-ol (2b)	47
C II.3	<i>In vitro</i> cascade starting from 2-methylcyclohex-2-en-1-ol (3b)	48
C II.4	<i>In vitro</i> cascade starting from 3-methylcyclohex-2-en-1-ol (4b)	49
C II.5	<i>In vitro</i> cascade starting from 2-benzylidenecyclohexanol (5b)	50
C II.6	Two cascades towards (3 <i>R</i> ,6 <i>S</i>)-abn-carvolactone (6e)	52
C II.6.1	<i>In vitro</i> cascade starting from (1 <i>R</i> ,5 <i>R</i>)-Carveol (1R-6b)	52
C II.6.2	<i>In vitro</i> cascade starting from (1 <i>S</i> ,5 <i>R</i>)-Carveol (1S-6b)	53
C II.7	<i>In vitro</i> cascade starting from (1 <i>S</i> ,5 <i>S</i>)-Carveol (1R-7b)	55
C II.7.1	Starting material concentration dependency on cascade performance	56
C II.8	Summary	57
C III	<i>In vivo</i> cascades – an enzymatic toolbox	58
C III.1	<i>E. coli</i> cell factory	58
C III.1.1	Expression system	58
C III.1.2	Reaction set-up	59
C III.2	<i>In vivo</i> cascade starting from cyclohex-2-en-1-ol (1b)	60
C III.3	<i>In vivo</i> cascade starting from 4-methylcyclohex-2-en-1-ol (2b)	61
C III.4	<i>In vivo</i> cascade starting from 2-methylcyclohex-2-en-1-ol (3b)	62
C III.5	<i>In vivo</i> cascade starting from 3-methylcyclohex-2-en-1-ol (4b)	63
C III.5.1	Analytical scale	63
C III.5.2	Preparative scale	64
C III.6	<i>In vivo</i> cascade starting from 2-benzylidenecyclohexanol (5b)	64
C III.7	Two cascades towards (3 <i>R</i> ,6 <i>S</i>)-abn-carvolactone (6e)	65
C III.7.1	<i>In vivo</i> cascade starting from (1 <i>R</i> ,5 <i>R</i>)-Carveol (1R-6b)	65
C III.7.2	<i>In vivo</i> cascade starting from (1 <i>S</i> ,5 <i>R</i>)-Carveol (1S-6b)	66
C III.7.2.1	Analytical scale	66
C III.7.2.2	Preparative scale	67
C III.8	<i>In vivo</i> cascade starting from (1 <i>S</i> ,5 <i>S</i>)-Carveol (1S-7b)	68
C III.8.1	Analytical scale	68
C III.8.1	Preparative scale	69
C III.9	Summary	69
C IV	Hydroxylation of cyclic alkenes	70
C IV.1	Cellulosimicrobium cellulans EB-8-4	71
C IV.1.1	Cultivation of <i>C. cellulans</i> EB-8-4	71
C IV.1.2	Biotransformations	73
C IV.1.3	Contamination of <i>C. cellulans</i> EB-8-4	74
C IV.2	Cumene dioxygenase (CumDO) in <i>P. putida</i> S12	75
C IV.2.1	Preparative scale - <i>R</i> -(+)-limonene (7a) to (1 <i>R</i> ,5 <i>S</i>)-carveol (1R-7b)	75

C IV.2.2	Expression of CumDO in <i>P. putida</i> S12	76
C IV.2.3	Influence of buffer	77
C IV.2.4	Influence of cell density	77
C IV.2.5	Influence of <i>R</i> -(+)-limonene concentration	78
C IV.2.6	Variations in <i>R</i> -(+)-limonene extraction	78
C IV.2.7	Influence of Triton X-100 on the hydroxylation reaction	79
C IV.2.8	Hydroxylation of other cyclic alkenes	79
C IV.3	CumDO in <i>Pseudomonas taiwanensis</i> VLB120ΔCAttgV	81
C IV.3.1	Cultivation and expression of CumDO in <i>P. taiwanensis</i> in LB	81
C IV.3.2	Cultivation and expression of CumDO in <i>P. taiwanensis</i> in M9	81
C IV.3.3	Limonene hydroxylation with CumDO in <i>P. taiwanensis</i>	82
C IV.4	Summary	83
C V	Metabolic engineering	84
C V.1	Identification of an <i>E. coli</i> background reaction	84
C V.2	<i>E. coli</i> BL21(DE3) Δ <i>nemA</i> – NemR deficient strain	85
C V.2.1	Verification of <i>nemA</i> disruption via PCR	86
C V.2.2	Confirmation of NemR deficiency via biotransformation tests	86
C V.2.3	Removal of kanamycin resistance	87
C V.3	<i>E. coli</i> BL21(DE3) Δ <i>nemA</i> Δ <i>fadH</i> – double knockout	88
C V.3.1	Biotransformations to test for DCR disruption	88
C V.3.2	<i>E. coli</i> BL21(DE3) Δ <i>nemA</i> Δ <i>fadH</i> -2+kan ^R	88
C V.4	Cloning of <i>nemA</i> and <i>fadH</i> from <i>E. coli</i>	90
C V.4.1	First expression of NemR and DCR	90
C V.5	Expression of pET-22b(+) _{<i>nemA</i>}	91
C V.6	Expression of pET-22b(+) _{<i>fadH</i>}	92
C V.7	Genomic integration	93
C V.8	Summary	94
C VI	From waste to value – Utilization of <i>R</i>-(+)-limonene from orange peel	95
C VI.1	Extraction enhancers - ionic liquids	96
C VI.1.1	Extraction of <i>R</i> -(+)-limonene from orange peel	96
C VI.1.1.1	Limonene content in orange peel	97
C VI.1.2	Growth of <i>E. coli</i> in presence of ILs	97
C VI.1.3	Growth of <i>P. putida</i> S12 in presence of ILs	98
C VI.1.4	Limonene hydroxylation by CumDO in presence of ILs	98
C VI.1.4.1	IL concentration	99
C VI.2	Orange peel as starting material for hydroxylation by CumDO	99
C VI.3	Mixed culture - extended pathway	101
C VI.3.1	Limonene to carvolactone	101
C VI.3.2	Orange peel to carvolactone	101
C VI.4	Summary	102
D	Conclusions and perspective	103
E	Experimental part	107
E I	Materials and methods – biotransformations	107
E I.1	Bacterial strains and enzymes	107
E I.2	Media, buffers and stock solutions	108
E I.3	Transformation of <i>E. coli</i>	109
E I.3.1	Chemical transformation	109
E I.3.2	Electroporation	109
E I.4	Preparation of permanent cultures	110
E I.5	Heterologous gene expression	110
E I.6	Cell free extracts (CFE)	111
E I.7	<i>E. coli</i> resting cells	111
E I.7.1	Method A	111
E I.7.2	Method B	111
E I.8	SDS-PAGE	112

E I.9	GC analysis	112
E II	Chemical syntheses	113
E II.1	Syntheses of starting material	113
E II.1.1	2-Bromo-4-methylcyclohexanone (16)	113
E II.1.2	4-Methylcyclohex-2-en-1-one (2c)	114
E II.1.3	4-Methylcyclohex-2-en-1-ol (2b)	114
E II.1.4	3-Isobutoxy-2-methylcyclohex-2-enone (19)	115
E II.1.5	2-Methylcyclohex-2-en-1-one (3c)	115
E II.1.6	2-Methylcyclohex-2-en-1-ol (3b)	116
E II.1.7	2-Benzylidenecyclohexanone (5c)	116
E II.1.8	2-Benzylidenecyclohexanol (5b)	117
E II.1.9	(1 <i>S</i> ,5 <i>R</i>)-2-Methyl-5-(prop-1-en-2-yl)cyclohex-2-en-1-yl acetate (22) and (1 <i>R</i> ,5 <i>R</i>)-Carveol (1R-6b)	117
E II.1.9.1	(1 <i>R</i> ,5 <i>R</i>)-Carveol (1R-6b)	118
E II.1.9.2	(1 <i>S</i> ,5 <i>R</i>)-Carvylacetate (22)	118
E II.1.10	(1 <i>S</i> ,5 <i>R</i>)-Carveol (1S-6b)	118
E II.1.11	(1 <i>S</i> ,5 <i>S</i>)-Carveol (1S-7b)	119
E II.2	Chemical syntheses of reference material	119
E II.2.1	Reduction of carvones to dihydrocarvones	119
E II.2.1.1	Cu/Zn-couple	119
E II.2.1.2	<i>R</i> -(-)-Carvone (6c) to <i>trans</i> - 6d and <i>cis</i> - 6d	119
E II.2.1.3	<i>S</i> -(+)-Carvone (7c) to <i>trans</i> - 7d and <i>cis</i> - 7d	120
E II.2.2	Baeyer-Villiger oxidation (BVOx) of ketones to lactones	120
E II.2.3	Reduction of ketones to alcohols	121
E III	<i>E. coli</i> biotransformations	122
E III.1	<i>In vitro</i> – single step	122
E III.2	<i>In vitro</i> – cascade	122
E III.2.1	Sequential cascade reaction	122
E III.2.2	Simultaneous cascade reaction	123
E III.3	<i>In vivo</i> – single step	123
E III.4	<i>In vivo</i> – cascade	123
E III.4.1	Preparative scale cascade reactions	123
E III.4.1.1	(<i>S</i>)-4-Methyloxepan-2-one ((<i>S</i>)-4-Methylcaprolactone, S-4f)	124
E III.4.1.2	(3 <i>R</i> ,6 <i>S</i>)-3-Methyl-6-(prop-1-en-2-yl)oxepan-2-one ((3 <i>R</i> ,6 <i>S</i>)-abn-carvolactone, 6e)	124
E III.4.1.3	(4 <i>S</i> ,7 <i>R</i>)-7-Methyl-4-(prop-1-en-2-yl)oxepan-2-one ((4 <i>S</i> ,7 <i>R</i>)-carvolactone, 7e)	124
E IV	Cyclic alkene hydroxylation	125
E IV.1	<i>Cellulosimicrobium cellulans</i> EB-8-4	125
E IV.1.1	Cultivation	125
E IV.1.2	Resting cells	126
E IV.1.3	Biotransformations	126
E IV.2	Cumene dioxygenase (CumDO) in <i>P. putida</i> S12	126
E IV.2.1	Resting cells	126
E IV.2.2	Growth in presence of ionic liquids (ILs)	126
E IV.2.3	Biotransformations	127
E IV.2.3.1	Preparative scale <i>R</i> -(+)-limonene hydroxylation	127
E IV.2.3.2	Cell density	127
E IV.2.3.3	Limonene concentration	127
E IV.2.3.4	Limonene hydroxylation in presence of Triton X-100	128
E IV.2.3.5	Limonene hydroxylation in presence of ILs	128
E IV.2.3.6	IL concentration	128
E IV.2.3.7	Hydroxylation of other cyclic alkenes	128
E IV.3	CumDO in <i>P. taiwanensis</i> VLB120Δ <i>CΔttgV</i>	128
E IV.3.1	Cultivation and expression of CumDO in LB	128
E IV.3.2	Cultivation in M9	128
E IV.3.3	Expression of CumDO in M9	129
E IV.3.3.1	Resting cells and biotransformation	129
E IV.4	Mixed-culture biotransformations	129
E IV.4.1	<i>P. putida</i> S12 expressing CumDO and <i>E. coli</i>	129
E IV.4.1.1	Simultaneous addition	129
E IV.4.1.2	Sequential addition	129

E V	Orange peel as starting material	130
E V.1	<i>P. putida</i> expressing CumDO	130
E V.1.1	<i>In situ</i> <i>R</i> -(+)-limonene conversion without additives	130
E V.1.2	<i>In situ</i> <i>R</i> -(+)-limonene conversion in presence of aqueous IL solutions	130
E V.1.3	Pre-dissolution of orange peel with following <i>R</i> -(+)-limonene conversion	130
E V.2	<i>P. putida</i> and <i>E. coli</i> - mixed-culture with orange peel	130
E V.2.1	Simultaneous addition	130
E V.2.2	Sequential addition	130
E VI	Materials and methods – molecular biology	131
E VI.1	Extraction of plasmid DNA	131
E VI.2	Extraction of genomic DNA (gDNA)	131
E VI.3	PCR	131
E VI.3.1	Colony PCR	131
E VI.4	Restriction enzyme digest	132
E VI.5	Agarose Gel electrophoresis	132
E VI.5.1	Agarose gel purification	132
E VII	Metabolic engineering	133
E VII.1	<i>E. coli</i> BL21(DE3) Δ <i>nemA</i>	133
E VII.1.1	Verification of intron insertion via PCR	133
E VII.1.2	Confirmation of <i>NemR</i> disruption via biotransformation test	134
E VII.1.3	Removal of the kanamycin resistance	134
E VII.2	<i>E. coli</i> BL21(DE3) Δ <i>nemA</i> Δ <i>fadH</i>	134
E VII.2.1	<i>E. coli</i> BL21(DE3) Δ <i>nemA</i> Δ <i>fadH</i> -2+kan ^R	135
E VII.3	Cloning of <i>nemA</i> into pET-22b(+)	135
E VII.4	Expression of <i>NemR</i>	135
E VII.5	Cloning of <i>fadH</i> and expression of DCR	136
E VIII	Primer list	137
F	Appendix	138
F I	Sequences	138
F II	Plasmid maps	139
F III	Publications resulting from this thesis	140
F IV	Curriculum vitae	141
F V	List of abbreviations	144
F VI	References	145

Acknowledgements - Danksagung

As I would like to thank some people in their own language, my apologies go to all non german readers of these acknowledgments. If you can't translate please consider every name mentioned here as a person without their contribution this work would not have been possible.

Mein erster Dank gilt Prof. Marko D. Mihovilovic, der mir die Möglichkeit gegeben hat meine Dissertation im Rahmen einer FWF Finanzierung (DACH FWF I-723) in seiner Forschungsgruppe durchzuführen. Ich durfte in den letzten Jahren interessante Projekte verfolgen, auf spannende Konferenzen fahren und habe durch die Arbeit in seiner interdisziplinären Gruppe viel gelernt.

Meinem direkten Betreuer Dr. Florian Rudroff gilt besonderer Dank. Nur durch die enge Zusammenarbeit und den konstanten wissenschaftlichen Austausch mit ihm war die Ausführung dieser Dissertation möglich. Lieber Florian, ich danke dir auch für deine tatkräftige Unterstützung beim Aufbau dieser Arbeit.

Herzlicher Dank gilt Prof. Uwe T. Bornscheuer für die hervorragende Kooperation in unserem gemeinsamen Forschungsprojekt, die interessanten wissenschaftlichen Diskussionen und die Begutachtung meiner Arbeit.

Prof. Robert Mach danke ich herzlichst für die Begutachtung meiner Dissertation und für die gute Kooperation mit seiner Forschungsgruppe bei unterschiedlichen Messungen oder Ideenaustausch.

I would like to thank Prof. Bruno Bühler, Prof. Marco Fraaije, Prof. Zhi Li and Privatdoz. Astrid Mach-Aigner for providing bacterial strains or plasmids for the forthcome of this project.

Prof. Peter Gärtner, Assistant Prof. Katharina Schröder und im Speziellen Dr. Anna Ressmann danke ich für die erfolgreiche Zusammenarbeit am „Limonen-Projekt“, wodurch im späten Stadium dieser Arbeit noch interessante Ergebnisse erzielt wurden.

Meinen Kollegen aus der Forschungsgruppe von Prof. Bornscheuer in Greifswald, Maria Kadow, Jan Muschiol, Christin Peters, Stefan Saß und Katja Zorn bin ich sehr dankbar für die gute Zusammenarbeit an unserem spannenden Projekt. Liebe Christin, lieber Jan, herzlichen Dank auch für eure Gastfreundschaft und den tollen Segelausflug bei unserem Projektmeeting in Greifswald.

Ohne die tatkräftige Unterstützung von Patricia Schaaf, als auch Waldemar Fahenstiel und Ramana Pydi bei chemischen Synthesen wäre diese Arbeit nicht durchführbar gewesen. Dankeschön liebe Patricia, thank you guys.

All present and former members of the „bio-group“, especially Letícia Gonçalves, Saima Ferroz, Sofia Milker, Thomas Wiesinger and Anna Ressmann I would like to thank for their cooperative teamwork.

Herzlichster Dank gilt Thomas Bayer für die gute Zusammenarbeit mit vielen konstruktiven Diskussionen und das eingespielte Teamwork im Labor. Ohne dich, lieber Donzi wären vor allem die Nacht- und Wochenendschichten nicht dasselbe gewesen und bestimmt nur viertel oder sogar achtel so lustig! #kükü

Vielschichtiger Dank gilt meinem besten Labor-Banknachbarn Dr. Michael J. Fink. Lieber Michi, dank dir für deine Ideen, deine Unterstützung, die Ablenkungen vom Labor-Alltag durch deine kleinen Streiche und last but not least, deine Freundschaft. Du hast mir im letzten Jahr ziemlich gefehlt und ich hoffe du lädst mich ein wenn du den Anruf aus Schweden bekommst... Keep on rocking!

All present and former members of the FGMDM I would like to thank for the great group atmosphere and a lot of fun at diverse activities. Thanks also to members of the FGHF and FGPG for a lot of at fun coffee breaks, institute activities and our legendary Christmas party. Es war mir eine Ehre!

Den beiden besten guten Feen des Institutes, Sabine Stiedry und Florian Untersteiner, möchte ich herzlichst für ihre Unterstützung bei allfälligen Problemchen in den letzten Jahren danken. Lieber Danko Milic vielen Dank für die vielen Pakete die du mir gebracht hast. Ihr seid die Herzen des IAS!

Den Mitgliedern unserer Kochgruppe, Anna, Gerit, Laurin, Lukas, Maria, Max und Navid gilt mein vollster Respekt, dass sie mich als einzige Vegetarierin in ihrer Mitte aufgenommen haben. Danke für das gute Essen! Děkuj Luki, you are an excellent cutter! Auch die Afterwork Erweiterung der Kochgruppe durch Flo, Kathi, Michi und Commandante Flotschi soll nicht unerwähnt bleiben. Danke liebe Fiaker für die lustigen Abende! Auch wenn wir jetzt ziemlich in der Welt verstreut sind – once a fiaker, always a fiaker...

Anna, Eva, Gerit, Hasi, Helene, Inge, Jasmin, Kathi, Maria, Meli, Mesi, Moni, Nani, Pizzi, Theresa, Vali und Verena: ihr seid alle individuelle, kuule und schöne Powerfrauen und ich bin sehr stolz euch meine Freundinnen nennen zu dürfen! Vielen Dank für alles!

Meinem Vater danke ich für seine Unterstützung und die Ermöglichung meines Studiums ohne welches diese Dissertation nie möglich gewesen wäre.

Manfred danke ich für seine Unterstützung durch das Borgen seines Autos womit ich in der Freizeit schöne Orte zum Energie tanken erreichen konnte.

Der lieben Familie Gritsch möchte ich danken, dass sie mich so herzlich aufgenommen haben. Man sagt ja immer (Schwieger)-Familie kann man sich nicht aussuchen, aber mit euch hab ich's mehr als gut erwischt. Danke für eure Unterstützung!

Meinen Seelenschwestern Eva, Hasi, Inge, Kathi, Maria und Moni danke ich für ihre verständnisvolle, ermutigende und unterstützende Wegbegleitung. Ihr macht mein Leben reicher, danke <3

Meiner Mami und meinem Bruder Johannes möchte ich danken, dass sie immer Verständnis für mich hatten. Danke dass ihr hinter mir gestanden seid auch wenn ich wenig Zeit für euch hatte, ich hab euch lieb!

Philipp, ich danke dir für deine Liebe. Ohne deine Unterstützung, deine Aufmunterungen und deinen Glauben an mich, wäre das alles nicht möglich gewesen. Ich liebe dich!

Meine liebste Omi, ich danke dir für alles! Es tut mir leid, dass es zu lang gedauert hat...

Abstract

Nature uses the principles of interconnected reactions, so called cascade reactions, since the beginning of evolution. These metabolic networks ensure the perpetuation of life, growth and reproduction. In a living cell these cascade reactions are executed in a one-pot-system in aqueous environment. The main actors of this highly regulated interactive reaction system are enzymes.

Taking nature's design principle as model, in this work the establishment of artificial cascade reactions is shown by combining naturally not connected enzymes. Parameters influencing such a cascade are studied in a simplified model system.

The model cascade was designed on the basis of the retrosynthetic approach, a regularly applied tool for intelligent synthesis planning in organic chemistry. This concept, where a desired valuable product is broken down to simple starting material, can also be employed in biocatalysis. Here the individual functional group interconversions are catalyzed by enzymes.

In the first step of the studied cascade a cyclic alkene should be activated by introduction of oxygen in a hydroxylation reaction exploited for further modifications. The produced unsaturated allylic alcohol is oxidized to an unsaturated ketone in the second step. Subsequent reduction yields a saturated cyclic ketone, which is functionalized towards a lactone in the last step via a Baeyer-Villiger oxidation.

All these steps of the cascade reaction can be efficiently and selectively catalyzed by enzymes. The composition of this cascade should enable to gain a deeper understanding of the interplay of different redox enzymes.

As the initial hydroxylation of cyclic alkenes proved difficult, a three-step cascade was implemented and investigated beforehand. Therefore, an alcohol dehydrogenase, an enoate reductase and a Baeyer-Villiger monooxygenase were introduced into the microbial host

Escherichia coli. This artificial system was thoroughly investigated *in vitro* and also in a whole-cell system. Through sensible choice of diverse starting material, overlapping of the individual substrate scopes was accomplished which led to the production of enantiopure chiral lactones.

Finally, the hydroxylation as the first step of the designed cascade could be realized in the microbial host organism *Pseudomonas putida* expressing the heterologous enzyme cumene dioxygenase. Therefore a mixed-culture system was tested for the implementation of cyclic alkenes as substrates. Through utilization of natural product limonene as starting material the production of chiral carvolactone could be achieved in a four-step cascade reaction.

In an application oriented approach the utilization of waste product orange peel was investigated as starting material. Here, the availability of limonene from orange peel was a crucial parameter which was addressed with different concepts. One approach was the addition of ionic liquids to enhance the *in situ* extraction of limonene.

Finally a cascade reaction from limonene from orange peel to carvolactone was achieved by combination of two microbial expression hosts in an aqueous system without the addition of extraction enhancers.

Kurzfassung

Die Natur nutzt seit Anbeginn der Evolution das Prinzip von miteinander verknüpften Reaktionen, sogenannte Kaskadenreaktionen. Diese metabolischen Netzwerke sichern die Aufrechterhaltung von Leben, Wachstum und Reproduktion. In einer lebenden Zelle laufen diese Kaskadenreaktionen quasi in einem Ein-Topf-System in wässrigem Milieu ab. Die Hauptakteure dieses hoch geregelten interaktiven Reaktionssystems sind Enzyme.

Das Designprinzip der Natur als Vorbild wird in dieser Arbeit die Entwicklung von artifiziellen Kaskadenreaktionen, durch die Zusammenführung von in der Natur nicht verknüpften Enzymen, gezeigt. An einem simplifizierten Modellsystem werden die Parameter, die eine solche Kaskade beeinflussen, studiert.

Durch den Einsatz des Prinzips der retrosynthetischen Zerlegung, ein in der Chemie oft angewendetes System zur intelligenten Syntheseplanung, wurde eine Modellkaskade entworfen. Auch in der Biokatalyse kann dieses System, bei dem ein hochwertiges Produkt auf simple Ausgangsmaterialien zurückgeführt wird, Anwendung finden. Die einzelnen Transformationen von funktionellen Gruppen werden in diesem Fall von Enzymen katalysiert.

Im ersten Schritt der studierten Kaskade sollte ein nicht aktiviertes cyclisches Alken durch die Addition von Sauerstoff in einer Hydroxylierung für weitere Modifikationen aktiviert werden. Der entstehende ungesättigte allylische Alkohol wird im zweiten Schritt durch Oxidation in ein ungesättigtes Keton überführt. Durch eine anschließende Reduktion entsteht ein gesättigtes cyclisches Keton, das im letzten Schritt mittels Baeyer-Villiger Oxidation zu einem Lakton funktionalisiert wird.

All diese Schritte der Kaskadenreaktion können effizient und selektiv von Enzymen katalysiert werden. Durch den Aufbau dieser

Kaskade sollte ein tieferes Verständnis des Zusammenspiels von Redox-Enzymen ermöglicht werden.

Da sich die initiale Hydroxylierung des cyclischen Alkens schwierig gestalten wurde vorerst eine drei-stufige Kaskadenreaktion genauer charakterisiert. Dafür wurden eine Alkoholdehydrogenase, eine Enoatreduktase und eine Baeyer-Villiger Monooxygenase in den mikrobiellen Wirtsorganismus *Escherichia coli* eingebracht. Dieses artifizielle System wurde sowohl *in vitro* als auch in der Ganzzelle genau untersucht. Durch die Auswahl von geeigneten Ausgangsmaterialien wurde die Überlappung der Substratprofile der einzelnen Kaskadenenzyme erreicht und dadurch der Zugang zu verschiedenen optisch reinen Laktonen ermöglicht.

Schließlich konnte die Hydroxylierung, der ersten Kaskadenschritt, im Wirtsorganismus *Pseudomonas putida* realisiert werden. Aus diesem Grund wurde ein Mischkultursystem zur Zugänglichmachung von cyclischen Alkenen als Startmaterialien getestet. Der Einsatz vom Naturstoff Limonen als Ausgangsmaterial ermöglichte so die Produktion von chiralen Carvolaktonen in einer vier-stufigen Kaskadenreaktion.

In einem anwendungsorientierten Versuch wurde der Einsatz des Abfallprodukts Orangenschale als Ausgangsmaterial untersucht. Die Verfügbarkeit von Limonen aus der Orangenschale war hierbei ein wichtiger Faktor, der in unterschiedlichen Strategien behandelt wurde. Ein Ansatz war die *in situ* Extraktion von Limonen durch den Einsatz von ionischen Flüssigkeiten zu verbessern.

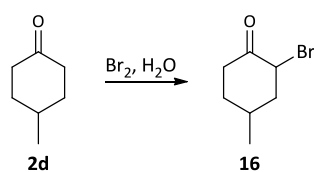
Schlussendlich zeigte sich, dass in einem simplen wässrigen System durch die Kombination der beiden mikrobiellen Wirtsorganismen eine Kaskadenreaktion von Limonen aus Orangenschale zu Carvolakton, ohne Extraktionszusätze, erreicht werden konnte.

A Synthetic schemes

A I Chemical syntheses

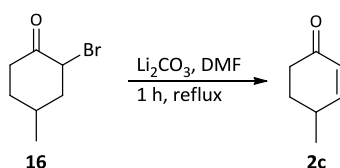
A I.1 Starting material

A I.1.1 2-Bromo-4-methylcyclohexanone (**16**)



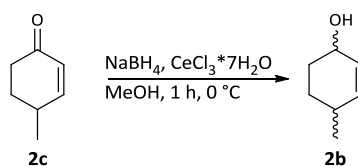
Scheme A-1. Bromination of 4-methylcyclohexanone (**2d**).

A I.1.2 4-Methylcyclohex-2-en-1-one (**2c**)



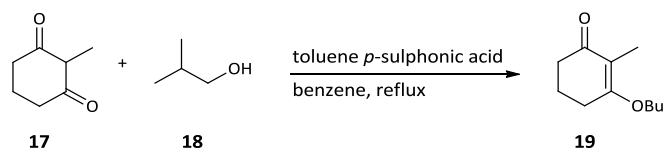
Scheme A-2. Elimination to yield 4-methylcyclohex-2-enone (**2c**).

A I.1.3 4-Methylcyclohex-2-en-1-ol (**2b**)

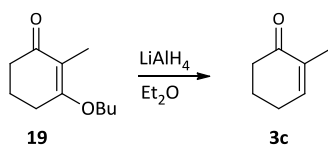


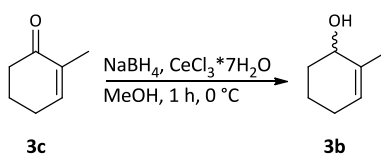
Scheme A-3. Luche reduction to give 4-methylcyclohex-2-en-1-ol (**2b**).

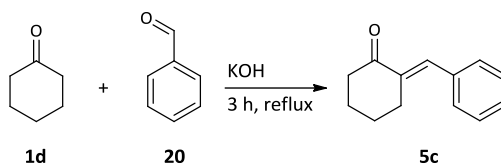
A I.1.4 3-Isobutoxy-2-methylcyclohex-2-enone (**19**)

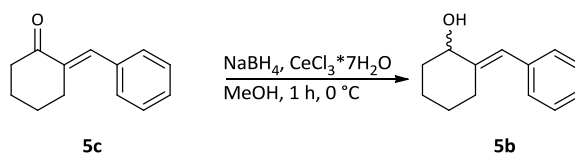


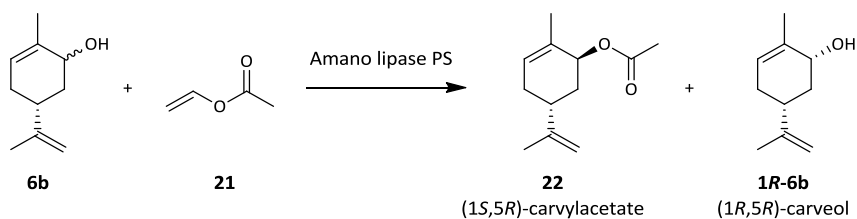
Scheme A-43. Condensation of 2-methyl-1,3-dione and isobutanol to yield isobutoxy-2-methylcyclohex-2-enone.

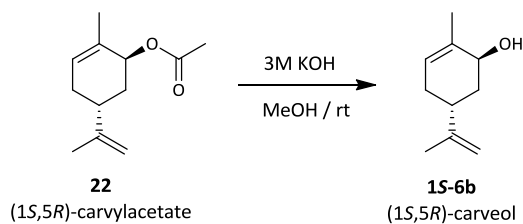
A 1.1.5 2-Methylcyclohex-2-en-1-one (**3c**)

Scheme A-5. LiAlH_4 reduction of 3-isobutoxy-2-methylcyclohex-2-enone to give 2-methylcyclohex-2-enone (**3c**).

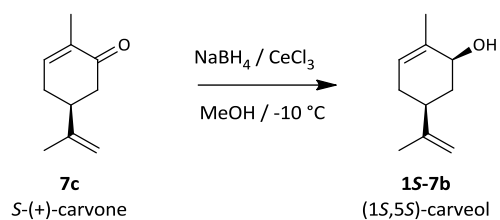
 A 1.1.6 2-Methylcyclohex-2-en-1-ol (**3b**)

Scheme A-6. Luche reduction of 2-methylcyclohex-2-enone (**3c**) to 2-methylcyclohex-2-en-1-ol (**3b**).

 A 1.1.7 2-benzylidenecyclohexanone (**5c**)

Scheme A-7. Knoevenagel condensation yielding in 2-benzylidenecyclohexanone (**5c**).

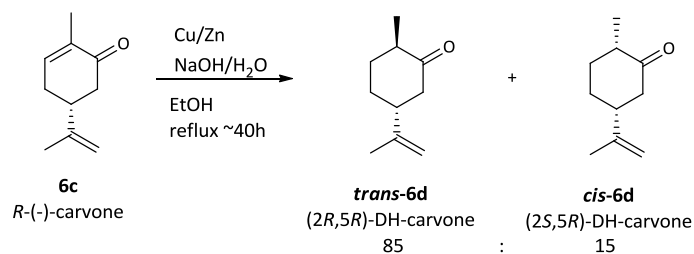
 A 1.1.8 2-benzylidenecyclohexanol (**5b**)

Scheme A-8. Luche reduction of 2-benzylidenecyclohexanone (**5c**) to 2-benzylidenecyclohexanol (**5b**).

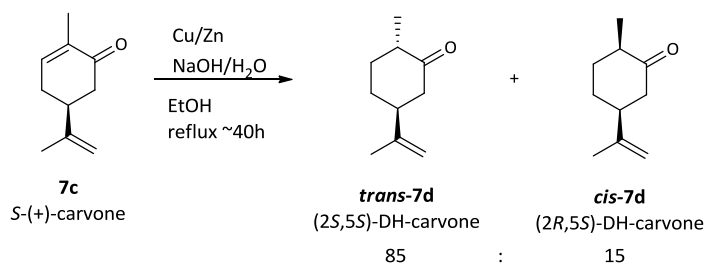
 A 1.1.9 (1*S*,5*R*)-2-methyl-5-(prop-1-en-2-yl)cyclohex-2-en-1-yl acetate (**22**) and (1*R*,5*R*)-Carveol (**1R-6b**)

Scheme A-9. Selective esterification of **6b** by Amano lipase yielding in (1*S*,5*R*)-carvyl acetate and **1R-6b**.

A I.1.10 (1*S*,5*R*)-Carveol (**1S-6b**)

 Scheme A-10. Basic hydrolysis of (1*S*,5*R*)-carvyl acetate to give **1S-6b**.

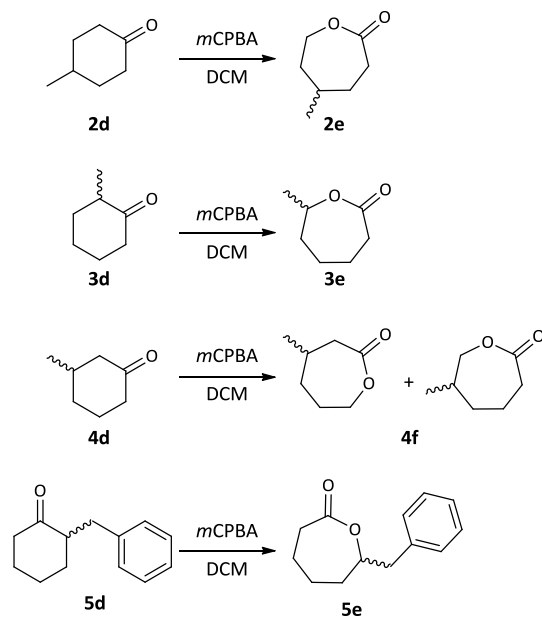
 A I.1.11 (1*S*,5*S*)-Carveol (**1S-7b**)

 Scheme A-11. Luche reduction of S-(+)-carvone (**7c**) yielding in **1S-7b**.

A I.2 Reference material

 A I.2.1 *R*-(-)-Carvone (**6c**) to *trans*-**6d** and *cis*-**6d**

 Scheme A-12. Reduction of *R*-(-)-carvone (**6c**).

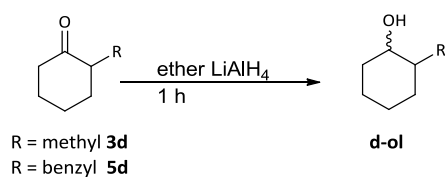
 A I.2.2 *S*-(+)-Carvone (**7c**) to *trans*-**7d** and *cis*-**7d**

 Scheme A-13. Reduction of *S*-(+)-carvone (**7c**).

A 1.2.3 Baeyer-Villiger oxidation (BVOx) of ketones to lactones



Scheme A-14. BVOx of cyclohexanone derivatives with mCPBA in DCM at RT o/n.

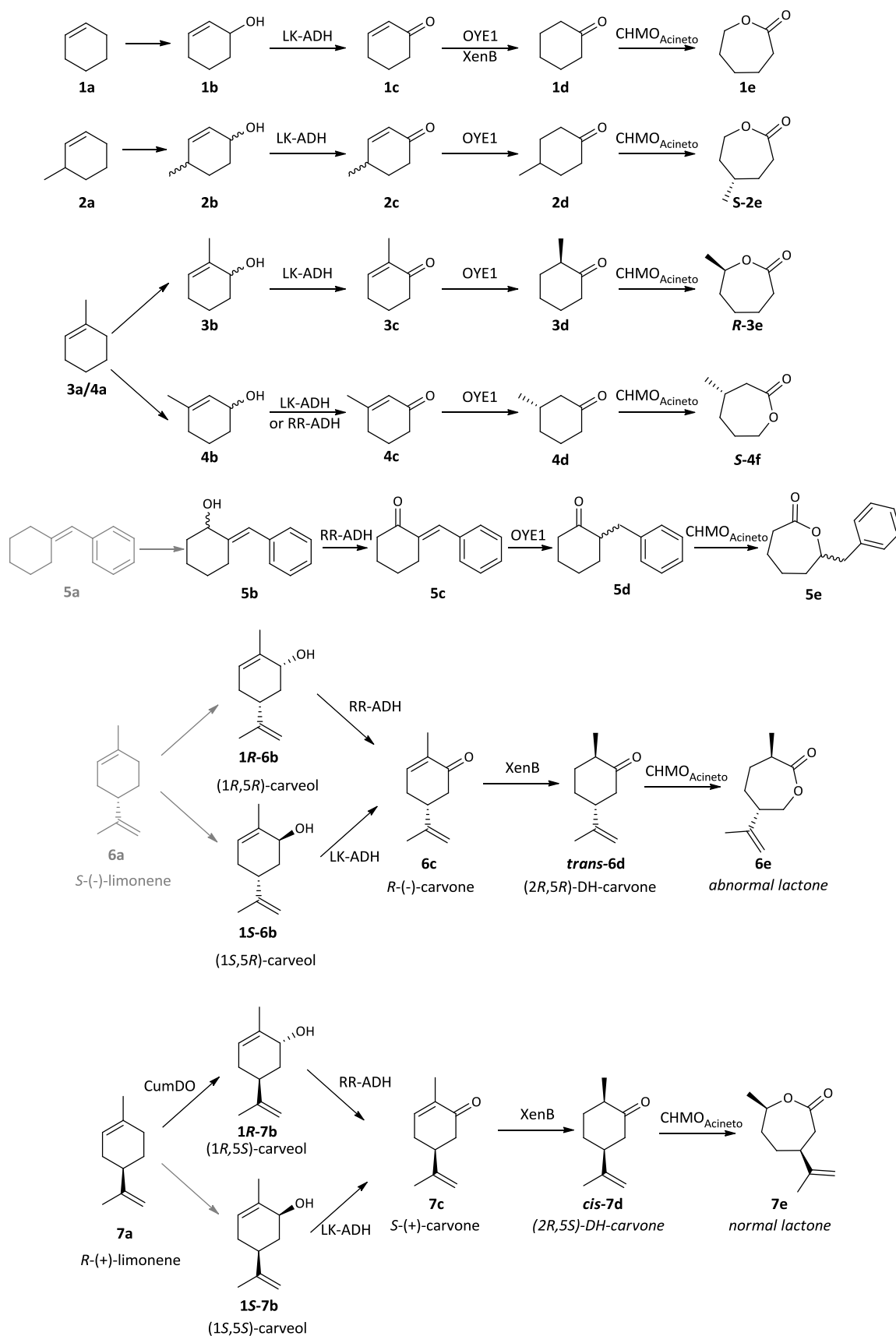
A 1.2.4 Reduction of ketones to alcohols



Scheme A-15. LiAlH₄ reduction of cyclohexanone derivatives.

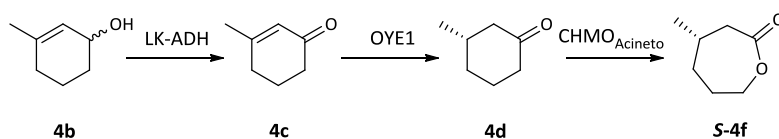
A II Biocatalytic reactions

A II.1 Analytical scale cascades



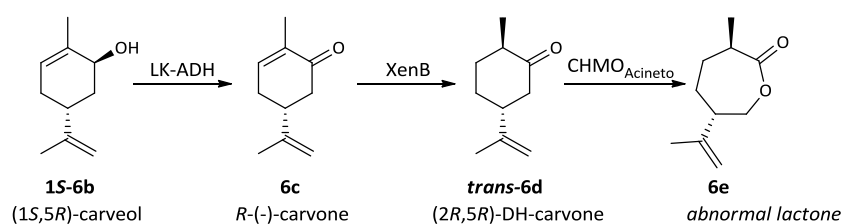
A II.2 Preparative scale cascades

A II.2.1 (S)-4-Methyloxepan-2-one ((S)-4-Methylcaprolactone, **S-4f**)



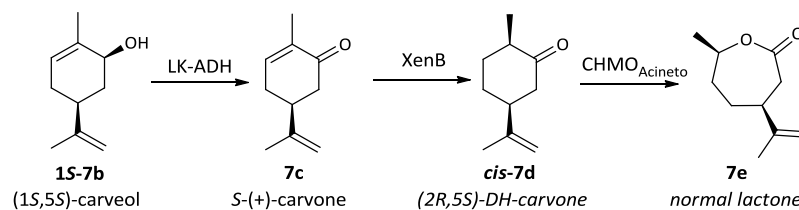
Scheme A-16

A II.2.2 (3R,6S)-3-Methyl-6-(prop-1-en-2-yl)oxepan-2-one ((3R,6S)-abn-carvolactone, **6e**)



Scheme A-17

A II.2.3 (4S,7R)-7-Methyl-4-(prop-1-en-2-yl)oxepan-2-one ((4S,7R)-carvolactone, **7e**)



Scheme A-18

B Introduction

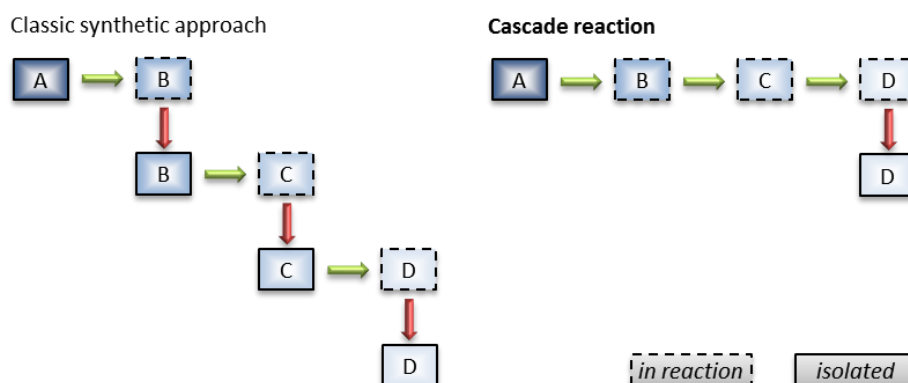
B I Cascade reactions

Nature has evolved a highly efficient system in form of cascade reactions which assemble the metabolic networks that ensure life (growth and reproduction) ^[1] In a living cell, basically a one-pot system, these complicated multistep synthetic reactions are catalyzed by numerous enzymes fine-tuned by evolution. The key part of the metabolic networks is the modulation of the catalytic activity of these enzymes by other molecules in the cell, including their own reactants and products, rendering catalysis critical for life. ^[2]

Cascades, when operated by a (bio)chemist, are generally described as a consecutive series of chemical reactions proceeding in concurrent fashion ^[3], and are often classified in the following groups: In domino reactions each catalyst triggers the formation of a reactive intermediate, which undergoes spontaneous transformation within a reaction sequence. Cascades with two or more catalysts can be executed in sequential or simultaneous mode. Whereas in simultaneous (or relay) cascades all the catalysts and reactants are present from the outset, in the sequential approach the next catalyst is added only after the completion of the previous step. ^[4]

B I.1 Chemocatalytic cascades

As chemists have been inspired by living cells, the mimicking of natural systems in chemical synthesis and performing catalytic cascade reactions in a one-pot manner was intensively investigated over the past decades. ^[5] Multistep cascades in living organisms commonly function without separation of intermediates; concentrations of all reactants are kept low, which allows high selectivity and avoids by-product formation. Taking nature as a model, application of cascade reactions in organic synthesis offers a lot of advantages over the classical step-by-step approach. As there is no need for purification, operating time, costs and waste are reduced, atom economy and overall yields are improved. Additionally, the problem of unstable or toxic intermediates can be overcome and reactivity as well as selectivity can be enhanced by evading equilibrium reactions by the cooperative effect of multiple catalysts (Scheme B-1). ^[4, 6-7]



Scheme B-1. Classic synthetic approach vs. cascade reactions adapted from Bruggink *et al.* ^[7]

Although significant research progress was achieved over the past decades, one-pot multistep reactions are still not of general applicability in chemocatalysis due to problems with compatibility of reaction conditions. ^[5]

B I.2 Enzymatic cascades

Multi-enzymatic cascade reactions can be classified in two groups: i) biotransformations, the conversion of arbitrary, non-native substrates into desired products and ii) fermentations, referring to product synthesis from a growth substrate involving native metabolism.^[8] Fermentations find application since a long time for example in brewing (*Saccharomyces* sp.) or vinegar production (*Acetobacter* sp.)^[9]. However the evolution from single-step biotransformations employing (purified) enzymes to complex multistep biocatalysis, which will be discussed in more detail later, only took place in the past decade.^[10]

Metabolic engineering has contributed significantly to the enhanced production of various value-added and commodity chemicals and materials from renewable resources.^[11] It involves the enhancement of native pathways for the overproduction of certain metabolites, e.g. shikimate in *E. coli*^[12] or the reconstruction of natural pathways in heterologous hosts as shown for the mevalonate pathway (MEV) from *S. cerevisiae* in *E. coli* towards the production of artemisinin^[13]. Also the disruption of hindering native reactions and the incorporation of heterologous enzymes in native pathways can lead to production of valuable compounds as reported for riboflavin^[14].

Synthetic biology aims to create novel and fine-controlled metabolic and regulatory circuits maximizing metabolic fluxes to the desired products in the strain being developed. This allows for engineering of host microorganisms to enhance their innate metabolic functions or to gain new capabilities in the production of target compounds.^[15] Combined strategies from biocatalysis, metabolic engineering and synthetic biology led to the establishment of artificial metabolic pathways.^[16] The above mentioned isoprenoid biosynthesis pathway (MEV) was later extended with two heterologous enzymes towards the production of limonene and perillyl alcohol.^[17] *De novo* designed pathways can be optimized by tuning the primary metabolism of the host as shown by the group of Prather through controlling the glycolytic flux.^[18] The same group showed customization of the host organism for a heterologous synthetic pathway towards vanillin by engineering *E. coli* for reduced aromatic aldehyde reduction (RARE).^[19]

Metabolic engineering of native and synthetic pathways was extensively studied and is topic of many comprehensive reviews. Lee *et al.* discussed trends in the field of systems metabolic engineering, combining systems biology, which aims at quantitative understanding of living cells and can thereby help to predict cellular behavior^[20], synthetic biology and evolutionary engineering.^[11] Computational approaches towards the sustainable production of chemical building blocks were reviewed by Chen *et al.*^[21]. Further reviews regarding the microbial production of fuels^[22-24], polymers^[25], isoprenoid-based C₅ alcohols^[26] and other fine chemicals^[27] have been published recently.

B I.3 Chemo-enzymatic cascades

Whereas enzymatic cascade reactions often benefit from a similar reaction milieu, chemo-enzymatic combinations encounter compatibility problems as either the biocatalyst is unstable in organic solvents or the organo- or metallo-catalyst is inactivated in aqueous environment.^[28] Several approaches have been investigated like the stabilization of enzymes or chemo-catalyst^[29] via different protein engineering approaches, compartmentalization by nanoparticles^[3], artificial metalloenzymes resulting from the encapsulation of an organometallic catalyst within a protein scaffold^[30] or immobilization.^[31]

B II Multistep biocatalysis

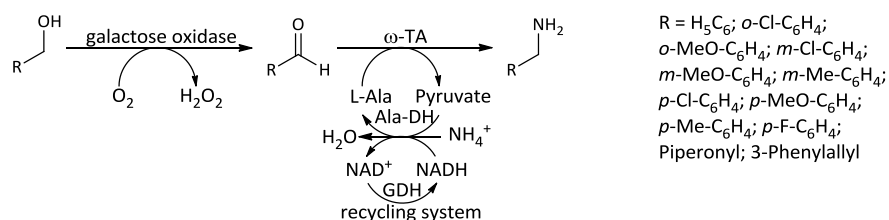
The one-pot combination of biocatalysts is often easy to realize as most enzymes reach their catalytic optimum at similar temperature and pH conditions in aqueous buffers. In these *in vitro* systems reaction parameters like substrate or enzyme concentrations, pH-value, temperature, and co-solvent additives can be varied and optimized in a systematic way. Preparation of the biocatalysts usually involves heterologous enzyme production in a microbial host, isolation and purification. Cell free extracts (CFE) of host cells after enzyme production or purified enzyme solutions show good storage capabilities and became of high value to the biocatalytic community. A major drawback of *in vitro* systems is that most redox enzymes are dependent on expensive cofactors which have to be either added in stoichiometric amounts or regenerated by enzymatic recycling systems.^[1, 16] Hence, all assets and drawbacks at hand, from a chemist's point of view an *in vitro* system with CFE, is often preferred as no special lab tools are required once the extracts are produced.

Using an *in vivo* whole cell system has the major advantage of a fully functional living organism providing an efficient enzyme production machinery, increased enzyme stability due to their natural environment, and an automated cofactor regeneration system^[1]. Additionally, no enzyme purification is required. However, in a multiple enzyme system usually preliminary genetic manipulations are required and therefore a different expertise is required.

B II.1 *In vitro* cascades

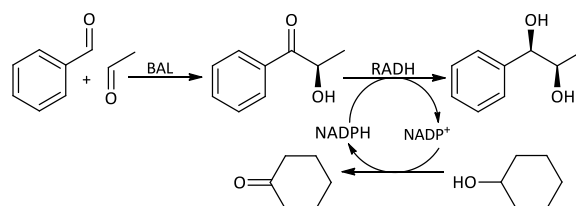
The scope of cascade reactions so far known in the literature last from simple combinations of one enzyme with a cofactor recycling system to coupling of thirteen different enzymes.^[32] There are comprehensive reviews on the topic of multi-enzymatic reactions^[1, 33-35] and only some examples from the literature regarding important issues will be highlighted here. Parameters such as cofactors and their recycling, co-solvents and the different preparation of the biocatalysts are of great influence to the performance of cascades.

The importance of proper secondary cofactor recycling enzymes was demonstrated for the direct conversion of benzylic and cinnamic primary alcohols to the corresponding amines based on a galactose oxidase from *Fusarium* NRRL 2903 and an ω -transaminase (Scheme B-2). An alanine dehydrogenase and a formate dehydrogenase (FDH) were tested as auxiliary enzymes, initially. Only the change from FDH to glucose dehydrogenase (GDH) gave an improvement from 81% to >99% conversion. This was attributed to the inhibitory effect of ammonium formate on galactose oxidase, which was then replaced by ammonium chloride with GDH. To demonstrate the applicability of this enzymatic oxidation–amination cascade, 3-phenyl-allylamine was used as the starting material for the preparation of the potent antifungal agent naftifine.^[36]



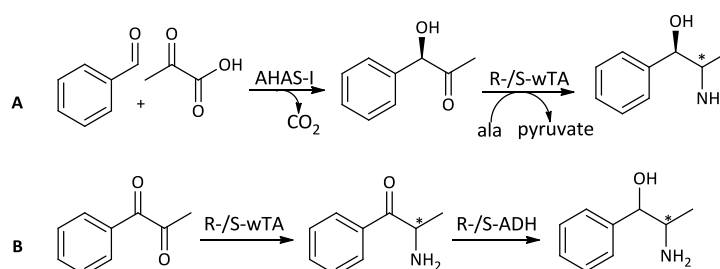
Scheme B-2. Oxidation-amination cascade by Fuchs *et al.*

Co-solvents or organic phases often play an important role in enzyme cascades for direct product extraction or increased substrate solubility. A cascade reaction by the group of Rother consisted of an asymmetric carbonylation by a benzaldehyde lyase (BAL) from *Pseudomonas fluorescens*, followed by stereoselective reduction of the intermediary α -hydroxy ketone by an alcohol dehydrogenase from *Ralstonia sp.* (RADH) (Scheme B-3). First, the reaction was done in pure organic solvent without any success. The addition of one equivalent of water to the dry catalyst resulted in a micro-aqueous environment ultimately activating the cascade. Out of nine tested organic solvents, MTBE was identified as most suitable choice for both enzymes. Also substrate concentration, enzyme concentration, enzyme ratio and buffer systems with different pH values were improved.^[37]



Scheme B-3. Carbonylation-reduction cascade by Jakobinnert *et al.*

When using *in vitro* cascades the preparation of the particular catalytic entity (CFE, lyophilized cells, immobilized cells/enzymes or purified enzymes) turned out as highly critical, in some cases affecting the resulting enantiomeric excess and conversion rates. For example, Sehl *et al.* developed cascades with enzymes from different toolboxes, which can be efficiently combined, yielding all stereoisomers of the desired nor-(pseudo)-ephedrine. Here, employing lyophilized whole cells or purified enzymes showed a significant difference with respect to enantiopurity. The combination of a purified (*R*)-selective thiamine diphosphate (ThDP)-dependent carbonylase (AHAS-I) and a purified (*S*)- or (*R*)-selective ω -transaminase resulted in the formation of (1*R*,2*S*)-norephedrine or (1*R*,2*R*)-norpseudoephedrine in excellent optical purities (>99% ee and >98% de, Scheme B-4-A). As an (*S*)-selective carbonylase was not available, the authors used a combination of an (*S*)-selective transaminase with an (*S*)- or (*R*)-selective alcohol dehydrogenase to afford (1*S*,2*S*)-norpseudoephedrine or (1*R*,2*S*)-norephedrine with >98% ee and >95% de (Scheme B-4-B). The use of the cheaper lyophilized whole cells decreased the diastereomeric excess (de) for (1*R*,2*S*)-norephedrine from >95% de to a diastereomeric ratio of approx. 8:2 due to the *E. coli* induced isomerization of the intermediate.^[38-39]



Scheme B-4. *In vitro* cascade reaction by Sehl *et al.*

B II.2 *In vivo* cascades

Many different bottlenecks could arise in complex biocatalytic multistep systems calling for diverse strategies to increase the flux through these reaction cascades. The most important challenges of artificial *in vivo* cascades for biotransformations are presented here.

B II.2.1 Enzyme activity and proximity

A very potent strategy to overcome challenges within *in vivo* cascades is to fine tune the requisite enzymes. In recent years, enzyme engineering was used to enhance a diverse set of proteins to realize new biosynthetic pathways and gain access to novel products.^[40] Mutagenesis of proteins by directed evolution^[41] for enhancement of activity, stereo- and regioselectivity, storage stability, temperature or solvent tolerance and widening of the substrate scope was well studied for their application in biocatalysis.^[42]

Protein engineering is indeed of great value, especially when a single enzyme is limiting the cascades overall output. A powerful example was the research by DeLoache *et al.* who, by using an enzyme-coupled biosensor, identified a tyrosine hydroxylase for the purpose to produce dopamine from glucose in yeast. Through enzyme mutagenesis they obtained a double mutant of the hydroxylase, co-expressed it with a L-3,4-dihydroxyphenylalanine (DOPA) decarboxylase and could achieve 7.4-fold improvement of dopamine titer.^[43]

A limiting factor in cascades combining several biocatalysts *in vivo* could be the diffusion of intermediates into the hosts' cytoplasm. The concept easiest to apply to deal with this separation of reaction partners is the production of fusion proteins. Linkage of cascade enzymes shortens the transit time between active sites which could protect unstable intermediates and limit side reactions.^[44-45] A very recent example for use of fusion proteins in cascade reactions was shown by Peters *et al.* who investigated the fusion of an alcohol dehydrogenase (ADH), an enoate reductase (ERED) and a Baeyer-Villiger Monooxygenase (BVMO). Whereas they could achieve successful linkage of an ERED with a BVMO, the ADH activity was lost upon fusion. This may be due to misfolding or displacement of important amino acids which is a common problem encountered with fusion proteins.^[46]

For another strategy to enhance synthetic multi-enzyme cascade reactions, nature provided the blue-prints with substrate channeling along spatially organized multi-enzyme structures. Very prominent examples are the polyketide synthases (PKSs) which present enzyme assembly lines for the synthesis of chemically diverse polyketide natural products.^[47] Efficient through-put is achieved by facilitated transfer of a reaction intermediate from the active site of one enzyme to the active site of a downstream enzyme without first diffusing into the bulk solution. Due to new developments in nucleic acid nanotechnology this system can be mimicked through protein scaffolding.^[48-49] This approach was exemplified by Dueber *et al.* by constructing synthetic protein scaffolds that spatially assemble enzymes in a designable manner. Scaffolds bearing interaction domains from metazoan signaling proteins were used to specifically recruit pathway enzymes tagged with their associated peptide ligands. With this system they targeted the bottleneck enzymatic step of a previously engineered mevalonate biosynthetic pathway^[50] for flux improvement. The three mevalonate biosynthetic enzymes were recruited to a synthetic scaffold, which optimized the stoichiometry and thereby a 77-fold improvement in product titer was achieved with low enzyme expression and reduced metabolic load.^[51]

B II.2.2 Host background

When introducing non-native cascades in host organisms, background reactions might be a challenge, leading to decreased conversion, side-product formation or similar undesired results. There is the possibility to shut down these activities by disrupting or deleting the gene sequences coding for these enzymes from the hosts' genome. This concept is referred to as gene knockout (KO) and can directly be connected with a knock-in (KI) where heterologous enzymes are used to exchange the background enzyme.^[52] Depending on the knocked out gene this could lead to growth deficiencies of the host which could in turn again limit the performance of the cascade. For the very frequently used host organism *E. coli* the group of Keio established a library of KO-strains, each characterized regarding their viability, which became a valuable tool for planning the disruption of background reactions.^[53]

Brockman and Prather developed a strategy for dynamically modulating the abundance of native enzymes within the host cell and applied this to a model system for *myo*-inositol production from glucose. They have been able to develop an *E. coli* strain with a growth mode close to wildtype and capable to be switched to production mode by inducer addition. By varying the induction time they achieved a two-fold improvement in yield and titers of *myo*-inositol.^[54]

B II.2.3 Growth deficiencies

Growth deficiencies might be a consequence of the mentioned knockout or by the introduction of the cascade itself, due to competition with the cell's metabolism for cascade precursors or the production of toxic intermediates. In the latter case, intracellular scaffolding as mentioned above or compartmentalization of the cascade might improve the viability of the host.

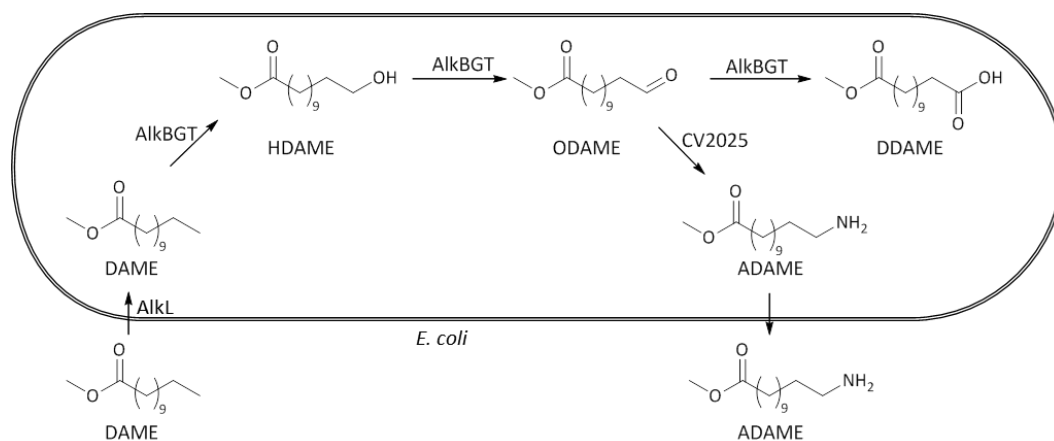
Confinement of enzymes in protein nanocompartments represents a potentially powerful strategy for controlling catalytic activity in cells. Wörsdörfer *et al.* successfully sequestered HIV (human immunodeficiency virus) protease, a toxic enzyme when produced in the cytoplasm, within an engineered lumazine synthase (from *Aquifex aeolicus*) capsid. The growth advantage resulting from protecting the *E. coli* host from the protease enabled directed evolution of improved capsids. After four rounds of mutagenesis and selection, they obtained a variant with a 5- to 10-fold higher loading capacity than the starting capsid, which permitted efficient growth even at high intracellular concentrations of HIV protease.^[55]

Bacterial microcompartments (MCPs) are a widespread family of proteinaceous organelles that consist of metabolic enzymes encapsulated within a protein shell.^[56] Sargent *et al.* designed a synthetic operon encoding the key structural components of a MCP based on the genes for the *Salmonella enterica* propanediol utilization (Pdu) MCP, whose mechanism was investigated by Fan *et al.*^[56]. An *in vivo* protease accessibility assay suggested that a GFP fusion protein could be protected from proteolysis when co-expressed with the synthetic MCP operon.^[57]

B II.2.4 Cell membrane

Permeability of the cell membrane is very often an issue in whole-cell biotransformations. Since the outer membrane of a bacterium is a lipid bilayer, only lipophilic substances can pass the membrane via diffusion. This limits the substrate uptake for cascade reactions not only in terms of polarity but for non-polar substances also in terms of uptake velocity since diffusion is a passive and, consequently, slow process. Different strategies can be applied for improving already existing cascade reactions and for establishing new cascades not feasible due to hindered substrate uptake.^[16]

To overcome limited substrate uptake, Bühler and coworkers identified a protein of the *Pseudomonas putida* GPo1 Alk-operon, which promotes uptake of hydrophobic substrates as exemplified by fatty acid methyl esters (FAMES) ^[58] and limonene. ^[59] This principle was applied for their described alternative route for the production of ω -aminocarboxylic acid methyl esters (ADAME) using the AlkBGT monoxygenase-reductase system from *P. putida* GPo1 and the transaminase from *Chromobacterium violaceum* CV2025. ^[60] Here, 1.4–2.9 mM substrate dodecanoic acid methyl ester (DAME) were used and resulted in approximately 5–16% yield. Furthermore, the overoxidation of the intermediary terminal aldehyde (ODAME) to the carboxylic acid (DDAME) by AlkBGT was observed. In their parallel work concerning the integral membrane porin AlkL, the co-expression of this protein led to a 62-fold increase of the activity towards FAMES. ^[58]



Scheme B-5. Production of ω -aminocarboxylic acid methyl esters utilizing membrane porin AlkL (adapted from Schrewe *et al.*) ^[61].

Furthermore, in a follow-up contribution the co-expression of AlkBGT, AlkL and AlkJ (an alcohol dehydrogenase, which will be discussed in more detail later) led to an enhanced production of dodecanedioic acid monomethyl ester (DDAME) ^[62], the application of AlkL for the production of perillyl alcohol from limonene gave a two-fold improvement of activity. ^[59] In both cases it was necessary to apply a two-phase system using bis(2-ethylhexyl)phthalate (BEHP) as substrate reservoir and product sink; this strategy is compromised by teratogenic and environmentally harmful properties of this solvent. By increasing the substrate uptake due to the expression of AlkL the intracellular level of DDAME was enhanced to toxic concentrations for the cell and BEHP was necessary to regulate the concentration level below the toxicity threshold. In summary, the application of AlkL significantly enhanced the uptake of hydrophobic substrates.

An additional challenge, as opposed to substrate uptake, might be the transport of the product to the exterior of the cell. This is important for microbial production of biofuels, as many compounds being considered as candidates for advanced fuels are toxic to microorganisms. ^[63] The utilization of active transporters is a particularly promising strategy for the efflux of biochemicals. ^[64] Dunlop *et al.* identified and heterologously expressed a library of 43 efflux pumps in *E. coli*, where they tested it against seven representative biofuels. By using a competitive growth assay, they efficiently distinguished pumps that improved survival in presence of α -pinene or limonene. For two of the fuels (n-butanol and isopentanol), none of the pumps improved tolerance. ^[63] The inability to find transporters for these alcohols may be due to a small number of putative pumps available, or because evolutionary pressures had not yet produced suitable transporters due to the lack of these chemicals in the environment of the sampled cells. ^[64]

B II.3 Redox enzymes in cascade reactions

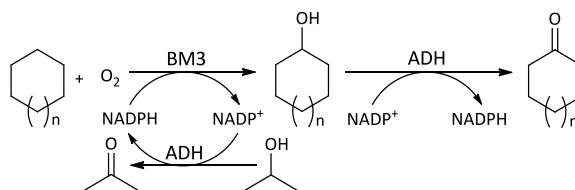
Redox reactions play a crucial role in the conversion from carbon sources to complex molecules. As such, every cascade design will have to deal with redox challenges, either in the conversion of material or the regeneration of cofactors. A very comprehensive overview of synthetically relevant biocatalytic redox reactions is given in a review by Blank *et al.* [65] Here, only enzyme classes relevant for this thesis will be discussed.

B II.3.1 Oxygenases

The biocatalytic incorporation of molecular oxygen into an organic molecule can be achieved with oxygenases presenting nature's variant of C-H-activation. Oxygenases can be categorized into two sub-groups. Monooxygenases insert one oxygen atom of molecular oxygen into the substrate while the other one is reduced at expense of a cofactor, generally nicotinamide adenine dinucleotide (phosphate) (NAD(P)H), resulting in water as by-product. The second subtype are dioxygenases where both oxygen atoms are incorporated into the substrate leading to an unstable peroxy-product which is often directly reduced to (di)hydroxy derivatives. Different types of oxidizing enzymes are oxidases, which catalyze electron transfer onto molecular oxygen, and peroxidases which use hydrogen peroxide as electron acceptor. [66]

Monooxygenases rely on either iron (Fe) or copper (Cu) containing cofactors or heteroaromatic cofactor systems (pteridin or flavin). Of the Fe-depending monooxygenases the majority belongs to the cytochrome P450 type enzymes which have been studied extensively (for reviews see Bernhardt [67]) and Urlacher and Girhard [68]).

A successful enzyme cascade utilizing a P450 monooxygenase for the direct oxidation of cycloalkanes to cycloalkanones in combination with an ADH was shown by Staudt *et al.* (Scheme B-6). Protein engineering of suitable P450 monooxygenases identified the BM3 variants 19A12 and F87V (originating from *Bacillus megaterium* BM3) as the best candidates for cycloalkane hydroxylation. Combination of the ADH from *Lactobacillus kefir* and the BM3 mutants enabled production of cyclooctanone (6.3 mM) and cyclohexanone (4.1 mM) starting from the corresponding cycloalkane (100 mM). Although the sequence gave the desired products, the low activity of the P450 monooxygenase turned out as bottleneck of the cascade. Protein engineering of the P450 monooxygenase with respect to activity, stability, and improvement of the "coupling efficiency" is still an ongoing challenge. [69]

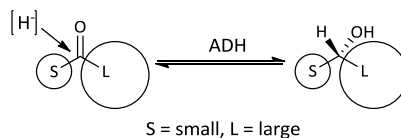


Scheme B-6. *In vitro* cascade combining a P450 monooxygenase with an ADH by Staudt *et al.*

B II.3.2 Alcohol dehydrogenases (ADHs)

In nature a vast variety of alcohol dehydrogenases [70] is present in nearly all organisms from prokaryotes to humans catalyzing diverse metabolic functions such as detoxification of alcohols or xenobiotics, regulation of hormones or taking part in signaling pathways. [71] An important structural attribute of dehydrogenases is the Rossmann-fold to bind the nicotinamide-based coenzymes. Based on distinct sequence motifs, protein chain length, mechanistic features, and structural comparisons, ADHs can be classified into aldo-keto reductases (AKRs), short- (SDRs), medium- (MDRs), and long-chain dehydrogenases/reductases (LDRs). [72]

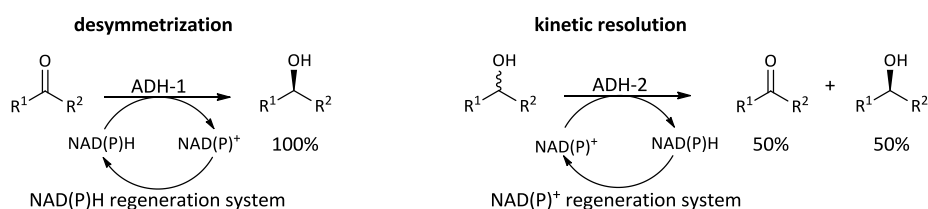
In biocatalysis ADHs are mainly studied and appreciated for their stereoselective reduction (desymmetrization, Scheme B-8) of aldehydes and ketones and emerged despite the highly competitive homogeneous organocatalysis as industrially relevant catalytic systems.^[73] The stereoselectivity of ADHs is mainly due to steric properties of the substrate and can for most dehydrogenases be predicted from a simple model, the Prelog's rule (Scheme B-7), introduced by Prelog^[74] already in 1964.^[75]



Scheme B-7. Prelog's rule for hydride attack in ADH reductions.

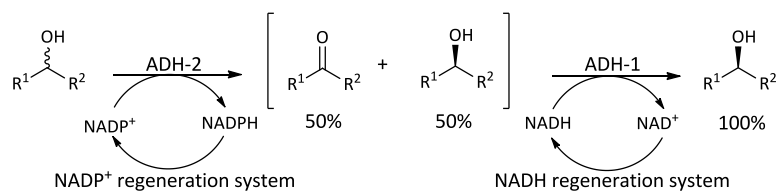
Frequently used and commercially available ADHs, such as horse liver ADH (HLADH) or ADH-A from *Rhodococcus ruber* follow the Prelog's rule and deliver (*S*)-alcohols. ADH from *Thermoanaerobium Brockii* (TBADH) exhibits special selectivity as it obeys the Prelog rule for large substrates but gives anti-Prelog products for small ketones. ADHs furnishing (*R*)-alcohols, therefore performing anti-Prelog, are produced by *Lactobacillus* sp. or *Pseudomonas* sp..^[75]

Selective oxidation of primary alcohols to yield aldehydes is challenging due to the reactivity of the product as over-oxidation to the acid is thermodynamically favored.^[76] Oxidation of chiral secondary alcohols by an ADH goes hand in hand with the elimination of a chiral center and is therefore of minor interest to the biocatalytic community. However, using an enantioselective enzyme allows accumulation of only one enantiomer in a kinetic resolution (Scheme B-8). The disadvantage of kinetic resolutions however is the maximum yield of only 50% (provided the catalyst exhibits perfect enantioselectivity). Thus, from the enantioselective synthesis point-of-view, desymmetrizations are usually preferred (100% yield).^[76]



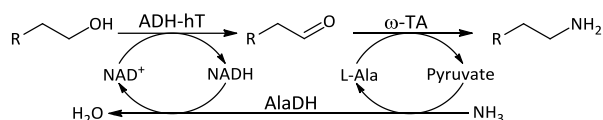
Scheme B-8. Valuable approaches for using ADHs in asymmetric synthesis (adapted from Schallmeyer *et al.*^[77])

A valuable strategy in asymmetric synthesis is the use of two enantiocomplementary ADHs for deracemizations, ultimately providing access to a theoretical 100% yield of chiral compound (Scheme B-9). Here the basic requirement is that at least one of the steps proceeds enantioselectively, ideally both steps are highly selective and complementary. One drawback of this methodology is that both ADHs need to differ in their cofactor requirements to prevent undesired cross-activities.^[76]



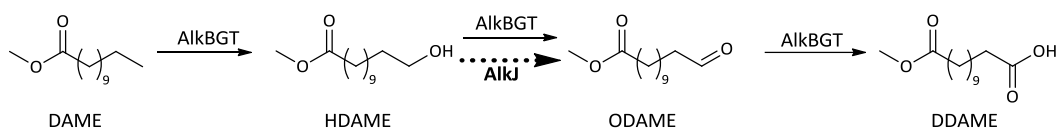
Scheme B-9. Deracemization by using two complementary ADHs (adapted from Hollmann *et al.*^[76-77])

Due to the fact that the oxidation reaction is thermodynamically unfavored the exclusive use of ADH catalyzed oxidations is limited but they are rather applied in cascade type reactions. Sattler *et al.* combined a thermostable ADH (ADH-hT) with a ω -transaminase (ω -TA) for the amination of primary alcohols in an *in vitro* reaction.^[78] By the addition of the cheap amine donor ammonia in connection with cofactor recycling L-alanine dehydrogenase they could shift the equilibrium of the reaction towards the product side (Scheme B-10).



Scheme B-10. Redox-neutral cascade for the bioamination of alcohols by Sattler *et al.*^[78].

The above mentioned AlkJ (from *P. putida*)^[79-80] is a cytoplasmic membrane protein and presents a special ADH as it is NAD(P)⁺ independent. AlkJ is supposed to transfer electrons to oxygen instead of a soluble cofactor^[80] and may therefore catalyze irreversible alcohol oxidation profiting from the thermodynamics of the O₂ reduction via the electron transport chain.^[62] Schrewe *et al.* made use of that by integrating AlkJ in the multistep oxidation of DAME, where substrate competition of ODAME and 12-hydroxydodecanoic acid methyl ester (HDAME) for AlkBGT was relieved by constant oxidation of HDAME by AlkJ (Scheme B-11).^[62]



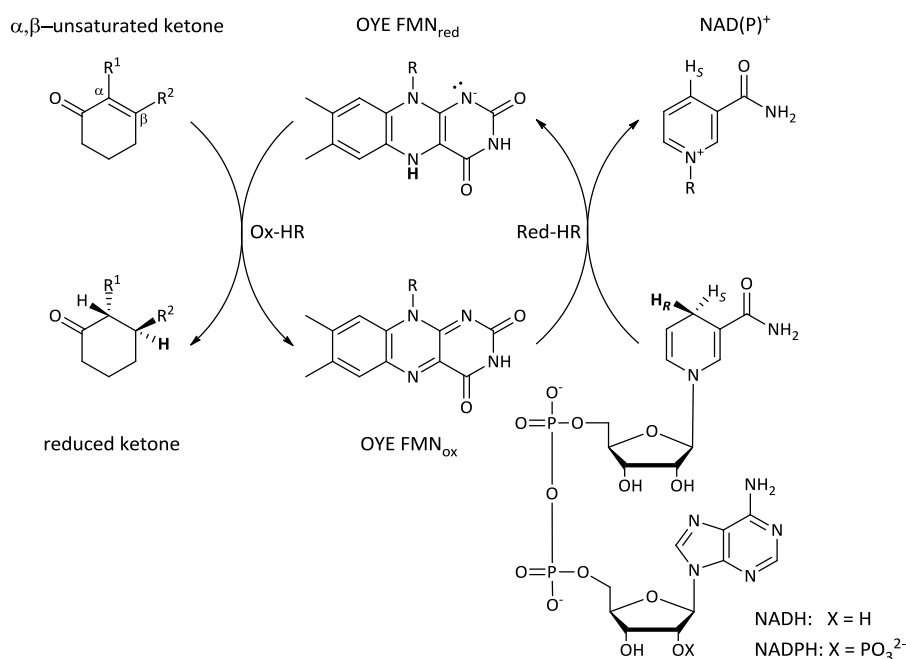
Scheme B-11. Multistep oxidation of DAME to DDAME by AlkBGT is enhanced by AlkJ (adapted from Schrewe *et al.*^[62]).

B II.3.3 Enoate reductases (EREDs)

Reductions of activated alkenes can be catalyzed by enoate reductases (ene-reductases, EREDs) resulting in the formation of up to two chiral centers. These well-studied flavin dependent enzymes are able to stereoselectively reduce activated C=C bonds presenting a highly useful asymmetric transformation method. A comprehensive review by Winkler *et al.*^[81] focused on industrially relevant ERED reaction products, Toogood *et al.*^[82] recently reviewed new developments in the field and Amato and Stewart highlighted applications of ERED engineering^[83].

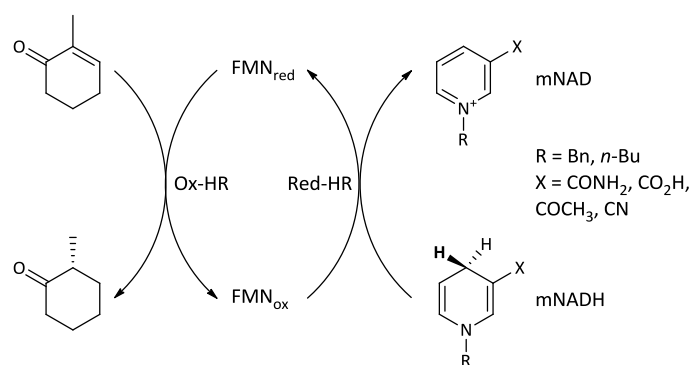
EREDs are highly abundant in plants and microorganisms, especially bacteria and fungi, where they are involved in fatty acid, morphine^[84] or jasmonate^[85] biosynthesis. They also play a role in degradative pathways catalyzing the detoxification of xenobiotics.^[86] Their substrate profile includes α,β -unsaturated carbonyl compounds, carboxylic acids, acid derivatives, nitro compounds and more complex ones such as steroids.^[87]

The most thoroughly studied EREDs are members of the old yellow enzyme (OYE) family, their color and consequently their name derived from the flavin cofactor, which were the first flavin mononucleotide (FMN) containing enzymes identified^[88]. The first described old yellow enzyme OYE1 was isolated from *Saccharomyces pastorianus* (formerly *S. carlsbergensis*)^[89] and its intensively studied catalytic mechanism^[90] is described in an oxidative (Ox-HR) and a reductive half reaction (Red-HR) as shown in Scheme B-12.



Scheme B-12. Catalytic mechanism of OYE enzymes (adapted from Kohli *et al.* [90])

The *trans*-hydrogenation proceeds via a hydride attack, derived from the reduced FMN cofactor (FMN_{Red} Scheme B-12), on the C β of the unsaturated ketone in a Michael-type fashion. Then a proton is added from the opposite side onto C α by a tyrosine residue of the protein. This oxidative half reaction is complemented by the Red-HR where the oxidized FMN cofactor is reduced at the expense of NAD(P)H. Most EREDs are rather unselective regarding their choice for nicotinamide adenine dinucleotide (NADH) or nicotinamide adenine dinucleotide phosphate (NADPH) but the cofactor has to be provided or recycled in an additional redox reaction. [86] Research to substitute the expensive and unstable native cofactors with synthetic nicotinamide biomimetics has been reviewed recently. [91] Application of synthetic nicotinamide mimics (mNAD) in ERED catalyzed reductions (Scheme B-13) has been investigated by the group of Hollmann. [92] Recently they could show that these inexpensive to manufacture and stable biomimetics outperformed the natural coenzymes in selected cases. [93]



Scheme B-13. ERED mediated reduction using synthetic nicotinamide mimics investigated by Paul *et al.* and Knaus *et al.*

In contrast to EREDs, ADHs are highly specific regarding their cofactor requirements and, therefore, lack activity towards until now studied synthetic nicotinamide mimics. This could be turned into an advantage, for example when using CFE where presence of ADHs can lead to unsatisfactory chemoselectivity. Despite overlapping substrate scopes these undesired side reactions could be limited by the use of synthetic nicotinamide cofactors. [91]

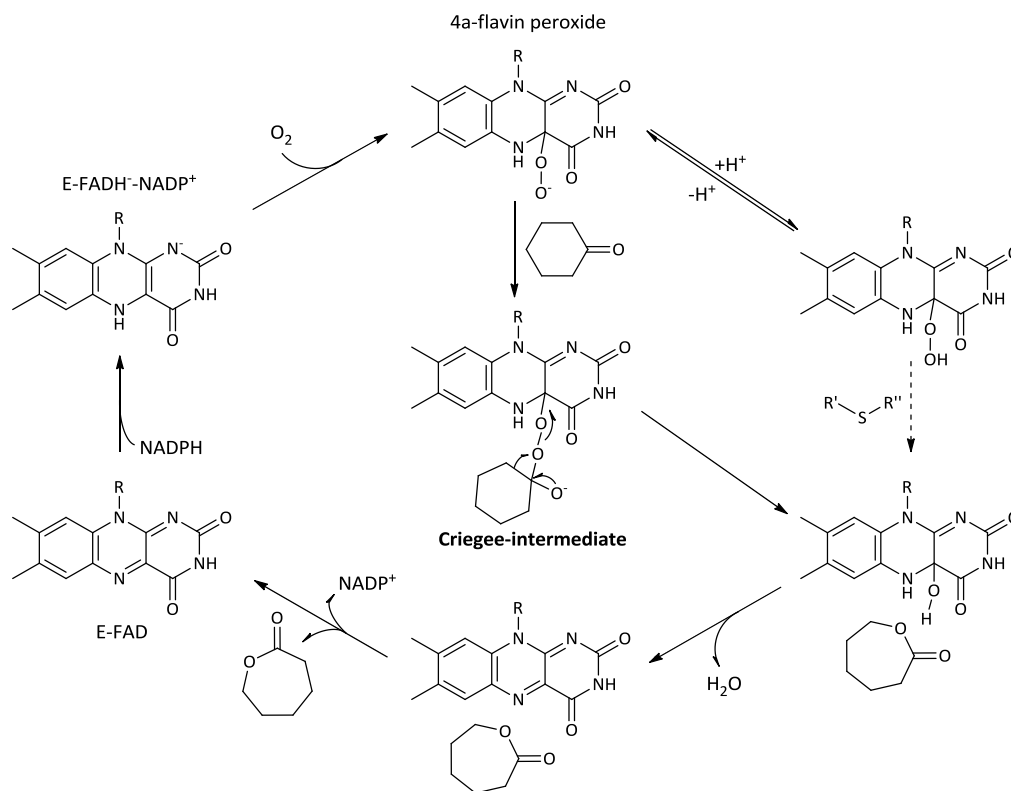
Cofactor addition is not required in whole-cell reactions, most prominently in baker's yeast, but they often suffer from side reactions such as the already mentioned carbonyl reduction by competing ADHs or ester hydrolysis. Expression systems for OYE1 in *E. coli* presented a possibility to circumvent by-products and characterize the enzyme regarding its stereoselective preferences.^[94] Protein engineering should drive the capacities of OYE1 even further and site saturation mutagenesis on a tryptophan residue (W116) led to stereocomplementary variants.^[95]

Agudo and Reetz investigated a cascade reaction with the ERED YqjM from *Bacillus subtilis* and a P450-BM3 triple mutant for the production of the enantiopure advanced pharmaceutical intermediate precursor methyl 3-oxocyclohexanecarboxylate. Three approaches were carried out with engineered *E. coli* cells, carrying an additional endogenous GDH for NADPH regeneration, to optimize the overall yield: (i) a mixed-cell approach by mixing recombinant cells harboring expression cassettes for either the P450-BM3 or the YqjM, (ii) use of *E. coli* cells harboring both enzyme encoding plasmids, and (iii) use of designer cells with genome-integrated YqjM and plasmid encoded P450-BM3. In the latter they exchanged the *nema* gene, coding for the *E. coli* native enoate reductase NemR, with the gene encoding for YqjM. Comparison of all three approaches in a 1.5 mM scale showed that using approach (i) a yield of 85% of the desired product was reached for both enantiomers in high purity (99% ee) after 75 min. In contrast, the other approaches gave a yield of approx. 50% after 60 min, but also in high purity. An upscaling of the first setup to 7.3 mM substrate concentration resulted in a yield of 69% for both enantiomers with an optical purity of 99% ee.^[96]

B II.3.4 Baeyer-Villiger monooxygenases (BVMOs)

The chemical Baeyer-Villiger-Oxidation (BVOx)^[97] is a major method for C-C bond cleavage by oxygen insertion and reliable for the preparation of esters or lactones from ketones. However, the chemical oxidants, peracids such as *meta*-chloroperbenzoic acid (*m*CPBA) or trifluoroperacetic acid, are toxic and generally result in racemic products.^[98] Baeyer-Villiger monooxygenases (BVMOs, Baeyer-Villigerases) are native in several bacteria and fungi for degradation of xenobiotics such as aromatic hydrocarbons. Trudgill and coworkers^[99] reported the isolation and characterization of cyclohexanone monooxygenase (CHMO) from *Acinetobacter* sp. NCIB 9871 (CHMO_{Acineto}) in 1976 from where on the importance of BVMOs has been rising steadily. The need for expertise and special equipment to handle microorganisms for synthesis and the pathogenicity of *Acinetobacter* sp. first triggered reluctance from organic chemists. But the potential of CHMO, a wide substrate scope alongside high enantioselectivity was shown^[100-101], and the "designer yeast", CHMO expressed in *Saccharomyces cerevisiae*,^[102] was a first step to general applicability. An engineered *E. coli* CHMO expression system eluded side-reactions occurring in baker's yeast and offered even easier handling^[103-104]. By now approx. 60 native BVMOs^[105] and numerous enzymes engineered by mutagenesis are well studied and also applied in industrial processes.^[106-110]

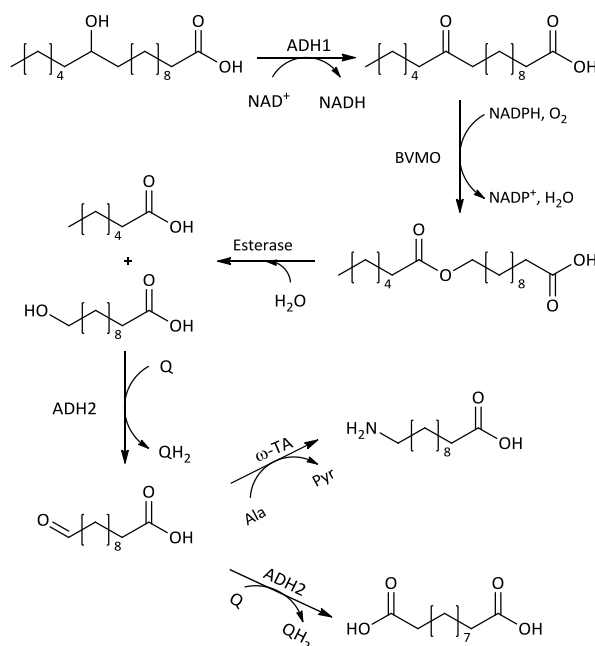
The catalytic mechanism of CHMO_{Acineto} was already investigated in 1982^[111], updated in 2001^[112] and is presented in Scheme B-14 (adapted from Kayser^[98]). BVMOs are flavin dependent monooxygenases and in the resting CHMO flavin adenine dinucleotide (FAD) is non-covalently bound and present in its oxidized form (E-FAD in Scheme B-14). Within the first step of the catalytic cycle it is reduced by the cofactor NADPH to the enzyme-NADP⁺ complex (E-FADH⁻-NADP⁺). Molecular oxygen then oxidizes this reduced complex to give 4a-flavin peroxide which acts as the equivalent of the peracid in chemical BVOx. The Criegee-intermediate is formed by a nucleophilic attack of the 4a-flavin peroxy anion on the carbonyl group of the ketone. Rearrangement leads to lactone and flavin hydroxide from where water is eliminated before lactone and NADP⁺ are released. NADP⁺ has to be reduced to NADPH before reentering the catalytic cycle which calls for an efficient cofactor recycling system as NADPH is very expensive.^[98]



Scheme B-14. Mechanism of CHMO. (E=enzyme) ^[98]

In BVOx the Criegee-intermediate is rearranged through the migration of the alkyl group antiperiplanar to the O–O bond for stereoelectronic reasons. When the conformation of the O–O bond is not regulated, the more electron-rich alkyl group will migrate preferentially. However, the 4a-flavin peroxide is installed in the chiral environment of the active site of a BVMO that may allow only a single conformation of the Criegee intermediate. When the conformation of the intermediate imposes placement of the less substituted group antiperiplanar to the O–O bond, it is that group which will migrate regardless of its nucleophilicity. The other possibility is that one enantiomer can assume the configuration where the more substituted group is antiperiplanar and migrates which will lead to the normal lactone. The other enantiomer would be forced into a configuration that leads to the migration of the less substituted carbon, rendering the abnormal product (the terms “normal” and “abnormal” lactone usually refer to the expected product of the chemical oxidation, which is essentially always governed by the nucleophilicity of the migrating carbon center). ^[98]

Additional to their long standing application in biocatalysis BVMOs have already been employed in cascade reactions. The group of Park used long-chain fatty acids as starting material for whole cell biotransformations towards α,ω -dicarboxylic acids and ω -aminocarboxylic acids. They first combined an ADH, a BVMO and an esterase ^[113] and later extended the established cascade towards the formation of ω -aminocarboxylic acids by applying an additional ADH (AlkJ from *P. putida* GPo1) and an ω -TA from *Silicibacter pomeroyi* (Scheme B-15). ^[114]



Scheme B-15. *In vivo* cascade towards the formation of ω -aminocarboxylic acids by Song *et al.*.

In general, 5 mM of saturated or unsaturated fatty acids were used and the corresponding products were obtained in 21 – 51% isolated yield. For two of the substrates used (ricinoleic and lesquerolic acid) a reduction of the *cis*-double bond was observed probably caused by the *E. coli* background. But in this case, it was not necessary to retain the double bond for the production of polyester precursors, although unsaturated building blocks also have certain interesting features. ^[115]

The group of Li encountered the same problem in their mixed-culture approach for the production of enantiopure δ -lactones using a non-engineered wild-type *Acinetobacter* sp. RS1 for unspecific reduction of a C=C bond, followed sequentially by Baeyer-Villiger oxidation carried out by *E. coli* cells harboring CHMO_{Acineto} and GDH from *Bacillus subtilis* for cofactor recycling. ^[116] Subsequently, hydrolysis of the (*S*)-lactone by *Acinetobacter* cells led to enantiopure (*R*)-lactone. The cascade had to be carried out in a sequential mode due to *E. coli* background reaction on the C=C bond. Cyclopentanone derivatives were used in a concentration of 6 mM as substrates and were converted with an isolated yield of 41 – 56% and an optical purity of 98% ee.

This chapter was mainly based on recently published reviews by Muschiol *et al.* ^[35] and Bayer *et al.* ^[16].

B III Scope of this thesis

This thesis describes the development of artificial metabolic pathways. For this, simple model systems were used to determine properties of enzyme cascades that could not develop in an evolutionary context, but were created *de novo*. In order to study as many parameters as possible in the model systems, cofactor-dependent redox biotransformations were explicitly chosen to be combined in the host organism *E. coli*. A particular aim of this study was to gain a deeper understanding of the interplay between synthetically active (redox)enzymes and the cells redox metabolism.

Following the design of the cascade reaction suitable biocatalysts with overlapping substrate profiles were chosen. As not all desired enzymes were available from the outset, a three-step cascade starting from different unsaturated allylic alcohols was implemented for a first proof of concept. The broad substrate scope of this synthetic cascade allowed focusing on the most important reaction types in chiral catalysis: kinetic resolution, desymmetrization and regiodivergent transformation. This should display the versatility of the system while gaining access to attractive lactone products.

Combination of the three biocatalysts and the required cofactors within *in vitro* experiments helped us to verify the compatibility of the single reaction steps. The implementation of this enzymatic toolbox in the well-studied microbial host *E. coli* BL21(DE3) allowed for a simple whole-cell reaction set-up for *in vivo* proof-of-concept. Bottlenecks of the multistep reaction were identified and measures were taken to circumvent these problems. Approaches of metabolic engineering on the host organism included native gene knockouts and the possibility of integrating heterologous genes in the *E. coli* genome. During these investigations native enzymes with enoate reductase activities were cloned from *E. coli* to be available for further use in common over-expression systems.

For the hydroxylation of cyclic alkenes, *R*-(+)-limonene was investigated as model substrate and different systems were considered. *Cellulosimicrobium cellulans* EB-8-4, a bacterial wildtype strain, reported to show hydroxylation activity, was investigated. Another approach, using a hydroxylating enzyme in *Pseudomonas putida* S12, led to promising results.

Finally, the direct conversion of *R*-(+)-limonene to carvolactone in a mixed-culture approach combining *E. coli* BL21(DE3) and *P. putida* S12 resting cells was aimed for. Additionally, the use of orange peel, a limonene-rich waste product, as starting material in a biocatalytic cascade reaction was studied. To increase *R*-(+)-limonene availability from orange peel different concepts, including the addition of ionic liquids as extraction enhancers, were investigated.

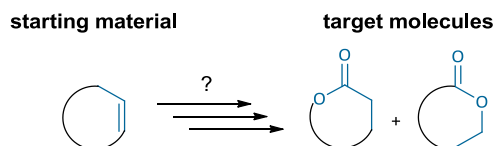
This thesis was conducted in the course of a joint project with the group of Prof. Uwe T. Bornscheuer at the Ernst-Moritz-Arndt-University of Greifswald (Germany). In-house collaboration with the group of Prof. Peter Gärtner was added for parts of the project.

C Results and discussion

This chapter comprises the approaches towards the realization of a non-native biocatalytic multistep reaction in *E. coli*. The first part describes the design of the cascade, and the choice of suitable biocatalysts for its establishment. The implementation of an enzymatic toolbox showed the versatility of the system *in vitro* and bottlenecks were investigated. The cascade was then established as *in vivo* synthetic mini-pathway in the microbial host organism *E. coli*. Finally, the potential of the title concept in an approach to produce carvolactone from natural limonene, which is directly extracted from orange peel waste, is demonstrated.

C I Enzymatic redox cascades by a retrosynthetic approach

The presented enzymatic redox cascade was designed on the basis of the retrosynthetic approach, where a target molecule is broken down to simple starting materials. This disconnection approach^[117] is well known in synthetic organic synthesis, and was recently also applied to biocatalytic systems^[118]. Simple cyclic alkenes were chosen to be functionalized to chiral lactones over several consecutive reaction steps. For these combined biotransformations, cofactor-dependent redox enzymes were explicitly chosen in order to gain a deeper understanding of the interaction of the biocatalysts. For the design of the cascade the structure of the starting materials and target molecules was generalized to cyclic compounds, only distinguished by the structural characteristics, marked in blue in Scheme C-1.



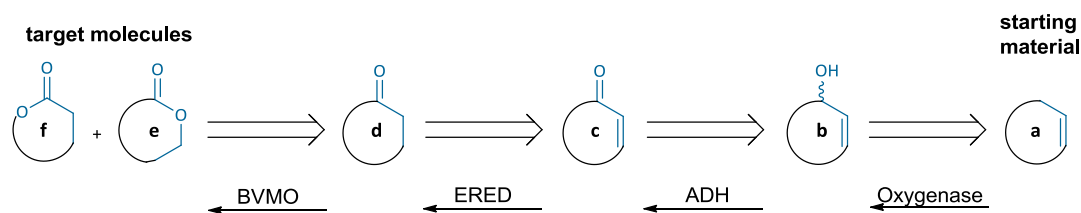
Scheme C-1. Generalized starting material and products for the design of the cascade.

Lactones are ubiquitous among fragrance compounds, and are attractive building blocks for the synthesis of bioactive or natural products^[119]. They can also serve as monomers for polymer production and therefore emerged as valuable target molecules. Their biocatalytic preparation was recently reported using lipase-catalyzed lactonization of hydroxy esters^[120], alcohol dehydrogenase (ADH) catalyzed reduction of a keto ester^[121], or oxidative lactonization of diols by an ADH^[122]. However, the most widely used biocatalytic approach to obtain a lactone is the transformation of a cyclic ketone by a Baeyer-Villiger monooxygenase (BVMO). To produce saturated cyclic ketones as substrates for the BVMOs, the use of alkanes as starting materials would require introduction of oxygen to the molecule. Although enzymatic alkane hydroxylation offers a possibility for oxygenation of an unactivated C-H bond, these enzymes are often highly specialized (e.g. steroid hydroxylation^[75]) or the particular transformation is only feasible after several rounds of mutagenesis^[123]. Conversely, allylic C-H bonds have a higher intrinsic reactivity towards oxygenation than regular sp^3 -C-H bonds. Therefore cyclic alkenes were chosen as starting materials for the cascade reaction. Considering also the availability of starting material, readily available natural products from the class of terpenes present interesting cyclic alkenes.

The next task was the search for suitable biocatalysts performing the functional group transformations that were required to convert the starting material to the target molecules. The first retrosynthetic step from the lactones (**e**, **f**) led back to a saturated cyclic ketone (**d**). As the starting material (**a**) contains a double bond it should be retrosynthetically derived from an unsaturated cyclic compound (**c**). Enoate reductases (EREDs) are very well studied for the reduction of activated C-C double bonds (C=C). Hence the next step was the reduction of an α,β -unsaturated ketone (**c**) by an ERED to give the saturated ketone (**d**). The availability of two ketone species, saturated (**d**) and unsaturated (**c**) would not lead to product mixtures, as BVMOs generally do not accept unsaturated substrates. Only recently the group of Alphand identified two new BVMOs that showed activity for unsaturated substrates, opening the possibility to gain access to ene-lactones.^[124]

An α,β -unsaturated ketone (**c**) could be obtained via oxidation of an allylic secondary alcohol (**b**) with alcohol oxidases (AOX)^[125], or ADHs: the latter are mainly appreciated for their ability to stereoselectively reduce ketones to the corresponding alcohols. Nevertheless, ADHs can also catalyze the oxidation of alcohols to ketones, and were therefore preferred, as byproduct of the AOX reaction is H_2O_2 , which would not be favorable in a redox-enzyme system.

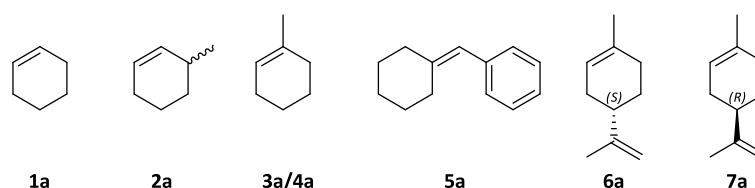
Finally, the last step was the attachment of the alcohol moiety (**b**) to a cyclic alkene (**a**) which could be achieved via hydroxylation with an oxygenase. The envisaged combination of an oxygenase, an ADH, an ERED and a BVMO, which are naturally not connected, presents an artificial mini-pathway. The retrosynthetic steps and the resulting choice of enzymes are depicted in Scheme C-2.



Scheme C-2. Final biocatalytic cascade designed with help of the retrosynthetic approach.

C I.1 Substrate scope

After the general design the next goal was the determination of the specific substrate scope of the cascade reaction. Starting from a pool of different cyclic alkenes the versatility of the approach should be shown. In this conceptual study the general applicability of the interacting redox enzymes should be exemplified in the conversion of different intermediates. As the simplest substrates cyclohexene (**1a**) and two methyl derivatives thereof, 3-methylcyclohex-1-ene (**2a**) and 1-methylcyclohex-1-ene (**3a/4a**) were chosen. (Cyclohexylidenemethyl)benzene (**5a**) presents a different motif, as it contains an exocyclic double bond. Structurally more complex cyclic alkenes are represented with the two natural monoterpenes *S*-(-)- (**6a**) and *R*-(+)-limonene (**7a**). All substrates are commercially available and are shown in Scheme C-3.

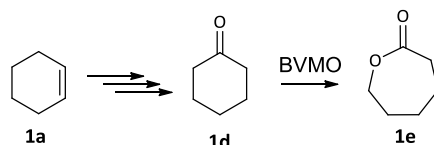


Scheme C-3. Pool of starting material.

It was envisaged to gain access to a broad variety of lactones while also displaying the selectivity potential of BVMOs. By choice of the starting material as described above, four different reaction types of BVMOs, which will be discussed in the following, were addressed.

C I.1.1 BVMO reaction types

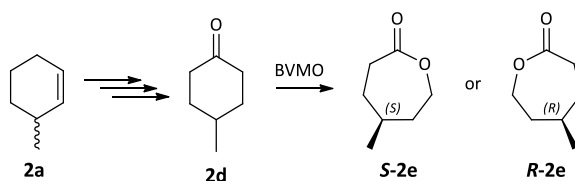
Starting from cyclohexene (**1a**) the intermediate cyclohexanone (**1d**) could be accessed. Through a simple achiral transformation by a BVMO **1d** could be converted to ϵ -caprolactone (**1e**) which is shown in Scheme C-4.



Scheme C-4. Achiral transformation via a BVMO.

C I.1.1.1 Desymmetrization

The introduction of chirality by desymmetrization of prochiral (symmetric) ketones is of great interest in chiral synthesis, as 100% theoretical yield of enantiopure material could be achieved. The ability of BVMOs to catalyze such reactions has been studied extensively^[100]. Starting the cascade with 3-methylcyclohex-1-ene (**2a**) the intermediate 4-methylcyclohexanone (**2d**) - a good model substrate for BVMO-catalyzed desymmetrization reactions - could be obtained (Scheme C-5).

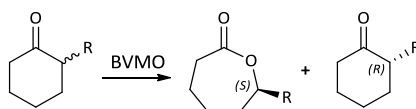


Scheme C-5. Desymmetrization of intermediate **2d** via BVMO reaction.

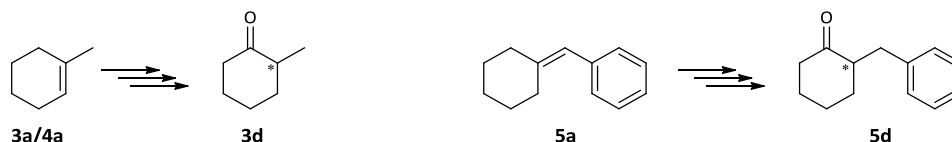
Regarding the desymmetrization of **2d** by different BVMOs, previous studies in our group found a significant clustering into two groups: while the majority of tested BVMOs belonging to the “CHMO type” gave *S*-(-)-5-methylcaprolactone (**S-2e**) in excellent enantiomeric excess (ee), CPMO_{Coma} (from *Comamonas*) and CHMO_{Brevi2} (from *Brevibacterium*) (“CPMO type”) gave the antipodal product **R-2e**.^[106] Both target enantiomers are thus available by choice of the particular biocatalyst.

C I.1.1.2 Kinetic resolution

Enantiopure lactones can be obtained from racemic ketones via kinetic resolution catalyzed by a BVMO. In kinetic resolution type reactions one enantiomer fits better into the active site of the enzyme and will therefore be converted at a higher rate. In an ideal case the ratio of reaction rates is so extreme that one enantiomer would be converted quickly and the other one not transformed at all, leading to a theoretical conversion of 50% with optically pure substrate and product being accumulated. In reality this reaction velocity ratio is not infinite, but measurable, resulting in a slowdown of reaction rate at 50% but not a complete standstill. Therefore the optical purity, given in enantiomeric excess (ee), of both substrate (ee_s) and product (ee_p) becomes a function of conversion.^[75] The kinetic resolution BVMO reaction is illustrated on the example of a 2-substituted cyclohexanone in Scheme C-6.

Scheme C-6. Kinetic resolution catalyzed by a BVMO (adapted from Stewart *et al.* [126]).

With two of the alkene substrates 2-substituted cyclohexanone derivatives would be formed as intermediates in the cascade reaction. 1-Methylcyclohex-1-ene (**3a/4a**) gives 2-methylcyclohexanone (**3d**) upon ERED-mediated reduction, and (cyclohexylidene)methyl)benzene (**5a**) gives 2-benzylcyclohexanone (**5d**) as intermediate (Scheme C-7).



Scheme C-7. Formation of two 2-substituted cyclohexanone derivatives through the cascade approach.

The transformation to lactones by different BVMOs was reported for both intermediates **3d** and **5d**, and is summarized in Table C-1.

Table C-1. Transformations of substrates **3d** and **5d** by BVMOs reported in the literature.

Entry	Substrate	BVMO	Conv. [%]	ee _s ^a [%]	ee _p ^b [%]	Lactone product	E ^c	Literature
1	 3d	CHMO _{Acineto}	51	60 (+)	63 (-)	 S-3e	7	Snajdrova PhD thesis [127], configuration in accordance to Kyte <i>et al.</i> [119]
2		CPMO _{Coma}	68	99 (-)	48 (+)	 R-3e	13	Snajdrova [127]
3		CDMO	58	99 (+)	92 (-)	 S-3e	125	Fink <i>et al.</i> [128] configuration in accordance to Kyte <i>et al.</i> [119]
4	 5d	CHMO _{Acineto}	44	78 (-)	99 (-)	 S-5e	200	Snajdrova [127]
5		CDMO	47	91 (-)	100 (-)	 R-5e	200	Fink <i>et al.</i> [128]

^a ee_s: enantiomeric excess of starting material; ^b ee_p: enantiomeric excess of product; ^c E = $\frac{\ln(1-ee_s) - \ln(1+\frac{ee_p}{ee_s})}{\ln(1+ee_s) - \ln(1+\frac{ee_p}{ee_s})}$

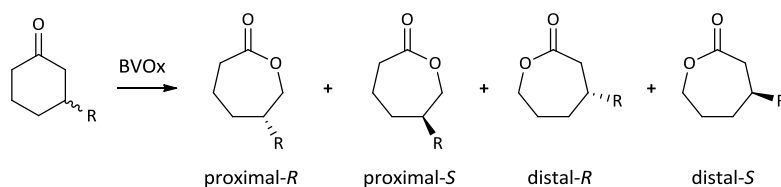
Table C-1 shows that both substrates **3d** and **5d** could be converted to both lactone enantiomers using different BVMOs. In the case of 2-methylcyclohexanone (**3d**) CHMO_{Acineto} preferentially produces (*S*)-7-methylcaprolactone (**S-3e**) (Table C-1, entry 1), whereas CPMO_{Coma} gives an excess of **R-3e** (Table C-1, entry 2). However, both enzymes are only poorly enantioselective (low E values). A better kinetic resolution

could be achieved with CDMO from *Rhodococcus* SC1 with an enantioference for (*S*)-7-methylcaprolactone (Table C-1, entry 3).

2-Benzylcyclohexanone (**5d**) could be converted to the enantiomeric lactones in a highly selective manner by either applying CHMO_{Acineto} and gaining access to the (*S*)-7-benzylcaprolactone (**S-5e**) or using CDMO, which selectively produced (*R*)-7-benzylcaprolactone (**R-5e**).

C I.1.1.3 Regiodivergent transformations

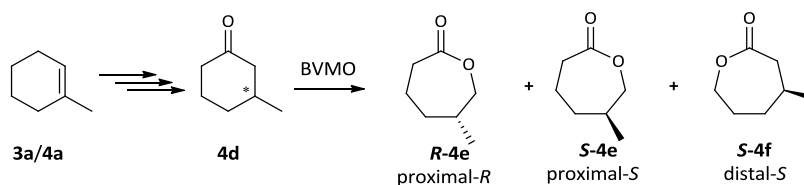
Regiodivergent biotransformations are a particularly valuable feature of BVMOs upon governing stereoelectronic and nucleophilic migration behavior: this type of conversion enables access to enantiopure regioisomeric lactones from a racemic starting material. Chemical BVOx of 3-substituted cyclohexanones would afford two enantiomeric pairs of regioisomeric lactones as there is hardly any electronic preference for migration of one of the two C-C bonds neighboring the carbonyl group.^[129] Scheme C-8 shows all possible products.



Scheme C-8. Transformation of 3-substituted cyclohexanones to different lactone products.

For enzymatic BVMO oxidations of 3-substituted cyclohexanones there are four possible reaction outcomes: i) high enantio- and regioselectivity, ii) high enantioselectivity but poor regioselectivity, iii) poor enantioselectivity with high regioselectivity, and iv) low enantio- and regioselectivity. While the first case is clearly the most desirable, cases two and three also have synthetic value and can be achieved by using different BVMOs.^[119]

Initiating the cascade reaction with 1-methylcyclohex-1-ene (**3a/4a**) the intermediate 3-methylcyclohexanone (**4d**) (Scheme C-9) could be produced; its conversion by BVMOs was already studied. CHMO_{Acineto} cleanly oxidized racemic **4d** to almost enantiopure regioisomers: (*R*)-6-methylcaprolactone (**R-4e**) and (*S*)-4-methylcaprolactone (**S-4f**).^[129] An interesting difference in regioselectivity was discovered between two BVMOs from *Brevibacterium* sp.: Whereas CHMO_{Brevi1} exhibited moderate enantioselectivity and no regioselectivity, giving proximal and distal product preferably in (*S*)-configuration (**S-4e** and **S-4f**), CHMO_{Brevi2} produced only the proximal enantiomers (**R-4e** and **S-4e**) in high regioselectivity.^[119] All products obtained from substrate **4d** by BVMO catalysis are shown in Scheme C-9.



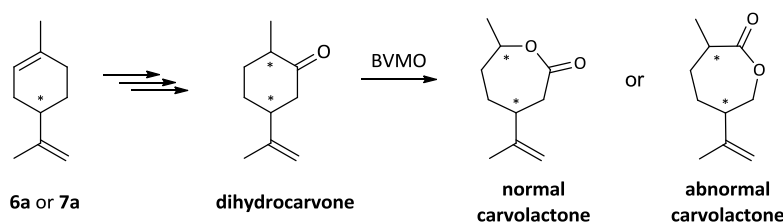
Scheme C-9. Regiodivergent biotransformation of 3-methylcyclohexanone (**4d**) by BVMOs.

By conversion of enantiopure ketone by a BVMO of choice one could obtain the desired enantiopure lactone as summarized in Table C-2.

Table C-2. Conversion of racemic or enantiopure 4d by two BVMOs.

BVMO	rac-4d	4d-R	4d-S	Literature
CHMO _{Acineto}	R-4e + S-4f	R-4e	S-4f	Stewart <i>et al.</i> [129]
CHMO _{Brevi2}	R-4e + S-4e	R-4e	S-4e	Kyte <i>et al.</i> [119]

Structurally more complex model substrates for regiodivergent transformations, dihydrocarvones could be obtained as intermediates from *S*-(-) (**6a**) or *R*-(+)-limonene (**7a**) as starting material in the model cascade reaction. The products of the BVMO reaction of dihydrocarvones are called carvolactones. Depending on the oxygen insertion, they are referred to as normal (migration of the more nucleophilic residue) or abnormal lactone (migration of the unsubstituted carbon under stereoelectronic control; Scheme C-10).

Scheme C-10. Obtaining dihydrocarvones from *R*-(+)-limonene and their conversion to carvolactones.

The conversion of all four dihydrocarvone isomers by different BVMOs was investigated by Cernuchova and Mihovilovic, and the results most relevant for this work are shown in Table C-3. [130]

Table C-3. Conversion of dihydrocarvones by BVMOs (results from Cernuchova *et al.* [130])

Entry	BVMO	<i>cis</i> -6d (+)- <i>cis</i> - or (2 <i>S</i> ,5 <i>R</i>)- dihydrocarvone	<i>trans</i> -6d (+)- <i>trans</i> - or (2 <i>R</i> ,5 <i>R</i>)- dihydrocarvone	<i>cis</i> -7d (-)- <i>cis</i> - (2 <i>R</i> ,5 <i>S</i>)- dihydrocarvone	<i>trans</i> -7d (-)- <i>trans</i> - or (2 <i>S</i> ,5 <i>S</i>)- dihydrocarvone
1	CHMO _{Acineto} [normal:abnormal]	64:36	0:100	100:0	100:0
2	CHMO _{Brevi1} [normal:abnormal]	100:0	55:45	100:0	100:0
3	CPMO _{Coma} [normal:abnormal]	37:63	0:100	0:100	0:100

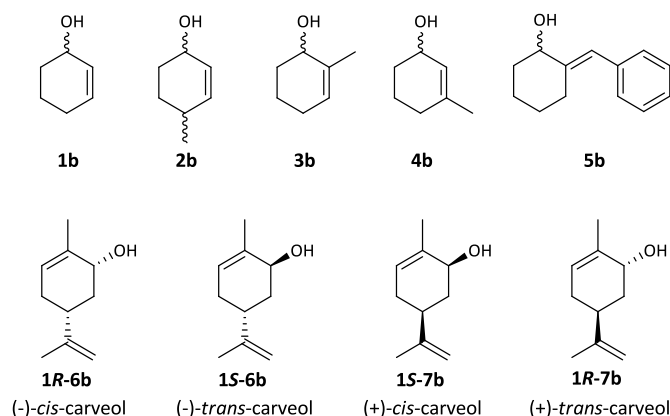
Table C-3 shows that both normal and abnormal carvolactones could be obtained from every dihydrocarvone isomer by choice of the appropriate BVMO. There was only a minimal regiopreference for the normal lactone from (2*R*,5*R*)-dihydrocarvone (**trans**-6d) exhibited by CHMO_{Brevi1}, whereas the normal lactones from **cis**-6d, **cis**-7d and **trans**-7d were derived in excellent selectivity. The abnormal lactone from **cis**-6d could only be obtained in a mixture with the normal lactone. Preference for the abnormal carvolactone from **cis**-6d was only shown by CPMO_{Coma} (Table C-3, entry 3) which converted the other dihydrocarvones to the abnormal lactones in highest regioselectivity. The study by Cernuchova *et al.* presented a good basis for the intention to convert the dihydrocarvone intermediates from the model cascade reaction with BVMOs to gain access to carvolactones.

C I.2 The enzymatic toolbox

After settling on a cyclic alkene substrate scope to address interesting BVMO reactions in the cascade reactions the next step was to identify specific biocatalysts for all the steps with broad overlapping substrate scopes. The first step of the designed cascade, the hydroxylation of cyclic alkenes, quickly emerged as a challenging task. The search for a suitable enzyme to tackle this hydroxylation reaction was mainly investigated by the collaborating group of Prof. Bornscheuer at the University of Greifswald. All further approaches to the realization of the alkene hydroxylation will be discussed in chapter C IV.

C I.2.1 Three-step cascade and its substrate scope

As it was not trivial to find a suitable oxygenase for the first step in time, a three-step cascade was implemented first to demonstrate the concept. The first intermediates in the designed cascade reaction after the hydroxylation of cyclic alkenes (**a**) are unsaturated alcohols (**b**), which should serve as starting material for this three-step cascade and are shown in Scheme C-11.

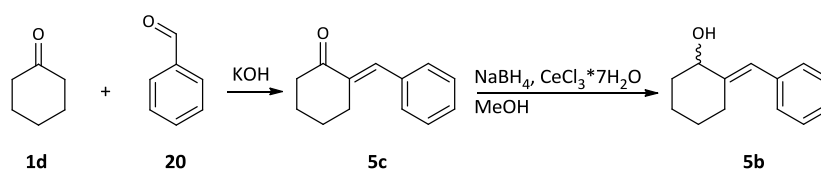


Scheme C-11. Substrate scope for the three-step cascade.

C I.2.1.1 Substrate accessibility

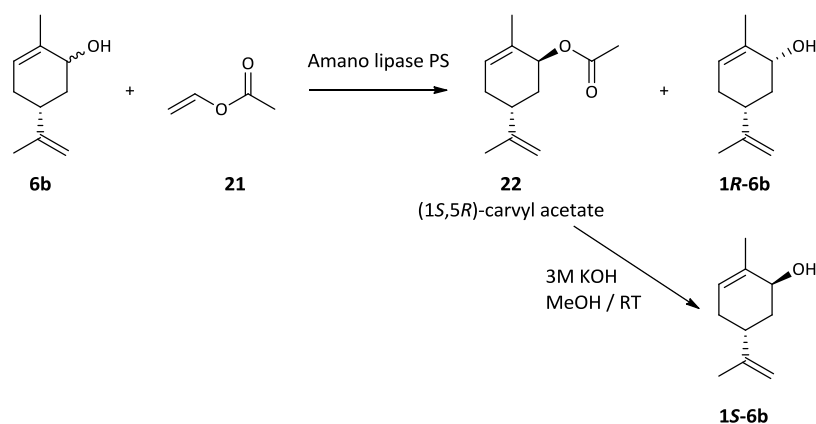
Cyclohex-2-en-1-ol (**1b**) and 3-methylcyclohex-2-en-1-ol (**4b**) were commercially available, whereas 4-methylcyclohex-2-en-1-ol (**2b**) and 2-methylcyclohex-2-en-1-ol (**3b**) had to be synthesized in-house. These syntheses, conducted in cooperation and by support of Patricia Schaaf, are described in detail in Oberleitner *et al.*^[131]. Briefly, commercially available 4-methylcyclohexanone (**2d**) was brominated to give 2-bromo-4-methylcyclohexanone (**16**), which was then used to produce 4-methylcyclohex-2-enone (**2c**) via elimination. 2-Methylcyclohex-2-enone (**3c**) was obtained via LiAlH_4 reduction of 3-isobutoxy-2-methylcyclohex-2-enone (**19**), which was synthesized via condensation of 2-methyl-1,3-dione (**17**) and isobutanol (**18**). Compounds **2c** and **3c** were both subjected to Luche reduction conditions to give 4-methylcyclohex-2-en-1-ol (**2b**), respectively 2-methylcyclohex-2-en-1-ol (**3b**).

The exocyclic unsaturated alcohol 2-benzylidenecyclohexanol (**5b**) was synthesized via Knoevenagel condensation yielding 2-benzylidenecyclohexanone (**5c**), therefore also making this intermediate available as reference compound. It was then subjected to Luche reduction to give substrate **5b** (Scheme C-12).



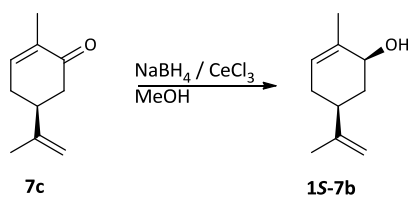
Scheme C-12. Synthesis workflow for **5b** and **5c**.

The carveols were commercially available only as isomeric mixtures of (-)-carveol (**6b**) and (+)-carveol (**7b**). Selective esterification of the mixture **6b** by Amano lipase yielded in (1*S*,5*R*)-carvyl acetate and **1*R*-6b**. Basic hydrolysis of (1*S*,5*R*)-carvyl acetate then gave **1*S*-6b** and the synthetic workflow is summarized in Scheme C-13 (conducted in-house by support of Ramana Pydi).



Scheme C-13. Preparation of enantiopure **1*R*-6b** and **1*S*-6b**.

Enantiopure **1*S*-7b** was synthesized via Luche reduction of *S*-(+)-carvone (**7c**) in cooperation with Ramana Pydi as shown in Scheme C-14.



Scheme C-14. Preparation of enantiopure **1*S*-7b**.

The synthesis of (1*R*,5*S*)-carveol (**1*R*-7b**) proved to be overly challenging for the scope of this project (conducted by Ramana Pydi). It was therefore omitted from further investigations, leaving five unsaturated alcohol derivatives (**1b** - **5b**) and three carveol isomers (**1*R*-6b**, **1*S*-6b** and **1*S*-7b**), as starting material for the three-step model cascade reaction.

C I.2.2 ADHs

After selecting the substrate scope for the three-step cascade, an unselective alcohol dehydrogenase to convert all unsaturated cyclic alcohols (Scheme C-11) should be identified. Preferably, this ADH would not be selective for any enantiomer in the starting material. Three ADHs were investigated in more detail by Maria Kadow in our partner group at the University of Greifswald; her results are listed in Table C-4. She found that LK-ADH from *Lactobacillus kefir*^[132] was active on our simplest substrate **1b** and converted an isomeric mixture of carveol to nearly 50%, which indicated a strong stereopreference of this enzyme (Table C-4, entry 1).

RR-ADH from *Rhodococcus ruber*^[133] was able to oxidize **1b** and also showed activity for the carveol mix (entry 2). The third investigated ADH from *Pseudomonas fluorescens* (PFDH) showed only minor conversion of the tested substrates and therefore proved unsuitable for our purpose. The other two enzymes were chosen for further substrate profiling.

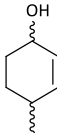
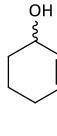
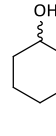
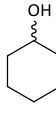
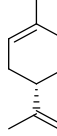
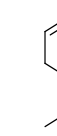

Table C-4. Oxidation of two unsaturated cyclic alcohols by different ADHs.

Entry	Enzyme	[%] ^a	[%] ^a
1	LK-ADH	60	49
2	RR-ADH	95	21
3	PFDH	12	3

Results by Maria Kadow. ^a Conversion determined by product formation after 20 h *in vitro* reaction

In preliminary tests LK-ADH and RR-ADH were assayed for their activity towards the other substrates of the unsaturated alcohol pool. Reactions were performed with CFE of the enzymes expressed in *E. coli* BL21(DE3) and the results are summarized in Table C-5.

Table C-5. Activity of ADHs towards alcohols measured by conversion of starting material.

Entry	Enzyme							
		2b	3b	4b	5b	1R-6b	1S-6b	1S-7b
1	LK-ADH	80	44	88	25	0	100	100
2	RR-ADH	47	19	n.a.	47	99	0	0

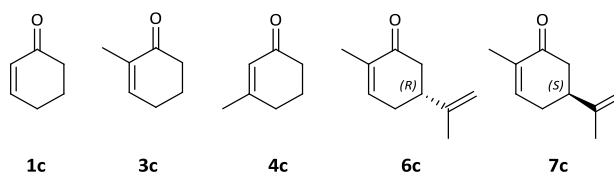
Results in % conversion of unsaturated alcohol. n.a.: not tested

Table C-5 shows that all unsaturated alcohols were accepted by at least one of the ADHs. 4-Methylcyclohex-2-en-1-ol (**2b**) and **4b** were well accepted by LK-ADH with values for conversion of up to 88%. Substrate **2b** and the exocyclic unsaturated alcohol **5b** were only converted to 47% by RR-ADH, which indicates a high stereoselectivity of this enzyme. The already expected complementary stereopreference of LK-ADH and RR-ADH for the carveol isomers could be proven. RR-ADH was only able to convert (1*R*,5*R*)-carveol (**1R-6b**) and showed no activity towards the 1*S*-isomers, and LK-ADH showed full consumption of **1S-6b** and **1S-7b** and no activity for **1R-6b**. 2-Methylcyclohex-2-en-1-ol (**3b**) - methyl substituted in 2-position just as carveol – was only converted to 44%, also suggesting stereopreference of LK-ADH for one enantiomer of this substrate.

Initially, the aim was to find an unselective ADH to convert all unsaturated alcohols, but these results showed that all tested ADHs were at least fairly stereoselective for some of the substrates. Nevertheless, activity for all unsaturated alcohols was achieved with these two enzymes, and their potential should be further investigated in the cascade reactions.

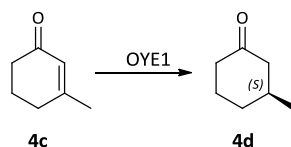
C 1.2.3 EREDs

To investigate a new ERED for the cascade reaction, Christin Peters at Greifswald cloned and characterized the enzyme XenB^[134] from *Pseudomonas putida*^[131]. In her PhD thesis she tested XenB for its activity towards some unsaturated cyclic ketones, the products of the preceding ADH reaction, which are shown in Scheme C-15^[135].



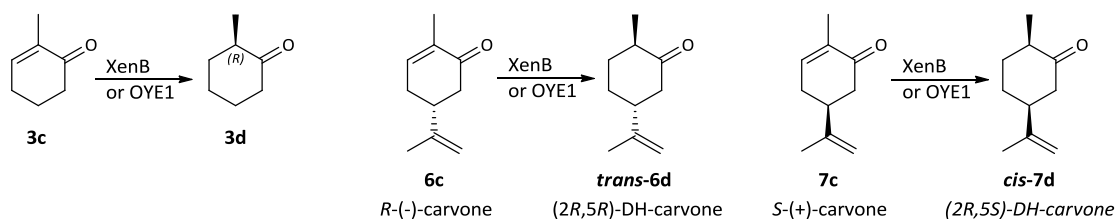
Scheme C-15. Substrates for ERED testing by Christin Peters.

XenB showed good activity for *R*-(-)-carvone (**6c**) and *S*-(+)-carvone (**7c**) and all tested cyclohexenone derivatives except 3-methyl-2-cyclohexen-1-one (**4c**). To also address this intermediate and realize the enzymatic toolbox, the very well-known OYE1 from *Saccharomyces carlsbergensis*, which was reported to stereoselectively reduce **4c** to (*S*)-3-methylcyclohexanone (**4d**) (Scheme C-16)^[94], should be used.



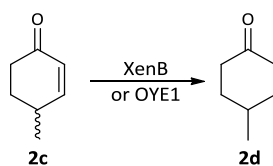
Scheme C-16. Reduction of **4c** catalyzed by OYE1.

Christin Peters reported high stereoselectivity of XenB towards 2-methyl substituted substrates - **3c**, *R*-(-)-carvone (**6c**), and *S*-(+)-carvone (**7c**) - as only (*R*)-products were obtained. The same selectivity was reported for OYE1 with substrate **3c**^[94] as well as with the carvones (**6c**, **7c**)^[95]. Scheme C-17 shows the stereoselective reductions of XenB and OYE1.



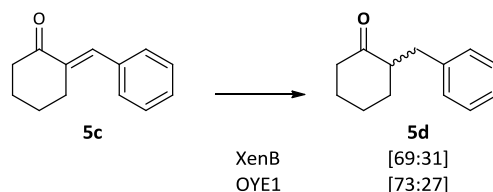
Scheme C-17. Stereoselectivity of XenB and OYE1.

Activity of XenB and OYE1 towards cascade intermediates 4-methyl-2-cyclohexen-1-one (**2c**) and 2-benzylidenecyclohexanone (**5c**) was tested in-house. Racemic **2c** was reduced to 4-methylcyclohexanone (**2d**, Scheme C-18) by both OYE1 and XenB: the former catalyst gave a marginally higher reaction rate, but both reached 99% conversion after 5h.



Scheme C-18. Reduction of **2c** by two EREDs.

The exocyclic unsaturated ketone **5c** was converted by both EREDs to a mixture of enantiomers of 2-benzylcyclohexanone (**5d**). Both EREDs gave 96% **5d** in a very similar isomeric ratio after 24 h (Scheme C-19).



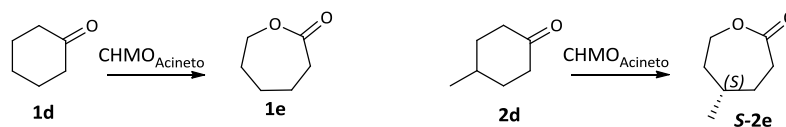
Scheme C-19. Reduction of **5c** to isomers of **5d**.

By using two different EREDs, XenB and OYE1, the reduction of all seven unsaturated ketone intermediates of the designed cascade could be addressed.

C I.2.4 BVMO

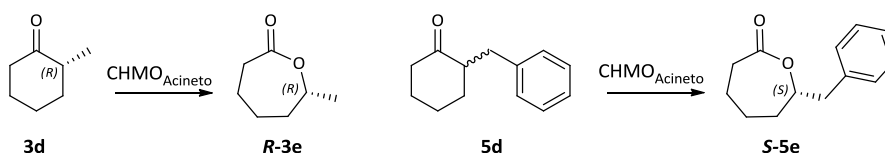
After identifying the last intermediates of the cascade reaction, the saturated ketones, the next goal was to select a BVMO for their conversion to lactones. From a large in-house library of BVMOs the well characterized CHMO_{Acineto} from *Acinetobacter* sp.^[136] was chosen. This promiscuous BVMO converted all saturated ketones that were produced from the preceding ERED, while accessing mostly optically pure lactones.

The name cyclohexanone monooxygenase already suggests that cyclohexanone (**1d**) is the natural substrate of CHMO_{Acineto} which was already reported in 1976 by Trudgill and coworkers.^[99] As already discussed in chapter C I.1.1.1 prochiral intermediate **2d** can be selectively converted to *S*-(-)-5-methylcaprolactone (**S-2e**) by CHMO_{Acineto}^[100]. Both biotransformations are shown in Scheme C-20.



Scheme C-20. Achiral transformation (**1d**) and desymmetrization (**2d**) by CHMO_{Acineto}.

For racemic 2-substituted cyclohexanones kinetic resolution is the common course of reaction as discussed in chapter C I.1.1.2. Here, optically pure 2-methylcyclohexanone intermediate (**3d**) was produced through the selective ERED reduction by either XenB or OYE1 (C I.2.3). As CHMO_{Acineto} was able to convert racemic 2-methylcyclohexanone, full conversion of **3d** to **R-3e** could be achieved. Snajdrova reported that CHMO_{Acineto} exhibited high enantioselectivity for (*S*)-2-benzylcyclohexanone as only (*S*)-7-benzylcaprolactone (**S-5e**) was produced from racemic starting material **5d**.^[127] Reported reactions for the 2-substituted cyclohexanones are shown in Scheme C-21.



Scheme C-21. Conversion of 2-substituted cyclohexanones by CHMO_{Acineto}.

An enantiomeric mixture of **5d** (**5d-1:5d-2** = 70:30, 0) was obtained as product of the preceding unselective ERED reduction where the absolute configuration of the isomers was not characterized. In a single biotransformation of racemic **5d** by CHMO_{Acineto}, a preference for **5d-2**, suggesting this enantiomer to be (*S*)-2-benzylcyclohexanone^[137], was observed. After 30 min reaction time, at 46% conversion, an ee_s of 67%

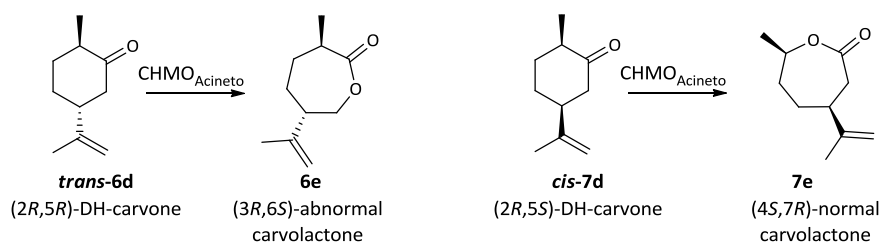
and an ee_p of 92% were detected. These results sum up to an E value of 48 which further decreased with prolonged reaction times. Unfortunately, this result is not in accordance with the literature where an E of greater 200 was reported.^[127]

In case of racemic 3-methylcyclohexanone $\text{CHMO}_{\text{Acineto}}$ would give a mixture of regiodivergent lactones as discussed in chapter C 1.1.1.3. As the intermediate after the ERED reaction was optically pure (S)-3-methylcyclohexanone (**4d**) $\text{CHMO}_{\text{Acineto}}$ would only produce the distal lactone by stereoelectronic control **S-4f** (Scheme C-22).



Scheme C-22. Regioselective conversion of optically pure **4d** by $\text{CHMO}_{\text{Acineto}}$.

With XenB and OYE1 two of the four possible dihydrocarvone isomers as intermediates could be accessed. $\text{CHMO}_{\text{Acineto}}$ exhibits interesting regioselectivity towards dihydrocarvones, as reported by Cernuchova^[130], and already discussed in chapter C 1.1.1.3. With $\text{CHMO}_{\text{Acineto}}$ the abnormal carvolactone could be obtained from **trans-6d** and the normal carvolactone from **cis-7d** (Scheme C-23).



Scheme C-23. Regioselective conversion of dihydrocarvones by $\text{CHMO}_{\text{Acineto}}$.

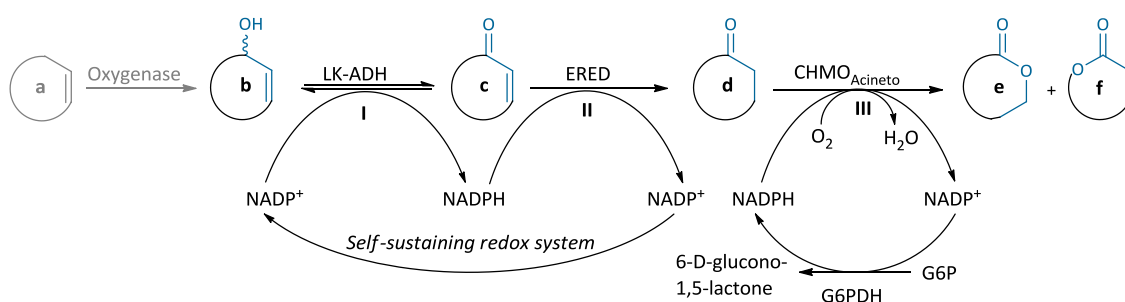
C 1.3 Summary

Eight different cyclic substrates were selected to show the feasibility of the enzymatic toolbox comprised of two stereocomplementary ADHs, two EREDs complementing each other's substrate profiles and one promiscuous BVMO. These versatile enzymes should be combined in biocatalytic redox cascades for investigation of their interplay and possible bottlenecks, finally resulting in the production of chiral lactones.

C II *In vitro* characterization of enzymatic redox cascades

After the design of the cascade, the set-up of the substrate scope and investigations regarding the single reaction steps, the three-step reaction cascade should be realized first, as a suitable oxygenase still was not available. A first proof-of-concept was accomplished in an *in vitro* system to get a better understanding of the interplay of the enzymes and to investigate possible cascade bottlenecks.

The *in vitro* cascade reactions were performed with cell free extracts (CFE) of *E. coli* BL21(DE3) with single overexpressed enzymes. In cascades with LK-ADH, an ERED of choice and CHMO_{Acineto} a self-sustaining redox system over step I and II was generated. LK-ADH is NADP⁺ dependent and produces NADPH in the oxidation of the unsaturated alcohol (**b**) to the unsaturated ketone (**c**). The NADPH can then be utilized by the ERED as cofactor for the reduction of the unsaturated ketone (**c**) to the saturated ketone (**d**). Here released NADP⁺ can also serve as cofactor for the LK-ADH reaction leading to a self-sustaining cofactor cycle. For step III, the BVMO reaction, NADPH is needed. To limit costs, NADP⁺ and a cofactor recycling system^[138] – glucose-6-phosphate (G6P) is transformed to 6-D-glucono-1,5-lactone by glucose-6-phosphate dehydrogenase (G6PDH) while reducing NADP⁺ to NADPH - were added to produce the NADPH. As soon as the cofactor recycling enzyme G6PDH is added it would compete with LK-ADH for the available NADP⁺, possibly limiting the first cascade step. Therefore it was decided on a sequential addition approach where the enzymes are added one after another to the same reaction vessel giving each step of the cascade (I, II, III) 1 h to react. Starting with LK-ADH and NADP⁺ no additional cofactor had to be added for the subsequently included ERED as NADPH should be present in the system. Cofactor recycling system and new NADP⁺ was then just added together with CHMO_{Acineto}. With this *in vitro* system, which is depicted in Scheme C-24, the general compatibility of all reaction components in a one-pot system should be investigated.



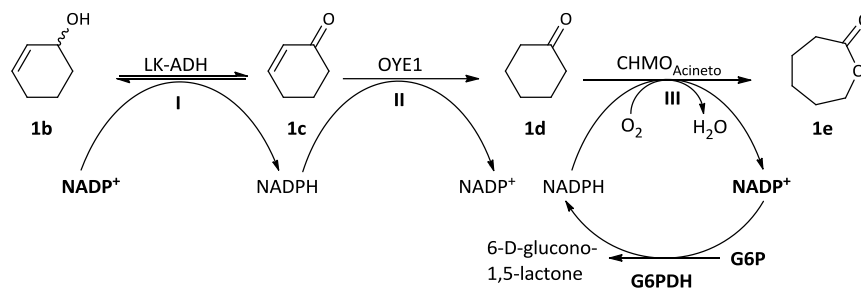
Scheme C-24. General scheme of the enzymatic three-step cascade *in vitro*.

The second ADH, RR-ADH is NAD⁺ dependent and would, hence, not compete with the recycling enzyme for the cofactor NADP⁺. Therefore, a simultaneous addition approach was tested in cascades with RR-ADH, where all enzymes, cofactors and cofactor regeneration system were mixed at once. This simultaneous system is more comparable to an *in vivo* approach, where all enzymes are present in the microbial host from the beginning, then the sequential addition. The differences between sequential and simultaneous addition in cascades with LK-ADH were investigated later. Both addition approaches were performed as one-pot reactions in aqueous buffer at ambient temperature.

The figures of this chapter show the time courses of the cascade reactions. As the first sample was drawn directly after mixing the first reactants, time point t_0 is defined as t_0^* . Black vertical lines mark the addition of the next enzyme and the bars above the diagram indicate the composition of the enzyme mix at the different phases of the reaction.

C II.1 *In vitro* cascade starting from cyclohex-2-en-1-ol (1b)

Investigations were started with the simplest substrate, cyclohex-2-en-1-ol (**1b**) to produce ϵ -caprolactone (**1e**) in a sequential *in vitro* cascade reaction. Enzymes, intermediates and cofactors of this model cascade are depicted in Scheme C-25.



Scheme C-25. *In vitro* cascade from cyclohex-2-en-1-ol to ϵ -caprolactone.

Interesting observations were made while incubating the starting material with CFE of the first enzyme LK-ADH and cofactor NADP^+ (Figure C-1, $t_0^* - t_1$). Oxidation to the α,β -unsaturated 2-cyclohexen-1-one (**1c**) progressed fast, so that transformation could be observed directly after mixing the reactants (t_0^*). Although no ERED was added yet traces of cyclohexanone (**1d**) and additionally an unidentified side-product (**X**) were detected.

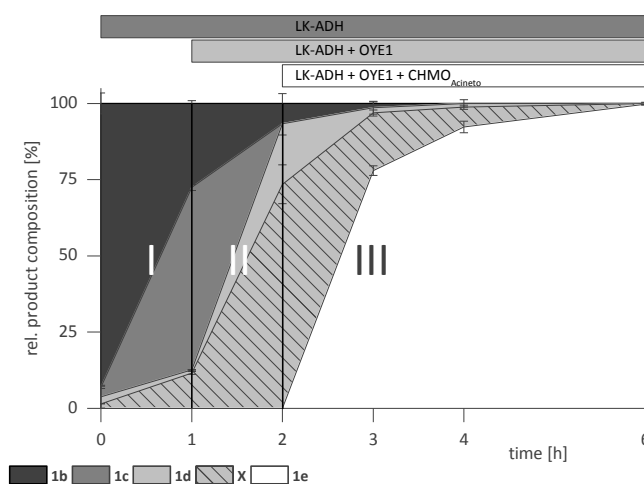


Figure C-1. The *in vitro* cascade reaction starting from cyclohex-2-en-1-ol.

As can be seen in Figure C-1 after one hour (t_1) nearly 60% of **1c** were produced. Again traces of **1d** and even 12% of the identified side-product (**X**) were detected.

In the second phase of the cascade reaction (Figure C-1, $t_1 - t_2$) CFE of the ERED OYE1 was added. There was no need to add cofactor as NADPH should be produced during the ADH reaction (Scheme C-25). After one hour of reaction with LK-ADH and OYE1 about 95% of the starting material cyclohex-2-en-1-ol (**1b**) was converted and the intermediate **1c** could not be detected. Interestingly only 20% of **1d** were found but the unidentified side-product was present with 75%.

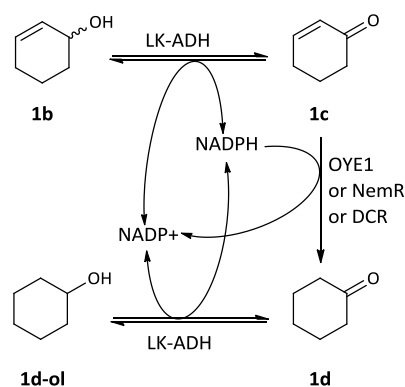
After adding the BVMO CHMO_{Acineto} in step III (Figure C-1, $t_2 - t_6$), at t_3 nearly no starting material was left, interestingly also the amount of side-product (**X**) declined and already 75% of final product ϵ -caprolactone could be detected. After only 6 h of total reaction time cyclohex-2-en-1-ol (**1b**) was completely converted to ϵ -caprolactone (**1e**).

Combination of three biocatalysts in a one-pot reaction showed proof-of-concept of a non-native enzymatic cascade. Nevertheless two unexpected occurrences were encountered in the model reaction: i) the formation of intermediate **1d** albeit the absence of the ERED in step I and ii) increasing amounts of an unidentified side-product (**X**) that fortunately completely disappeared in the last step of the cascade.

Investigations of these circumstances were started with the examination of the untimely formation of **1d**. The *in vitro* reactions were performed rather with CFE of *E. coli* with over-expressed biocatalysts instead of purified enzymes. Therefore these CFE also contained *E. coli* native enzymes that could catalyze background reactions. *E. coli* native EREDs which could be responsible for the reduction of **1c** to **1d** were found through sequence analysis. The identification of two potential *E. coli* background enzymes, N-ethylmaleimide reductase (NemR) and 2,4-dienoyl CoA reductase (DCR) and the construction of *E. coli* ERED-disruption strains will be discussed in detail later (C V.1 and C V.2).

N-Ethylmaleimide reductase (NemR) was already characterized by Mueller *et al.*^[139], whereas DCRs substrate profile was not investigated in the literature. NemR was reported to have high activity towards 2-methylcyclohex-2-en-1-one (**3c**) and *R*-(-)-carvone (**6c**) and show low conversion of 3-methylcyclohex-2-en-1-one (**4c**). NemR was reported to exhibit the same stereoselectivity for these substrates as OYE1 and XenB. Although unsubstituted 2-cyclohexen-1-one (**1c**), for which the background reaction was observed as described above, was not examined in the literature it was very likely that NemR was responsible for the untimely formation of **1d**.

The unidentified side-product (**X**) was detected up to 75% but then disappeared again. This indicated the occurrence of a reversible side-reaction as 100% of the desired lactone product could be obtained (as determined by calibrated GC). All available reaction components in step II, where the amount of side-product was the highest, had to be taken into consideration. Substrate **1b** was oxidized to **1c** by LK-ADH at the expense of NADP⁺ and subsequent reduction of **1c** to **1d** was performed by OYE1 and also by *E. coli* native EREDs, NemR and DCR. After 1 h of LK-ADH and OYE1 reacting together no intermediate **1c** was left but just 20% of **1d** could be detected, indicating the consumption of **1d** to the prominent side-product. As LK-ADH was reported to have activity for 2-methylcyclohexanone (**3d**)^[132] it was hypothesized it could also be active on the saturated ketone **1d** leading to the formation of cyclohexanol (**1d-ol = X**). The resulting reaction cycle is illustrated in Scheme C-26.



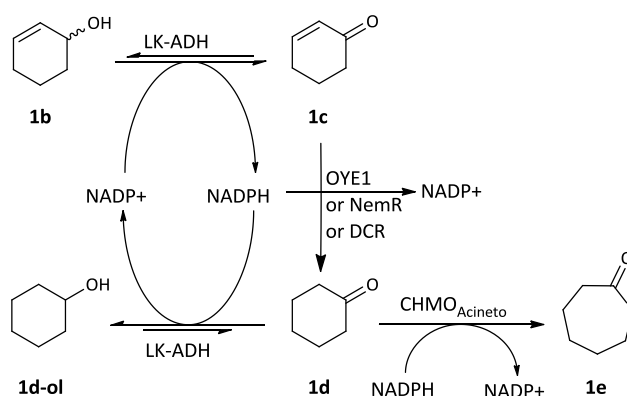
Scheme C-26. Hypothesized reaction cycle of LK-ADH and EREDs.

Indeed the side-product (**X**) was identified as cyclohexanol (**1d-ol**) via GC by comparison to commercially available cyclohexanol and to explain our observations the individual LK-ADH reactions were investigated in more detail by Christin Peters (University of Greifswald)^[140]. Enzyme activity measurements were performed and the results are depicted in Table C-6.

Table C-6. Activity of LK-ADH towards different cascade intermediates.

Entry	Reaction	Enzyme activity [U mg ⁻¹]
1	1b → 1c cyclohex-2-en-1-ol + NADP ⁺ → 2-cyclohexen-1-one + NADPH	0.91
2	1c → 1b 2-cyclohexen-1-one + NADPH → cyclohex-2-en-1-ol + NADP ⁺	0.29
3	1d-ol → 1d cyclohexanol + NADP ⁺ → cyclohexanone + NADPH	1.59
4	1d → 1d-ol cyclohexanone + NADPH → cyclohexanol + NADP ⁺	30.08

The oxidation of cyclohex-2-en-1-ol (**1b**) to the corresponding α,β-unsaturated ketone **1c** was slightly favored by LK-ADH (Table C-6, entry 1, enzyme activity threefold higher than for the reduction - entry 2). In case of the saturated substrates LK-ADH activity was almost 19 times higher for the reduction of cyclohexanone (**1d**) to the unwanted cyclohexanol (**1d-ol**, entry 4).



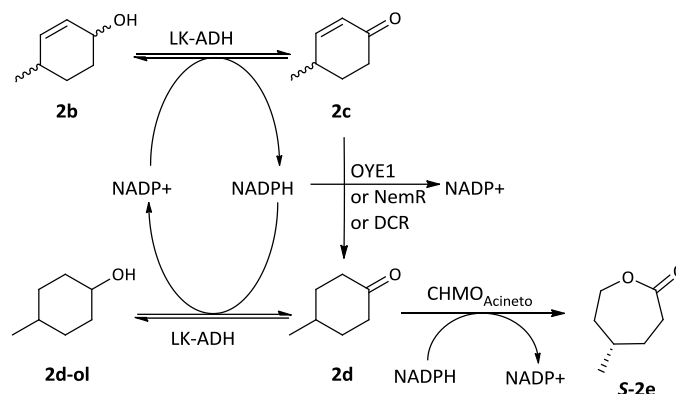
Scheme C-27. Back reaction cycle of LK-ADH resulting in formation of cyclohexanol as by-product.

These results confirmed the observations in the model cascade reaction. As the oxidation was favored the first reaction proceeded smoothly and provided enough 2-cyclohexen-1-one (**1c**) for the subsequent ERED reaction which is irreversible at the conditions used. The observed highly pronounced production of side-product cyclohexanol (**1d-ol**) is underlined by the high activity of LK-ADH towards cyclohexanone. Albeit high preference for the by-product, completion of the cascade reaction was realized by addition of CHMO_{Acineto} as the BVMO reaction is irreversible. Oxygenation of cyclohexanone to ε-caprolactone (**1e**) caused a continuous equilibrium shift (Scheme C-27) and full conversion could be achieved (Figure C-1).

In the *in vitro* reaction system with the simplest substrate cyclohex-2-en-1-ol (**1b**) a background reaction and an additional reaction of the ADH were observed. After these first investigations all unsaturated alcohols should be converted in *in vitro* cascade reactions. This finding can be considered as a “reservoir-pool” accumulation of a side product, which finally is “funneled” into the ultimate cascade target product by means of an irreversible reaction.

C II.2 *In vitro* cascade starting from 4-methylcyclohex-2-en-1-ol (**2b**)

According to the model reaction cascade starting with cyclohex-2-en-1-ol (**1b**) an *in vitro* cascade reaction starting from 4-methylcyclohex-2-en-1-ol (**2b**) was then investigated to address a desymmetrization reaction of the BVMO (Scheme C-28). Similar observations were made as in the above case after 1 h, where only CFE of *E. coli* BL21(DE3) with over-expressed LK-ADH was present, the intermediate 4-methylcyclohexanone (**2d**) and side-product 4-methylcyclohexanol (**2d-ol**, commercially available) could be detected. This showed that background enzymes NemR and possibly also DCR could reduce 4-methylcyclohex-2-en-1-one (**2c**) which was not reported in the literature.^[139] The formation of **2d-ol** indicated activity of LK-ADH for **2d** and the cascade with the side-reaction by LK-ADH is shown in Scheme C-28.



Scheme C-28. *In vitro* cascade reaction starting from **2b** with LK-ADH, OYE1 and CHMO_{Acineo}.

The conversion of **2b** by LK-ADH was slower compared to the model reaction and seemed to be the rate limiting step of this cascade. Nevertheless, in comparison to a single reaction where LK-ADH only consumed 80% of the unsaturated alcohol **2b** full conversion in the cascade was achieved. This may be due to an equilibrium shift of the first ADH reaction as the ERED constantly consumed the oxidation product **2c**. After 20 h the transformation of **2b** reached completion (Figure C-2) and final product (S)-5-methylcaprolactone (**S-2e**) was obtained with >99% ee.

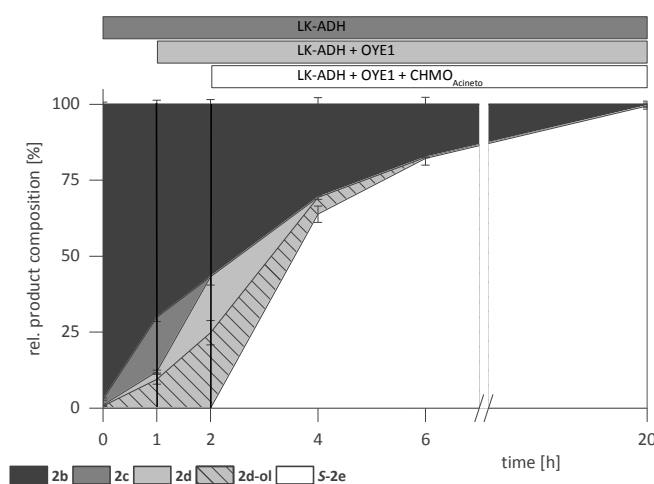
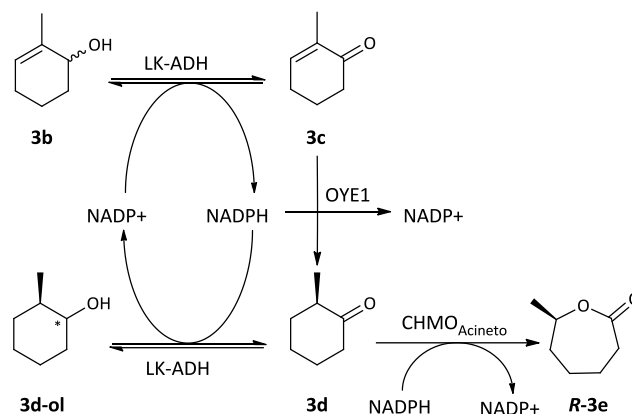


Figure C-2. Time course for the sequential *in vitro* cascade starting from 4-methylcyclohex-2-en-1-ol (**2b**).

C II.3 *In vitro* cascade starting from 2-methylcyclohex-2-en-1-ol (**3b**)

As discussed before racemic 2-methylcyclohex-2-en-1-ol (**3b**) was converted by LK-ADH in single reactions in a kinetic resolution fashion (C I.2.2). This was also observed in the cascade reaction as the transformation of **3b** to **3c** first progressed fast and slowed down after 50% conversion. Although **3c** was reported as substrate for NemR^[139] a background reaction was not detected here. After addition of CFE of OYE1 the reduction to **3d** took place and also the formation of 2-methylcyclohexanol (**3d-ol**) was observed due to LK-ADH back-reaction. Compound **3d-ol** was synthesized as reference material for comparison by LiAlH₄ reduction of **3c**. In the cascade reaction the addition of CFE of CHMO_{Acineto} pulled the equilibrium of the LK-ADH back-reaction towards the final product **R-3e** (Scheme C-29).



Scheme C-29. *In vitro* cascade reaction starting from **3b** with LK-ADH, OYE1 and CHMO_{Acineto}.

In controversy to the single reaction of LK-ADH, the starting material was converted beyond 50%, indicating also the conversion of the unfavored enantiomer of **3b** (which can be considered favorable for the overall progress of this cascade due to the destruction of chirality in this initial step). Nevertheless this very slow reaction embarked as the limitation of the cascade and the reaction was stopped after 30 h at 74% (*R*)-7-methylcaprolactone (**R-3e**) with an ee of 93% (Figure C-3).

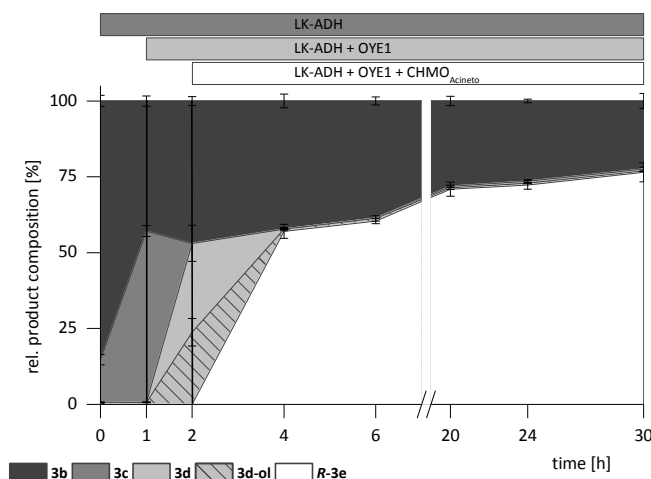
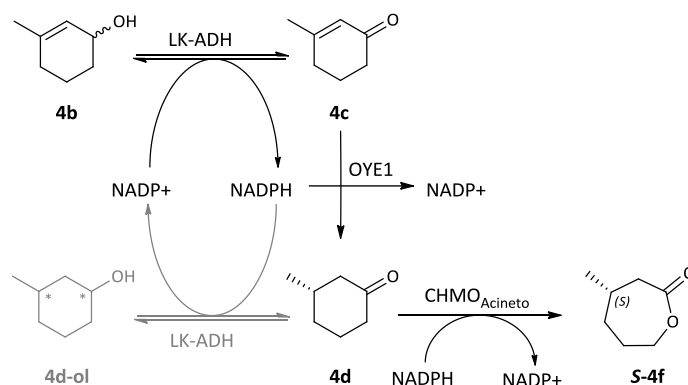


Figure C-3. Time course for the sequential *in vitro* cascade starting from 2-methylcyclohex-2-en-1-ol.

To reach full conversion from starting material to final product in this cascade reaction the implementation of an unselective ADH (displaying even lower selectivity compared to LK-ADH) could be a solution. Another possibility would be the utilization of enantiopure starting material. Nevertheless, the practicability of the chiral synthesis of starting material would have to be questioned.

C II.4 *In vitro* cascade starting from 3-methylcyclohex-2-en-1-ol (**4b**)

The *in vitro* cascade reaction starting from 3-methylcyclohex-2-en-1-ol (**4b**) was accomplished with CFE of LK-ADH, OYE1 and CHMO_{Acineto} without any difficulties. A background reaction of NemR or DCR could not be observed and no back-reaction of LK-ADH to the saturated alcohol occurred. Starting material and intermediates are shown in Scheme C-30.



Scheme C-30. *In vitro* cascade reaction starting from **4b** with LK-ADH, OYE1 and CHMO_{Acineto}.

After 24 h final product (S)-4-methylcaprolactone (**S-4f**) was present in about 83% (ee >99%) GC yield but also all intermediates could be detected. The ADH reaction again seemed to be slower than the other reactions. Although the CHMO_{Acineto} reaction progressed very fast, its activity declined after 22 h (t_{24}) as intermediate **4d** was found in the final intermediate composition (Figure C-4).

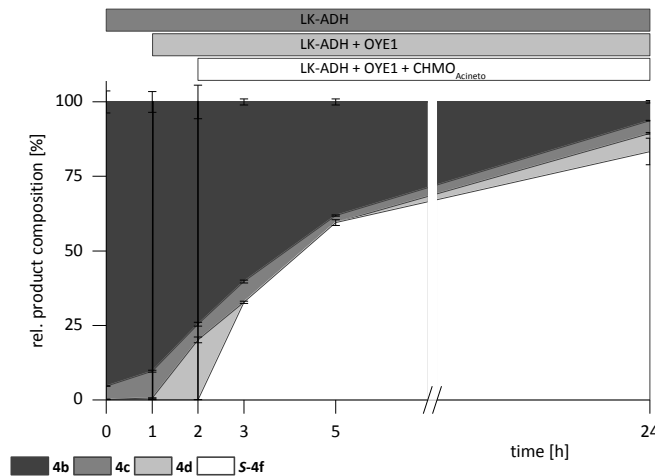


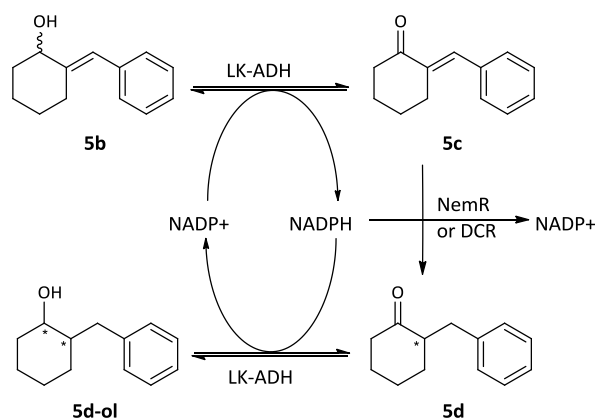
Figure C-4. Time course for the sequential *in vitro* cascade starting from 3-methylcyclohex-2-en-1-ol (**4b**).

To reach full conversion in this cascade reaction it would be beneficial to increase the rate of the LK-ADH reaction. As can be seen in Figure C-4 the ADH reaction progressed faster upon the addition of OYE1 after 1 h which is possibly due to an equilibrium shift. To add the ERED sooner or even to start with ADH and ERED from the beginning could be a solution.

C II.5 *In vitro* cascade starting from 2-benzylidenecyclohexanol (**5b**)

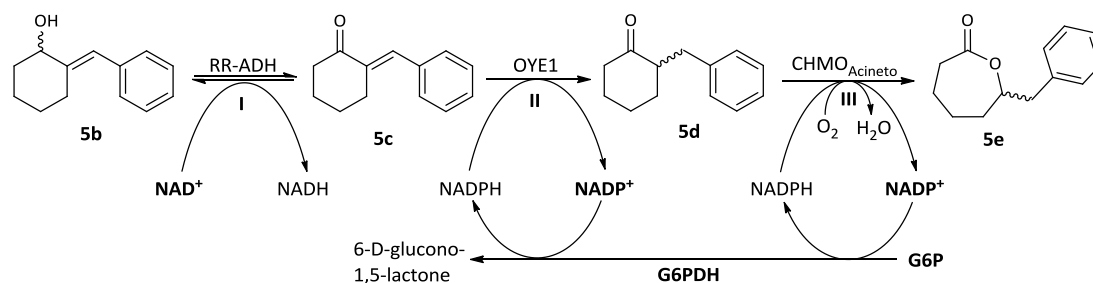
Before combining all biocatalysts for the cascade reaction from 2-benzylidenecyclohexanol (**5b**) the ADH reactions were investigated in detail. In the single reaction of CFE of LK-ADH expressed in *E. coli* BL21(DE3) the produced 2-benzylidenecyclohexanone (**5c**) was further converted to 2-benzylcyclohexanone (**5d**) as detected by GC and small amounts of unknown by-products which were not noticed in the RR-ADH reaction. As known from the previous studies native *E. coli* enzymes can cause background ERED reactions. Neither NemR nor DCR were reported to reduce 2-benzylidenecyclohexanone **5c** until now. Reduction activity for substrate **5c** has been reported for whole cells of baker's yeast^[141] and *Shewanella yellow* enzyme (SYE-4)^[142].

The additional by-products which were detected in the LK-ADH reaction but not with RR-ADH indicated that the produced 2-benzylcyclohexanone (**5d**) also serves as a substrate for LK-ADH, which would lead to 2-benzylcyclohexanol (**5d-ol**) as a product. LiAlH₄ reduction of 2-benzylcyclohexanone (**5d**) gave an isomeric mixture of **5d-ol** as reference material which was thereby identified as the detected by-product. The possible side- and back-reactions are shown in Scheme C-31.



Scheme C-31. Back-reaction of LK-ADH and background reaction of *E. coli* EREDs.

To realize the cascade from **5b** to benzylcaprolactone (**5e**) RR-ADH was chosen – as it showed better conversion of the starting material (C I.2.2) and the back-reaction of LK-ADH to **5d-ol** could be avoided – OYE1 and CHMO_{Acineto}. RR-ADH is NAD⁺ dependent, therefore a simultaneous addition approach was selected for this *in vitro* cascade. The addition of cofactor recycling system from the beginning does not interfere with the first reaction as G6PDH only converts NADP⁺. Therefore RR-ADH, OYE1, CHMO_{Acineto}, NAD⁺, NADP⁺, G6P and G6PDH were added to one reaction vessel altogether to start the reaction cascade which is shown in Scheme C-32.



Scheme C-32. *In vitro* system for the cascade from **5b** to **5e**.

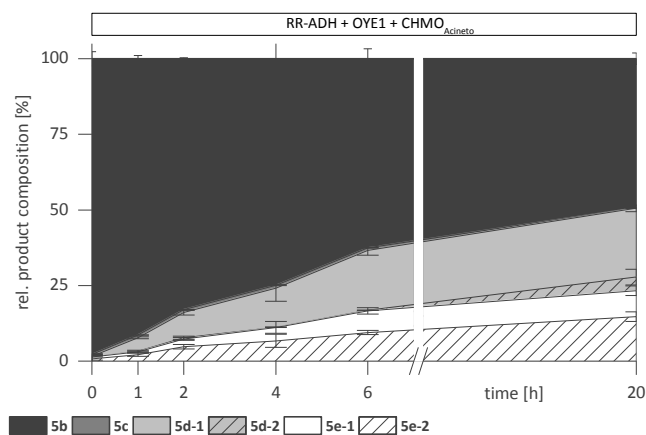
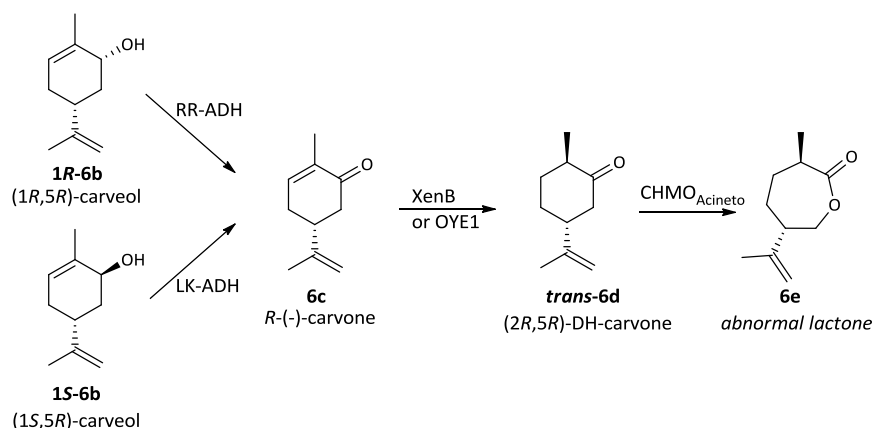


Figure C-5. *In vitro* cascade reaction from 2-benzylidenecyclohexanol (**5b**) to benzylcaprolactone (**5e**).

The time course of the reaction is shown in Figure C-5. The main limiting factor of the cascade reaction from 2-benzylidenecyclohexanol (**5b**) to benzylcaprolactone (**5e**) was the RR-ADH reaction. Conversion of starting material **5b** only proceeded until 50% due to strong stereoselectivity of RR-ADH (C I.2.2) towards one of the 2-benzylidenecyclohexanol enantiomers. While the subsequent ERED reaction, catalyzed by OYE1, and putatively the native *E. coli* enzymes NemR and DCR, progressed very fast, the CHMO_{Acineto} reaction was rather slow. As can be seen in Figure C-5 intermediate **5d-1**, the more abundant enantiomer after ERED reduction (C I.2.3) accumulates while **5d-2**, presumably the *S*-enantiomer^[137] which should be preferred by CHMO_{Acineto}, is converted to **5e-2**. Possibly due to the unfortunate ratio of **5d** enantiomers produced by the ERED the final product **5e** could only be detected in about 18% conversion with an ee_p of 26%. To enhance the outcome of this cascade reaction an unselective ADH and the implementation of another BVMO could be beneficial.

C II.6 Two cascades towards (3*R*,6*S*)-abn-carvolactone (6e)

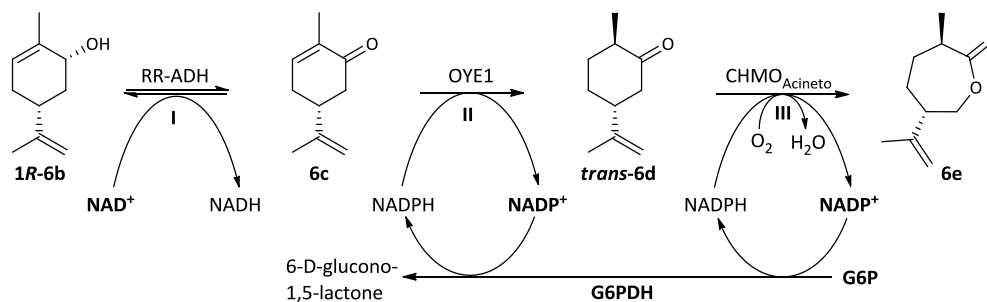
To produce an abnormal carvolactone two carveol isomers could be used as starting material for cascade reactions. With the flexible enzymatic toolbox the appropriate ADH could be chosen: (1*R*,5*R*)-carveol (**1R-6b**) could be converted by RR-ADH and (1*S*,5*R*)-carveol (**1S-6b**) by LK-ADH. Their common intermediate *R*-(-)-carvone (**6c**) could be reduced to (2*R*,5*R*)-DH-carvone (**trans-6d**) by XenB or OYE1 and the final product (3*R*,6*S*)-abn-carvolactone was produced by CHMO_{Acineto} (Scheme C-33).



Scheme C-33. Two substrates could be converted to (3*R*,6*S*)-abn-carvolactone (**6e**).

C II.6.1 *In vitro* cascade starting from (1*R*,5*R*)-Carveol (**1R-6b**)

For the conversion of (1*R*,5*R*)-carveol (**1R-6b**) to (3*R*,6*S*)-abn-carvolactone (**6e**) by RR-ADH, OYE1 and CHMO_{Acineto} a simultaneous CFE addition mode (E III.2.2) was chosen as RR-ADH is NAD⁺ dependent and therefore the first reaction is uncoupled from the subsequent ones which require NADPH (Scheme C-34).



Scheme C-34. *In vitro* cascade reaction from (1*R*,5*R*)-carveol (**1R-6b**) to (3*R*,6*S*)-abn-carvolactone (**6e**).

As can be seen in Figure C-6 the reaction was mainly limited by the transformation of (1*R*,5*R*)-carveol (**1R-6b**) by RR-ADH. All intermediates were present in low concentrations and final product (3*R*,6*S*)-abn-carvolactone (**6e**) was detected in 55% yield (>99% ee) after 30 h.

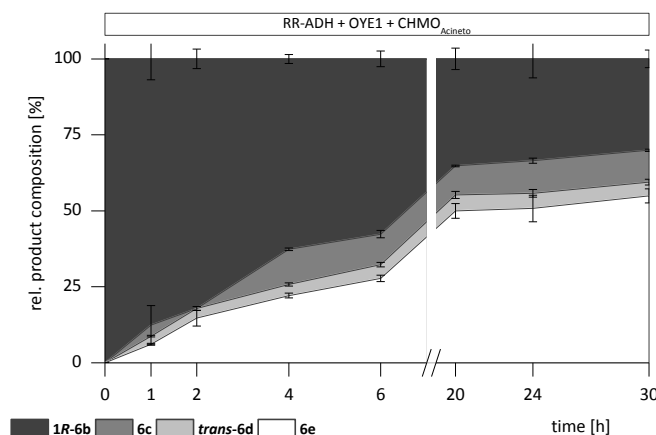


Figure C-6. Time course for a simultaneous *in vitro* cascade starting from (1*R*,5*R*)-carveol (**1R-6b**).

Background reaction of NemR or DCR could not be surveyed here as OYE1 was present from the beginning. If a background reaction occurred it did not produce different intermediates and it was also stated in the literature that NemR converts **6c** to **trans-6d**, therefore exhibiting the same stereoselectivity as OYE1 or XenB.

The slow conversion of **1R-6b** by RR-ADH limited the overall performance of the cascade. Especially within *in vitro* systems enzyme and cofactor stability decrease over time, hence a rate limiting first reaction is not beneficial. Addition of new cofactor after longer reaction times may enhance the outcome but is inappropriate in terms of expenses.

C II.6.2 *In vitro* cascade starting from (1*S*,5*R*)-Carveol (**1S-6b**)

(1*S*,5*R*)-Carveol (**1S-6b**) was used to investigate differences between a sequential and a simultaneous addition approach, the latter being more comparable to an *in vivo* system where all catalysts are present from the beginning. In Figure C-7 the time course of the sequential addition experiment can be seen.

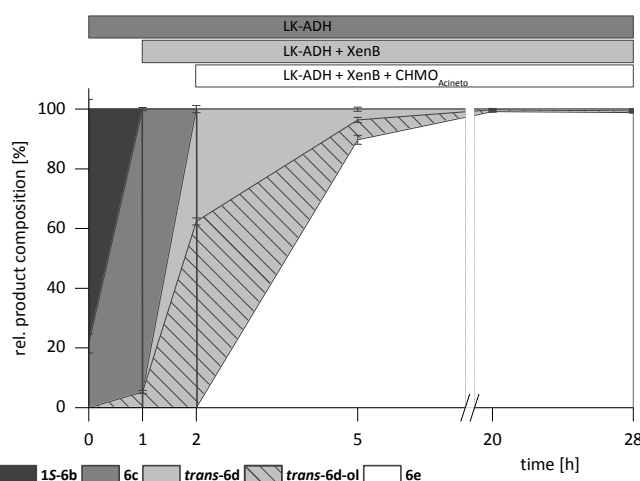


Figure C-7. Time course for the sequential *in vitro* cascade starting from (1*S*,5*R*)-carveol (**1S-6b**).

Full conversion of starting material **1S-6b** to **6c** by LK-ADH was accomplished very fast and after addition of XenB **6c** was reduced to **trans-6d** also within an hour. Background activity of NemR or DCR and back-reaction of LK-ADH could be seen as the by-product which was identified as an isomer of dihydrocarveol (**trans-6d-ol**) was already detected in the first hour. Significant amounts of **trans-6d-ol** were present which showed fast reductive activity of LK-ADH towards dihydrocarvone (**trans-6d**). Through addition of CHMO_{Acinetor} performance of the

cascade reaction was facilitated by an equilibrium shift and after 20 h 99% (3*R*,6*S*)-abn-carvolactone (**6e**) were present with perfect regio- and stereoselectivity. Application of a simultaneous addition approach resulted in significant increase in the formation of undesired by-product *trans*-**6d-ol** as can be seen in Figure C-8.

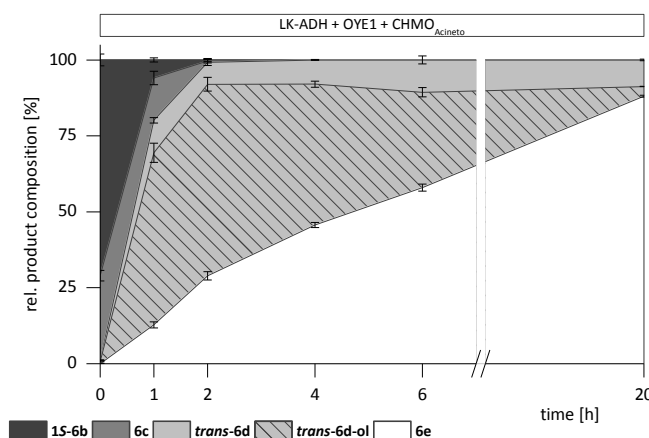
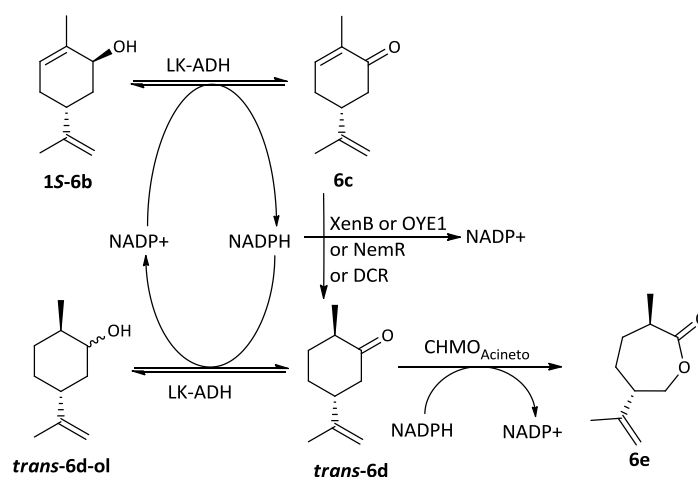


Figure C-8. Time course for a simultaneous *in vitro* cascade starting from (1*S*,5*R*)-carveol (**1S-6b**).

The cascade, possible side-reactions and the required cofactors are shown in Scheme C-35.

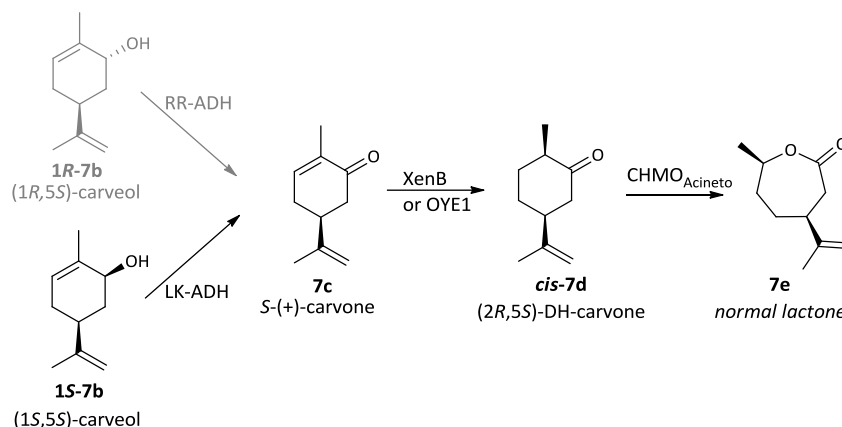


Scheme C-35. *In vitro* cascade reaction from (1*S*,5*R*)-carveol (**1S-6b**) to (3*R*,6*S*)-abn-carvolactone (**6e**).

Besides possible BVMO stability decrease in a simultaneous approach, an explanation for the difference between sequential and non-sequential addition could be the cofactor dependency and availability. In a sequential approach during the conversion of (1*S*,5*R*)-carveol (**1S-6b**) to *R*(-)-carvone (**6c**) by LK-ADH, NADPH is produced which is then consumed by subsequently added XenB, resulting in a self-sustaining redox system. Upon addition of CHMO_{Acineto} and cofactor recycling system (NADPH) the reaction is pulled towards the lactone (**6e**). In the simultaneous reaction set-up (Figure C-8) unlimited amounts of NADPH were present from the beginning resulting in direct competition of the high affinity of LK-ADH towards **6c** and the BVMO reaction. The formation of by-product *trans*-**6d-ol** was very prominent and the Baeyer-Villiger oxidation turned out to be the rate-limiting step as can be seen in the time course in Figure C-8. Nevertheless due to equilibrium shift by the irreversible last reaction final product (3*R*,6*S*)-abn-carvolactone (**6e**) was obtained in 88% (<99% ee) after 20 h in the simultaneous addition approach.

C II.7 *In vitro* cascade starting from (1*S*,5*S*)-Carveol (1*R*-7*b*)

The normal carvolactone **7e** could only be produced from one carveol isomer, as (1*R*,1*S*)-carveol (**1*R*-7*b***) was not available as starting material. Both theoretically possible cascades towards (4*S*,7*R*)-carvolactone (**7e**) are shown in Scheme C-36.



Scheme C-36. Cascades towards (4*S*,7*R*)-carvolactone (**7e**).

This *in vitro* reaction cascade with LK-ADH, OYE1 and CHMO_{Acineto} was conducted in simultaneous addition mode, as the example of (1*S*,5*R*)-carveol (**1*S*-6*b***, C II.6.2) showed that the overall cascade performance was not decreased significantly, in comparison to the sequential addition, and allowed for an easier experiment set-up. (1*S*,5*S*)-Carveol (**1*S*-7*b***) was very well accepted by LK-ADH, the subsequent cascade reaction progressed smoothly and the reaction was nearly completed after 20 h (Figure C-9).

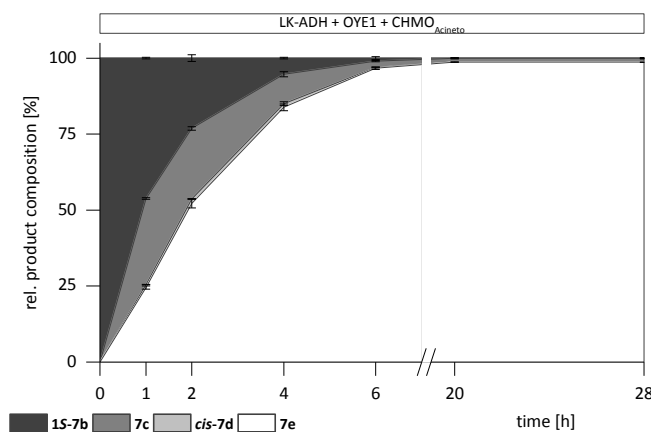
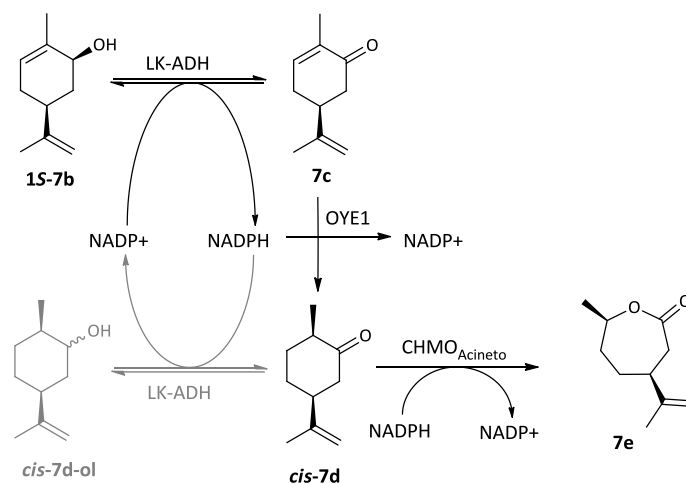


Figure C-9. Time course for a simultaneous *in vitro* cascade starting from (1*S*,5*S*)-carveol (**1*S*-7*b***).

As can be seen in Figure C-9 no formation of dihydrocarveol (*cis*-**7d-ol**) as by-product of LK-ADH could be observed, which was rather surprising as from *trans*-**6d** (Figure C-8) nearly 70% by-product was produced. This interesting observation could possibly be due to some steric hindrance of the *cis*-dihydrocarvone *cis*-**7d** in the binding pocket of LK-ADH. Additionally, CHMO_{Acineto} exhibits very strong activity towards *cis*-**7d**, leaving hardly any of this intermediate available for a possible back-reaction of LK-ADH. The cascade reaction is depicted in Scheme C-37.



Scheme C-37. *In vitro* cascade reaction starting from (1S,5S)-carveol (**1S-7b**).

Again due to the simultaneous addition where OYE1 was present from the beginning no background reaction of NemR or DCR could be analyzed. Only intermediate **cis-7d** could be detected, so either no background reaction occurred or the *E. coli* native EREDs exhibited the same stereopreference as OYE1.

C II.7.1 Starting material concentration dependency on cascade performance

A study to investigate the concentration of starting material was performed with the cascade reaction starting from (1S,5S)-carveol (**1S-7b**) to (4S,7R)-carvolactone (**7e**) as it proceeded without significant bottlenecks. Additionally to the standard concentration of 4 mM also 10 mM, 25 mM and 50 mM **1S-7b** were used in simultaneous cascade reactions with CFE of LK-ADH, OYE1 and CHMO_{Acineto}.

Increasing the substrate load to 10 mM significantly decreased the reaction speed of LK-ADH. Also the reduction of **7c** by OYE1 seemed inhibited by the higher concentration. The activity of CHMO_{Acineto} was not influenced but only declined after 20 h where final product of the cascade was already present in 90% GC-yield.

At 25 mM starting material, productivity of LK-ADH and OYE1 was further decreased in comparison to 10 mM **1S-7b**. Starting material **1S-7b** was here not fully converted to **7c**, which indicates either product inhibition of LK-ADH or substrate inhibition for the subsequent OYE1 reaction. CHMO_{Acineto} still performed fast in the beginning but its activity started to drop now already after 6 h. Still final product (4S,7R)-carvolactone (**7e**) was observed up to 50% GC yield.

The LK-ADH reaction was strongly inhibited with 50 mM **1S-7b**. The produced **7c** was still reduced by OYE1 rendering the earlier hypothesized substrate inhibition for the ERED as unlikely. CHMO_{Acineto} transformed **trans-7d**, which was only available in lower concentrations. This high concentration of starting material did not prove feasible for the overall outcome of the cascade reaction. The time courses for the different concentrations of starting material are combined in Figure C-10.

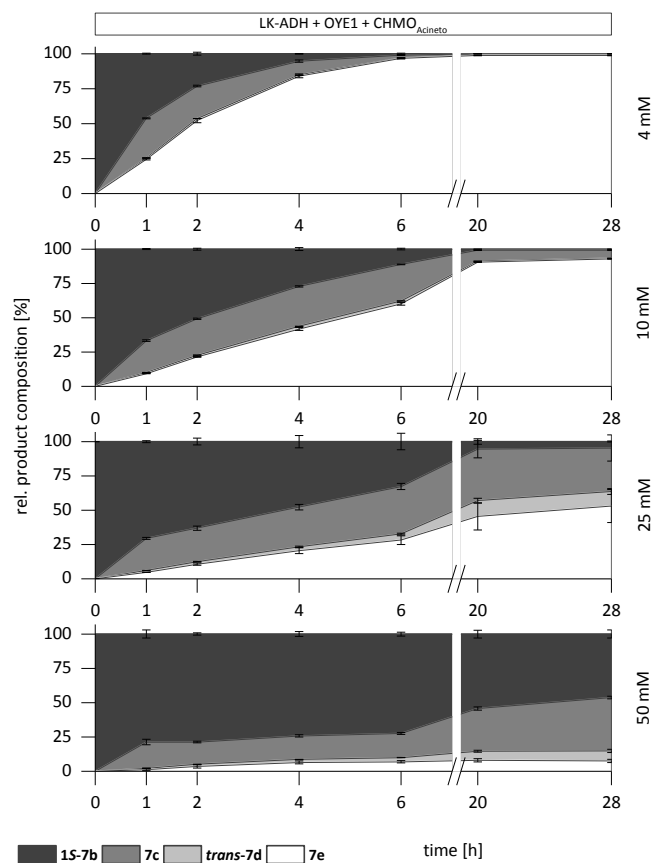


Figure C-10. Time courses for simultaneous *in vitro* cascades starting from different concentrations of (1S,5S)-carveol (1S-7b).

C II.8 Summary

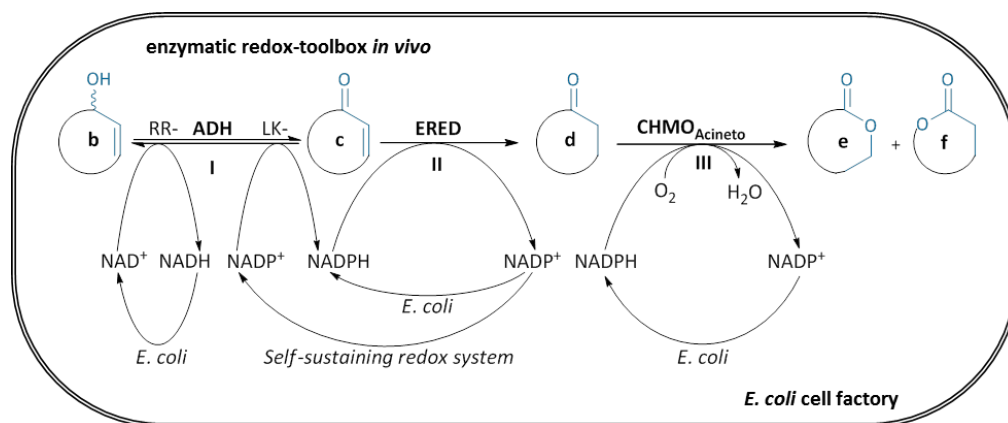
An enzymatic toolbox comprised of three biocatalysts was investigated in an *in vitro* system. The conversion of eight different substrates showed the versatility of our approach. Background reactions by *E. coli* native enzymes and side-reactions caused by LK-ADH were identified. These deeper insights were the basis for the implementation of an *in vivo* enzymatic toolbox in the microbial host *E. coli*.

C III *In vivo* cascades – an enzymatic toolbox

After thorough investigations of the interplay of the chosen redox enzymes *in vitro*, the transfer of the system to a microbial host organism to study non-native pathways was addressed. The plasmid based expression system was optimized for multiple enzymes and genomic integration of cascade enzymes was contemplated, which will be discussed in detail later (C V.7). The initially planned four-step cascade starting from cyclic alkenes could not be investigated as an oxygenase for the first step was not available. Therefore the focus was set on the three step cascade, starting from unsaturated cyclic alcohols.

C III.1 *E. coli* cell factory

To set up the cascade reaction as metabolic mini-pathway in a host organism, the use of *E. coli* was aspired as it is thoroughly studied and well characterized. Additionally, the expression of active biocatalysts in this host was confirmed in previous experiments for all involved enzymes. The realization of an enzymatic cascade *in vivo* may have its challenges but comes with a number of advantages. If the first reaction step of the cascade is catalyzed by LK-ADH the first two steps represent a self-sustaining cofactor RedOx system. With RR-ADH as being NAD^+ dependent this is not the case and therefore two cofactors plus recycling system had to be added in the *in vitro* approach. Also for the final step NADPH had to be provided. In resting – not growing - *E. coli* cells, supplemented with carbon source (e.g. glucose), the central metabolism of the bacterium is producing redox equivalents: NADH is product of the glycolysis and NADPH is released from the pentose phosphate pathway (PPP). This constant availability of cofactors, provided by the metabolism of the living host cell, not only reduces the costs but also simplifies the system. The idea of an *in vivo E. coli* “cell factory” containing an enzymatic toolbox for the cascade reactions is visualized in Scheme C-38.



Scheme C-38. *In vivo E. coli* “cell factory”.

C III.1.1 Expression system

As the chosen enzymes derive from different organisms and are not native in *E. coli*, they had to be heterologously expressed. Therefore different concepts were investigated. The first approach was the implementation of a conventional plasmid overexpression system where each heterologous gene was presented on one plasmid (3-plasmid system). Here, the host organism had to cope with the metabolic burden of three plasmids which could lead to reduced productivity.^[16] Hence, also a two plasmid system was approached where the ADH was expressed from one plasmid and the ERED and the BVMO were coproduced

from another expression vector. Here, the metabolic burden was reduced but modularity of the system was maintained as the ADH could be chosen upon its suitability for the starting material.

The co-expression system for the EREDs and the BVMO was constructed at the University of Greifswald and cotransformed with the ADHs into *E. coli* BL21(DE3) in-house. The enzymatic toolbox was therefore implemented by choosing different combinations of plasmids, which are listed in Table C-7.

Table C-7. Combinations of plasmids offering an enzymatic toolbox.

System	Enzymes	Plasmids
3 plasmids	RR-ADH, XenB and CHMO _{Acineto}	pRRADH + pGASTON_XenB + pET28a_CHMO
2 plasmids	LK-ADH, XenB and CHMO _{Acineto}	pET22b_LKADH + pET28_CHMO_XenB
2 plasmids	LK-ADH, OYE1 and CHMO _{Acineto}	pET22b_LKADH + pET28_CHMO_OYE
2 plasmids	RR-ADH, XenB and CHMO _{Acineto}	pRRADH + pET28_CHMO_XenB
2 plasmids	RR-ADH, OYE1 and CHMO _{Acineto}	pRRADH + pET28_CHMO_OYE

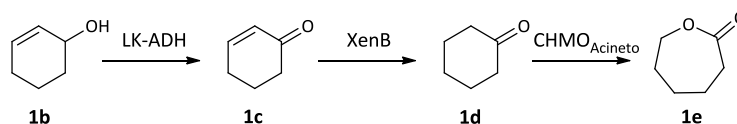
Additionally the genomic integration of the ADHs was investigated, which is discussed in detail later (C V.7). In this system the genome of host organism *E. coli* would be genetically modified to contain the genes for the ADHs. This would further minimize the amount of plasmids which would be beneficial for the extension of the cascade with the oxygenase to the four step cascade. Then four enzymes could be expressed in *E. coli* with one plasmid for the oxygenase, a genome-integrated gene for an ADH and a co-expression plasmid for the ERED and the BVMO.

C III.1.2 Reaction set-up

The enzymes of choice were coproduced in *E. coli* BL21(DE3) and resting cells were used for the reactions. The addition of glucose ensured the viability of the cells and hence the availability of cofactors provided by the bacterial host.

C III.2 *In vivo* cascade starting from cyclohex-2-en-1-ol (**1b**)

The simplest starting material cyclohex-2-en-1-ol (**1b**) was subjected to a cascade reaction to produce ϵ -caprolactone (**1e**) for a first proof of concept. *E. coli* BL21(DE3) resting cells with expression systems pET22b_LK-ADH and pET28_CHMO_XenB were prepared according to Procedure A (E I.7.1) and supplemented with 4 mM cyclohex-2-en-1-ol (**1b**). Starting material, enzymes, intermediates and product are shown in Scheme C-39.



Scheme C-39. Three-step cascade converting cyclohex-2-en-1-ol (**1b**) to ϵ -caprolactone (**1e**).

As can be seen in Figure C-11 starting material **1b** was converted to **1c** shortly after adding it to the resting cells with the biocatalysts. Final product **1e** was detected with 60% yield already after 1 h demonstrating the power of the one-pot cascade reaction as one intermediate is converted to the next one as soon as it is available. The reaction cascade had progressed to over 90% after 3 h and reached completion in 20 h.

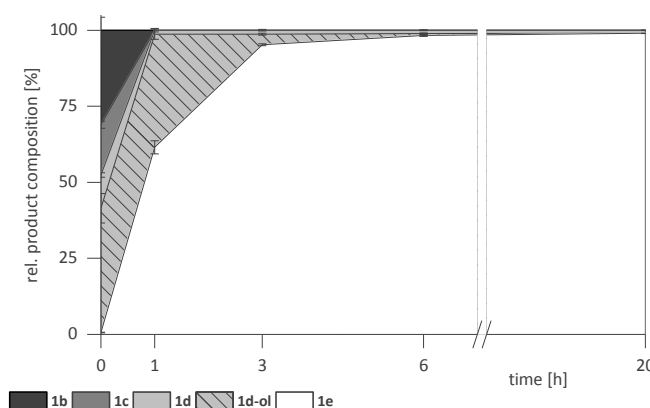
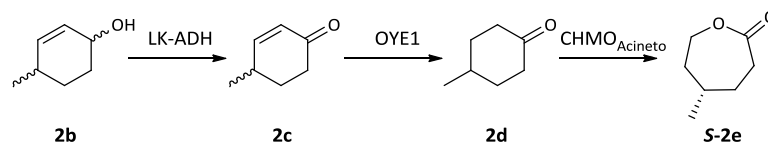


Figure C-11. Time course of *in vivo* cascade from cyclohex-2-en-1-ol (**1b**) to ϵ -caprolactone (**1e**).

This simple model cascade performed also very well in the *in vitro* system (C II.1), but there the side-product cyclohexanol (**1d-ol**) was produced due to a LK-ADH back-reaction up to 75%. This by-product **1d-ol** was only detected up to 40% in the *in vivo* system in the first hours of the reaction. Here the *in vivo* system, where all enzymes are present from the outset of the cascade reaction, shows its benefits. As CHMO_{Acineto} is available from the beginning it could directly compete with the LK-ADH back-reaction hence limiting the amount of produced by-product **1d-ol**. The irreversible BVMO reaction leads to an equilibrium shift and full conversion to the final product **1e**.

C III.3 *In vivo* cascade starting from 4-methylcyclohex-2-en-1-ol (**2b**)

Having accomplished the *in vivo* cascade starting from simple cyclohex-2-en-1-ol (**1b**) the system was challenged with the more complex substrate (**2b**) resulting in desymmetrization of 4-methylcyclohexanone (**2d**) (Scheme C-40).



Scheme C-40. Cascade from 4-methylcyclohex-2-en-1-ol (**2b**) to (S)-5-methylcaprolactone (**S-2e**).

Resting cells of *E. coli* BI21(DE3) with co-expressed pET22b_LK-ADH and pET28_CHMO_OYE (prepared according to E 1.7.1) were supplemented with 4 mM **2b**. Oxidation of **2b** by LK-ADH progressed much slower than compared to the fast conversion of unsubstituted cyclohex-2-en-1-ol (**1b**) as already seen in the *in vitro* system (C II.2). Subsequent reduction of the double bond by the ERED OYE1 to prochiral 4-methylcyclohexanone (**2d**) and final desymmetrization by the CHMO_{Acineto} performed so fast that intermediates **2c** and **2d** were - if at all - only detected in low amounts (Figure C-12).

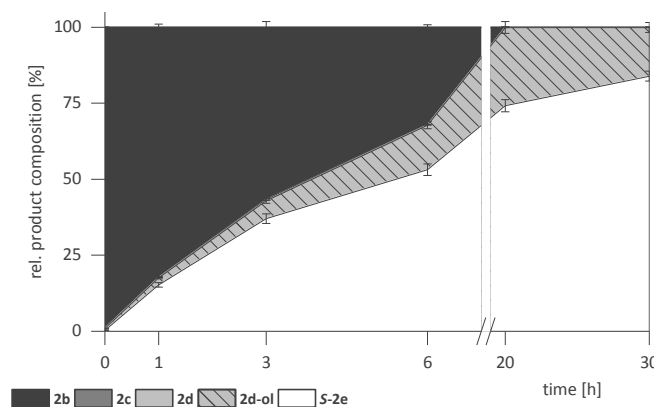
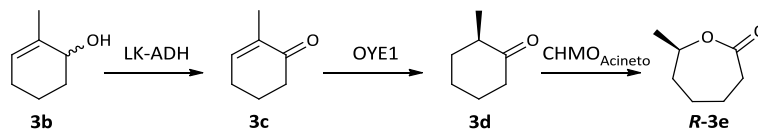


Figure C-12. Time course of *in vivo* cascade from 4-methylcyclohex-2-en-1-ol (**2b**) to (S)-5-methylcaprolactone (**S-2e**).

The generation of side-product **2d-ol** by LK-ADH as encountered in the *in vitro* system (C II.2) occurred differently in the *in vivo* system. After 2 h 20% of **2d-ol** were detected in the *in vitro* sequential addition approach, as CHMO_{Acineto} was not yet added to compete against the LK-ADH back-reaction. In the *in vivo* system with all enzymes present from the beginning, the side-product was only detected after 3 h. From this point on LK-ADH and CHMO_{Acineto} compete over intermediate **2d** and a maximum of **2d-ol** is present after 20 h. Due to the irreversible BVMO reaction this amount is reduced to about 16% after 30 h, where lactone **S-2e** was the only other detectable product and showed perfect optical purity (>99% ee).

C III.4 *In vivo* cascade starting from 2-methylcyclohex-2-en-1-ol (**3b**)

E. coli BL21(DE3) resting cells with expression systems pET22b_LK-ADH and pET28_CHMO_OYE were prepared according to Procedure A (E I.7.1) and supplemented with 4 mM 2-methylcyclohex-2-en-1-ol (**3b**) and reaction of the cascade is illustrated in Scheme C-41.



Scheme C-41. *In vivo* cascade from 2-methylcyclohex-2-en-1-ol (**3b**) to (R)-7-methylcaprolactone (**R-3e**).

Oxidation of **3b** progressed relatively slow after 50% of the starting material were converted to **3c** due to the stereospecificity of LK-ADH as already observed in the *in vitro* system (C II.3). Intermediate **3c** was continuously reduced by OYE1 and delivered optically pure (R)-2-methylcyclohexanone (**3d**). As CHMO_{Acineto} shows only limited enantioselectivity towards racemic 2-methylcyclohexanone^[119] no stereoselective limitations were encountered for the conversion of **3d** and enantiomerically pure lactone **R-3e** (74% GC yield, >99% ee) was produced. The time course of the cascade can be seen in Figure C-13.

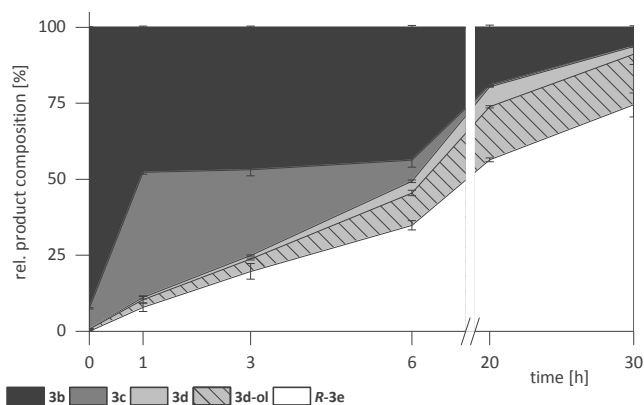


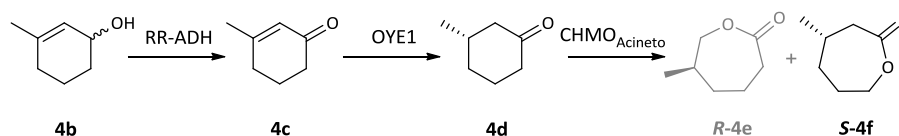
Figure C-13. Time course of *in vivo* cascade from 2-methylcyclohex-2-en-1-ol (**3b**) to (R)-7-methylcaprolactone (**R-3e**).

The differences for the production of side-product **3d-ol** in *in vitro* and *in vivo* system showed the same pattern as in the cascade starting from 4-methylcyclohex-2-en-1-ol (**2b**, 0). Whereas **3d-ol** was produced in the first hours of the *in vitro* reaction in quantities up to 20%, it was only detected in lower amounts later in the *in vivo* reaction. The cascade again benefits from the irreversible BVMO reaction as no additional side-product is produced in the last hours of the reaction but more final product lactone **R-3e** is present. A further decrease of side-product towards complete conversion could eventually be achieved with even longer reaction times but could be limited due to declining enzyme activity.

C III.5 *In vivo* cascade starting from 3-methylcyclohex-2-en-1-ol (**4b**)

C III.5.1 Analytical scale

For the conversion of substrate 3-methylcyclohex-2-en-1-ol (**4b**) resting cells of *E. coli* BL21(DE3) expressing pRR-ADH and pET28_CHMO_OYE (prepared according to E I.7.1) were applied resulting in a cascade reaction shown in Figure C-19.



Scheme C-42. *In vivo* cascade from 3-methylcyclohex-2-en-1-ol (**4b**) to (*S*)-4-methylcaprolactone (**S-4f**).

Substrate **4b** was oxidized by RR-ADH to 3-methyl-2-cyclohexen-1-one (**4c**) which was reduced to optically pure (*S*)-3-methylcyclohexanone (**4d**) by OYE1. Intermediate **4d** was converted by CHMO_{Acineto} to the distal lactone **S-4f** (86% GC yield, >99% ee) so fast that intermediate **4d** was hardly detected. Proximal lactone **R-4e** was not produced as only (*S*)-3-methylcyclohexanone (**4d**) was present and CHMO_{Acineto} is known to exhibit strong regioselectivity for in position 3 methylated cyclohexanone^[143]. A time course of the reaction is shown in Figure C-14.

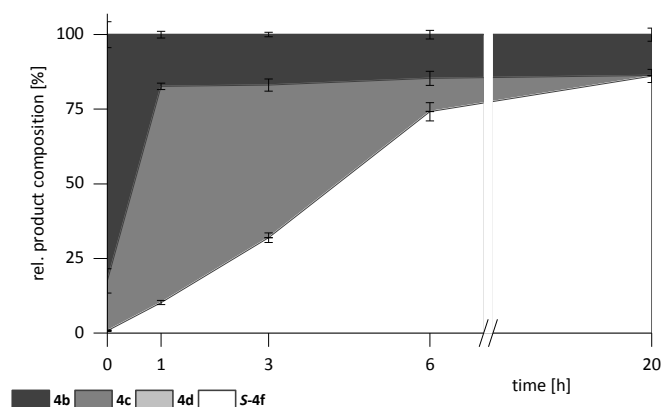
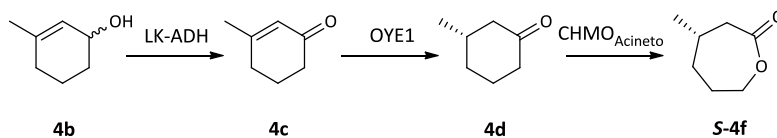


Figure C-14. Time course of *in vivo* cascade from 3-methylcyclohex-2-en-1-ol to (*S*)-4-methylcaprolactone in an analytical scale experiment.

RR-ADH exhibited strong stereopreference for one isomer of starting material **4b** which was converted within the first hour. The remaining amounts of **4b** belonged to the other isomer which was oxidized very slowly, which may also be due to activity decrease of RR-ADH over time. The reaction of OYE1 seems to be the rate defining step of the cascade as intermediate **4d** was not even detected because it was converted to **S-4f** CHMO_{Acineto} instantly.

C III.5.2 Preparative scale

To demonstrate the power of whole cell cascade reactions an up-scaled experiment with 100 mg 3-methylcyclohex-2-en-1-ol (**4b**) as starting material was performed. Therefore LK-ADH was chosen to avoid the strong stereopreference of RR-ADH (C III.5.1). The combination of LK-ADH, OYE1 and CHMO_{Acineto} (Scheme C-43) already operated well in the *in vitro* studies (C II.4).



Scheme C-43. Preparative scale cascade from **4b** to **S-4f**.

E. coli BL21(DE3) resting cells expressing pET-22b(+)_LK-ADH and pET28_CHMO_OYE were treated according to E III.4.1 and the time course of the reaction can be seen in Figure C-15.

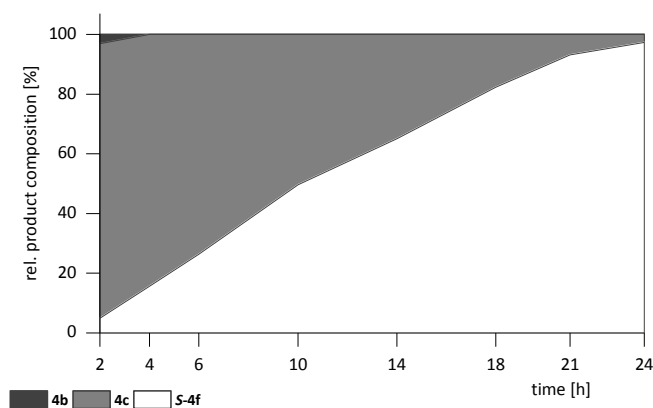


Figure C-15. Time course of the preparative scale *in vivo* cascade from 3-methylcyclohex-2-en-1-ol to (S)-4-methylcaprolactone.

Also here it was observed that the limiting reaction of the cascade was the reduction of **4c** to **4d** by OYE1. Intermediate **4d** on the other hand was transformed by the BVMO so quickly that it could not be detected. Nevertheless, after 24 h approx. 95% of final product were detected. The cells were separated from the reaction suspension by centrifugation and the aqueous supernatant was extracted with diethylether (Et₂O). After evaporation of Et₂O *in vacuo* the product was purified over column chromatography that yielded in 54 mg distal (S)-4-methylcaprolactone (**S-4f**) (ee 95%). This amount of product corresponds to 47% isolated yield and an average of 78% yield per individual step of the cascade could be achieved.

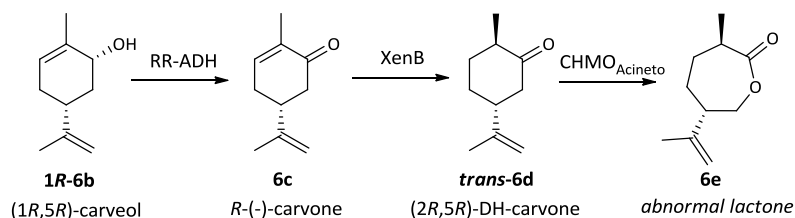
C III.6 *In vivo* cascade starting from 2-benzylidenecyclohexanol (**5b**)

The *in vitro* cascade starting from 2-benzylidenecyclohexanol as discussed in C II.5 did not deliver satisfying results as only 18% not enantiopure final product were observed. Therefore substrate **5b** was not investigated in the *in vivo* studies.

C III.7 Two cascades towards (3*R*,6*S*)-abn-carvolactone (**6e**)

C III.7.1 *In vivo* cascade starting from (1*R*,5*R*)-Carveol (**1R-6b**)

For the conversion of (1*R*,5*R*)-carveol (**1R-6b**) an *E. coli* BL21(DE3) resting cell system with expression systems pRRADH, pGASTON_XenB and pET28a_CHMO (prepared according to E I.7.1) was employed. Starting material, intermediates, product and enzymes are shown in Scheme C-44.



Scheme C-44. *In vivo* cascade from (1*R*,5*R*)-carveol to (3*R*,6*S*)-abn-carvolactone.

The available ADHs exhibited high stereoselectivity for the hydroxyl group, therefore RR-ADH was used to convert (1*R*,5*R*)-carveol to *R*-(-)-carvone (**6c**). Unfortunately, the conversion is not complete but the resulting **6c** was nevertheless reduced by XenB very well and the resulting (2*R*,5*R*)-dihydrocarvone (**trans-6d**) is known as good substrate for CHMO_{Acineto}^[130], hence about 66% of (3*R*,6*S*)-abn-carvolactone (**6e**) could be detected after 20 h reaction time (Figure C-16).

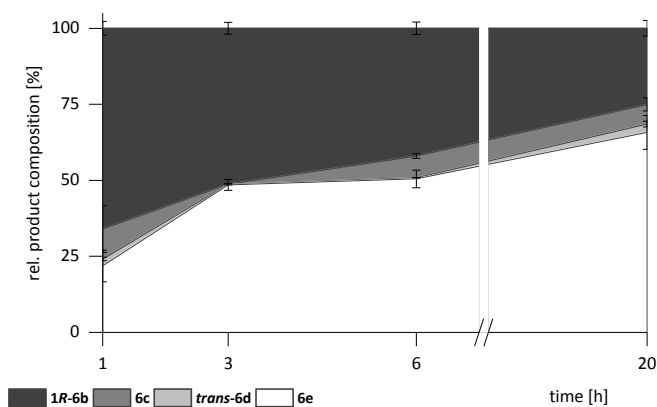
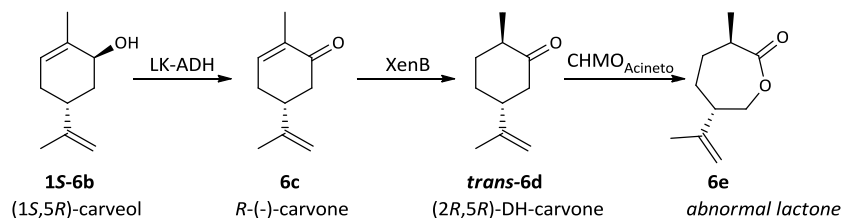


Figure C-16. Time course of *in vivo* cascade from (1*R*,5*R*)-carveol to (3*R*,6*S*)-abn-carvolactone.

C III.7.2 *In vivo* cascade starting from (1*S*,5*R*)-Carveol (**1S-6b**)

C III.7.2.1 Analytical scale

(1*S*,5*R*)-Carveol (**1S-6b**) was transformed with *E. coli* BL21(DE3) resting cells with expression systems pET22b_LK-ADH and pET28_CHMO_XenB via the cascade shown in Scheme C-45. Final product was again (3*R*,6*S*)-abn-carvolactone (**6e**), as the first intermediate was as well *R*-(-)-carvone (**6c**).



Scheme C-45. *In vivo* cascade from (1*S*,5*R*)-carveol (**1S-6b**) to (3*R*,6*S*)-abn-carvolactone.

As can be seen in Figure C-17 LK-ADH showed high activity towards **1S-6b** as it was converted instantly after addition to the resting cells. The high affinity of LK-ADH for the carveol/carvone structure goes hand in hand with high activity also for the unsaturated ketone **trans-6d** leading to production of **trans-6d-ol**, as already noticed in the *in vitro* system C II.6.2.

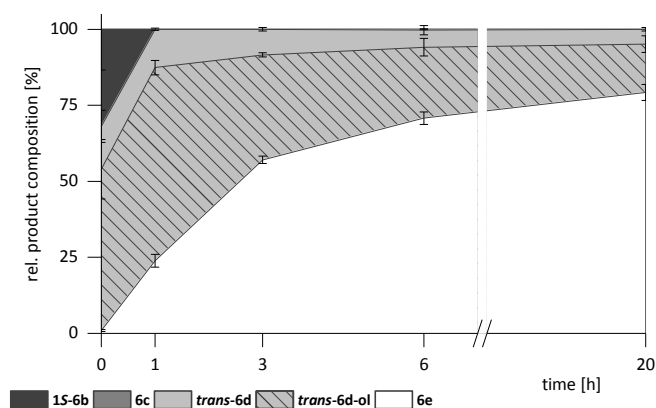


Figure C-17. Time course of *in vivo* cascade from (1*S*,5*R*)-carveol (**1S-6b**) to (3*R*,6*S*)-abn-carvolactone.

A maximum of by-product **trans-6d-ol** production is reached after 1 h, after which the equilibrium is constantly shifted by the irreversible BVMO reaction. The final product **6e** could be detected with approx. 80% after 20 h. Further decrease of by-product **trans-6d-ol** could maybe be achieved with longer reaction times.

C III.7.2.2 Preparative scale

This cascade from (1*S*,5*R*)-carveol (**1S-6b**) towards (3*R*,6*S*)-abn-carvolactone (**6e**) was additionally investigated in a preparative scale experiment (E III.4.1): 100 mg of **1S-6b** were added to resting cells with expression systems pET22b_LK-ADH and pET28_CHMO_XenB, glucose and pH levels kept constant and reaction control done with GC. The time course can be seen in Figure C-18.

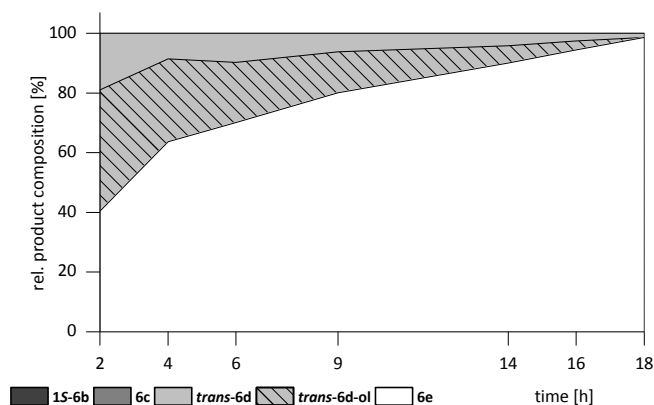


Figure C-18. Preparative scale cascade from (1*S*,5*R*)-carveol (**1S-6b**) to (3*R*,6*S*)-abn-carvolactone (**6e**).

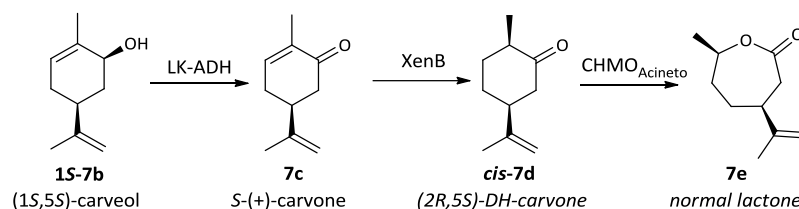
Starting material **1S-6b** and intermediate **6c** are fully converted already after 2 h reaction time. The competition of LK-ADH and CHMO_{Acineto} over intermediate **trans-6d** was identified as rate defining step. Here the irreversible BVMO reaction led to nearly full conversion to final product **6e** already after 18 h. In the analytical scale experiment after 20 h still about 16% **trans-6d-ol** were present. This difference could be explained by stricter control of reaction conditions in the preparative scale experiment. Here pH and glucose were maintained constant as good as possible whereas in the analytical scale such control was not performed. These optimized conditions could lead to more active and stable enzymes and therefore enhanced flux through the cascade.

After 20 h the cells were separated from the reaction suspension by centrifugation and the aqueous supernatant extracted with Et₂O. Following evaporation of the organic solvent the crude product was purified over column chromatography yielding in 69 mg (3*R*,6*S*)-abn-carvolactone (**6e**). This amount of final product corresponds to 62% yield and a calculated yield of 85% per individual cascade reaction (over three steps).

C III.8 *In vivo* cascade starting from (1*S*,5*S*)-Carveol (1*S*-7b)

C III.8.1 Analytical scale

(1*S*,5*S*)-Carveol (1*S*-7b) was added to *E. coli* BL21(DE3) resting cells with pET22b_LK-ADH and pET28_CHMO_XenB (prepared according to E 1.7.2) and the resulting cascade reaction can be seen in Scheme C-46.



Scheme C-46. *In vivo* cascade from (1*S*,5*S*)-carveol to (4*S*,7*R*)-carvolactone.

Here, access to another final product was achieved, as the first intermediate was *S*-(+)-carvone (7c) and product of the XenB reaction was the (-)-*cis*-dihydrocarvone (*cis*-7d) which was selectively transformed to the normal carvolactone (7e) by CHMO_{Acineto}^[130]. The cascade progressed very fast with hardly detectable intermediates and reached completion after 20 h (Figure C-19).

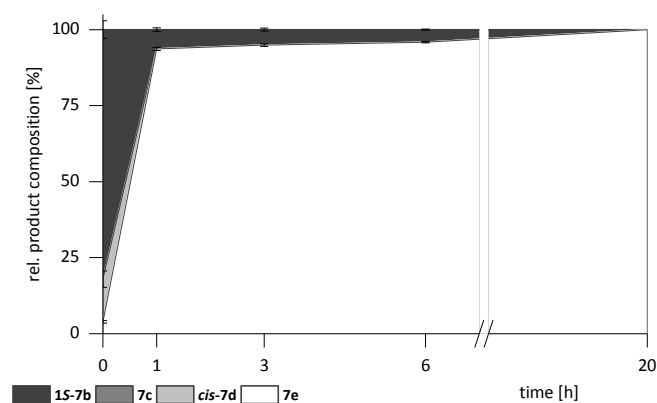


Figure C-19. Time course of *in vivo* cascade from (1*S*,5*S*)-carveol to (4*S*,7*R*)-carvolactone in an analytical scale experiment.

C III.8.1 Preparative scale

The cascade reaction from (1*S*,5*S*)-carveol (**1S-7b**) to (4*S*,7*R*)-carvolactone (**7e**) (Scheme C-46) was also chosen for an upscaling experiment. *E. coli* BL21(DE3) resting cells with pET22b_LK-ADH and pET28_CHMO_XenB were treated as described in E III.4.1 and the time course of the reaction can be seen in Figure C-20. The reaction speed of the cascade was just limited by the ADH reaction as no other intermediates could be detected and the reaction was worked up after 18 h at about 91% conversion. The yield of normal (4*S*,7*R*)-carvolactone (**7e**) was 65 mg which corresponds to 59% isolated yield. For each individual step of the cascade this would be an average of 84% yield per reaction.

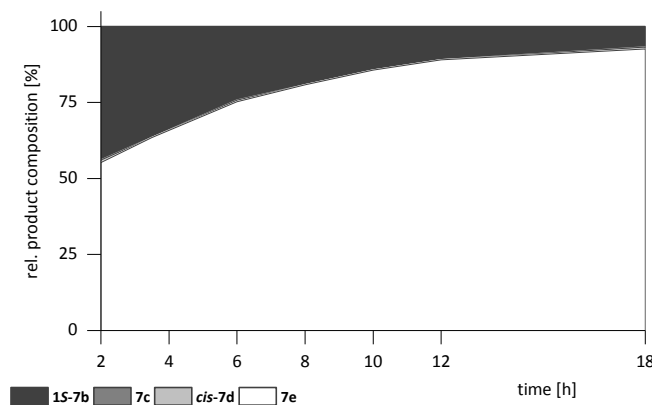


Figure C-20. Time course of the preparative scale *in vivo* cascade from (1*S*,5*S*)-carveol to (4*S*,7*R*)-carvolactone.

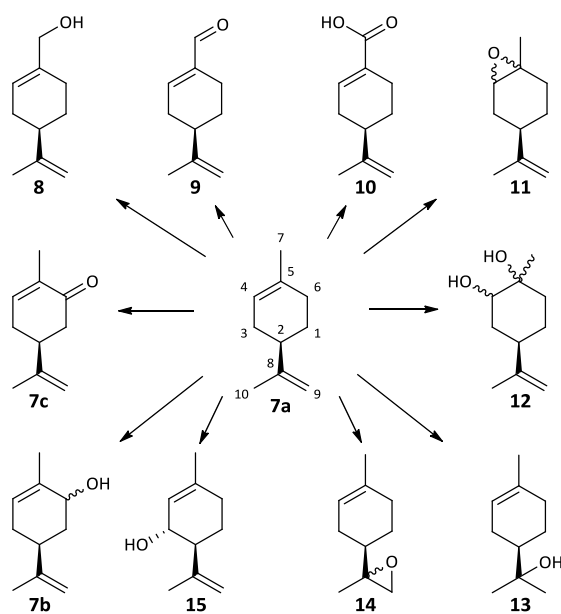
C III.9 Summary

In cascade reactions starting from seven different substrates the versatility and applicability of our enzymatic toolbox was also shown in the host organism *E. coli*. The approach was realized in an *in vivo* resting cell system with three heterologous enzymes which were natively not connected in a metabolic context. The constant availability of redox equivalents provided by the microbial host is advantageous compared to the *in vitro* system. The equilibrium of the first reaction of the three-step cascade, the oxidation catalyzed by an ADH which is reversible, could be shifted by the subsequent ERED reaction. The inversion of an ERED reduction was shown with *GkOYE* at elevated temperatures^[144] but reactions of XenB or OYE1 at our reaction conditions are irreversible. Hence the equilibrium was pulled towards the last intermediate. Undesired production of a side-product caused by a back-reaction of LK-ADH could in the most cases be limited due to another equilibrium shift induced by the irreversible reaction of BVMO leading to the desired lactone product.

C IV Hydroxylation of cyclic alkenes

To utilize cyclic alkenes as starting material in the four-step cascade reaction their hydroxylation had to be achieved. Literature dealing with hydroxylation of natural product limonene was consulted in the search for a suitable biocatalyst. An enzyme capable of limonene hydroxylation could prospectively also exhibit activity for the unnatural cyclic alkene substrates.

Hydroxylated derivatives of limonene such as perillyl alcohol (**8**), carveol (**7b**) or carvone (**7c**) have great market potential not only due to their pleasant fragrances^[145] but also have been reported to have anticancer or antifungal activities^[146]. Besides the disadvantage of using toxic reagents, chemical oxidations of limonene mostly resulted in a vast mixture of products. Biotransformation of limonene has been studied since the 1960s beginning with R-(+)-limonene feeding experiments of bacterial strains and detection of produced metabolites.^[147] Since then a lot of regio- and also stereoselective enzymatic hydroxylation reactions of limonene have been found. Van Beilen *et al.* reported the identification and cloning of a cytochrome P450 from *Mycobacterium sp.*, catalyzing the conversion of limonene to perillyl alcohol (**8**, hydroxylation in position 7)^[148], which has been applied in several interesting studies^[17, 59]. Hydroxylation of limonene in position 6 by *Solanum aviculare* and *Dioscorea deltoidea* plant cells lead to racemic carveol and carvone products.^[149] Caraway (+)-limonene-6-hydroxylase from *Carum carvi* exhibited strict regio- and enantiospecificity as the product consisted of over 95% (+)-*trans*-carveol^[150] and Duetz *et al.* used toluene-grown *Rhodococcus opacus* PWD4 (*Pseudomonas sp.* PWD32) to obtain the same product.^[151] The gene cluster coding for the enzyme, potentially responsible for this reaction, cumene dioxygenase (CumDO) was only very recently cloned into *P. putida* S12 allowing toluene-free enzyme production.^[152] Oxygenation of R-(+)-limonene in other positions (Scheme C-47) yielding in perillaldehyde (**9**), perillic acid (**10**), limonene-1,2-epoxide (**11**), limonene-1,2-diol (**12**), α -terpineol (**13**), limonene-8,9-epoxide (**14**) or isopiperitenol (**15**) was reviewed in detail by Duetz *et al.*^[147]



Scheme C-47. Diverse hydroxylations of R-(+)-limonene (**7a**), (adapted from Duetz *et al.*^[147])

The search for a suitable enzyme to be heterologously expressed in *E. coli* BL21(DE3) was mainly carried out by the project partner group at the University of Greifswald. Investigations on cytochrome P450-monooxygenase mutants from *Bacillus megaterium* (P450-BM3)^[153] have been conducted by Stefan Saß and Jan Muschiol^[154] who worked with a homologous enzyme from *Bacillus licheniformis* (CYP102A7)^[155] and the limonene-6-hydroxylase (L6H) from *Mentha spicata*^[156]. Unfortunately, all these approaches did not deliver a hydroxylating enzyme to be incorporated into our cascade reaction in *E. coli*. Therefore, other bacterial strains which were reported to regioselectively hydroxylate *R*-(+)-limonene to carveol were investigated.

C IV.1 Cellulosimicrobium cellulans EB-8-4

A bacterial wildtype strain was first investigated for its hydroxylation activity. *Cellulosimicrobium cellulans* EB-8-4 was described by the group of Prof. Li^[157] (National University of Singapore) to stereoselectively transform *R*-(+)-limonene (**7a**) to (1*R*,5*S*)-carveol (**1R-7b**).

C IV.1.1 Cultivation of *C. cellulans* EB-8-4

C. cellulans EB-8-4 was reported to show hydroxylation activity if grown on ethyl benzene (EtPh) as sole carbon source.^[157] As it was not stated specifically in the literature if the strain was cultivated under aerobic or anaerobic conditions, first cultivations were performed in closed Erlenmeyer flasks (plastic cap plus parafilm) as EtPh is volatile and flammable. To reproduce the literature *C. cellulans* EB-8-4 was cultivated in M9 medium either supplemented with glucose or in its absence and a 15 mL falcon tube (without cap) containing 1 mL EtPh was placed in the Erlenmeyer flask (see Figure C-21). After 26 h resting cells were prepared from these cultivations and biotransformations were performed, which only showed *R*-(+)-limonene hydroxylation activity when ethyl benzene was the sole C source. Therefore, all further cultivations were done without the addition of glucose.

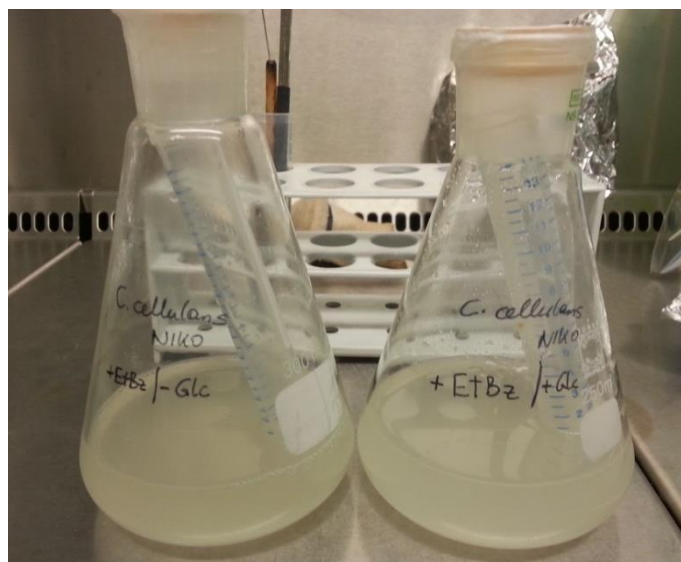


Figure C-21. First set-up for *C. cellulans* EB-8-4 cultivation.

Wang *et al.* reported a final cell dry weight (cdw) of 2.9 g L⁻¹ (corresponds to an OD₄₅₀ of about 10) whereas only about 0.4 g cdw L⁻¹ could be obtained in-house after the same incubation time of 24 h. To further investigate *C. cellulans* growth and in order to reproduce the literature values a cultivation experiment with 10 biological replicates in individual flasks was performed. While monitoring the growth, for each time-point a new flask was opened to minimize loss of carbon source EtPh. Cultivation time was extended to 42 h and these cultures were not used to prepare resting cells. At the end of this cultivation one culture showed significantly

higher cell density than the rest. A closer look showed that the glass stopper of this flask was quite loose, therefore the cultivation was rather aerobic than anaerobic.

After this insight, aerobic cultivation was further investigated and incubation time was shortened as Wang et al. [157] reported maximum hydroxylation activity after 24 h of cultivation. First experiments were performed on a small shaker at room temperature (RT) under the fume hood to observe the volatility of the flammable EtPh. No significant loss of EtPh was noted over the whole cultivation time (approx. 300 μ L in 28 h) and *C. cellulans* EB-8-4 showed much better growth under aerobic conditions as can be seen in Figure C-22. Reduced growth of the anaerobic cultivation in comparison to the previous cultivation can be explained by lowered incubation temperature.

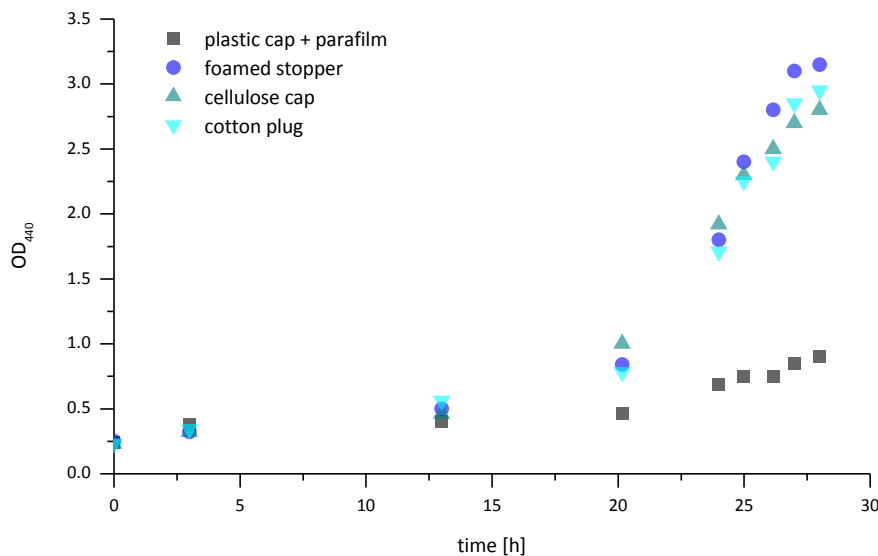


Figure C-22. Cultivation of *C. cellulans* EB-8-4 on a small shaker at 300 rpm and RT with different stoppers under the fume hood.

As no critical evaporation of EtPh could be detected the cultivations were subsequently performed in the large orbital shaker at 30 °C. For optimization of carbon source utilization, falcons with additional holes at different positions were used in the next cultivations to investigate the EtPh flow. The attempt to direct the EtPh flow through holes in the falcon nearer to the cell suspension, by closing the falcon and just piercing a hole into the cap, did not prove better than a normal falcon without cap. Usage of an EtPh falcon without cap and pierced openings at the mL markings 6, 7 and 10 led to higher cell densities, therefore offered better C source supply. Growth curves of the different approaches are visualized in Figure C-23.

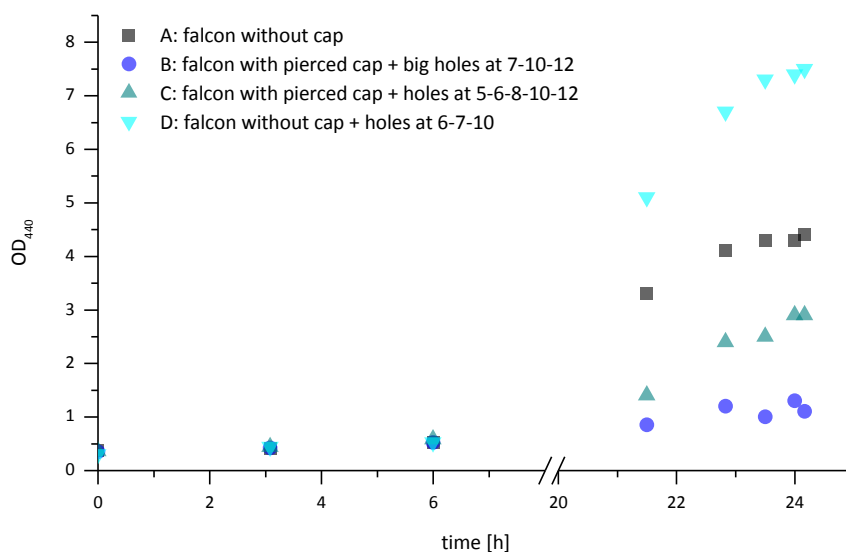
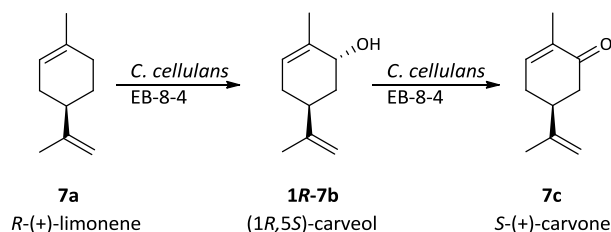


Figure C-23. Cultivation of *C. cellulans* EB-8-4 in an orbital shaker at 200 rpm and 30 °C with different EtPh falcons.

C IV.1.2 Biotransformations

C. cellulans EB-8-4 resting cells (130 mg cww mL⁻¹) from the first cultivations were tested for hydroxylation activity by adding 20 mM *R*-(+)-limonene and 100 mM glucose and samples were taken from single experiments. The high concentration of *R*-(+)-limonene was chosen as higher conversion rates were reported by Wang *et al.* (maximum at 62 mM) who also discovered overoxidation towards *S*-(+)-carvone (**7c**, Scheme C-48).



Scheme C-48. Hydroxylation of **7a** reported by Wang *et al.*

As can be seen in Figure C-24 recovery of starting material and product is rather poor. After 2 h reaction time the main product is (1*R*,5*S*)-carveol (**1R-7b**) but already **7c** could be detected. After 21 h more *S*-(+)-carvone (**7c**) than **1R-7b** was detected, although Wang *et al.* reported only small amounts of carvone.

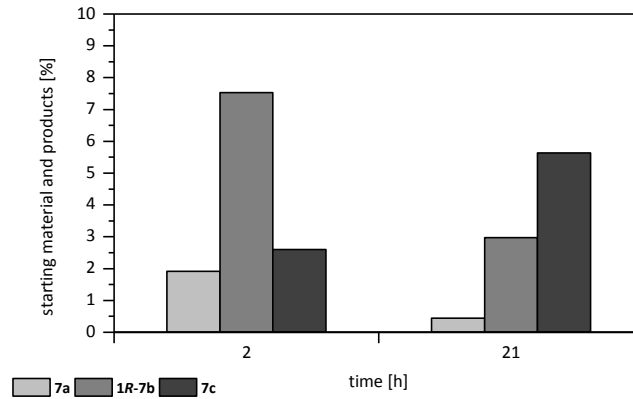


Figure C-24. 130 mg cww mL⁻¹ *C. cellulans* EB-8-4 resting cells supplemented with 20 mM *R*-(+)-limonene and 100 mM glucose.

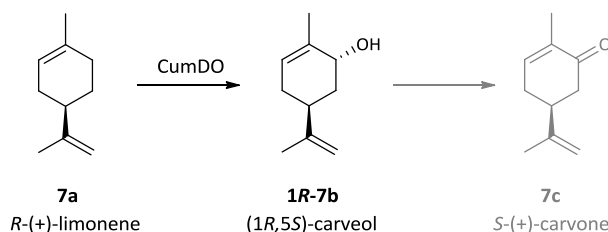
C IV.1.3 Contamination of *C. cellulans* EB-8-4

In the last cultivations color differences in the cell pellets were observed. In addition to the normally yellowish colored pellet also pink cells could be seen which indicated the presence of a second bacterial species. This problem was reported to our collaborating group in Greifswald where they already came across the problem. Katja Zorn cut protein bands from SDS-PA gels from cell lysate of *C. cellulans* cultivations and analyzed them via MALDI-MS. Checking the results in the NCBI protein databank only delivered matches with *Rhodococcus* but not *Cellulosimicrobium* enzymes. One of the databank hits was benzene-1,2-dioxygenase (gi|491396703) from *Rhodococcus* which shares 63.4% sequence identity with CumDo from *Rhodococcus opacus* PWD4^[151].

Katja was able to separate the differently colored strains and performed further experiments. The pinkish colored bacteria were identified as *Rhodococcus* sp. strain which also showed the *R*-(+)-limonene hydroxylation activity in contrast to the independently investigated *C. cellulans* strain. *C. cellulans* EB-8-4 was therefore not able to produce carveol from *R*-(+)-limonene as stated by Wang *et al.*^[157]. As the newly discovered transformation by *Rhodococcus* sp. did not show high conversions to carveol and the strain is S2 pathogenic, therefore would require special safety measures, this approach was not further investigated. Details on this part of the cooperative project can be found in the report by Katja Zorn (University of Greifswald) and the PhD thesis of Jan Muschiol^[154].

C IV.2 Cumene dioxygenase (CumDO) in *P. putida* S12

The expression system for cumene dioxygenase (CumDO) in *Pseudomonas putida* S12 was delivered from Prof. Marco W. Fraaije (Groningen) and CumDO was first tested for its limonene hydroxylation activity. Groeneveld *et al.* [152] reported that *R*-(+)-limonene (**7a**) was selectively transformed to (1*R*,5*S*)-carveol (**1R-7b**) and no overoxidation to *S*-(+)-carvone (**7c**) was observed (Scheme C-49).



Scheme C-49. Hydroxylation of **7a** by CumDO as reported by Groeneveld *et al.*.

Hydroxylation of *S*-(-)-limonene (**6a**) gave a mixture of products, including (1*R*,5*R*)-carveol (**1R-6b**) and (1*S*,5*R*)-carveol (**1S-6b**) [152]. The other cyclic alkenes which were planned as starting material for the cascade reaction should be tested after verification of **7a** hydroxylation and optimization of the reaction conditions.

C IV.2.1 Preparative scale - *R*-(+)-limonene (**7a**) to (1*R*,5*S*)-carveol (**1R-7b**)

A preparative scale experiment with 108 mg *R*-(+)-limonene (**7a**, 6 mM) was performed to verify the production of (1*R*,5*S*)-carveol (**1R-7b**) from *R*-(+)-limonene by *P. putida* S12 expressing CumDO resting cells (E IV.2.1, OD₅₉₀ = 3). An amount of 35 mg (1*R*,5*S*)-carveol (**1R-7b**) could be extracted from the resting cell suspension which relates to a yield of 29%. The value for specific rotation $\alpha_D^{25} = 140.2$ (*c* 0.87, CHCl₃) is in the range of the literature values [157-158]. The structure was confirmed via NMR and chiral GC measurement and showed that the retention of (1*R*,5*S*)-carveol (**1R-7b**) was in the same range as the other carveol isomers (Figure C-25).

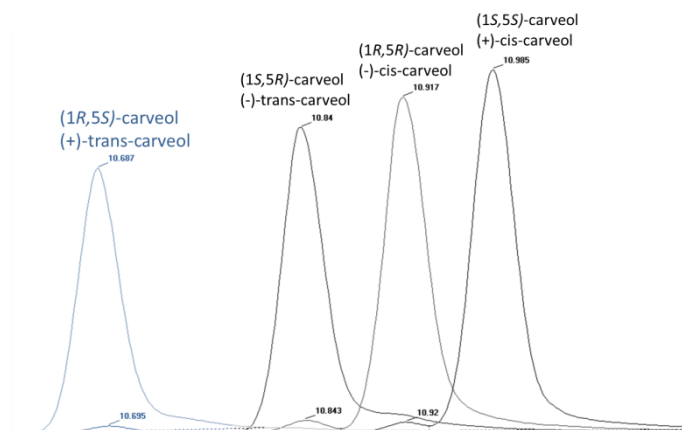


Figure C-25. Overlay of GC-chromatograms (BGB175) of all carveol isomers.

This result proved the production of (1*R*,5*S*)-carveol (**1R-7b**) from *R*-(+)-limonene (**7a**) by CumDO expressed in *P. putida* S12 and delivered access to the fourth carveol isomer which was not available through chemical synthesis (C I.2.1).

C IV.2.2 Expression of CumDO in *P. putida* S12

Expression was verified via SDS-PAGE and was comparable to the literature^[152] as the α -subunit of CumDO (52 kDa) as well as its β -subunit (22 kDa) could clearly be seen on SDS-PA gels (Figure C-26).

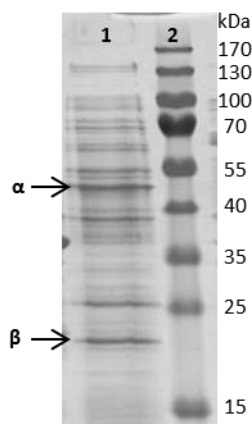


Figure C-26. SDS-PA gel of CumDO expression in TB medium; 1 – *P. putida* S12 pBTBX-2_CumDO whole cell sample, 2 – protein ruler

Cultivation of *P. putida* S12 was first performed in LB medium as described in the literature but a change to cultivation in TB medium for 6 h showed higher hydroxylation activity as can be seen in Figure C-27.

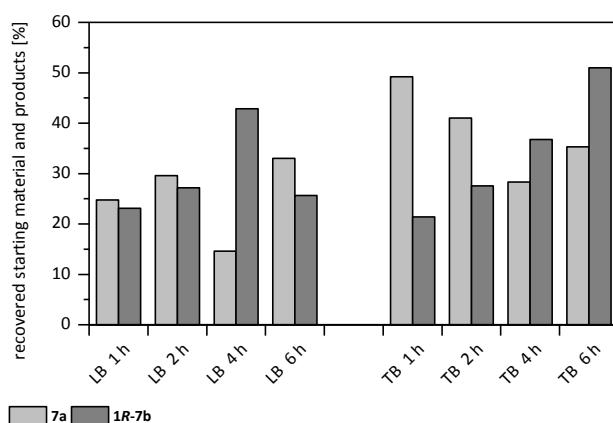


Figure C-27. Comparison of hydroxylation activity (12 h reaction) after expression for 1, 2, 4 or 6 h in LB or TB (single samples directly from culture).

C IV.2.3 Influence of buffer

As described in the literature^[152] resting cell suspensions of *P. putida* S 12 expressing CumDO with an OD₅₉₀ of 3 were prepared in K-buffer. The influence of the buffer on the hydroxylation reaction was investigated as our standard resting cell system was prepared with Tris-HCl buffer. Therefore resting cells were prepared from the same cultivation in K-buffer as well as Tris-HCl (E IV.2.1) and supplemented with *R*-(+)-limonene (**7a**). As can be seen in Figure C-28 the change to Tris-HCl buffer proved beneficial for the reaction as more carveol **1R-7b** could be detected.

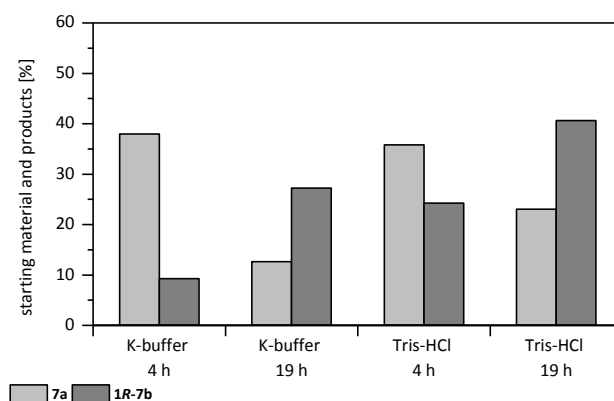


Figure C-28. Influence of the buffer on the hydroxylation reaction in single experiments.

C IV.2.4 Influence of cell density

Hydroxylation reactions with resting cells of *P. putida* S12 expressing CumDO (E IV.2.1) in different cell densities showed that increasing the OD₅₉₀ from 3 to approx. 20 improved the yield of **1R-7b** as can be seen in Figure C-29. Increasing the cell density significantly higher was not beneficial for the whole cell reaction.

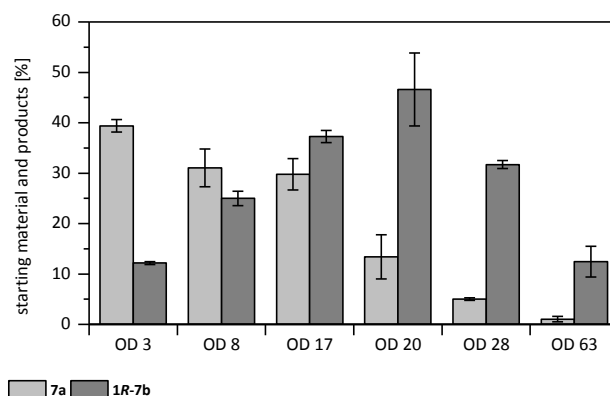


Figure C-29. Influence of cell density on the hydroxylation reaction of 4 mM *R*-(+)-limonene (**7a**) after 12 h reaction time.

C IV.2.5 Influence of *R*-(+)-limonene concentration

The literature stated that hydroxylation worked best with a *R*-(+)-limonene concentration of 6.2 mM^[152]. To investigate the influence of concentration of starting material on the reaction resting cells of *P. putida* S12 with expressed CumDO (for preparation see E IV.2.1) were supplemented with different concentrations of *R*-(+)-limonene. As depicted in Figure C-30, with decreasing concentrations of *R*-(+)-limonene better conversions to (1*R*,5*S*)-carveol (**1R-7b**) could be achieved. While reaching only about 40% conversion at a *R*-(+)-limonene (**7a**) concentration of 4 mM, with 0.5 mM **7a** nearly 80% carveol (**1R-7b**) could be detected.

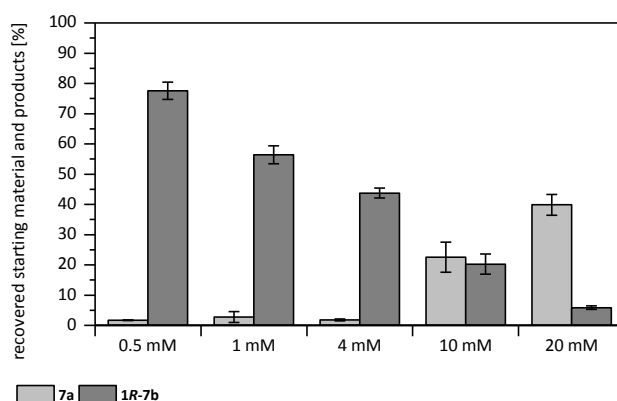


Figure C-30. Influence of *R*-(+)-limonene concentration on the hydroxylation reaction.

C IV.2.6 Variations in *R*-(+)-limonene extraction

As can be seen in the previous figures recovery of *R*-(+)-limonene from the reactions was rather unreliable and varying due to the high volatility of *R*-(+)-limonene and its minimal water solubility. Several experiments were performed to achieve better *R*-(+)-limonene recovery including testing of different organic solvents for extraction of the reactions and the addition of a surfactant to enhance phase transfer. For these experiments 1% Triton X-100 was added to aqueous buffer supplemented with *R*-(+)-limonene (**7a**) and *S*-(+)-carvone (**7c**) which was then extracted with chloroform (CHCl₃), dichloromethane (DCM), ethyl acetate (EtOAc), 2-methyltetrahydrofuran (Me-THF) and methyl tert-butyl-ether (MTBE). The comparison of the different solvents and the influence of Triton X-100 are shown in Figure C-31.

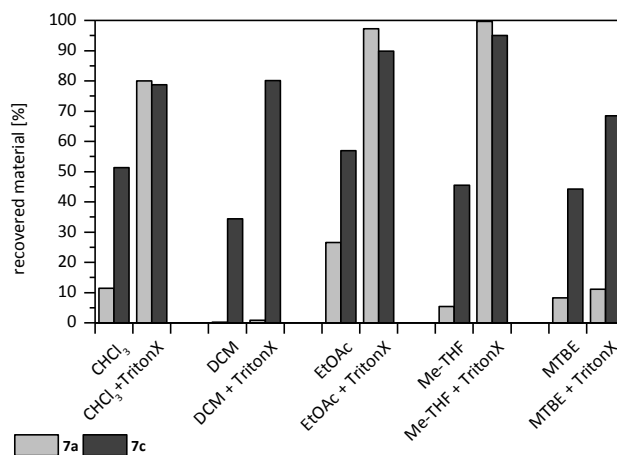


Figure C-31. Recovery of *R*-(+)-limonene and carvone from aqueous buffer extracted with different organic solvents with or without the addition of Triton X-100.

The recovery of *R*-(+)-limonene (**7a**) as well as of *S*-(+)-carvone (**7c**) was enhanced by the addition of Triton X-100 in combination with all organic solvents except with DCM, which rendered unfeasible for *R*-(+)-limonene extraction even after addition of surfactant. With addition of Triton X-100 to the extracted solution, Me-THF emerged as the best extraction solvent but nearly full recovery was achieved with Triton X-100 and EtOAc. Additionally EtOAc is cheaper than Me-THF and gave the best results without the addition of Triton X-100 and was therefore maintained as standard extraction solvent.

C IV.2.7 Influence of Triton X-100 on the hydroxylation reaction

As the addition of Triton X-100 enhanced the recovery of *R*-(+)-limonene the influence of the addition of this surfactant to the *P. putida* S12 expressing CumDO resting cell hydroxylation reaction was tested. Supplementing either the TB culture directly after expression or resting cells concentrated to OD 50 in Tris-HCl with 1% Triton X-100 interfered with the hydroxylation reaction as conversion to carveol **1R-7b** was lowered. Also the improvement of *R*-(+)-limonene (**7a**) recovery was only minimal as can be seen in Figure C-32.

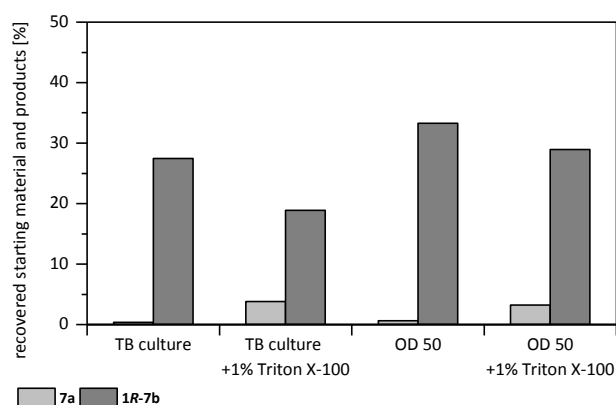
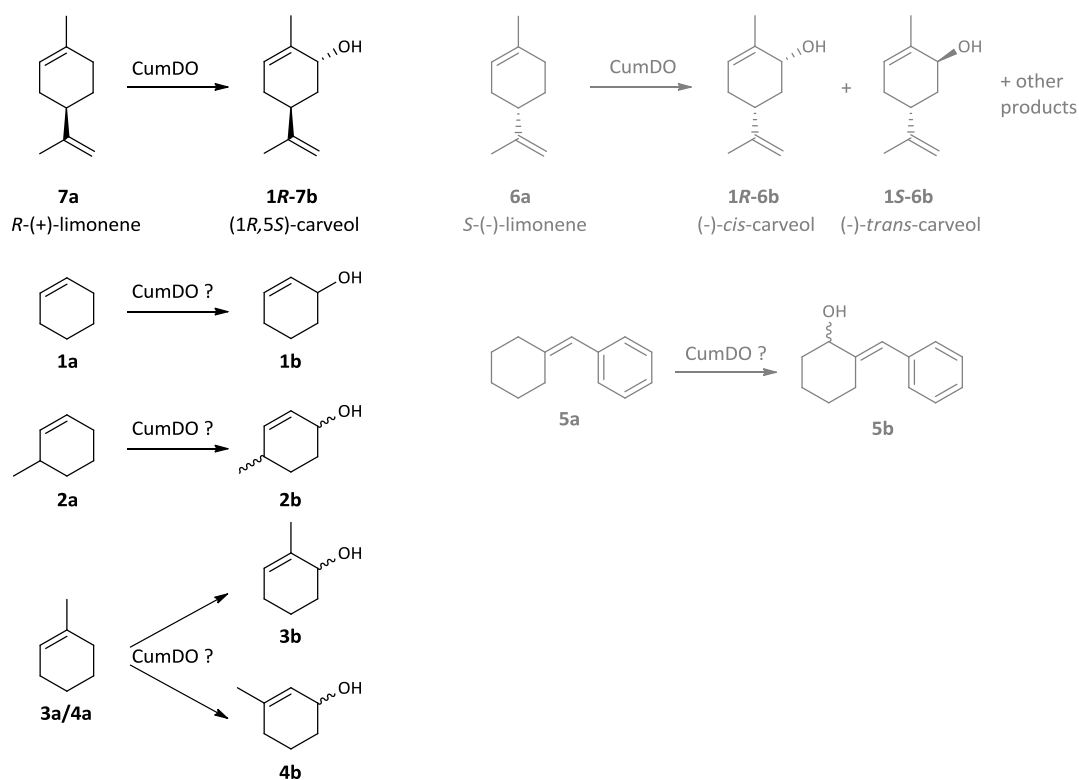


Figure C-32. Influence of Triton X-100 addition on hydroxylation reaction.

C IV.2.8 Hydroxylation of other cyclic alkenes

After evaluating the hydroxylation of *R*-(+)-limonene which was reported, the activity of CumDO towards the cyclic alkenes which were planned as starting material for extended cascade reactions should be tested. According to the literature *S*-(-)-limonene (**6a**) was converted to a mixture of products which was not desirable for our purpose and therefore not included in this study. The three-step-cascade starting from **5b** as discussed in C II.5 did not deliver satisfying results, hence the use of substrate **5a** was omitted. As CumDO stereoselectively hydroxylated **7a**, hydroxylation of the other cyclic alkenes **1a**, **2a** and **3a/4a** was hypothesized in corresponding positions as shown in Scheme C-50.



Scheme C-50. Possible hydroxylation of cyclic alkenes according to **7a** hydroxylation.

Resting cells of *P. putida* S12 with expressed CumDO were supplemented with 1 mM of cyclic alkene and the reactions were performed according to the *R*-(+)-limonene hydroxylation (C IV.2.5). The results are summarized in Table C-8.

Table C-8. Hydroxylation of cyclic alkenes.

Entry	Substrate	Product	GC yield [%]
1	1a	1b	25
2	2a	2b	3
3	3a/4a	3b	23
4	3a/4a	4b	6

As can be seen in Table C-8, hydroxylation of the cyclic alkenes did not proceed very well. The best result (entry 1) was obtained with the simplest substrate cyclohexene (**1a**) which was converted to cyclohex-2-en-1-ol (**1b**) in 25% yield. Substrate **3a/4a** was hydroxylated preferably in 2-position, most probably due to the highest stereochemical similarity to the natural reaction from **7a** to **1R-7b**, but unfortunately yielding only 23% **3b**. The transformations to **2b** and **4b** both yielded fewer than 10% rendering further applications as unfeasible. Additionally to low yields recovery of material was insufficient maybe due to volatility of the substrates.

C IV.3 CumDO in *Pseudomonas taiwanensis* VLB120 Δ C Δ ttgV

Pseudomonas taiwanensis VLB120 Δ C Δ ttgV was reported by the group of Prof. Bruno Bühler for its constitutive solvent tolerance^[159], a characteristic which would be an interesting feature for a microbial host used for limonene hydroxylation. Intolerance of the host to solvents possibly used for two-liquid phase systems^[59] or problems with toxic effects by limonene itself^[160] could be circumvented with a solvent tolerant strain. *P. putida* S12 can also be adapted to solvents^[161] but this is a tedious and time consuming procedure which could be avoided by the utilization of a constitutive solvent tolerant strain.

Therefore *P. taiwanensis* VLB120 Δ C Δ ttgV (*P. taiwanensis*) should be tested as expression host for the *R*-(+)-limonene hydroxylating enzyme CumDO. The strain was provided by Prof. Bruno Bühler and transformed with the expression plasmid for CumDO (pBTBX-2_CumDO) extracted from *P. putida* S12 (provided by Prof. Marco Fraaije).

C IV.3.1 Cultivation and expression of CumDO in *P. taiwanensis* in LB

First cultivation experiments with three positive clones of *P. taiwanensis* pBTBX-2_CumDO were performed in LB medium with *P. taiwanensis* and *P. putida* S12 pBTBX-2_CumDO as controls. Here it was observed that the *P. taiwanensis* pBTBX-2_CumDO clones showed slower growth (longer lag phase) than the wildtype *P. taiwanensis* as well as *P. putida* S12 pBTBX-2_CumDO. Figure C-33 presents a crude SDS-PA gel showing expression 3 h and 9 h after induction.

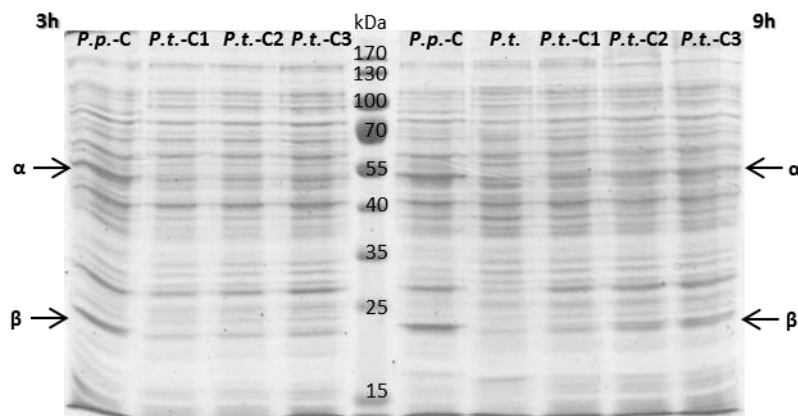


Figure C-33. Crude SDS-PA gel of CumDO expression test in *P. taiwanensis* in LB.

P.p.-C – *P. putida* S12 pBTBX-2_CumDO; *P.t.-C1*, *P.t.-C2*, *P.t.-C3* – *P. taiwanensis* pBTBX-2_CumDO clones 1-3; *P.t.* – *P. taiwanensis*

As can be seen in Figure C-33 expression of CumDO in *P. taiwanensis* is decreased in comparison to its production in *P. putida* S12. Especially the α -subunit is poorly present even after 9 h expression time.

C IV.3.2 Cultivation and expression of CumDO in *P. taiwanensis* in M9

Due to low expression levels in LB medium cultivation of *P. taiwanensis* pBTBX-2_CumDO clones was tested in M9 medium, which was also used by Volmer *et al.*^[159]. L-Arabinose was used as inducer for the expression of pBTBX-2_CumDO which would not be utilized if cultures are grown on D-glucose, which M9 is generally supplemented with. Therefore, glycerol was tested as C source for the minimal medium which led to much slower growth compared to D-glucose as C source. Resting cells of these expression experiments were prepared 17 h after induction. Expression can be seen in a crude SDS-PA gel shown in Figure C-34.

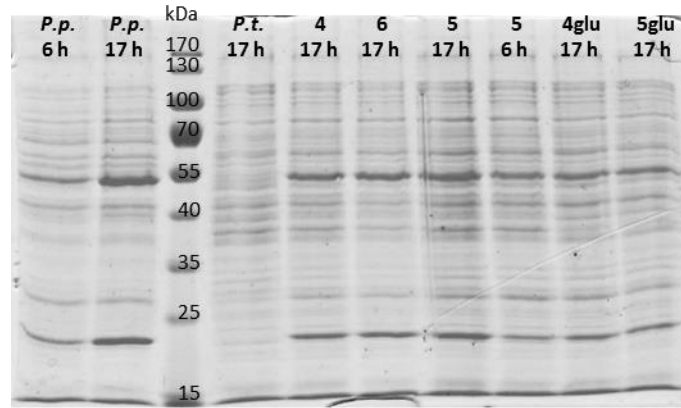


Figure C-34. Crude SDS-PA gel of CumDO expression test in *P. taiwanensis* in M9 medium after different expression times.
P.p. – *P. putida* S12 pBTBX-2_CumDO; *P.t.* – *P. taiwanensis*; 4,5,6 – *P. taiwanensis* pBTBX-2_CumDO clones 4-6;
 4glu, 5glu – *P. taiwanensis* pBTBX-2_CumDO clones 4-5 expressed in M9 with glucose.

In Figure C-34 it can be observed that CumDO expression in M9 is still better in *P. putida* S12 than in *P. taiwanensis* but has improved from the expression in LB medium. Despite expected carbon catabolite repression, CumDO is expressed in presence of glucose, possibly due to the high concentration of inducer L-arabinose.

C IV.3.3 Limonene hydroxylation with CumDO in *P. taiwanensis*

Resting cells of the expression described in C IV.3.2 were supplemented with *R*-(+)-limonene to test hydroxylation activity of CumDO expressed in *P. taiwanensis*. A single experiment with *P. putida* S12 resting cells expressing CumDO was performed as control reaction. The results after 3 h and 5 h reaction time are depicted in Figure C-35.

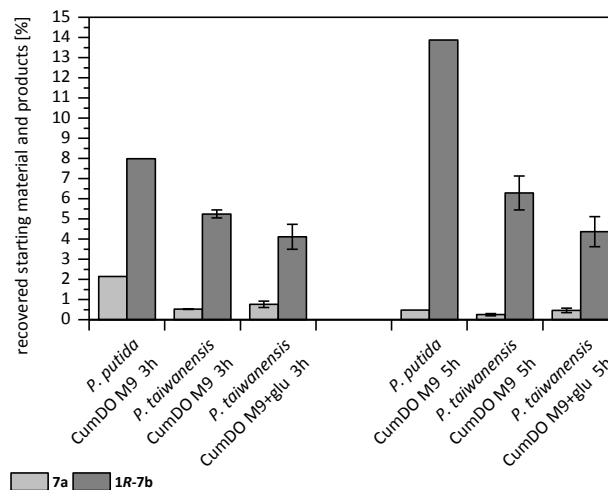


Figure C-35. Hydroxylation of *R*-(+)-limonene by CumDO expressed in different microbial hosts and in different media.
P. taiwanensis CumDO M9 gives mean values of 3 clones of *P. taiwanensis* pBTBX-2_CumDO expressed in M9 medium and *P. taiwanensis* CumDO M9+glu gives mean values of 2 clones of *P. taiwanensis* pBTBX-2_CumDO expressed in M9 supplemented with glucose.

Albeit very poor recovery for this hydroxylation experiment, general observations could be made. Hydroxylation activity of CumDO expressed in *P. taiwanensis* is decreased in comparison to CumDO expressed in *P. putida* S12. Slightly lowered expression could be observed when glucose was supplemented to M9, which possibly accounts for the lowered hydroxylation activity of CumDO expressed in this medium.

C IV.4 Summary

As the search for an oxygenase to be implemented in the microbial host *E. coli* for the hydroxylation of cyclic alkenes, the first step of the designed cascade reaction, was unsuccessful, other bacterial strains were investigated. *C. cellulans* EB-8-4, that was reported to hydroxylate *R*-(+)-limonene, which was also in the planned substrate scope, was tested first. Hydroxylation of *R*-(+)-limonene as well as further oxidation of carveol to carvone could be detected but the results were not consistent. Unfortunately, a contamination in *C. cellulans* was discovered and identified as a *Rhodococcus* strain, which was responsible for the hydroxylation. As *Rhodococcus* is a pathogenic strain it proved unfeasible for our work and this approach was not further investigated.

The second approach was the use of *P. putida* S12 with heterologously expressed CumDO which was reported to hydroxylate *R*-(+)-limonene to (1*R*,5*S*)-carveol. This finding could be replicated and the reaction conditions optimized before the other cyclic alkenes from the substrate scope were also tested. Unfortunately no good conversions could be achieved here but the specific hydroxylation of *R*-(+)-limonene opened the possibility to investigate a mixed-culture approach to extend the three-step cascade reaction which will be discussed in chapter C VI.

The integration of CumDO in the constitutively solvent tolerant strain *P. taiwanensis* VLB120 was also investigated. Although production of CumDO was achieved, its hydroxylation activity was decreased compared to if the enzyme was produced in *P. putida* S12. Improvement of the expression system could not be realized in the course of this thesis. As solvent tolerance would be an advantageous feature for a microbial host used for biotransformations of non-native substrates this concept should be investigated in future work.

C V Metabolic engineering

In this chapter different approaches on engineering of the host organism *E. coli* BL21(DE3) are described. Observation of background reactions led to the desire to construct knockout (KO) strains to eliminate these native activities. Furthermore, a plan to integrate heterologous genes into the *E. coli* genome to reduce the metabolic burden of multiple plasmid systems was set up.

C V.1 Identification of an *E. coli* background reaction

After observing a native *E. coli* ERED reaction (C II.1), the amino acid (aa) sequence of the ERED OYE1 was subjected to BLAST® analysis limiting the results to *E. coli* BL21(DE3) enzymes and two highly similar hits were retrieved. N-Ethylmaleimide reductase (NemR) was found to have a query cover of 94% (max. score of 220) and 2,4-dienoyl-CoA reductase (DCR) covered the query with 64% (may. score 86.3) (Figure C-36).

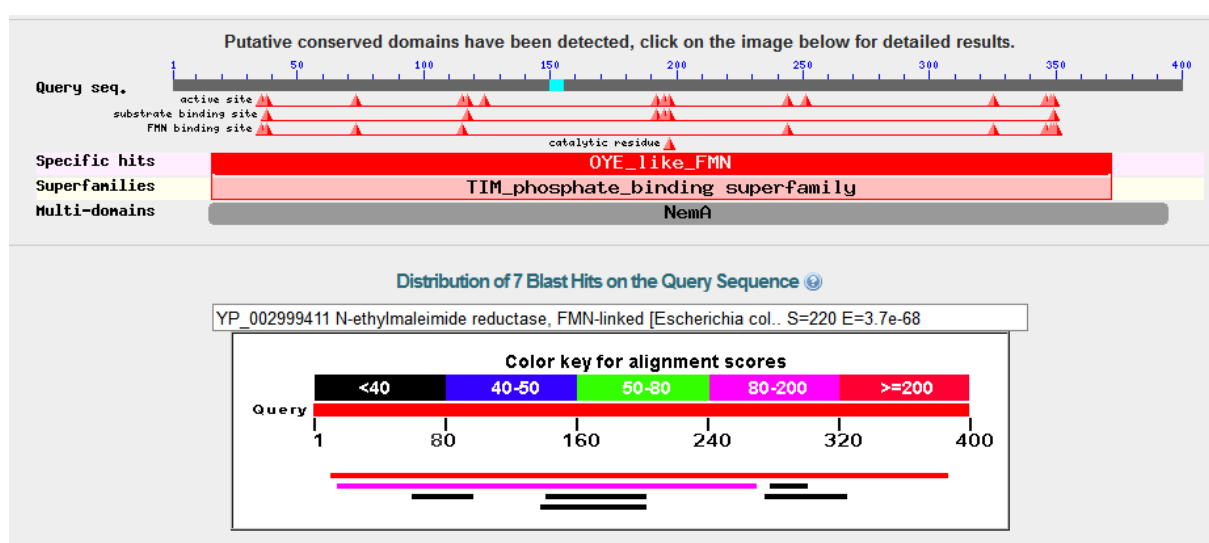
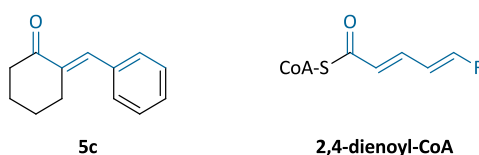


Figure C-36. Screenshot of the BLAST® search results.

Searching the literature for these *E. coli* enzymes, the work of the group of Prof. Faber was consulted where the first BLAST® hit NemR was amongst other EREDs characterized regarding its substrate spectrum^[139]. Here NemR was reported to have activity towards 2-methylcyclohex-2-en-1-one (**3c**), 3-methylcyclohex-2-en-1-one (**4c**) and *R*-(-)-carvone (**6c**). Unsubstituted 2-cyclohexen-1-one (**1c**), where we first observed the background reaction, was not examined in the literature.

The second hit, DCR was found to be characterized regarding its structure and reaction mechanism but was not reported to be applied in biocatalysis.^[162-166] The enzymes natural substrate 2,4-dienoyl-CoA exhibits similarities to the core structure of 2-benzylidenecyclohexanone (**5c**, Scheme C-51) which was reduced to **5d** by an *E. coli* BL21(DE3) background reaction (C II.5).

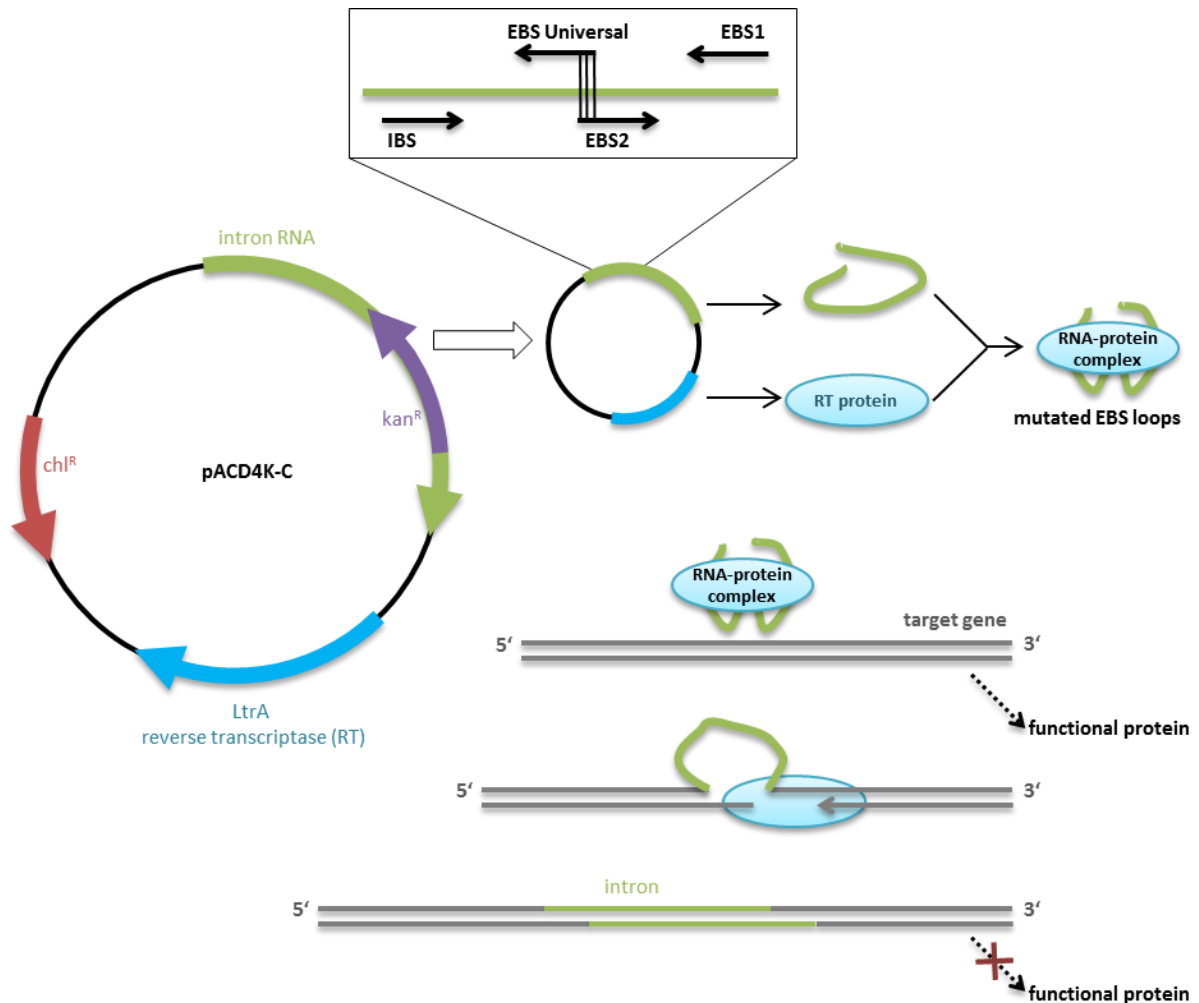


Scheme C-51. Structural similarities between **5c** and 2,4-dienoyl-CoA marked in blue.

Therefore the construction of a double KO strain, which should be deficient of native ERED activities and could serve as expression host for heterologous EREDs, was planned. As NemR was identified as background enzyme with the higher similarity it was decided to first create an *E. coli nemA* (gene coding for NemR) knockout (KO) strain and later disrupt *fadH*, the gene coding for DCR, resulting in the double KO strain *E. coli* BL21(DE3) $\Delta nemA \Delta fadH$. Both the single KO strains *E. coli* $\Delta nemA$ and *E. coli* $\Delta fadH$ were available through the keio collection and were not reported to have any striking growth defects.^[53] Although the influence of the disruption of both *nemA* and *fadH* in one strain was not reported in the literature and despite the difference that the keio collection was based on *E. coli* K-12 and we were working with *E. coli* BL21(DE3) the reported unchanged physiology of the KO strains encouraged our plans.

C V.2 *E. coli* BL21(DE3) $\Delta nemA$ – NemR deficient strain

The TargetTron® Gene Knockout System (Sigma Aldrich) was chosen to generate *E. coli* BL21(DE3) $\Delta nemA$ by disrupting the *nemA* gene with a group II intron^[167] via a RNA protein complex (Scheme C-52). The RNA protein complex is expressed via the pACD4K-C vector which is delivered with the kit and customized with individual re-targeting primers (IBS, EBS1, EBS2) to later direct the intron to the desired site. The intron bears a kanamycin resistance (kan^R) marker to select strains with disrupted genes of interest.



Scheme C-52. Group II intron insertion via the TargetTron® Gene Knockout System adapted from the manual.

C V.2.1 Verification of *nemA* disruption via PCR

According to the TargeTron® manual the intron should be approx. 2000 bp long but after sequence analysis of the pACD4K-C intron expression vector in Geneious® the intron length was assigned with 2289 bp. This length was used to calculate the PCR product sizes for the verification of the disrupted gene.

To confirm group II intron insertion, PCR with primers flanking the gene *nemA* was first performed in a colony PCR to directly identify positive clones. However only for some clones a negative PCR product (1199 bp), signaling intact *nemA*, and for the other clones no product could be seen on agarose gels. This led to the conclusion that the PCR product size (3488 bp) of *E. coli* BL21(DE3) $\Delta nemA+kan^R$ clones is too big for colony PCR. Hence genomic DNA (gDNA) of *E. coli* BL21(DE3) and putative *E. coli* BL21(DE3) $\Delta nemA+kan^R$ clones was extracted and used as PCR templates. Albeit all different primer combinations gave PCR products with this approach, the product sizes of the putative KO clones were smaller than expected.

Due to the length inconsistencies between the PCR products on agarose gels and the calculated sizes, a PCR product putatively containing the intron was sent for sequencing, which revealed a 393 bp shorter intron size. The actual size of the intron inserted from pACD4K-C was therefore reduced to 1896 bp. The revised PCR product sizes conferred with the products visualized on agarose gels consequently confirming the construction of *E. coli* BL21(DE3) $\Delta nemA+kan^R$.

C V.2.2 Confirmation of NemR deficiency via biotransformation tests

To verify that the enzyme NemR is not produced anymore after disruption of *nemA*, a possible candidate of *E. coli* BL21(DE3) $\Delta nemA+kan^R$ was subjected to biotransformation reactions. CFE of the wildtype *E. coli* BL21(DE3) and the disruption strain *E. coli* BL21(DE3) $\Delta nemA+kan^R$ were prepared and incubated with NADP⁺, cofactor regeneration system and *R*-(-)- (**6c**) as well as *S*-(+)-carvone (**7c**). As can be seen in Figure C-37 the wildtype strain shows reductive activity for both carvone isomers which is lost in *E. coli* BL21(DE3) $\Delta nemA+kan^R$ proving the construction of a NemR deficient strain.

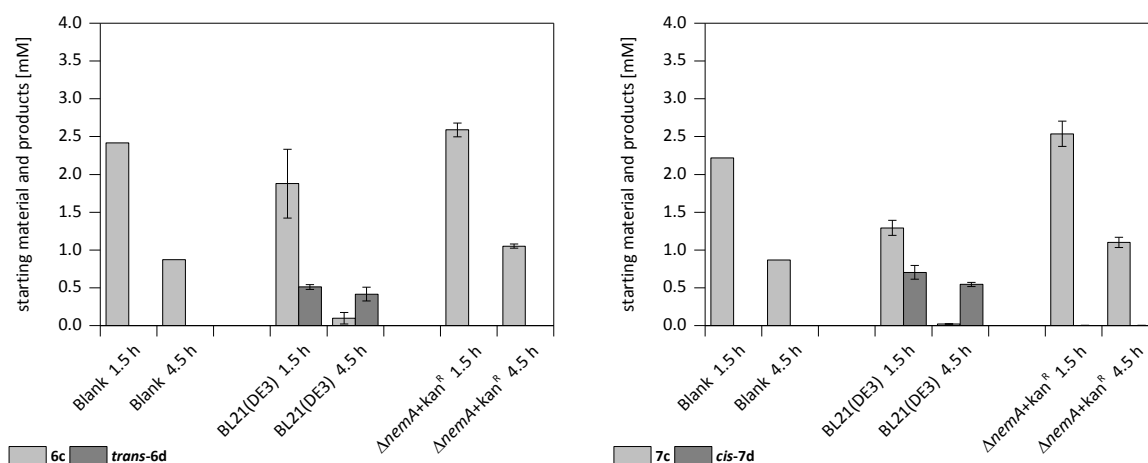


Figure C-37. *In vitro* biotransformations for the verification of *E. coli* BL21(DE3) $\Delta nemA$.

To further investigate the discovered background reactions, cell free extracts of both *E. coli* BL21(DE3) and *E. coli* BL21(DE3) $\Delta nemA+kan^R$ expressing no heterologous enzyme were also supplemented with 2-benzylidenecyclohexanone (**5c**) and cofactors. With both strains this resulted in conversion to the stereoisomers of 2-benzylcyclohexanone (**5d-1** and **5d-2**) in a highly similar manner (Figure C-38). Thus the observed background reaction cannot be accounted for solely by NemR and the involvement of the second native *E. coli* ERED DCR in this background reaction was hypothesized.

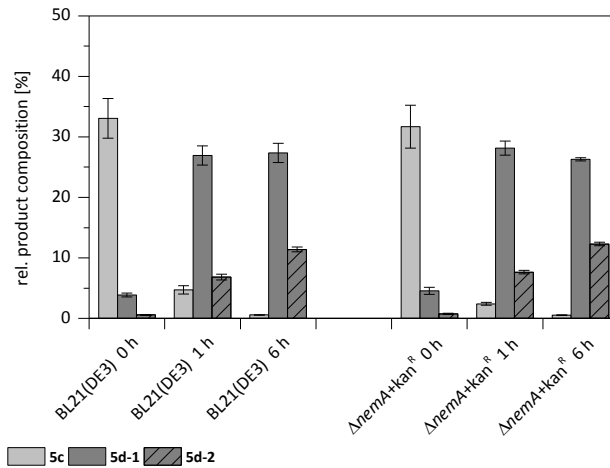
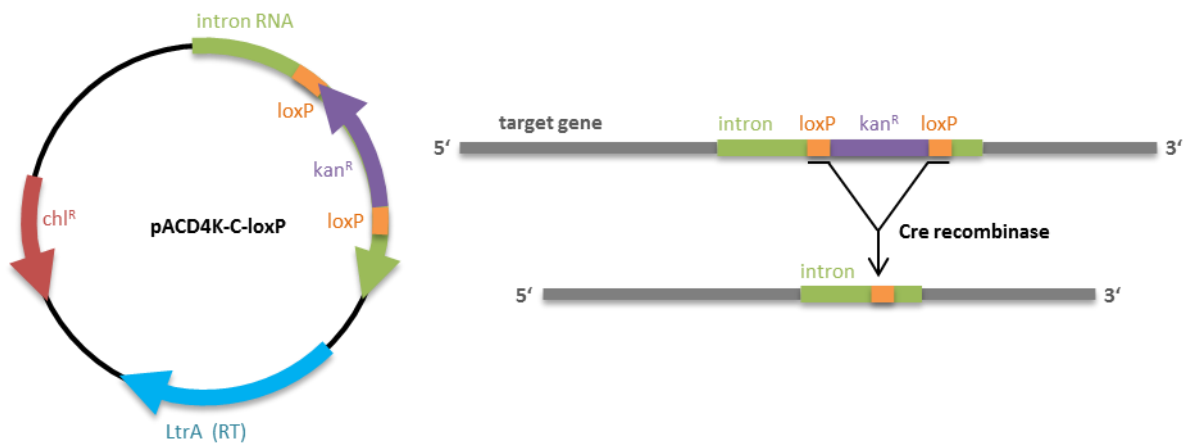


Figure C-38. Conversion of **5c** to stereoisomers **5d-1** and **5d-2** by CFE of *E. coli* BL21(DE3) and *E. coli* BL21(DE3) $\Delta nemA+kan^R$ not expressing any heterologous enzyme.

C V.2.3 Removal of kanamycin resistance

As *E. coli* BL21(DE3) $\Delta nemA$ should consequently be objected to the disruption of the gene *fadH*, the kanamycin resistance introduced through the TargeTron® Gene Knockout System used for selection emerged troublesome. Additionally expression plasmids with kan^R could not be maintained in *E. coli* BL21(DE3) $\Delta nemA+kan^R$ as the strain itself held the antibiotic resistance. Thus it was decided on the use of the TargeTron® knockout vector pACD4K-C-loxP which provides the possibility to remove the resistance marker via loxP site recombination. After the initial disruption strain is constructed the loxP sites flanking kan^R can be recombined by a Cre recombinase, hence cutting out the antibiotic resistance (Scheme C-53).



Scheme C-53. Principal of the removal of kan^R with Cre recombinase (according to the product information for TargeTron® pACD4K-C-loxP).

So the TargeTron® Gene Knockout procedure was executed again with pACD4K-C-loxP and the disruption of *nemA* confirmed via PCR. The size of the intron inserted by pACD4K-C-loxP was a little bit longer (1963 bp) due to the loxP sites. A positive clone of *E. coli* BL21(DE3) $\Delta nemA-loxP$ was transformed with the 706-Cre plasmid and after expression of the Cre recombinase positive clones were checked for kanamycin resistance via replica-plating. Colonies which lost the antibiotic resistance were checked via PCR verifying the construction of kan^R free *E. coli* BL21(DE3) $\Delta nemA$.

C V.3 *E. coli* BL21(DE3) $\Delta nemA$ $\Delta fadH$ – double knockout

The same KO strategy as for the NemR deficient strain, the TargeTron[®] system using the pACD4K-C-loxP, was chosen but now the disruption of *fadH* was done in *E. coli* BL21(DE3) $\Delta nemA$ to obtain a double KO strain. Removal of kanamycin resistance was executed according to the procedure performed on *E. coli* BL21(DE3) $\Delta nemA+kan^R$ and all steps were verified via PCR.

C V.3.1 Biotransformations to test for DCR disruption

After identifying the first clone of the double disruption strain, biotransformation tests with 2-benzylidenecyclohexanone (**5c**) and *R*-(-)-carvone (**6c**) were performed in single experiments and the results are shown in Figure C-39.

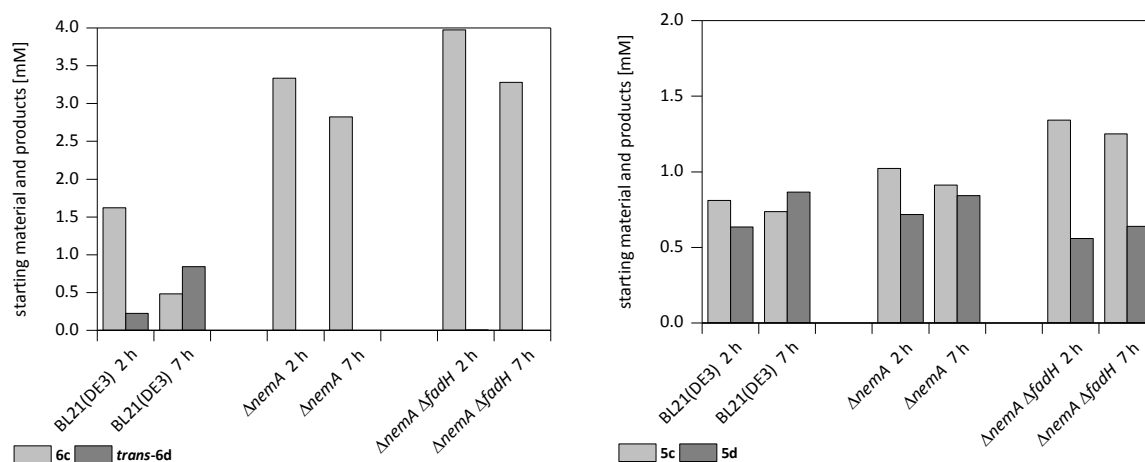
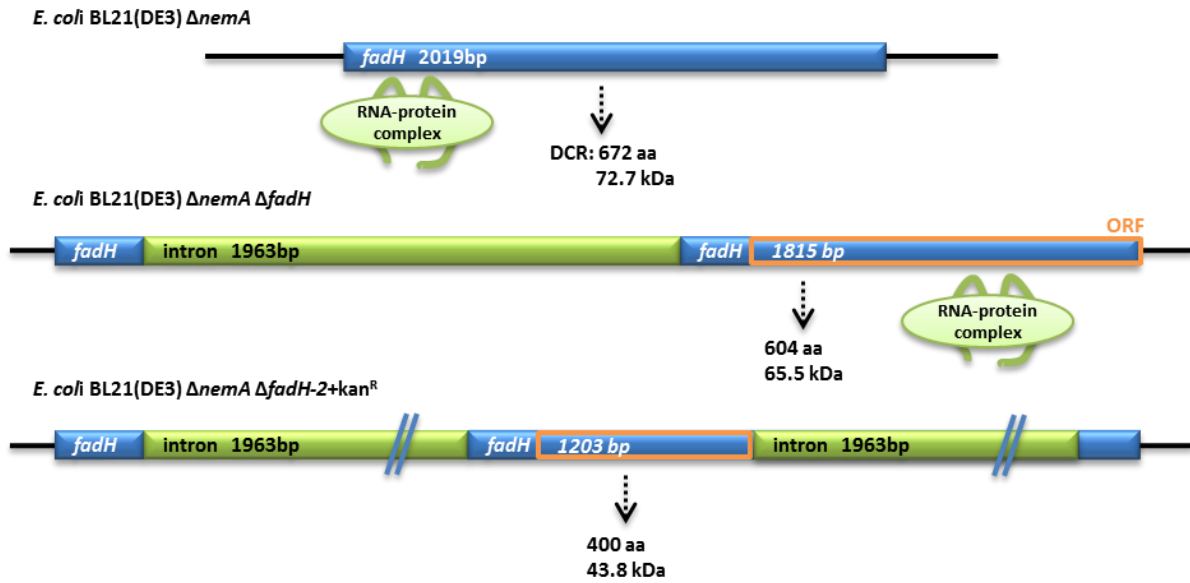


Figure C-39. Biotransformation tests with resting cells of *E. coli* BL21(DE3), *E. coli* BL21(DE3) $\Delta nemA$ and *E. coli* BL21(DE3) $\Delta nemA \Delta fadH$.

As can be seen in the above figure the activity for reducing *R*-(-)-carvone (**6c**) is lost in *E. coli* BL21(DE3) $\Delta nemA$ as well as in *E. coli* BL21(DE3) $\Delta nemA \Delta fadH$. As already shown before the disruption of *nemA* did not have an influence on the conversion of **5c**. Unfortunately also resting cells of *E. coli* BL21(DE3) $\Delta nemA \Delta fadH$, where the background enzyme DCR should not be produced anymore, still exhibited reduction of **5c** to **5d**. Although the ERED activity was a little reduced it was assumed that the disruption of DCR had not been efficient.

C V.3.2 *E. coli* BL21(DE3) $\Delta nemA \Delta fadH-2+kan^R$

Through sequence analysis it was discovered that the group II insertion left an open reading frame (ORF) of 1815 bp available therefore only shortening DCR of 68 aa. As the shortened enzyme could maybe still have activity it was decided to perform a second group II intron insertion in the gene *fadH*. The KO procedure was again performed on *E. coli* BL21(DE3) $\Delta nemA \Delta fadH$ and the resulting strain with two insertions in *fadH* was named *E. coli* BL21(DE3) $\Delta nemA \Delta fadH-2+kan^R$. The procedure of the two group II intron insertions is illustrated in Scheme C-54.



Scheme C-54. Group II intron insertion in the *fadH* gene, available ORFs and resulting protein sizes.

With a positive clone of *E. coli* BL21(DE3) $\Delta nemA \Delta fadH-2+kan^R$ biotransformation tests with **5c** were performed as before. As controls resting cells of *E. coli* BL21(DE3) and *E. coli* BL21(DE3) $\Delta nemA \Delta fadH$ were also supplemented with the substrate and the results are depicted in Figure C-40.

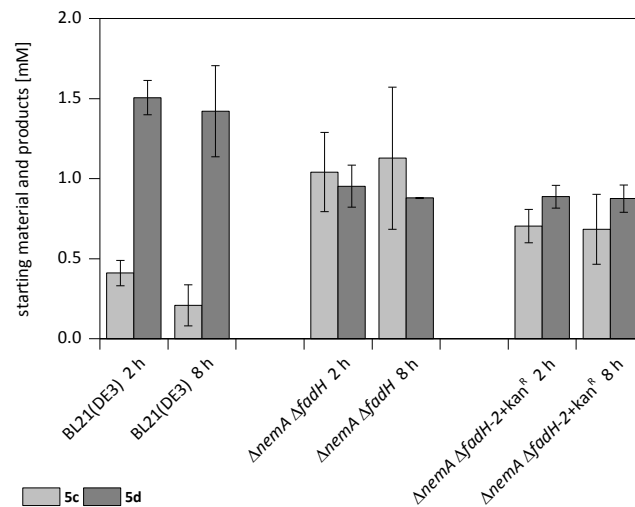


Figure C-40. Reduction of **5c** by resting cells of *E. coli* BL21(DE3), *E. coli* BL21(DE3) $\Delta nemA \Delta fadH$ and *E. coli* BL21(DE3) $\Delta nemA \Delta fadH-2+kan^R$.

As already shown before reduction activity of *E. coli* BL21(DE3) $\Delta nemA \Delta fadH$ was decreased but not extinguished as anticipated. This decreased activity of *E. coli* BL21(DE3) $\Delta nemA \Delta fadH$ for **5c** could unfortunately not be minimized through another group II intron insertion in the gene *fadH* as *E. coli* BL21(DE3) $\Delta nemA \Delta fadH-2+kan^R$ shows similar reduction activity (Figure C-40). As it is highly unlikely that an even shorter version of DCR (400 aa) still has activity, these results strongly indicate that DCR is not solely responsible for the reduction of **5c** but rather indicate the presence of another native *E. coli* reducing background enzyme.

Further sequence searches in BLAST® did not reveal any other putative *E. coli* native EREDs so that the investigations were stopped at this point due to scope and timeline restrictions of this thesis. Nevertheless *E. coli* BL21(DE3) $\Delta nemA \Delta fadH$ was established as an expression host with reduced native ERED activity, rendering it feasible for future whole cell studies on heterologously expressed EREDs.

C V.4 Cloning of *nemA* and *fadH* from *E. coli*

After obtaining *E. coli* BL21(DE3) $\Delta nemA \Delta fadH$ as a background minimized platform for ERED expression we were interested in the activities of the *E. coli* native EREDs NemR and DCR. Whilst NemR was already quite elaborately characterized regarding its substrate scope, DCR was only cloned but to our knowledge not tested for its biocatalytic activities towards unnatural substrates.

To have overexpression systems for NemR and DCR, their respective genes *nemA* and *fadH* were cloned into expression plasmid pET-22b(+). Genomic DNA of *E. coli* BL21(DE3) served as template for PCR reactions over the whole genes using primers with incorporated restriction sites. The PCR product as well as pET-22b(+) were digested with the same restriction enzymes, then ligated and the ligation mixes transformed in *E. coli* DH5 α for the selection of positive clones. Colony PCR was performed with the standard primers pET94F and pET417R to verify insertion of *nemA* or *fadH* in pET-22b(+).

C V.4.1 First expression of NemR and DCR

Three positive pET-22b(+)*_nemA* and pET-22b(+)*_fadH* clones were extracted from *E. coli* DH5 α and transformed into *E. coli* BL21(DE3) $\Delta nemA$ where first expression tests were performed (E VII.4). A SDS-PA gel of the crude samples after 3 h expression can be seen in Figure C-41. NemR (39.5 kDa) as well as DCR (72.7 kDa) could clearly be expressed in *E. coli* BL21(DE3) $\Delta nemA$ and the expression levels which can be seen in the gel (Figure C-41) were basically the same after 20 h.

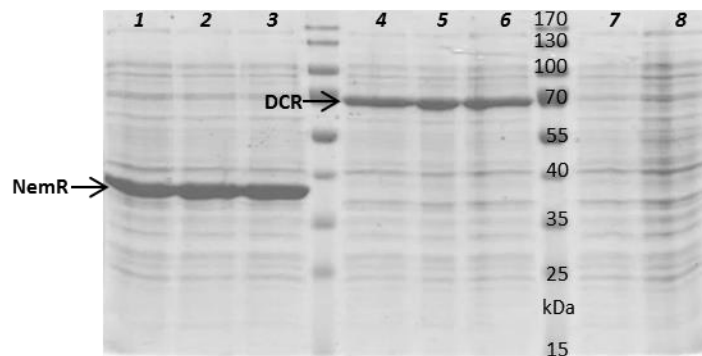


Figure C-41. SDS-PA crude gel after 3 h expression. 1 – pET-22b(+)*_nemA*_1, 2 – pET-22b(+)*_nemA*_2, 3 – pET-22b(+)*_nemA*_3, 4 – pET-22b(+)*_fadH*_1, 5 – pET-22b(+)*_fadH*_2, 6 – pET-22b(+)*_fadH*_3, 7 – BL21(DE3), 8 – BL21(DE3) $\Delta nemA$

C V.5 Expression of pET-22b(+)*_nemA*

Further expression experiments of pET-22b(+)*_nemA* in *E. coli* BL21(DE3) $\Delta nemA$ were conducted at 25°C in LB and TB with different concentrations of inducer IPTG. The SDS-PA gels of the soluble and insoluble fractions of samples from 2 h, 4 h and 22 h expression time are presented in Figure C-42.

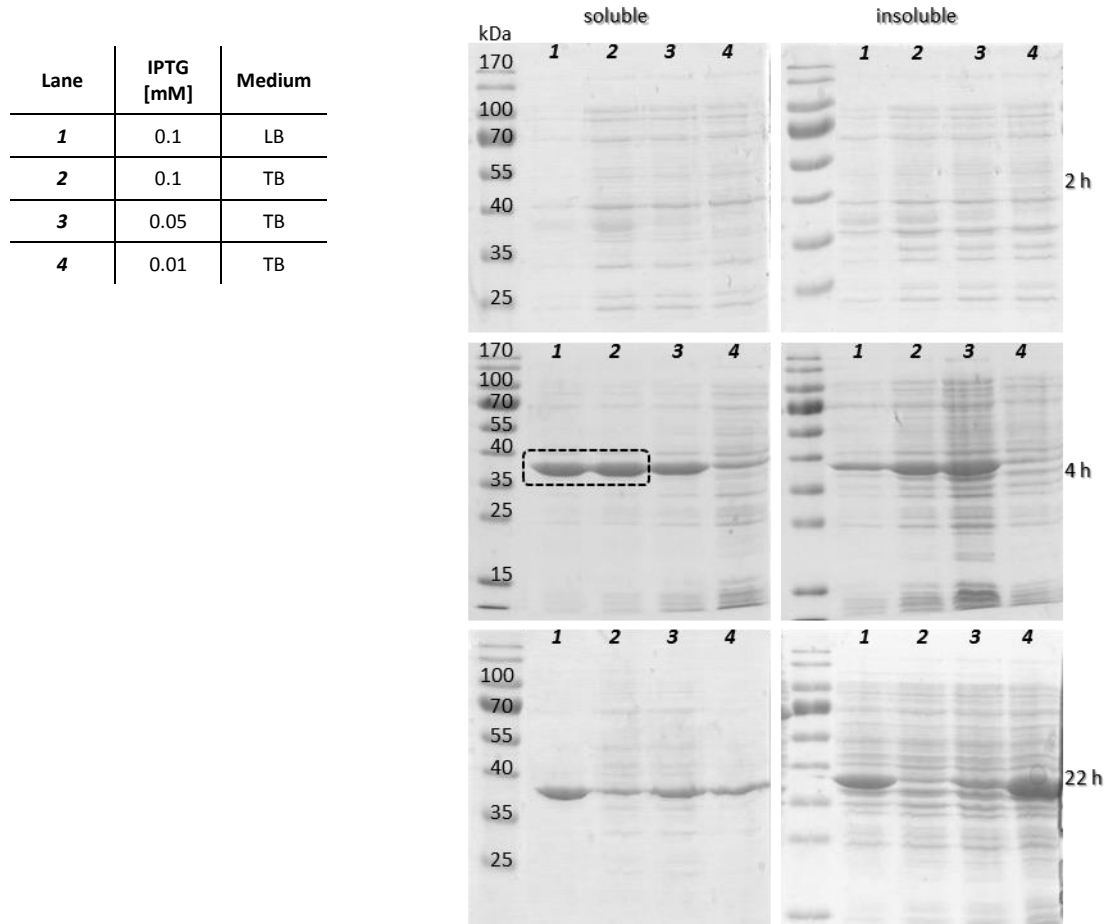


Figure C-42. SDS-PA gels of soluble and insoluble samples of pET-22b(+)*_nemA* expression tests

As can be seen in the SDS-PA gels best soluble expression was achieved 4 h after induction with 0.1 mM IPTG in LB or TB medium. Lower concentrations of IPTG were not beneficial. For longer expression times LB medium seems better than TB. With this expression protocol sufficient amounts of soluble NemR can be produced making it available for further substrate screening, which was not within the scope of this thesis.

C V.6 Expression of pET-22b(+)*fadH*

DCR production through expression of pET-22b(+)*fadH* in *E. coli* BL21(DE3) $\Delta nemA$ was investigated at different temperatures in LB or TB medium with different concentrations of inducer IPTG. The SDS-PA gels of soluble and insoluble fractions from samples after 2 h and 4 h expression time are shown in Figure C-43.

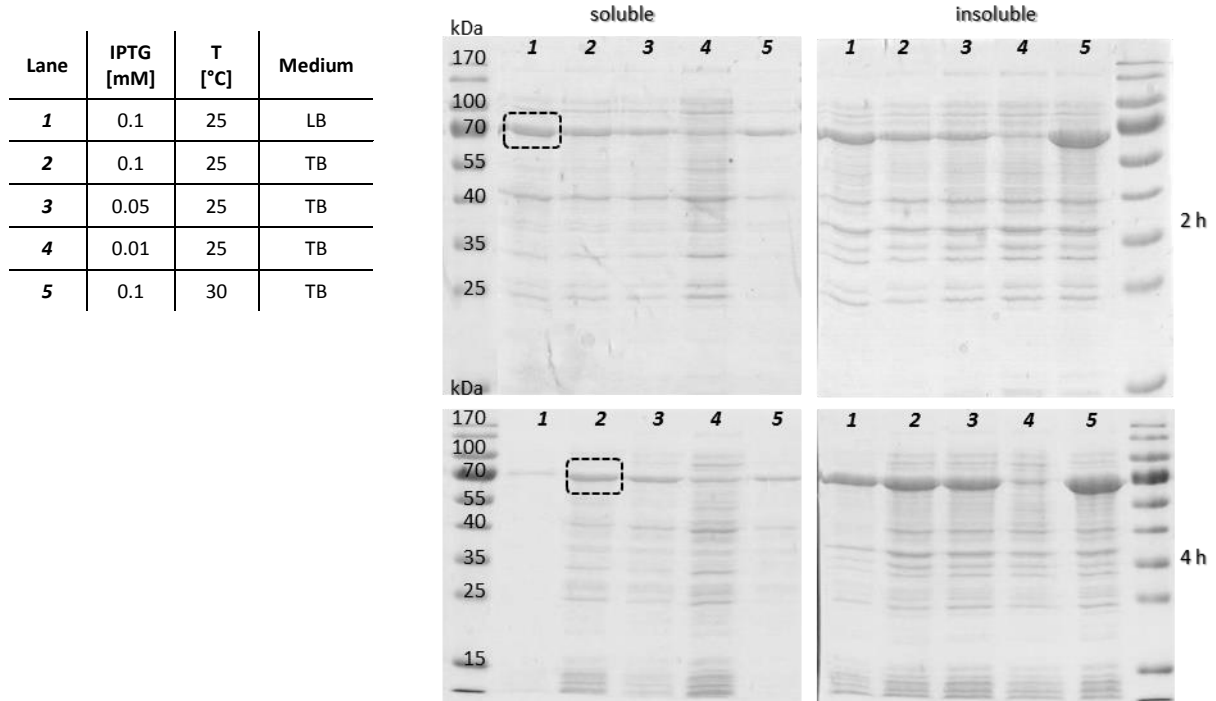


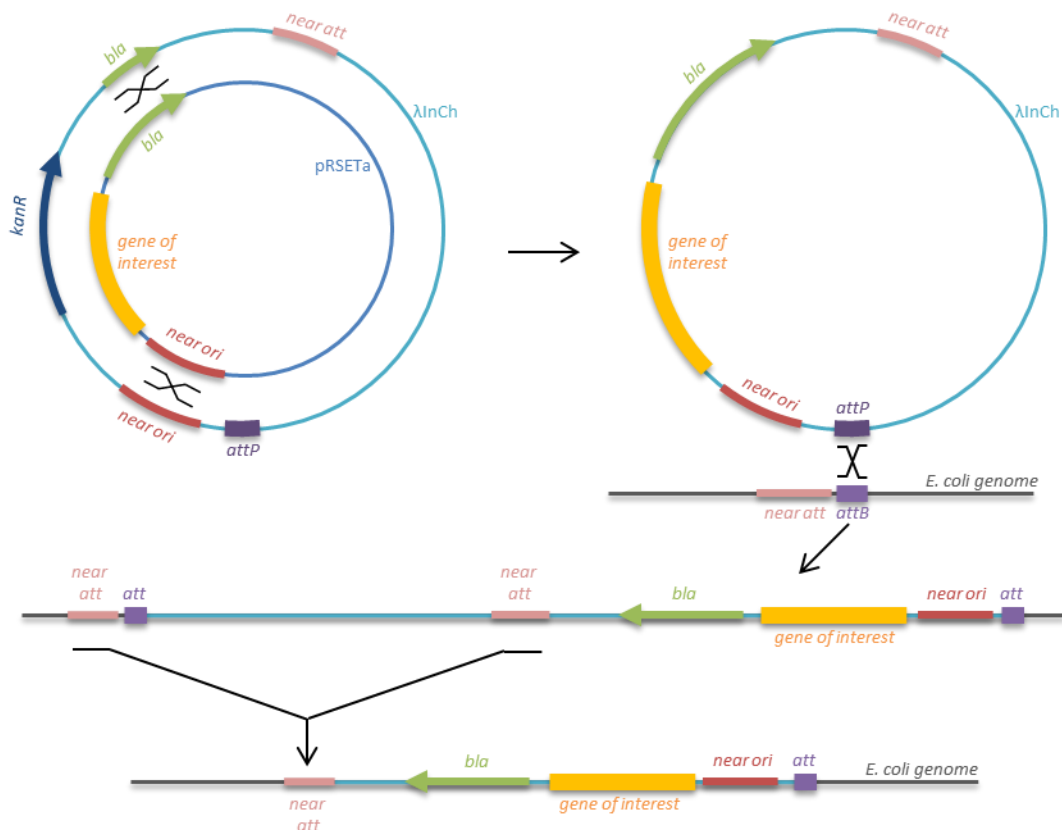
Figure C-43. SDS-PA gels of soluble and insoluble samples of pET-22b(+)*fadH* expression tests.

In the SDS-PA gels it can be observed that expression of pET-22b(+)*fadH* performed rather poorly. Some soluble protein could be achieved in LB medium 2 h after induction with 0.1 mM IPTG at 25 °C as well as in TB medium after 4 h at the same conditions. More protein was produced at 30 °C but unfortunately all of it was insoluble. In the literature^[162] a different expression system was used but could serve as lead for further expression optimization.

C V.7 Genomic integration

To reduce the metabolic burden of a multi-plasmid approach, which the expression system for our enzymatic toolbox consisted of, genomic integration (GI) was considered to engineer the host organism *E. coli* BL21(DE3). The genes of the two ADHs, LK-ADH and RR-ADH, should be incorporated in the *E. coli* BL21(DE3) genome via λ -phage recombination^[168]. Considerations towards this approach were planned together with Thomas Bayer and the λ -phage-containing *E. coli* strain was received from Privatdoz. Astrid Mach-Aigner (TU Wien).

The principle of GI with the λ -phage system relies on the infection cycle of the phage and consists of three homologous recombination events *in vivo*. The first recombination occurs from the phage vector λ InCh to a plasmid bearing the gene of interest in a phage infected *E. coli* strain. Through recombination of the *near ori* sites and *bla* sites the gene of interest and the full sequence for the ampicillin resistance (*bla*) are transferred to the λ InCh vector, whereupon it loses its kanamycin resistance (*kanR*). Instead it gains ampicillin resistance which allows for selection of positive clones. In the next step the *attP* site in the modified λ InCh vector recombines with the *attB* site in the *E. coli* genome during transfection of the bacteria through the λ -phage. Hence the λ -phage DNA including the gene of interest is integrated in the *E. coli* genome. The last recombination of the *near att* sites in the *E. coli* genome removes the inserted λ -phage DNA. Consequently the *E. coli* strain is cured from the λ -phage and the gene of interest is integrated in the genome of *E. coli*. An illustration of the recombination events is shown in Scheme C-55.



Scheme C-55. Illustration of the recombination events during genomic integration through λ -phage recombination (adapted from Boyd *et al.*^[168]).

The two genes of LK-ADH and RR-ADH should be integrated in one GI approach handling them as one “gene of interest”. For the purpose of the enzymatic toolbox the possibility to induce the expression of the ADH genes independently was desirable. Therefore the implementation of two new inducers different to IPTG, which is the

inducing agent for standard plasmid based expression systems, should be tested. After research by Thomas Bayer it was decided on the use of anhydrotetracycline (*tetR*) for LK-ADH and cumate (*cymR*) for RR-ADH as individual inducers. The gene sequences of LK-ADH and RR-ADH were codon-optimized for *E. coli* via the GeneArt Gene Synthesis Software (ThermoFisher) and then assembled together with the inducer sequences in Geneious.

As the whole construct would have been too big for one gene synthesis order at GeneArt the sequence was equipped with several well placed unique restriction sites. Therefore the gene synthesis job could be parted in LK-ADH plus *tetR* (*tetLK*) and RR-ADH plus *cymR* (*cymRR*) allowing for later combination through classic restriction-ligation cloning. A simplified illustration of the designed construct is depicted in Scheme C-56.



Scheme C-56. Simplified illustration of the sequence construct for GI of LK-ADH and RR-ADH plus individual inducer regions.

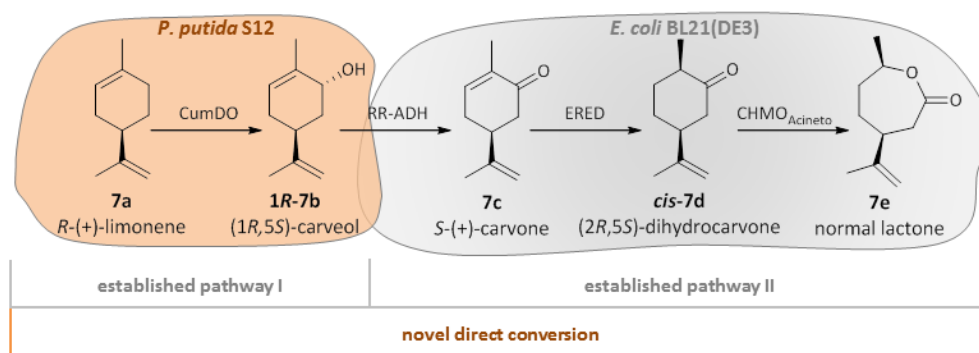
The sequence construct of LK-ADH plus *tetR* (*tetLK*) was ordered from GeneArt in the plasmid pRSETa which is highly similar to pGEM5Z-f(+) which is normally used with the λ -phage system by Astrid Mach-Aigner. Therefore the pRSETa_ *tetLK* vector should have the desired properties to recombine with the λ InCh vector and transfer the *tetLK* construct. Before combining *tetLK* and *cymRR* through cloning to get the whole construct the GI method was tested with pRSETa_ *tetLK* alone. Unfortunately, the protocol could not be taken further than the first recombination event. The problems which occurred with the λ -phage system could not be overcome in the timeline of this thesis. For a continuation of this project different genomic integration approaches may be considered where the versatile sequence construct described above could be of good use.

C V.8 Summary

After discovering background reactions from the microbial host *E. coli* BL21(DE3) its native EREDs NemR and DCR were disrupted via genetic modification of their genes. The background reduction of most of the cascade intermediates could hence be diminished. Only one substrate was still converted by the developed double knockout strain, suggesting the involvement of a third background enzyme. Nevertheless the *E. coli* BL21(DE3) double knockout presents a good platform for background-free heterologous ERED expression. The two *E. coli* native EREDs were additionally cloned into standard expression plasmids to be available for biocatalytic testing. To further optimize the production of multiple enzymes for cascade reactions in one microbial host the concept of genomic integration was investigated. A system to introduce two ADH genes into the genome of *E. coli* was designed. Although this approach could not be finalized during the course of this thesis this modular system could be applied for other genes and forms a good basis for further work in this direction.

C VI From waste to value – Utilization of *R*-(+)-limonene from orange peel

In this chapter the conversion of natural product *R*-(+)-limonene (**7a**) to chiral carvolactone (**7e**) is discussed. Therefore the hydroxylation step had to be combined with the existing heterologous three-step pathway in *E. coli* BL21(DE3). As hydroxylation by CumDO heterologously expressed in *P. putida* S12 is performed in a bacterial strain other than *E. coli*, a mixed culture set-up (Scheme C-57) had to be investigated.



Scheme C-57. *R*-(+)-limonene to carvolactone – by combination of two existing pathways in a mixed-culture approach.

In an application oriented approach it was aimed for the valorization of FSCW (food supply chain waste) orange peel^[169], as more than 15 million tons of peel are produced annually as waste of the citrus juice industry. *R*-(+)-Limonene is the main oil component of citrus peel and is commercially extracted by energy intensive steam distillation or cold expression^[170]. To directly utilize the orange peel and convert the *R*-(+)-limonene *in situ* to valuable compounds would offer certain advantages.

To implement orange peel as starting material in a mixed culture cascade reaction towards chiral carvolactone several factors had to be considered. The availability of limonene, which is volatile and hardly soluble in water had to be assured. Therefore different concepts towards the *in situ* conversion of *R*-(+)-limonene from orange peel were investigated. A two liquid phase approach^[171] as it is commonly applied in biotechnology, also for limonene^[59, 172], rendered unfeasible for our purpose. Due to its hydrophobicity *R*-(+)-limonene would mainly accumulate in the organic solvent hence limiting its availability in the aqueous phase of the resting cells where the hydroxylation takes place.

The easiest approach although attached with some challenges, is the use of a solely aqueous system making use of the orange peel itself as substrate reservoir, applying the concept of SFPR (substrate feed product removal)^[173]. Hence the problem of volatility of starting material *R*-(+)-limonene could be circumvented as already minimal amounts would directly be converted via the biocatalytic cascade.

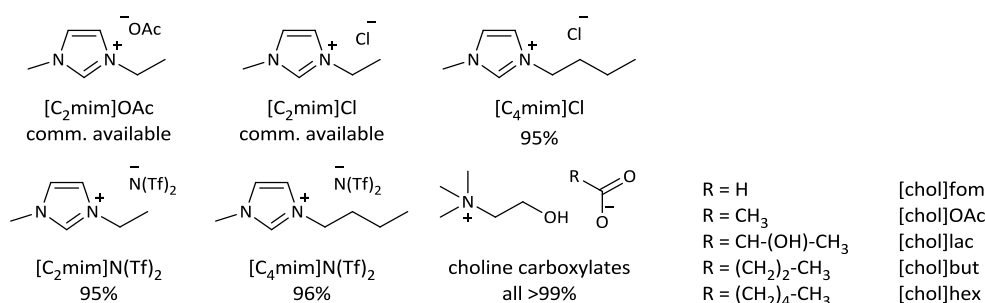
Another concept is the addition of water soluble extraction enhancers where the tolerance of the bacterial strains towards these chemicals is a crucial factor. Ionic liquids (ILs), salts with a melting point below 100 °C, are already commonly applied as biocompatible additives in biocatalytic processes^[174-175]. For this approach we started a collaboration project with Dr. Anna K. Ressmann from the group of Prof. Peter Gärtner (TU Wien) as she conducted her PhD thesis^[176] with Assistant Prof. Katharina Schröder (Bica) whose main research topic are ILs.

C VI.1 Extraction enhancers - ionic liquids

Two approaches on the implementation of ILs were investigated, as they could be directly added to the aqueous system in low concentration to enhance *R*-(+)-limonene extraction or be used in concentrated form to completely dissolve orange peel^[177] prior to biocatalysis. All experiments were conducted in close cooperation with Dr. Anna K. Ressmann.

For the choice of ionic liquids different requirements had to be fulfilled: they should not only be tolerated by the two bacterial strains *E. coli* BL21(DE3) and *P. putida* S12, therefore being suitable for the cascade reaction, but also be able to extract *R*-(+)-limonene from orange peel.

As shown by Wood et al. long-chain ionic liquids are rather toxic for bacteria.^[178] Therefore ionic liquids with a maximum chain length of 6 carbon atoms were chosen. Imidazolium ([C_{2/4}mim]) ILs with hydrophilic (chloride, acetate) and hydrophobic anions (N(Tf)₂) were chosen, as well as the environmentally benign choline ([chol]) ILs with variable chain length from formate (fom) to hexanoate (hex) (Scheme C-58).



Scheme C-58. Ionic liquids used for the combination with microbial expression hosts. Percentage gives yield achieved by Anna Ressmann.

C VI.1.1 Extraction of *R*-(+)-limonene from orange peel

The *R*-(+)-limonene (**7a**) extraction ability of the chosen ILs was tested by Anna Ressmann^[176] with pure ILs at elevated temperature and relevant results are shown in Figure C-44.

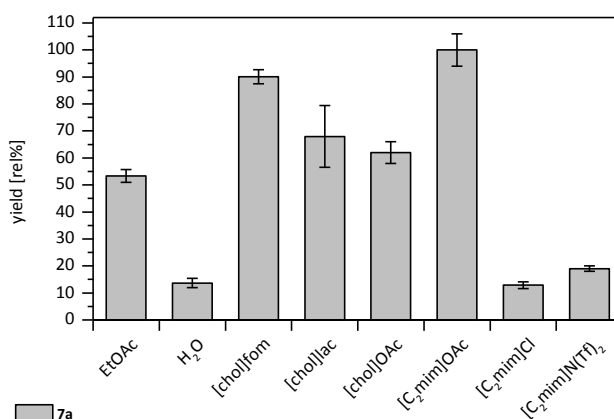


Figure C-44. From orange peel extracted amounts of *R*-(+)-limonene (**7a**). Results from Anna Ressmann, values are relative percent to the best result ([C₂mim]OAc).

As can be seen in the above figure most of the ILs exhibited much better *R*-(+)-limonene extraction ability than the organic solvent EtOAc, which would additionally not be compatible with microbial cells.

C VI.1.1.1 Limonene content in orange peel

To get an estimation of the amount of *R*-(+)-limonene (**7a**) present in orange peel, extraction experiments were conducted with different batches of orange peel and the results are depicted in Figure C-45.

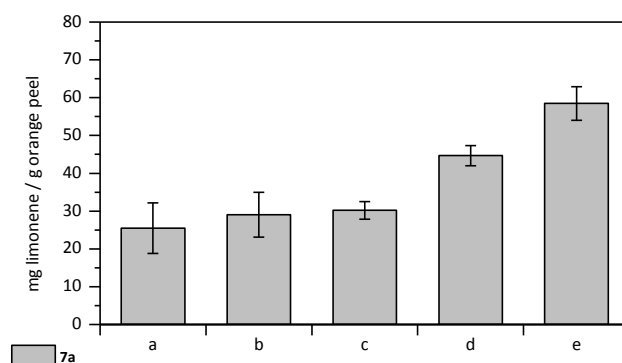


Figure C-45. *R*-(+)-Limonene (**7a**) extracted from different batches of orange peel with [C₂mim]OAc. Results from Anna Ressmann.

As can be seen above, *R*-(+)-limonene contents in orange peel vary from 25-60 mg *R*-(+)-limonene per g peel which is in the range of reported literature values (approx. 3.8%)^[179].

C VI.1.2 Growth of *E. coli* in presence of ILs

The bacterial expression host for the cascade enzymes *E. coli* BL21(DE3) was investigated towards its tolerance towards the chosen ILs. Growth in presence of 50 mM and 100 mM IL was monitored and the influences can be seen in Figure C-46.

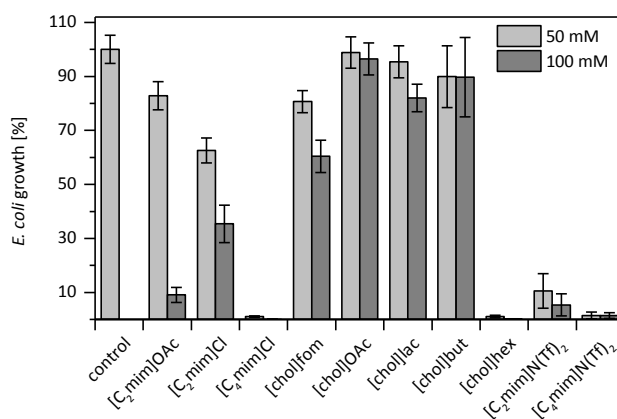


Figure C-46. Influence of the addition of ILs on the growth of *E. coli* BL21(DE3).

Short chained choline carboxylates (formate, acetate, lactate and butyrate) had only small impact on bacterial growth. Strong concentration dependence was observed with 1-ethyl-3-methyl-imidazolium acetate ([C₂mim]OAc) where 100 mM showed much higher growth interference than 50 mM IL. The hydrophobic [C₂mim]N(Tf)₂ and [C₄mim]N(Tf)₂ also showed incompatibility with growing *E. coli* BL21(DE3) cells. (Figure C-46)

C VI.1.3 Growth of *P. putida* S12 in presence of ILs

To evaluate the compatibility of *P. putida* S12, the expression host for CumDO, with the chosen ILs, first the effect of ILs on the growth of the bacteria was investigated. Therefore growing *P. putida* S12 cells were supplemented with 50 mM and 100 mM IL and their growth monitored. The influences of the addition of the ILs can be seen in Figure C-47.

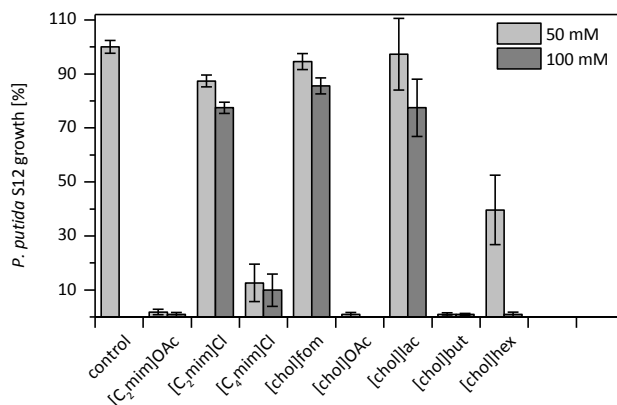


Figure C-47. Influence of the addition of ILs on the growth of *P. putida* S12.

Growth of *P. putida* S12 was in most cases strongly impaired by the addition of IL. (Figure C-47) Only two choline derivatives [chol]fom and [chol]lac were well tolerated in a 50 mM concentration. Choline derivatives with higher chain length and with an acetate anion inhibited the growth. The acetate anion seemed to have a negative effect in general since no growth was observed with the imidazolium derivative [C₂mim]OAc as well. If the anion was exchanged to chloride a significant difference was observed and the chloride ionic liquid only slightly reduced the growth of *P. putida* S12. This is in accordance with the literature where full inhibition of yeast growth and biofuel production with the presence of only 0.25% of [C₂mim]OAc was observed, whereas [C₂mim]Cl influenced yeast growth to a lesser extent.^[180] Again, elongation of the side chain length of the ionic liquid resulted in a decreased growth rates which was also observed by Wood *et al.*^[178]

The biphasic bistriflimide (N(Tf)₂) ionic liquids were not tested as they showed incompatibility with growing *E. coli* cells (C VI.1.1). Additionally, it was shown in the literature that imidazolium bistriflimide ionic liquids inhibit bacterial growth^[178] and affect membrane integrity.^[181-182] The concentration of the ionic liquid had a significant influence on bacterial growth as greater inhibition was observed with 100 mM in all cases.

C VI.1.4 Limonene hydroxylation by CumDO in presence of ILs

Four ILs were selected to further investigate their compatibility with the hydroxylation reaction in resting cells of *P. putida* S12 with expressed CumDO. [C₂mim]OAc and [chol]OAc were chosen due to their good to excellent *R*-(+)-limonene extraction ability although they inhibited growing cells of *P. putida* S12. [C₂mim]Cl and [chol]fom showed best compatibility with growing *P. putida* cells and [chol]fom additionally exhibited superior biomass extraction performance.

Resting cells of *P. putida* S12 expressing CumDO were supplemented with *R*-(+)-limonene in the presence of ILs in the optimum concentration of 50 mM. Interestingly [C₂mim]OAc, which showed no compatibility with growing cells, only slightly inhibited the hydroxylation reaction. [C₂mim]Cl also showed minor interference with the reaction therefore the two 1-ethyl-3-methyl-imidazolium ILs could be tested as extraction enhancers (Figure C-48).

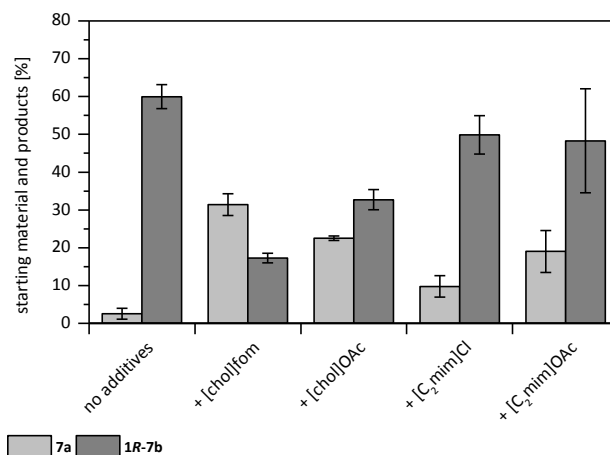


Figure C-48. Hydroxylation of 0.5 mM *R*-(+)-limonene by CumDO in presence of ILs.

C VI.1.4.1 IL concentration

Hydroxylation of *R*-(+)-limonene was tested in resting cells of *P. putida* S12 with expressed CumDO in presence of different concentrations of [C₂mim]OAc. 50 mM IL were well tolerated whereas already 100 mM interfered with the biotransformation and 250 mM strongly impaired the reaction shown in Figure C-49.

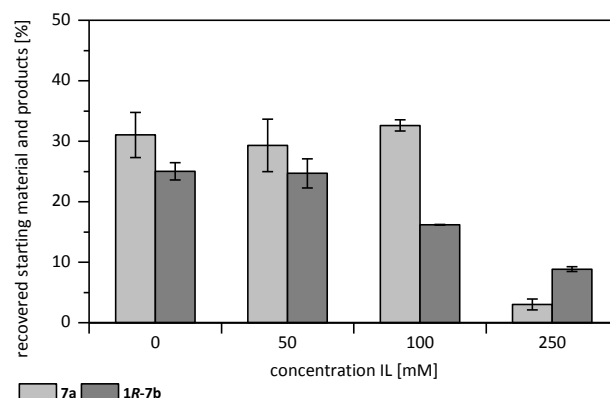
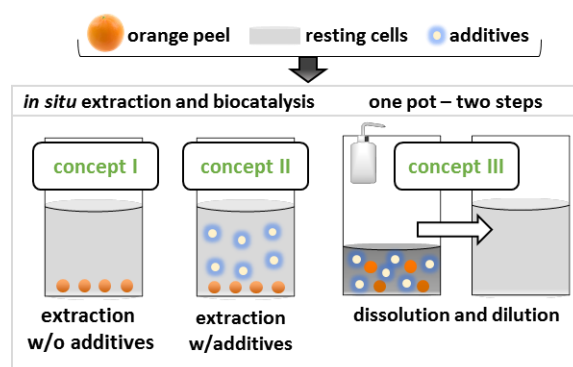


Figure C-49. Hydroxylation of 4 mM *R*-(+)-limonene with and without the addition of different concentrations of [C₂mim]OAc.

C VI.2 Orange peel as starting material for hydroxylation by CumDO

The first attempt towards the valorization of waste product orange peel was its use as starting material for the *R*-(+)-limonene hydroxylation in resting *P. putida* S12 cells expressing CumDO. Here three different concepts as illustrated in Scheme C-59 were investigated.



Scheme C-59. Three applied concepts to the utilization of orange peel as starting material.

Concept I representing the easiest approach is a solely aqueous system with orange peel itself acting as substrate reservoir. The addition of extraction enhancers for *in situ* *R*-(+)-limonene conversion is utilized in concept II. Concept III, the dissolution of orange peel in ILs prior to biocatalysis, needs an intermediary dilution step. The latter concept was tested by dissolving orange peel in [C₂mim]OAc, which was the best candidate due to its extraction ability (C VI.1.1) and good compatibility with the hydroxylation reaction (C VI.1.4), and then diluting the extract into *P. putida* S12 resting cells expressing CumDO. This additional handling step did not prove feasible as a higher amount of resting cells was needed – due to the optimal concentration of 50 mM IL – and furthermore the recovery for the experiment was very poor and sufficient amounts of product could not be detected. Concept III was therefore not investigated any further.

As extraction enhancers for concept II the same ILs were chosen, which were already investigated as additives in the hydroxylation reaction with *R*-(+)-limonene as starting material (C VI.1.4). The aqueous system according to concept I was based only on resting cells of *P. putida* S12 expressing CumDO in Tris-HCl buffer. Orange peel was cut in small pieces and added to the reactions in a biomass loading of 3% (w/v). This loading was chosen, as orange peel contains about 2-6% *R*-(+)-limonene (C VI.1.1.1), to augment an acceptable *R*-(+)-limonene concentration in the aqueous phase while staying below any toxicity level^[160]. Due to variations in *R*-(+)-limonene contents in orange peel it was decided on a representation of the results in mg product per g orange peel instead of percentage of conversion of limonene. The results obtained from an experiment with 3% (w/v) biomass loading of a batch of orange peel with 13.8 ± 4.0 mg *R*-(+)-limonene per g biomass are shown in Figure C-50.

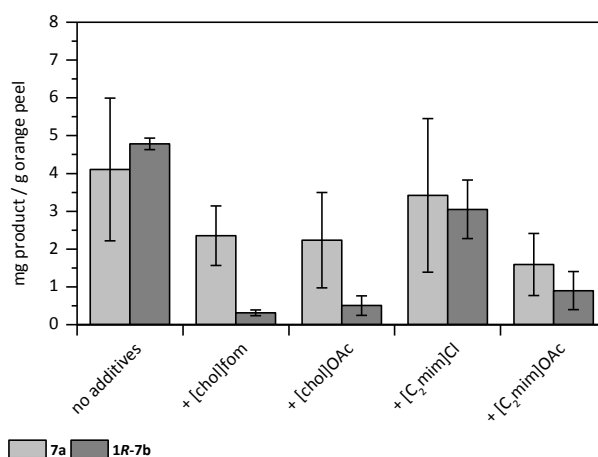


Figure C-50. *R*-(+)-Limonene hydroxylation by CumDO starting from orange peel with and without addition of ILs.

As can be seen in Figure C-50 the solely aqueous system (concept I) delivered the best result with 4.8 mg carvedol per g orange peel to be detected (GC). The addition of the ILs [chol]fom, [chol]OAc and [C₂mim]OAc strongly interfered with the hydroxylation reaction. [C₂mim]Cl influenced the whole cell reaction only minor but its addition did not improve the *in situ* conversion of limonene.

C VI.3 Mixed culture - extended pathway

For the direct conversion of *R*-(+)-limonene to carvolactone the biocatalytic cascade starting from carveol had to be combined with the hydroxylation of limonene. As the three cascade enzymes are expressed in *E. coli* and CumDO is expressed in *P. putida* S12 a mixed culture system for the first proof of concept was envisaged.

C VI.3.1 Limonene to carvolactone

To convert *R*-(+)-limonene (**7a**) to carvolactone (**7e**) in a one-pot resting cell mixed culture system two approaches were tested. In a simultaneous addition approach resting cells of both expression hosts, *P. putida* S12 and *E. coli* BL21(DE3) were directly combined with *R*-(+)-limonene to start the reaction cascade. In a sequential addition approach the preceding hydroxylation by CumDO was performed first and resting cells of *E. coli* BL21(DE3) with expressed RR-ADH, XenB and CHMO_{Acineto} were added to the same pot after 10 hours. Recovered starting material, intermediate and product are shown in Figure C-51.

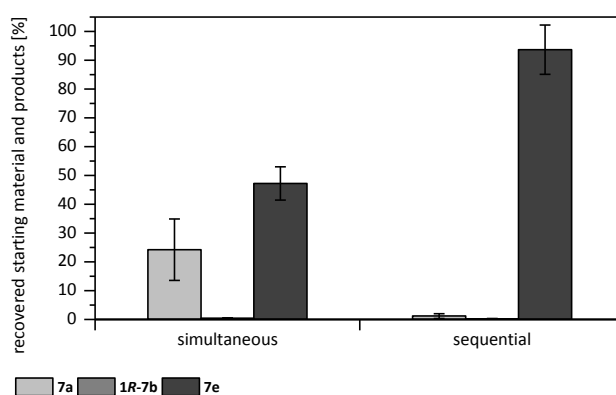


Figure C-51. Production of carvolactone from 0.5 mM *R*-(+)-limonene with simultaneous and 1 mM *R*-(+)-limonene with sequential addition after 20 h.

As can be seen in Figure C-51 in a simultaneous addition approach approx. 50% carvolactone could be detected after 20 h reaction time. In the sequential approach, where after 10 h *R*-(+)-limonene hydroxylation to carveol was nearly complete, almost quantitative conversion to carvolactone could be achieved. This proved the one-pot compatibility of the two microbial expression hosts as well as the suitability of the enzymes for a combined cascade reaction.

C VI.3.2 Orange peel to carvolactone

Finally the direct valorization of waste product orange peel to chiral building block carvolactone was explored. The different concepts, discussed for the utilization of orange peel in the hydroxylation reaction (C VI.2) were applied, except unfeasible concept III (the pre-dissolution of biomass), on the simultaneous and sequential addition investigated for the mixed culture system (C VI.3.1).

Initial biomass loading was 3% (w/v) as this proved feasible in the hydroxylation reaction starting from orange peel, resulting in 4.8 mg carveol per g peel (C VI.2, Figure C-50). With this biomass loading from a batch of orange peel (limonene [c] = 17.9 mg ± 3.7 mg g⁻¹ biomass) 3.2 mg carvolactone per g orange peel could be obtained in a sequential addition approach in an aqueous system (concept I). Here concept II was also investigated by adding 50 mM [C₂mim]Cl as extraction enhancer to this system. As can be seen in Figure C-52 this concept did not inhibit the reaction significantly but also did not improve the yield of carvolactone.

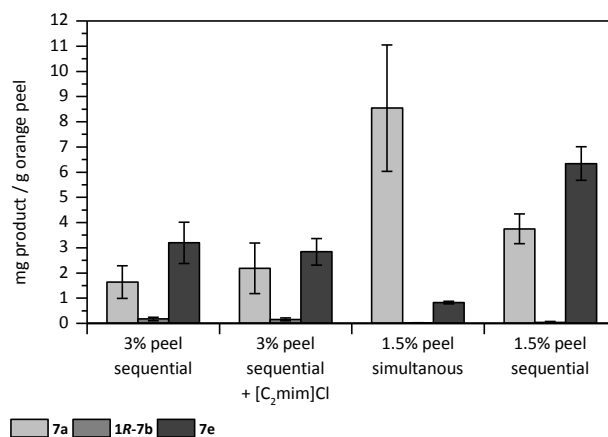


Figure C-52. Production of carvolactone from orange peel in different approaches with altered biomass loadings.

To ascertain no overloading with orange peel resulting in a toxic effect which could limit the reaction, a lower biomass loading of 1.5% (w/v) was tested with the solely aqueous system since concept II did not provide improvement. A simultaneous addition approach only delivered low amounts of carvolactone as already noticed in the same experiment starting from limonene. However in an approach with sequential addition of *P. putida* S12 and *E. coli* BL21(DE3) resting cells and the lowered biomass loading, 6.3 mg carvolactone per g orange peel (limonene [c] = 17.9 mg ± 3.7 mg g⁻¹ biomass) could be detected. With a yield of 29% calculated on the concentration of *R*-(+)-limonene over 4 steps (73% per step) this result, achieved in an aqueous system relying on orange peel as substrate reservoir, renders rather promising.

C VI.4 Summary

In this final chapter the realization of an enzymatic four-step cascade from *R*-(+)-limonene to carvolactone by the use of a one-pot mixed-culture system was shown. Additionally, application oriented investigations, on the utilization of waste product orange peel, were conducted. Enhancement of *R*-(+)-limonene availability from orange peel was tested with ionic liquids in different concepts. Although ionic liquids are excellent biomass extraction solvents and could also be used in diluted form *in situ* no benefits could be drawn from their use. The simple system with orange peel and resting cells of two microbial hosts in aqueous buffer resulted in the transformation of waste product to carvolactone.

D Conclusions and perspective

Cascade reactions present a synthesis concept towards more sustainable chemistry. The application of enzymatic multistep reactions comes with a lot of advantages as the biocatalysts are in general easily compatible. The design, implementation and extension of biocatalytic redox cascade reactions were investigated in this thesis.

Main focus was the interplay of different enzymes connected in a cascade reaction. Due to cofactor dependency of most redox enzymes these reactions could become quite cost intensive. Hence the implementation of an enzymatic multistep reaction in a microbial host organism, where cofactors are provided by its metabolism, was desirable. The transfer of the developed cascade reaction into the well characterized bacteria *E. coli* was therefore the next step. After set-up of the cascade reaction system *in vitro* this established non-native mini-pathway was investigated *in vivo*.

An enzymatic redox cascade was designed on the basis of the retrosynthetic approach where a valuable target compound is systematically dissected to cheap starting material. Lactones were chosen as final product and four retrosynthetic steps led back to simple cyclic alkenes as starting material. The enzymes chosen to address these steps were an oxygenase, to hydroxylate the cyclic alkene, an ADH to oxidize the resulting unsaturated alcohol to a ketone and an ERED to reduce the C-C double bond towards a saturated ketone which was substrate for a BVMO reaction to result in a lactone product. To show the versatility of our approach it was decided on a set of differently substituted cyclohexenes, a cyclohexane with an exocyclic double bond and the two isomers of natural product *R*-(+)-limonene as the substrate scope.

While identifying suitable enzymes for each cascade step, problems finding a feasible oxygenase for the first hydroxylation were encountered. For the three subsequent steps two stereocomplementary ADHs, LK-ADH and RR-ADH, two EREDs, XenB and OYE1, and the well-studied CHMO_{Acinetobacter} were found to be able to convert all cascade intermediates. To reach first milestones, this three-step cascade was investigated with a set of unsaturated cyclic alcohols as starting material.

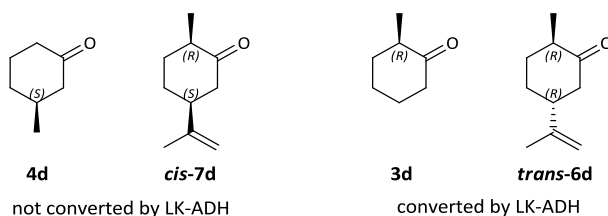
The set-up of an *in vitro* reaction system was realized with cell free extracts (CFE) of the enzymes heterologously produced in *E. coli* BL21(DE3). Different addition concepts were applied depending on the enzymes in use. In cascades utilizing LK-ADH it was decided on a sequential addition approach, starting the cascade reaction with unsaturated alcohol as substrate, LK-ADH and NADP⁺ as cofactor. After an hour the ERED of choice was added and no additional cofactor was needed as the NADPH produced from the ADH reaction served as the required redox equivalent. These first two steps presented a self-sufficient redox system only when adding CFE of CHMO_{Acinetobacter} additional NADP⁺ and cofactor recycling system, as NADPH is needed for the BVMO reaction, was included. In a simultaneous approach where all enzymes are present from the outset the cofactor recycling enzyme glucose-6-phosphate dehydrogenase would compete with LK-ADH over the available NADP⁺ which could limit the first reaction step. RR-ADH is NAD⁺ dependent and therefore uncoupled from the cofactor recycling system why a simultaneous addition approach was chosen for cascades with this ADH.

In the first *in vitro* cascade reaction with our simplest substrate cyclohex-2-en-1-ol (**1b**) some interesting observations were made. While only CFE of *E. coli* BL21(DE3) with expressed LK-ADH was present, intermediate **1d** - the product of an ERED reaction - was already detected, suggesting an *E. coli* background reaction. Two *E. coli* native EREDs were identified through sequence comparison as possible background enzymes. N-Ethylmaleimide reductase (NemR) was already reported to have activity on some of the substrates while 2,4-dienoyl CoA reductase (DCR) was not characterized regarding its substrate profile in the literature.

The second observation was also made during the first hour of the reaction as an unknown side-product was detected. Considering all present enzymes and intermediates at this stage a LK-ADH back-reaction was hypothesized. This was proven as the side-product was identified as cyclohexanol (**1d-ol**) the product of the reduction of cyclohexanone (**1d**) by LK-ADH. As the side-product was highly abundant this was a rather unfortunate finding. Nevertheless after adding the ERED and finally CHMO_{Acinetobacter} full conversion to the final product caprolactone could be obtained in about six hours. Through the irreversible BVMO reaction the equilibrium of the unwanted side-reaction of LK-ADH was continuously shifted and the cascade reaction was driven to completion.

After these first insights into the interplay of the enzymes, the other unsaturated alcohol substrates were investigated in the three-step *in vitro* cascade reactions. The background and side-reactions discovered in the cyclohex-2-en-1-ol cascade were also observed with most of other substrates. No background reaction of NemR or DCR could be observed with intermediates **3c** and **4c**. In simultaneous reaction set-ups the background reactions of NemR or DCR could not be analyzed as the cascade ERED was present from the outset. As no other stereoisomers were detected in these reactions same stereoselectivity of the background enzymes is possible and it was also reported that NemR shows the same selectivity as OYE1.^[139]

Only intermediate 3-methylcyclohexanone (**4d**) and dihydrocarvone **cis-7d** were not converted to side-products by LK-ADH. In the cascade reaction starting from (1*S*,5*R*)-carveol (**1S-6b**) the side-product dihydrocarveol **trans-6d-ol** was abundant in highest amounts. Whereas dihydrocarvone **cis-7d** was not reduced at all, the activity of LK-ADH towards dihydrocarvone **trans-6d** was very high. This suggests very strong stereoselectivity of LK-ADH for dihydrocarvone in 5-position. Also **4d** which shows the same stereochemistry in the correlating position is not converted by LK-ADH. The structural similarities of the intermediates are shown in Scheme D-1.



Scheme D-1. Intermediates of cascade reactions and the activity of LK-ADH towards them.

Apart from background and side-reactions all *in vitro* cascades progressed very well. In the most cases the ADH reaction was the rate limiting step. This was either due to stereoselectivity of the enzyme towards one isomer of starting material or low reaction speed in general. The very well accepted substrate (1*S*,5*S*)-carveol (**1S-7b**) was subjected to a substrate concentration study. Also here it became clear that the reaction impaired mainly by higher concentrations of starting material was the ADH reaction. Whilst 10 mM of substrate still led to satisfying results the cascade reaction was unfeasible with 50 mM **1S-7b**.

The implementation of these three enzymes, which were naturally not connected in a single organism in a metabolic context, in a non-native mini-pathway in the microbial host *E. coli* BL21(DE3) was the next step. Also this *in vivo* approach delivered promising results. The side-reaction of LK-ADH could in most cases be decreased due to the presence of CHMO_{Acinetobacter}, therefore being able to compete over the saturated ketone intermediate from the outset. In three preparative scale experiments the power of the whole cell one-pot cascade reaction was shown as an average yield of 82% per individual cascade step could be achieved (calculated from isolated yield over three steps). Both the *in vitro* and the *in vivo* cascade reactions benefited from the irreversible BVMO reaction shifting the equilibrium towards the final product.

Although the *E. coli* native enzymes did not interfere with the outcome of the cascade reactions, as they showed same stereoselectivity as our EREDs, the discovered background reaction should be eliminated. Therefore an *E. coli* BL21(DE3) double knockout strain was constructed by disrupting the genes coding for NemR and DCR. It could be shown that the activity of NemR was shut down but intermediate **5c**, which was thought to be converted by DCR due to structural similarity with its natural substrate, was still reduced by the double knockout strain. This suggests the presence of yet another enzyme or interplay of more enzymes native in *E. coli* which caused this background reaction. The identification of further background enzymes and the disruption of their genes could be part of the work towards the construction of a totally background free expression host for EREDs.

Due to co-expression of the ERED and the BVMO from one plasmid the metabolic burden on the expression host could be limited to two plasmids. For future work when an oxygenase should be added for the hydroxylation of cyclic alkenes the amount of plasmids could lead to decreased viability of *E. coli*. Therefore the approach of genomic integration was envisaged to produce a bacterial strain with genes coding for heterologous enzymes introduced in its genome. A system for the genomic integration of LK-ADH and RR-ADH with individually inducible promoters was designed. With this system it should be possible to selectively express one ADH from the genome of *E. coli* and only one plasmid for the ERED and BVMO would be needed, leaving space for an additional plasmid with another enzyme. Unfortunately the genomic integration could not be finalized during the course of this thesis but the designed integration system forms a good basis for future research.

After thorough investigations on the three-step cascade where side-reactions and bottlenecks were identified, the extension of the cascade with an oxygenase to start from cyclic alkenes should finally be realized. As a suitable enzyme to be integrated in *E. coli* could not be found implementation of another bacterial strain was tested. The search in the literature was focused on hydroxylation activity reported for limonene, as most recently discovered microbial entities are tested towards their biodegradation abilities of natural products. *C. cellulans* EB-8-4 was reported to hydroxylate *R*-(+)-limonene to (1*R*,5*S*)-carveol^[157] which could be converted in the three-step cascade. Unfortunately a mix-strain with a pathogenic *Rhodococcus* strain, being responsible for the hydroxylation, was discovered therefore rendering unfeasible for our use.

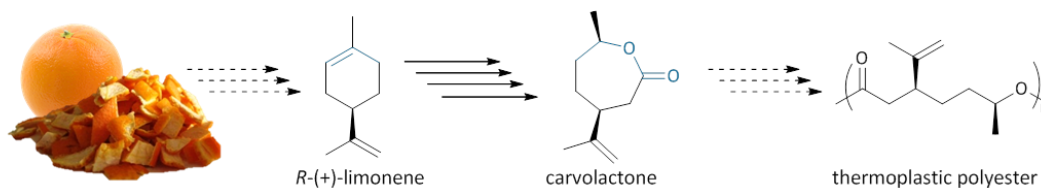
Also cumene dioxygenase (CumDO) was reported to selectively produce (1*R*,5*S*)-carveol from *R*-(+)-limonene.^[152] This enzyme was expressed in *P. putida* S12 and its hydroxylation activity proven in a preparative scale experiment from which enantiopure (1*R*,5*S*)-carveol was extracted and characterized. This stereoselective transformation of *R*-(+)-limonene enabled access to a carveol isomer which was not available through chemical synthesis showing the advantages of biocatalysis in chiral synthesis. *P. putida* S12 resting cells with expressed CumDO were also tested for hydroxylation activity for the other cyclic alkene substrates. First test reactions did not proceed very well, possibly also due to volatility of the substrates.

A two-liquid-phase approach could be beneficial for several optimizations of the cascade reactions. The volatility of hydrophobic substrates could be limited as they would be submerged in the organic phase. Although *P. putida* S12 is known as a solvent-tolerant strain it has to be adapted to organic liquids, which is a tedious procedure. Therefore the expression of CumDO in the constitutively solvent-tolerant strain *P. taiwanensis* VLB120 was investigated. Unfortunately first tests did not show better hydroxylation activity. Further improvements could be achieved through optimizing the cultivation of *P. taiwanensis* VLB120 and expression of CumDO.

As the hydroxylation by CumDO in *P. putida* S12 worked fine it was decided to investigate a mixed-culture approach to realize a cascade from *R*-(+)-limonene to chiral carvolactone. Resting cells of *P. putida* S12 with expressed CumDO and *E. coli* BL21(DE3) with expressed RR-ADH, XenB and CHMO_{Acinetobacter} were mixed in

one-pot. With a sequential approach where CumDO reaction was performed first and *E. coli* added later excellent conversion of *R*-(+)-limonene to carvolactone was achieved. In a simultaneous approach where both were added from the beginning *E. coli* seemed to inhibit the hydroxylation reaction.

These very promising results led to the idea to utilize *R*-(+)-limonene containing orange peel as starting material. High amounts of orange peel are produced as food supply chain waste (FSCW) during the production of orange juice. Valorization of waste products presents an appealing concept in green chemistry.^[169, 183-185] The utilization of orange peel in our cascade reaction would present such a valorization as the final product carvolactone could serve as building block for the synthesis of thermoplastic polyesters.^[186-187] Enzymatic polymerization was recently reported for other lactones^[188] and may also be applied for carvolactones.



Scheme D-2. Transformation of *R*-(+)-limonene from orange peel and possible further utilization of the final product carvolactone.

As *R*-(+)-limonene is hydrophobic different concepts to ensure its availability in the aqueous resting cell phase were investigated. Ionic liquids were used to dissolve orange peel prior to the whole cell reaction but albeit their excellent biomass extraction abilities^[177] the dilution of the extract to the resting cells did not render feasible. Also the addition of diluted ionic liquids to the mixed-culture cascade as *in situ* extraction enhancers did not improve our results. Recently induction systems for ionic liquid resistance in *E. coli* have been investigated.^[189-190] Application of these concepts may also enhance the IL tolerance of our system and could be investigated in future projects.

Very fortunately the simplest system with orange peel suspended in the aqueous phase of the resting cells delivered most promising results. Here the orange peel served as substrate reservoir, continuously releasing *R*-(+)-limonene to the aqueous phase where it could directly be converted. Due to moderate percentage of *R*-(+)-limonene in orange peel toxicity levels^[160], which could impair the viability of the microbial host, were not reached.

The implementation of the complete enzymatic cascade system, i.e. CumDO, an ADH, an ERED and a BVMO in one microbial organism is highly desired. As CumDO was reported not to express in *E. coli* a *Pseudomonas* strain could eventually be of use. If the decreased activity of CumDO in *P. taiwanensis* VLB120 could be overcome this strain could provide the optimal platform as it is constitutively solvent-tolerant^[159]. This feature would be beneficial for the implementation of a two-liquid phase system or the utilization of biphasic ionic liquids^[191]. The organic layer would contain the main share of the hydrophobic substrate, enabling higher concentrations of starting material and limiting toxic effects on the microbial host. The feasibility of a two-liquid-phase system for the use with orange peel as starting material would have to be thought through in detail. As all *R*-(+)-limonene, i.e. the hydrophobic substrate would accumulate in the organic phase; high amounts of orange peel would be needed to transfer enough substrate to the aqueous phase.

E Experimental part

E I Materials and methods – biotransformations

Unless noted otherwise, all reagents were purchased from commercial suppliers and used without further purification. All plastic consumables were either sterile upon purchase (Greiner) or sterilized prior to use, like standard glass equipment, by autoclaving (121°C, 15 min, elevated pressure; Tuttnauer 2540EL autoclave).

E I.1 Bacterial strains and enzymes

All bacterial strains used in this study are listed in Table E-1. *Escherichia* strains were available in the research group or constructed from these, *Cellulosimicrobium* and *Pseudomonas* strains were received from the cooperation partners referred to in the references.

Table E-1. Bacterial strains

Entry	Bacterial strain	Abbreviation	Reference
1	<i>Escherichia coli</i> BL21(DE3)	<i>E. coli</i> BL21(DE3)	
2	<i>Escherichia coli</i> BL21(DE3) $\Delta nemA$ +kan ^R	$\Delta nemA$ +kan ^R	this work
3	<i>Escherichia coli</i> BL21(DE3) $\Delta nemA$	$\Delta nemA$	this work
4	<i>Escherichia coli</i> BL21(DE3) $\Delta nemA \Delta fadH$	$\Delta nemA \Delta fadH$	this work
5	<i>Escherichia coli</i> BL21(DE3) $\Delta nemA \Delta fadH-2$ +kan ^R	$\Delta nemA \Delta fadH-2$ +kan ^R	this work
6	<i>Escherichia coli</i> DH5 α	<i>E. coli</i> DH5 α	
7	<i>Escherichia coli</i> Top10	<i>E. coli</i> Top10	
8	<i>Cellulosimicrobium cellulans</i> EB-8-4	<i>C. cellulans</i>	[157]
9	<i>Pseudomonas putida</i> S12	<i>P. putida</i>	[152]
10	<i>Pseudomonas taiwanensis</i> VLB120 $\Delta C\Delta ttgV$	<i>P. taiwanensis</i>	[159]

All enzymes regularly used and implemented in cascade reactions, their origin and GenBank accession number can be found in Table E-2. Protein sizes, expression plasmids and correlated antibiotic resistances are depicted in Table E-3.

Table E-2. Used enzymes and their origin.

Entry	Enzyme name	Origin	GenBank accession number	Ref.
1	RR-ADH	<i>Rhodococcus ruber</i>	CAD36475.1	[133]
2	LK-ADH	<i>Lactobacillus kefir</i>	AY267012.1	[132]
3	XenB	<i>Pseudomonas putida</i> ATCC 17453	AGS77941.1	[131]
4	OYE1	<i>Saccharomyces</i> sp.	Q02899.3	[95]
5	CHMO _{Acineto}	<i>Acinetobacter calcoaceticus</i>	BAA86293.1	[104]
6	CumDO	<i>Pseudomonas</i> sp. PWD32	KT160226.1	[152]

Table E-3. Enzymes with corresponding plasmids and expression hosts.

Entry	Enzyme name	Enzyme class	Size [kDa]	Plasmids (ori)	Antibiotic resistance (concentration)	Ref.
1	RR-ADH	ADH	35 (band appears at 25)	pRRADH (p15A)	chl (34 $\mu\text{g mL}^{-1}$)	[133]
2	LK-ADH	ADH	26.7	pET21_LKADH (pBR322 + F1)	amp (100 $\mu\text{g mL}^{-1}$)	[132]
3	XenB	ERED	38.7	pGASTON_XenB (pBR322)	amp (100 $\mu\text{g mL}^{-1}$)	[131]
4	OYE1	ERED	45 + 25 GST-tag	pDJB5 (ColE1 + F1)	kan (50 $\mu\text{g mL}^{-1}$)	[95]
5	CHMO _{Acineto}	BVMO	60.9	pET28a_CHMO (pBR322 + F1)	kan (50 $\mu\text{g mL}^{-1}$)	[192]
				pMM4 (pBR322 + F1)	amp (100 $\mu\text{g mL}^{-1}$)	[104]
6	CumDO	Oxygenase	Alpha-unit: 52 beta-unit: 22	pBTBX-2_CumDO (pBBR-1)	kan (40 $\mu\text{g mL}^{-1}$)	[152]

E I.2 Media, buffers and stock solutions

Bacteria on agar plates were incubated in an Heraeus Instruments FunctionLine incubator under air. Agar plates were prepared with LB medium supplemented by 1.5% w/v Agar Agar. Bacterial liquid cultures were cultivated in orbital shakers (InforsHT Multitron 2 Standard) at defined temperatures and shaking speed. Cell density of liquid cultures was measured in a WPA colourwave CO7500 Colorimeter (Biochrom, Harvard Apparatus Inc., Holliston, MA, USA) at a wavelength of $\lambda = 590$ nm (optical density OD_{590}) if not noted otherwise. $\text{OD}_{590} = 1$ correlates to a value of 0.43 g L^{-1} cell dry weight (cdw) for *E. coli*. All materials and biotransformation media were sterilized by autoclaving at 121°C for 20 min.

Table E-4. Constituents of complex bacterial growth media and frequently used buffers.

LB Medium		TB Medium		50 mM Tris-HCl pH 7.5	
10 g	peptone	12 g	tryptone	6.06 g	Tris
5 g	yeast extract	24 g	yeast extract	700 mL	dH ₂ O
10 g	NaCl	16.4 g	K ₂ HPO ₄ · 3 H ₂ O		
		2.3 g	KH ₂ PO ₄		
Concentrations on 1000 mL deionized water				Adjust pH to 7.5 with 2 N HCl, make to 1000 mL	

Table E-5. Antibiotic stock solutions.

Reagent	Abbreviation	Concentration	Solvent	Sterilization by
Ampicillin	amp	50 mg mL ⁻¹	dH ₂ O	0.2 μm filtration
Kanamycin	kan	50 mg mL ⁻¹	dH ₂ O	0.2 μm filtration
Tetracycline	tet	5 mg mL ⁻¹	dH ₂ O	0.2 μm filtration
Streptomycin	sm	100 mg mL ⁻¹	dH ₂ O	0.2 μm filtration
Chloramphenicol	chl	34 mg mL ⁻¹	EtOH	

Table E-6. Stock solutions of sugars, inducers and cofactors.

Reagent	Concentration	Solvent	Sterilization by
IPTG	100 mM	dH ₂ O	0.2 µm filtration
L-rhamnose	20% (w/v)	dH ₂ O	0.2 µm filtration
D-glucose	20% (w/v)	dH ₂ O	0.2 µm filtration
Glycerol	50% (w/v)	dH ₂ O	autoclaving
MgCl ₂	2 M	dH ₂ O	autoclaving
L-arabinose	40% (w/v)	dH ₂ O	0.2 µm filtration
NAD ⁺	0.1 M	dH ₂ O	0.2 µm filtration
NADH	0.1 M	dH ₂ O	0.2 µm filtration
NADP ⁺	0.1 M	dH ₂ O	0.2 µm filtration
NADPH	0.1 M	dH ₂ O	0.2 µm filtration
G6P	0.5 M	dH ₂ O	0.2 µm filtration

E I.3 Transformation of *E. coli*

For the transformation of bacterial strains with plasmids two different approaches were available.

E I.3.1 Chemical transformation

A LB culture (containing the appropriate antibiotic if necessary) was inoculated with 1% (v/v) of an o/n culture in the same medium and grown to an OD₅₉₀ of 0.2-0.4 at 37 °C. This culture was then dispensed in 1.5 mL aliquots which were centrifuged at 2300 x g at 4 °C for 10 min. Supernatant was discarded, the cell pellet resuspended in 0.5 mL ice cold 0.1 M CaCl₂ and kept on ice for 15 min. The centrifugation step was then repeated and the cells were resuspended in 100 µL ice cold 0.1 M CaCl₂ to obtain chemically competent cells. Typically 50-100 ng of plasmid were added to one aliquot of competent cells and kept on ice for 1 h. After a heat shock at 42 °C for 1 min cells were cooled on ice for 2 min before addition of 500 µL LB medium. This cell suspension was shaken at 37 °C for 1 h for recovery. 100 µL of this suspension were plated on a LB agar plate containing the selection marker of the plasmid and the plate incubated at 37 °C o/n.

E I.3.2 Electroporation

A LB culture (containing the appropriate antibiotic if necessary) was inoculated with 1% (v/v) of an o/n culture in the same medium and grown to an OD₅₉₀ of 0.5 at 37 °C. This culture was centrifuged at 4000 x g at 4 °C for 15 min and the supernatant was discarded. Resuspension in sterile dH₂O, centrifugation and discarding of the supernatant was performed two times for washing. The pellet was then resuspended in 10% sterile glycerol (same volume as culture) and centrifuged at the above conditions. After discarding of the glycerol the pellet was taken up in half the volume of 10% glycerol and dispensed in 100 µL aliquots which could be stored at -80 °C until further use.

Electroporation cuvettes and competent cells were cooled on ice and SOC medium (preparation see Table E-7) was tempered to 37 °C for at least 30 min prior to transformation. 1-100 ng of plasmid DNA were mixed with 40 µL of electrocompetent cells and filled into a cooled cuvette. The closed and from the outside dried cuvette was placed in the PEP (Personal Electroporation Pak) unit and electroporated at 1.6 kV for 4 ms in a BTX Genetronics ECM399 electroporation device (Harvard Apparatus, Inc., Holliston, MA, USA). 500 µL of pre-warmed SOC medium were immediately added in the cuvette, the transformation mix was transferred to an

Eppendorf tube and shaken at 37 °C for 1 to 1.5 h. On one pre-warmed LB agar plate containing the appropriate antibiotic 100 µL were plated, the rest of the mix on another plate and incubated at 37 °C o/n.

Table E-7. Preparation of SOC medium.

SOx		SOC	
4 g	tryptone	50 mL	SOx
1 g	yeast extract	0.25 mL	2 M MgCl ₂
0.1 g	NaCl	0.9 mL	20% Glucose
190 mL	dH ₂ O		
shake until dissolved			
0.5 mL	1 M KCl		
Adjust pH to 7.0 with 5 N NaOH, make to 200 mL and autoclave		Sterile preparation	

E I.4 Preparation of permanent cultures

Bacterial strains were incubated (*E. coli* at 37 °C, both *Pseudomonas* strains at 30 °C) on LB agar plates containing the appropriate antibiotic concentrations (Table E-3) for 12–24 h. A 5 mL pre-culture was inoculated with a single colony and incubated (5 mL LB+antibiotic, PP round bottom culturing tube, 30 °C/37 °C, 12–24 h). Aliquots of this culture were added to 50% sterile glycerol (5:4, ~22% glycerol final concentration) in Eppendorf tubes and stored at -80 °C until further use.

E I.5 Heterologous gene expression

In general, the cultivation of bacteria was carried out by inoculation of cultivation media supplied with the specified antibiotic with overnight culture to a calculated OD₅₉₀ of 0.05. The cultivation was continued at 30 °C or 37 °C until OD₅₉₀ = 0.6-0.7 was reached. Then, expression of the heterologous genes for enzyme production was started by addition of the appropriate inducer and carried out for a specific duration, at given temperatures and shaking speed. Deviations from this standard protocol and specific requirements are listed in Table E-8.

Table E-8. Expression protocols for single enzymes.

Entry	Enzymes	Expression strain (plasmid)	Expression protocol
1	LK-ADH	<i>E. coli</i> BL21(DE3) (pET22b_LKADH)	LB _{amp} , 37 °C, 120 rpm; at OD ₅₉₀ 0.6 + 0.1 mM IPTG, 20 h, 30 °C
2	RR-ADH	<i>E. coli</i> BL21(DE3) (pRRADH)	LB _{chl} , 37 °C, 120 rpm; at OD ₅₉₀ 0.4 + 1 mM ZnCl ₂ ; 30 min 25 °C; + 0.1 mM IPTG, 20 h
3	XenB	<i>E. coli</i> BL21(DE3) (pGASTON_XenB)	LB _{amp} , 37 °C, 180 rpm; at OD ₅₉₀ 0.6 + 0.2% (w/v) L-rhamnose; 20 h, 25 °C
4	OYE1	<i>E. coli</i> BL21(DE3) (pDJB5)	LB _{amp} , 37 °C, 180 rpm; at OD ₅₉₀ 0.6 + 0.1 mM IPTG; 20 h, 25 °C
5	CHMO _{Acineto}	<i>E. coli</i> BL21(DE3) (pMM04)	LB _{amp} , 37 °C, 180 rpm; at OD ₅₉₀ 0.6 + 0.1 mM IPTG; 20 h, 25 °C
6	CumDO	<i>P. putida</i> S12 (pBTBX-2_CumDO)	TB _{kan} , 30 °C, 200 rpm; at OD ₅₉₀ 0.6 + 2% (w/v) L-arabinose, 6 h, 30 °C

The same general procedure was used for the simultaneous co-expression of multiple enzymes in one expression host. The requirements for the specific combinations are depicted in Table E-9.

Table E-9. Protocols for co-expression of enzymes in *E. coli*.

Entry	Enzymes	Expression strain (plasmids)	Expression protocol
1	RR-ADH, XenB and CHMO _{Acineto}	<i>E. coli</i> BL21(DE3) (pRRADH + pGASTON_XenB + pET28a_CHMO)	TB _{chl+amp+kan} , 37 °C, 120 rpm; at OD ₅₉₀ 0.3 + 1 mM ZnCl ₂ ; 30 min 25 °C; + 0.2% (w/v) L-rhamnose + 0.1 mM IPTG, 22 h, 25 °C
2	LK-ADH, XenB and CHMO _{Acineto}	<i>E. coli</i> BL21(DE3) (pET28_CHMO_XenB + pET22b_LKADH)	TB _{amp+kan} , 37 °C, 200 rpm; at OD ₅₉₀ 0.7 + 0.1 mM IPTG; 20 h, 25 °C
3	LK-ADH, OYE1 and CHMO _{Acineto}	<i>E. coli</i> BL21(DE3) (pET28_CHMO_OYE + pET22b_LKADH)	TB _{amp+kan} , 37 °C, 200 rpm; at OD ₅₉₀ 0.7 + 0.1 mM IPTG; 20 h, 25 °C
4	RR-ADH, XenB and CHMO _{Acineto}	<i>E. coli</i> BL21(DE3) (pET28_CHMO_XenB + pRRADH)	TB _{chl+kan} , 37 °C, 200 rpm; at OD ₅₉₀ 0.3 + 1 mM ZnCl ₂ ; 30 min 25 °C; at OD ₅₉₀ 0.7 + 0.1 mM IPTG; 20 h, 25 °C
5	RR-ADH, OYE1 and CHMO _{Acineto}	<i>E. coli</i> BL21(DE3) (pET28_CHMO_OYE + pRRADH)	TB _{chl+kan} , 37 °C, 200 rpm; at OD ₅₉₀ 0.3 + 1 mM ZnCl ₂ ; 30 min 25 °C; at OD ₅₉₀ 0.7 + 0.1 mM IPTG; 20 h, 25 °C

E 1.6 Cell free extracts (CFE)

After the end of cultivation described in E 1.5, 50-200 mL of the culture were centrifuged at 6000 x g at 4 °C for 15 min. The supernatant was decanted and the cells were resuspended in 10 ml 50 mM Tris-HCl pH 7.5 and again centrifuged at 6000 x g at 4 °C for 15 min. After resuspension of the cells in 4-6 ml 50 mM Tris-HCl pH 7.5 supplemented with 0.1 mM PMSF (phenylmethylsulfonyl fluoride) sonication was performed with a Bandelin KE 76 sonotrode connected to a Bandelin Sonopuls HD 3200 wave generator. The cell suspension was repeatedly (9 cycles) sonicated for 5 s followed by 55 s pause on ice. Insoluble cell residues were cut off by centrifugation at 14000 x g at 4 °C for 20 min. The supernatant cell free extract was sterilized by 0.2 µm filtration. Protein concentration was determined with Bio-Rad Protein Assay (Bio-Rad Laboratories, Inc., Hercules, CA, USA) according to instruction manual.

E 1.7 *E. coli* resting cells

For *in vivo* biotransformations resting (not growing) cells of bacteria were prepared according to the following.

E 1.7.1 Method A

Resting cells could be prepared directly in the cultivation medium after production of the enzymes in *E. coli* (E 1.5) by cooling the cell culture to 4 °C and supplementing it with 1% (w/v) D-glucose.

E 1.7.2 Method B

For concentrated resting cells the cultures were centrifuged at 4500 x g at 4 °C for 10 min after cultivation. The supernatant was discarded and the cells were gently resuspended in nitrogen free (N-free) M9 medium

(adapted from Sambrook^[193]) or 50 mM Tris-HCl pH 7.5, both supplemented with 1% (w/v) D-glucose, to a calculated OD₅₉₀ of 100 if not otherwise noted.

Table E-10. Preparation of N-free M9 medium.

N-free M9 salts (5x)		N-free M9	
2.5 g	NaCl	N-free M9 salts (5x)	20 mL
64 g	Na ₂ HPO ₄ · 7 H ₂ O	Glucose (20%, sterile)	2 mL
15 g	KH ₂ PO ₄	MgSO ₄ (1 M, autoclaved)	200 µL
		CaCl ₂ (1 M, autoclaved)	10 µL
Concentrations on 1000 mL deionized water, autoclaved.		Amounts on 100 mL sterile deionized water	

E I.8 SDS-PAGE

Sodium dodecyl sulfate polyacrylamide gel electrophoresis (SDS-PAGE) was performed with a Mini-PROTEAN® system from Bio-Rad and all buffers and gels were prepared according to the instruction manual. SDS-PA gels were normally prepared with 12.5% acrylamide/bis-acrylamide as a resolving gel and 4% acrylamide/bis-acrylamide for the stacking gel. For the estimation of protein size a Fermentas PageRuler™ Prestained Protein Ladder (#SM0671) was used. Staining of SDS-PA gels was done with Coomassie Brilliant Blue R-250 from Bio-Rad or SimplyBlue™ SafeStain from Thermo Fisher Scientific following the manufacturer's instructions.

CFE samples were diluted with SDS-PAGE sample buffer (Mini-PROTEAN instruction manual) supplemented with β-mercaptoethanol to a concentration of 1 µg µL⁻¹. Whole cell samples for "crude" gels were normalized to OD₅₉₀=8, where the cells were mixed with sample buffer in a ratio of 1:2. Cultures with higher cell density were diluted accordingly with more sample buffer. Lower cell density samples were concentrated by centrifugation, the supernatant discarded and the pellet resuspended in sample buffer. All samples were denatured at 95°C for 4 min, shortly centrifuged and 20 µL loaded onto the gel.

E I.9 GC analysis

Conversion and product purity were determined by gas chromatography (GC) using a Thermo Finnigan Focus GC / DSQ II equipped with a standard capillary column (BGB5, 30 m x 0.25 mm ID, 0.50 µm film). Enantiomeric excess was determined by GC analysis using a BGB175 (30 m x 0.25 mm ID, 0.25 µm film) or BGB173 (30 m x 0.25 mm ID, 0.25 µm film) column on a ThermoQuest Trace GC 2000 and a ThermoFocus GC, both with FID detector.

Table E-11. Methods for GC analysis

	Column	Temperature program (r = [°C/min])	Duration
Method A	BGB5	100 °C 2 min – 18r → 280 °C 5 min	17 min
Method B	BGB175	80 °C 2 min – 5r → 130 °C 1 min – 50r → 220 °C 6.2 min	21 min
Method C	BGB175	95 °C 2 min – 2r → 115 °C 0.5 min – 50r → 190 °C 0.5 min – 20r → 220 °C 2 min	18 min
Method D	BGB173	90 °C 2 min – 5r → 96 °C 2 min – 5r → 100 °C – 20r → 135 °C – 4r → 145 °C 0.25 min – 50r → 220 °C 1 min	13 min
Method E	BGB175	110 °C 2 min – 10r → 118 °C – 2r → 122 °C – 25r → 200 °C 1 min – 50r → 220 °C 1.68 min	11 min
Method F	BGB173	80 °C 1 min – 1r → 84 °C 1.4 min – 14r → 140 °C – 50r → 220 °C 1 min	13 min
Method G	BGB175	100 °C 2 min – 2r → 110 °C – 1.5r → 120 °C 2 min – 1.5r → 125 °C – 5r → 150 °C – 1.5r → 165 °C – 2r → 180 °C 1 min – 50r → 220 °C 1 min	45 min

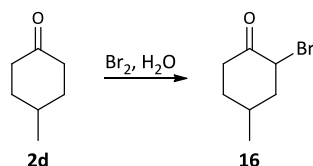
E II Chemical syntheses

E II.1 Syntheses of starting material

Chemical syntheses of not commercially available starting material and intermediates were conducted in close cooperation and support by Waldemar Fahrenstiel, Ramana Pydi and Patricia Schaaf and are partly published.^[131]

Unless noted otherwise, all reagents were purchased from commercial suppliers and used without further purification. Dichloromethane, diethylether (Et₂O), 1,4-dioxane, methanol (MeOH), tetrahydrofuran (THF) and toluene intended for water-free reactions were pre-distilled and then desiccated on Al₂O₃ columns (PURESOLV, Innovative Technology). Chromatography solvents were distilled prior to use. For all other solvents quality grade is given in the reaction procedures. Column chromatography was performed on a BüchiSepacore Flash System (2 x Büchi Pump Module C-605, Büchi Pump Manager C-615, Büchi UV Photometer C-635, Büchi Fraction Collector C-660) or standard manual glass columns using silica gel from Merck (40-63 µm) using LP and Et₂O or EtOAc mixtures. Desiccation of organic solvents after extraction in reaction workup was performed using anhydrous sodium sulfate and subsequent filtration. NMR spectra were recorded from CDCl₃, CD₂Cl₂ or d₆-DMSO solutions on a Bruker AC 200 (200 MHz) or Bruker Advance UltraShield 400 (400 MHz) spectrometer and chemical shifts are reported in ppm using tetramethylsilane as internal standard. Whenever possible, calibration was performed via residual solvent peaks. Peak assignment was based on correlation experiments or software prediction.

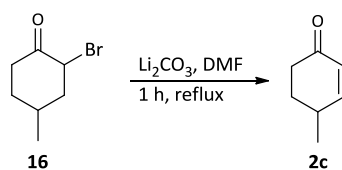
E II.1.1 2-Bromo-4-methylcyclohexanone (**16**)



Scheme E-1. Bromination of 4-methylcyclohexanone (**2d**).

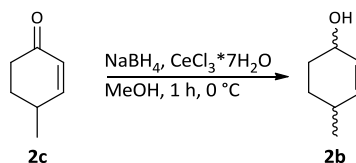
Br₂ (2.39 ml, 41.3 mmol) was added dropwise to a stirred mixture of 5 g 4-methylcyclohexanone (**2d**) and 15 ml H₂O. The temperature was kept at 30 °C with an ice bath. Addition of bromine took 30 min. The aqueous layer was extracted with CH₂Cl₂ (3×150 ml) after separation and the combined ethereal solution was dried over Na₂SO₄. The solvent was evaporated and the product was purified by vacuum distillation, bp 23-29 °C (0.09 mbar).^[194]

Yield	4.668 g (59%)
Sum formula, m.w.	C ₇ H ₁₃ BrO, 193.08
¹H-NMR (200 MHz, CDCl₃)	δ = 0.99-1.04 (m, 3H), 1.28-1.54 (m, 2H), 1.84-2.70 (m, 7H), 3.03-3.20 (m, 1H), 4.30-4.34 (m, 1H), 4.60-4.70 (m, 1H) ppm.
¹³C-NMR (50 MHz, CDCl₃)	δ = 20.5, 20.7, 26.2, 33.5, 34.5, 34.9, 35.4, 40.1, 42.1, 47.4, 50.9, 55.3, 201.6, 204.7 ppm.

E II.1.2 4-Methylcyclohex-2-en-1-one (**2c**)Scheme E-2. Elimination to yield 4-methylcyclohex-2-enone (**2c**).

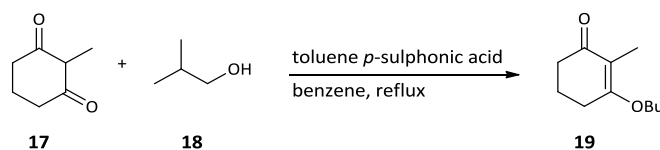
2-Bromo-4-methylcyclohexanone (**16**, 2.5 g, 13.16 mmol) and Li_2CO_3 (1.948 g, 26.32 mmol) in 20 ml DMF were heated under reflux in argon for 1 h. The mixture was cooled, diluted with H_2O and extracted with CH_2Cl_2 (3×100 ml). The organic layer was washed with brine and dried over Na_2SO_4 and concentrated *in vacuo*.^[195]

Yield	833 mg (58%)
Sum formula, m.w.	$\text{C}_7\text{H}_{10}\text{O}$, 110.15
$^1\text{H-NMR}$ (200 MHz, CDCl_3)	$\delta = 0.78\text{-}0.93$ (m, 1H), 1.12-1.24 (m, 3H), 1.55-1.75 (m, 1H), 2.02-2.16 (m, 1H), 2.25-2.61 (m, 3H), 5.94 (dd, 1H, $J = 10.1, 2.4$ Hz), 6.79 (ddd, 1H, $J = 10.1, 2.6, 1.3$ Hz) ppm.
$^{13}\text{C-NMR}$ (50 MHz, CDCl_3)	$\delta = 20.2, 30.9, 31.1, 36.9, 128.6, 156.3, 199.8$ ppm.

E II.1.3 4-Methylcyclohex-2-en-1-ol (**2b**)Scheme E-3. Luche reduction to give 4-methylcyclohex-2-en-1-ol (**2b**).

NaBH_4 (94 mg, 2.47 mmol) was added to a solution of the ketone (272 mg, 2.47 mmol) and $\text{CeCl}_3 \cdot 7\text{H}_2\text{O}$ (1.020 g, 2.74 mmol) in 15 ml MeOH at -70 °C. The reaction mixture was stirred at -70 °C for 1 h and was quenched by the addition of 150 ml of saturated NH_4Cl solution. The aqueous phase was washed with Et_2O (3×50 ml). The combined organics were washed with saturated NaCl solution (2×50 ml), followed by H_2O (3×50 ml), dried over NaSO_4 and concentrated *in vacuo*.^[196]

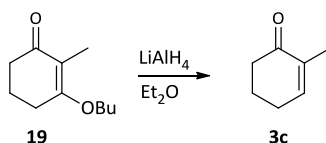
Yield	196 mg (71%) <i>trans</i> isomer ^[197] <i>cis</i> isomer: minor component, 33%, shorter retention time ^[195]
Sum formula, m.w.	$\text{C}_7\text{H}_{12}\text{O}$, 112.17
$^1\text{H-NMR}$ (200 MHz, CDCl_3)	$\delta = 0.91\text{-}1.01$ (m, 3H), 1.12-2.23 (m, 6H), 4.10-4.22 (m, 1H), 5.56-5.70 (m, 1H) ppm.
$^{13}\text{C-NMR}$ (50 MHz, CDCl_3)	$\delta = 21.0, 21.2, 26.3, 29.0, 30.2, 30.3, 30.4, 31.8, 64.3, 66.8, 128.1, 129.7, 139.9, 137.3$ ppm.

E II.1.4 3-Isobutoxy-2-methylcyclohex-2-enone (**19**)

Scheme E-4. Condensation of 2-methyl-1,3-dione and isobutanol to yield isobutoxy-2-methylcyclohex-2-enone.

A solution of 2-methyl-1,3-dione (**17**, 4.889 g, 38.8 mmol) and toluene *p*-sulphonic acid (hydrate) in 75 ml benzene and isobutanol (**18**, 5.742 g, 77.6 mmol) was heated to reflux on a Dean stark separator for 2 h. The reaction mixture was cooled, washed with 5% NaOH_{aq} (3×50 ml), with H₂O (3×50 ml), dried over Na₂SO₄ and concentrated *in vacuo*.^[198]

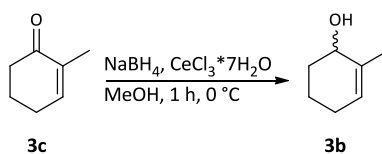
Yield	3.874 g (55%)
Sum formula, m.w.	C ₁₁ H ₁₈ O ₂ , 186.26
¹H-NMR (200 MHz, CDCl₃)	δ = 0.97-1.00 (d, 6H, <i>J</i> = 6.8 Hz), 1.67-1.69 (m, 3H), 1.93-1.99 (m, 3H), 2.30-2.37 (m, 2H), 2.52-2.59 (m, 2H), 3.78 (d, 2H, <i>J</i> = 6.5 Hz) ppm.
¹³C-NMR (50 MHz, CDCl₃)	δ = 7.4, 19.0, 21.0, 25.5, 28.8, 36.3, 114.9, 171.6, 198.9 ppm.

E II.1.5 2-Methylcyclohex-2-en-1-one (**3c**)

Scheme E-5. LiAlH₄ reduction of 3-isobutoxy-2-methylcyclohex-2-enone to give 2-methylcyclohex-2-enone (**3c**).

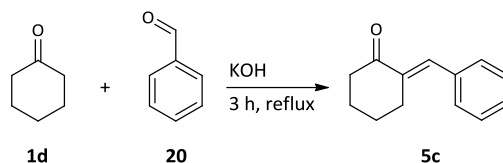
3-Isobutoxy-2-methylcyclohex-2-enone (**19**, 2.002 g, 11 mmol) in 15 ml dry Et₂O was added dropwise to LiAlH₄ (LAH, 167 mg, 4.4 mmol) in 15 ml dry Et₂O at such a rate that steady refluxing was maintained. The mixture was stirred for a further 1 h, cooled and 15 ml of 10% H₂SO₄ were added. The aqueous layer was extracted with Et₂O and the combined ethereal solutions were dried over Na₂SO₄ and concentrated *in vacuo*. The product was purified by column chromatography (LP/Et₂O; 1:2).^[198]

Yield	715 mg (59%)
Sum formula, m.w.	C ₇ H ₁₀ O, 110.15
¹H-NMR (200 MHz, CDCl₃)	δ = 1.77 (dd, 3H, <i>J</i> = 3.3, 1.6 Hz), 1.92-2.05 (m, 2H), 2.28-2.46 (m, 4H), 6.73-6.76 (m, 1H) ppm.
¹³C-NMR (50 MHz, CDCl₃)	δ = 16.0, 23.3, 26.0, 38.3, 135.7, 145.6, 200.1 ppm.

E II.1.6 2-Methylcyclohex-2-en-1-ol (**3b**)Scheme E-6. Luche reduction of 2-methylcyclohex-2-enone (**3c**) to 2-methylcyclohex-2-en-1-ol (**3b**).

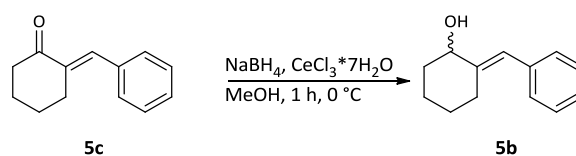
NaBH_4 (43 mg, 1.14 mmol) was added to a solution of the ketone (110 mg, 1.00 mmol) and $\text{CeCl}_3 \cdot 7\text{H}_2\text{O}$ (413 mg, 1.11 mmol) in 5 ml MeOH at -21°C . The reaction mixture was stirred at 0°C for 1 h and was quenched by the addition of 30 ml of saturated NH_4Cl solution. The aqueous phase was washed with Et_2O (3×15 ml). The combined organics were washed with saturated NaCl solution (2×15 ml), followed by H_2O (3×15 ml), dried over Na_2SO_4 and concentrated *in vacuo*.^[196]

Yield	40 mg (36%)
Sum formula, m.w.	$\text{C}_7\text{H}_{12}\text{O}$, 112.17
$^1\text{H-NMR}$ (200 MHz, CDCl_3)	$\delta = 1.52\text{--}2.02$ (m, 10H), 3.98 (s, 1H), 5.54 (s, 1H) ppm.
$^{13}\text{C-NMR}$ (50 MHz, CDCl_3)	$\delta = 18.1, 20.6, 25.4, 32.1, 68.4, 125.4, 135.2$ ppm.

E II.1.7 2-Benzylidenecyclohexanone (**5c**)Scheme E-7. Knoevenagel condensation yielding in 2-benzylidenecyclohexanone (**5c**).

A mixture of benzaldehyde (**20**, 530 mg, 5 mmol), cyclohexanone (**1d**, 735 mg, 7.5 mmol) and 1 N KOH solution (5 ml) was refluxed for 3 h. After cooling to room temperature, diethylether (10 ml) was added, the aqueous layer was separated and extracted with diethylether (3×10 ml). The combined ethereal solution was washed to neutrality with H_2O and dried over Na_2SO_4 . The solvent was evaporated and the product was purified by column chromatography (PE/EE; 20:1).^[137]

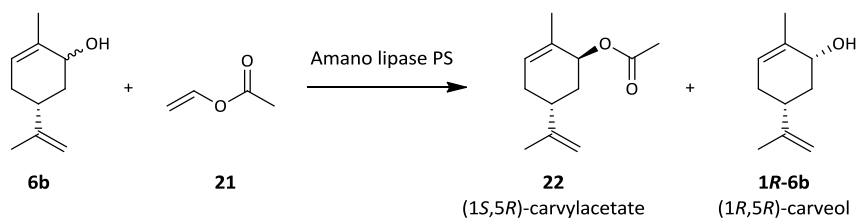
Yield	353 mg (38%)
Sum formula, m.w.	$\text{C}_{13}\text{H}_{14}\text{O}$, 186.25
Appearance	slightly yellow solid
$^1\text{H-NMR}$ (200 MHz, CDCl_3)	$\delta = 1.76\text{--}1.93$ (m, 4 H), 2.54 (t, $J = 6.7$ Hz, 2 H), 2.81–2.84 (m, 2 H), 7.34–7.51 (m, 6 H) ppm.
$^{13}\text{C-NMR}$ (50 MHz, CDCl_3)	$\delta = 23.4, 23.9, 28.9, 40.3, 128.3, 128.5, 130.3, 135.6$ (2 x C), 136.7, 201.8.

E II.1.8 2-Benzylidenecyclohexanol (**5b**)

Scheme E-8. Luche reduction of 2-benzylidenecyclohexanone (**5c**) to 2-benzylidenecyclohexanol (**5b**).

To a $0\text{ }^\circ\text{C}$ solution of the ketone (1.001 g, 5.38 mmol) and $\text{CeCl}_3 \cdot 7\text{H}_2\text{O}$ (2.221 g, 5.97 mmol) in 10 ml MeOH was added NaBH_4 (233 mg, 6.13 mmol). The reaction mixture was stirred at $0\text{ }^\circ\text{C}$ for 1 h and was quenched by the addition of 150 ml of saturated NH_4Cl solution. The aqueous phase was washed with Et_2O ($3 \times 150\text{ ml}$). The combined organics were washed with saturated NaCl solution ($2 \times 100\text{ ml}$), followed by H_2O ($3 \times 100\text{ ml}$), dried over Na_2SO_4 and concentrated in vacuo. The product was purified by column chromatography (PE/EE; 20:1).^[196]

Yield	626 mg (62%)
Sum formula, m.w.	$\text{C}_{13}\text{H}_{16}\text{O}$, 188.27
$^1\text{H-NMR}$ (200 MHz, CDCl_3)	$\delta = 1.52\text{-}1.98$ (m, 8 H), $2.66\text{-}2.78$ (m, 1 H), $4.21\text{-}4.24$ (m, 1 H), 6.52 (s, 1 H), $7.20\text{-}7.31$ (m, 5 H) ppm.
$^{13}\text{C-NMR}$ (50 MHz, CDCl_3)	$\delta = 23.2, 27.0, 27.4, 36.6, 73.8, 120.8, 126.2, 128.1, 128.9, 137.7, 144.4$ ppm.

E II.1.9 (1*S*,5*R*)-2-Methyl-5-(prop-1-en-2-yl)cyclohex-2-en-1-yl acetate (**22**) and (1*R*,5*R*)-Carveol (**1R-6b**)

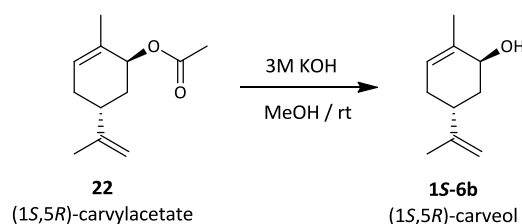
Scheme E-9. Selective esterification of **6b** by Amano lipase yielding in (1*S*,5*R*)-carvyl acetate and **1R-6b**.

A mixture of *cis/trans*-L-carveol (**6b**, 2.4 g, 15.8 mmol), lipase (0.25 g, Amano lipase PS), vinyl acetate (**21**, 0.68 g, 7.88 mmol, 0.5 eq) and *tert*-butyl methyl ether (15 ml) was stirred at room temperature and the formation of the desired acetate (**22**) was monitored by TLC and chiral GC analysis. The reaction was stopped by filtration of the enzyme and subsequent evaporation of the solvent at reduced pressure. Column chromatography of the residue in PE/EE afforded (1*R*,5*R*)-Carveol (**1R-6b**) and the desired acetate (**22**) in very good yields.

E II.1.9.1 (1*R*,5*R*)-Carveol (**1R-6b**)
Yield 1.06 g (44%)
Sum formula, m.w. C₁₀H₁₆O, 152.23
¹H-NMR (200 MHz, CDCl₃) δ = 1.38-1.60 (m, 1H), 1.66-1.78 (m, 6H), 1.88-2.37 (m, 3H), 4.09-4.26 (m, 1H), 4.72 (s, 2H), 5.49 (bs, 1H) ppm.
¹³C-NMR (50 MHz, CDCl₃) δ = 18.9, 20.6, 30.9, 37.9, 40.4, 70.8, 109.1, 123.8, 136.1, 148.9 ppm.

E II.1.9.2 (1*S*,5*R*)-Carvylacetate (**22**)
Yield 1.49 g (45%)
Sum formula, m.w. C₁₂H₁₈O₂, 194.27
¹H-NMR (200 MHz, CDCl₃) δ = 1.54-1.66 (m, 1H), 1.70 (s, 3H), 1.73 (s, 3H), 1.73-1.80 (m, 2H), 2.08 (s, 3H), 2.12-2.41 (m, 2H), 4.68-4.79 (m, 2H), 5.27 (bs, 1H), 5.69-5.79 (m, 1H) ppm.
¹³C-NMR (50 MHz, CDCl₃) δ = 20.6, 20.8, 21.4, 30.9, 33.6, 35.8, 70.6, 109.2, 127.9, 130.9, 148.7, 170.9 ppm.

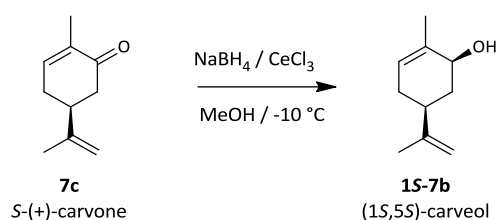
E II.1.10 (1*S*,5*R*)-Carveol (**1S-6b**)



Scheme E-10. Basic hydrolysis of (1*S*,5*R*)-carvyl acetate to give **1S-6b**.

(1*S*,5*R*)-2-Methyl-5-(prop-1-en-2-yl)cyclohex-2-en-1-yl acetate (**22**, 1.49 g, 7.09 mmol) was dissolved in 3 M KOH/MeOH (7.5 ml) and stirred at room temperature until no starting material was detected by TLC. The mixture was diluted with water (35 ml) and extracted three times with Et₂O (20 mL). The organic layers were combined, washed with brine, dried over Na₂SO₄ and concentrated *in vacuo* to give pure carveol **1S-6b**.

Yield 815 mg (68%)
Sum formula, m.w. C₁₀H₁₆O, 152.23
¹H-NMR (200 MHz, CDCl₃) δ = 1.47-1.70 (m, 2H), 1.75 (s, 3H), 1.76-1.82 (m, 3H), 1.86-2.45 (m, 4H), 4.03 (bs, 1H), 4.74 (bs, 2H), 5.50-5.66 (m, 1H) ppm.
¹³C-NMR (50 MHz, CDCl₃) δ = 20.8, 20.9, 30.9, 35.2, 36.7, 68.5, 109.0, 125.4, 134.3, 149.2 ppm.

E II.1.11 (1*S*,5*S*)-Carveol (**15-7b**)Scheme E-11. Luche reduction of *S*-(+)-carvone (**7c**) yielded in **15-7b**.

S-carvone (1 g, 6.66 mmol) and CeCl₃ were dissolved in dry MeOH (40 ml). The mixture was cooled to -10 °C and after 10 minutes NaBH₄ (375 mg, 9.9 mmol, 1.5 eq) was added slowly in portions. The cooling bath was removed and the mixture was stirred at room temperature until full conversion was detected by TLC (2 h). Afterwards, the solvent was removed under vacuum, the crude mixture was treated with water (35 ml) and extracted three times with CH₂Cl₂. The combined organic phases were washed with brine, dried over Na₂SO₄ and the solvent was removed under reduced pressure. No further purification was necessary.

Yield	730 mg (73%)
Sum formula, m.w.	C ₁₀ H ₁₆ O, 152.23
¹H-NMR (200 MHz, CDCl₃)	δ = 1.38-1.60 (m, 1H), 1.66-1.78 (m, 6H), 1.88-2.37 (m, 3H), 4.09-4.26 (m, 1H), 4.72 (s, 2H), 5.49 (bs, 1H) ppm.
¹³C-NMR (50 MHz, CDCl₃)	δ = 18.9, 20.6, 30.9, 37.9, 40.4, 70.8, 109.1, 123.8, 136.1, 148.9 ppm.

E II.2 Chemical syntheses of reference material

Following chemical syntheses were performed in small scale to obtain reference material for GC analysis.

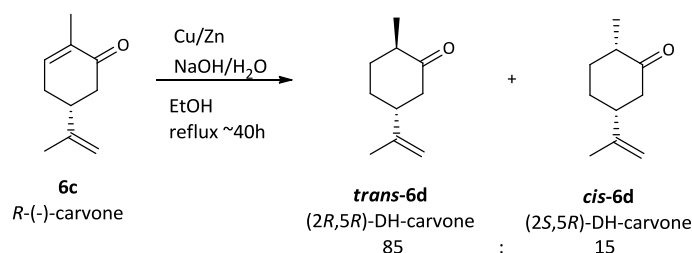
E II.2.1 Reduction of carvones to dihydrocarvones

E II.2.1.1 Cu/Zn-couple

A stirred suspension of zinc dust (10 g, 0.15 mol) in water (40 mL) was degassed by passing through N₂ for 15 min. Subsequently, CuSO₄ (750 mg, 4.7 mmol) was added at once and the black suspension was stirred while N₂ was passed through for an additional 45 min. The Copper-Zinc (Cu/Zn)-couple was collected on a sintered glass funnel, washed successively with 100 mL degassed water and acetone, dried *in vacuo* and stored (max. 2 d) under N₂.

E II.2.1.2 *R*-(-)-Carvone (**6c**) to *trans*-**6d** and *cis*-**6d**

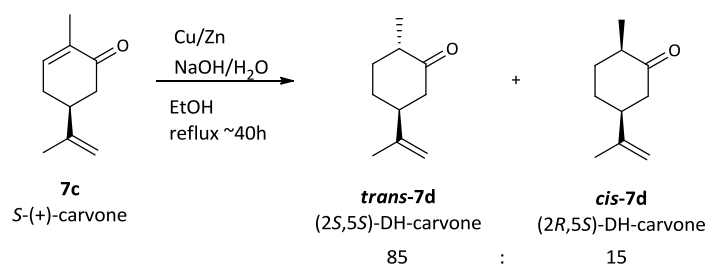
As reported by Petra Cernuchova this reaction results in a mixture of about 85% *trans*-**6d** and 15% *cis*-**6d** ^[199] (Scheme E-12).

Scheme E-12. Reduction of *R*-(-)-carvone (**6c**).

Cu/Zn-couple (2.4 g, E II.2.1.1) was added to a stirred solution of NaOH (2.5 g, 0.063 mol, 6.3 equiv.) in a mixture of water (10 mL) and ethanol (20 mL). Subsequently pure enantiomer of **6c** (1.5 g, 0.01 mol) was added and the resulting mixture was heated to reflux for several hours. The conversion of starting material was determined by GC. The mixture was filtered through a pad of Celite and extracted with diethylether (ether, 3x30 mL). The combined extracts were washed with saturated ammonium chloride, dried over sodium bicarbonate and evaporated. The crude product was dissolved in EtOAc, subjected to GC analysis and the peaks of *trans-6d* and *cis-6d* assigned according to their abundance reported by Cernuchova.

E II.2.1.3 S-(+)-Carvone (**7c**) to *trans-7d* and *cis-7d*

The reduction of S-(+)-carvone (**7c**, Scheme E-13) was also reported by Cernuchova and performed according to the procedure for **6c** described in E II.2.1.2.



Scheme E-13. Reduction of S-(+)-carvone (**7c**).

E II.2.2 Baeyer-Villiger oxidation (BVOx) of ketones to lactones

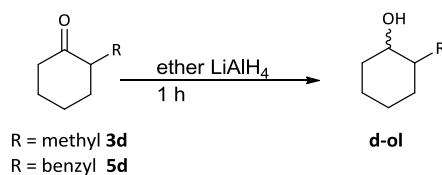
Racemic ketone (50 mg, Table E-12) was dissolved in dichloromethane (DCM, 0.25 mL), added to *meta*-chloroperoxybenzoic acid (mCPBA, 1.5 equiv.) in DCM (0.25 mL) and stirred at RT overnight. The mixture was diluted with water and DCM (1 mL each) and added to triethylamine (100 μL) upon cooling on ice. After vigorous stirring for 15-30 min a sample was taken from the organic phase and diluted for GC analysis (E I.9, Table E-11) where the lactone product mixture was separated.

Table E-12. Ketones objected to chemical BVOx and amount of mCPBA added.

Ketone	mCPBA [g]	Lactones	GC method
 2d 4-methylcyclohexanone	0.149	 2e	D
 3d 2-methylcyclohexanone	0.149	 3e	E
 4d 3-methylcyclohexanone	0.149	 4e + 4f	F
 5d 2-benzylcyclohexanone Literature values for optical rotation: <i>R</i> : $\alpha_D^{20} = +73.2$ (c 0.5, CHCl_3) ^[200] <i>S</i> : $\alpha_D^{21} = -32.4$ (c 0.9, CHCl_3) ^[137]	0.089	 5e Literature values for optical rotation: <i>R</i> : $\alpha_D^{20} = -45.8$ (c 1.3, CHCl_3) ^[201]	H

E II.2.3 Reduction of ketones to alcohols

To obtain saturated alcohols as reference material saturated ketones were subjected to lithium aluminum hydride (LiAlH_4) reduction as shown in Scheme E-14.



Scheme E-14. LiAlH_4 reduction of cyclohexanone derivatives.

Ketone (Table E-13) was dissolved in Et_2O (1 mL) and 1 equiv. LiAlH_4 added while stirred under ice/ NaCl cooling. After one hour the reaction progress was checked via TLC and the mixture was then quenched with saturated ammonium chloride. A sample was taken from the ether phase, diluted in EtOAc supplemented with methylbenzoate as standard and subjected to GC analysis.

Table E-13. Amounts of ketone and LiAlH_4 used for the reductions.

Ketone		[mg]	LiAlH_4 [mg]
3d	2-methylcyclohexanone	110	37.4
5d	2-benzylcyclohexanone	77.5	15.6

E III *E. coli* biotransformations

Sampling of biotransformation reactions was in general conducted by taking 100 μL of reaction suspension and mixing it with 500 μL EtOAc supplemented with 1 mM methyl benzoate as GC standard in glass vials. For better phase separation, transfer of the mixture to an Eppendorf tube and short centrifugation was possible. The organic phase was dried over Na_2SO_4 , transferred to a GC vial and measured according to E I.9.

E III.1 *In vitro* – single step

In vitro biotransformation reactions were conducted with CFE (preparation see E I.6) in closed glass vials while shaking at 24 °C and 200 rpm. For standard conditions the minimum reaction volume was 500 μL in 50 mM Tris-HCl pH 7.5. CFE was used in 5 mg mL^{-1} total protein concentration and 4 mM starting material were added from 1 M ethanolic stock solution. Additionally required cofactors and additives for specific enzyme reactions are listed in Table E-14.

Table E-14. Cofactors and recycling system added to *in vitro* reactions.

Enzyme	Cofactor	Concentration	Cofactor recycling	
			G6P-DH	G6P
LK-ADH	NADP^+	4.8 mM (1.2 equiv.)		
RR-ADH	NAD^+	4.8 mM (1.2 equiv.)		
EREDs	NADP^+	4.8 mM (1.2 equiv.)	1 U mL^{-1}	4.8 mM (1.2 equiv.)
$\text{CHMO}_{\text{Acineto}}$	NADP^+	4.8 mM (1.2 equiv.)	1 U mL^{-1}	4.8 mM (1.2 equiv.)

E III.2 *In vitro* – cascade

Two different reaction setups were chosen for *in vitro* cascade reactions: (i) a sequential cascade reaction where the three enzymes were added one after another, enabling a discrete initiation phase for each reaction step; (ii) a simultaneous approach with all enzymes, cofactors and recycling system mixed at once. All reactions were performed in closed glass vials at 24 °C and were shaken at 200 rpm.

E III.2.1 Sequential cascade reaction

The first reaction of the cascade, the oxidation of the unsaturated alcohol to the ketone, was performed with CFE of LK-ADH with a total protein concentration of 5 mg mL^{-1} . Reaction volume was 1 mL in a 50 mM Tris-HCl buffer at pH 7.5. NADP^+ (4.8 mM, 1.2 equiv.) was added as cofactor and the reaction started upon addition of 4 mM unsaturated alcohol (as a 1 M ethanolic stock solution). First sampling was conducted within a few minutes after mixing of the components (time point zero; $t_0 = t_0^*$). After one hour another sample was taken and then the ERED was added to the reaction mixture to a final total protein concentration of 5 mg mL^{-1} . In this step there was no need to add additional cofactor as NADPH was produced in the LK-ADH reaction. After another hour reaction progress was sampled and $\text{CHMO}_{\text{Acineto}}$ (CFE with 5 mg mL^{-1} total protein), 4.8 mM NADP^+ , 8 mM glucose-6-phosphate (G6P) and 1 U mL^{-1} glucose-6-phosphate dehydrogenase (G6P-DH) as cofactor recycling system were added. Sampling was performed after another hour (3 h) and continued up to 30 h.

E III.2.2 Simultaneous cascade reaction

For all cascade reactions with RR-ADH the simultaneous addition of the enzymes was performed, due to NAD^+ dependence of this ADH. CFEs of the ADH, the ERED and the BVMO were used at a total protein concentration of 5 mg mL^{-1} . 4.8 mM NAD^+ (1.2 equiv.) and 4.8 mM NADP^+ (1.2 equiv.) were added; 2 equiv. of G6P (8 mM) and 1 U mL^{-1} of G6P-DH served as cofactor recycling system. All CFEs, the cofactors, the recycling system and 4 mM substrate were mixed together at once in 50 mM Tris-HCl pH 7.5.

The simultaneous cascade applying LK-ADH was performed accordingly just without addition of NAD^+ . Samples were taken at regular time intervals to be comparable to the sequential approach.

E III.3 *In vivo* – single step

For *in vivo* biotransformations resting cells (E I.7) were supplemented with 4 mM substrate (from 1 M stock prepared in EtOH) in a closed glass vial with a volume approx. 10-fold higher than the cell suspension. Biotransformation was conducted at $24 \text{ }^\circ\text{C}$ and 200 rpm for a maximum of 48 h.

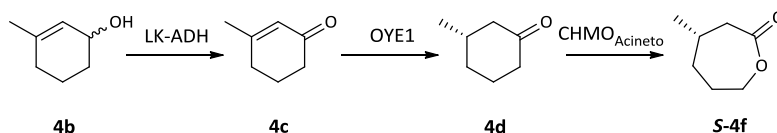
E III.4 *In vivo* – cascade

In vivo cascade reactions were either done by combining resting cells of individually expressed enzymes (Table E-8) in one pot or by using resting cells where all enzymes were coproduced in one host (Table E-9). The biotransformation procedure was done according to the single step reaction (E III.3).

E III.4.1 Preparative scale cascade reactions

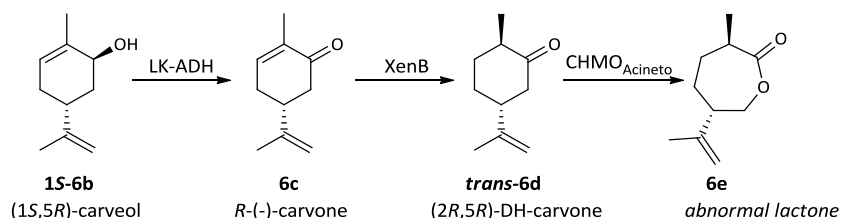
For preparative scale biotransformations concentrated resting cells (E I.7.2) were used. 100 mg of unsaturated alcohol as starting material were dissolved in $200 \text{ } \mu\text{L}$ EtOH and added to *E. coli* BL21(DE3) pET28_CHMO_XenB + pET22b_LKADH resting cells (164 mL) supplemented with 10 g L^{-1} glucose. The reaction was performed in a 1 L Schottflask at $24 \text{ }^\circ\text{C}$ and 160 rpm. Glucose concentration was checked every few hours with an Accu-Check Performa (Roche diagnostics) and maintained at 10 g L^{-1} . The pH was checked every 30 min to 1 h and adjusted to 6.5 – 8 with 3 N NaOH. For GC reaction control $50 \text{ } \mu\text{L}$ of cell suspension were extracted with $250 \text{ } \mu\text{L}$ EtOAc supplemented with 1 mM methyl benzoate.

For reaction workup the cell suspension was centrifuged at $4500 \times g$ at $4 \text{ }^\circ\text{C}$ for 10 min and the supernatant was transferred to a separation funnel and extracted with ether (3 x 100 mL). The cells were resuspended in approx. 50 mL dH_2O , disrupted through sonication, centrifuged at $15000 \times g$ at $4 \text{ }^\circ\text{C}$ for 15 min and the supernatant was extracted with ether. Combined organic layers were washed with satd. NaCl, dried over Na_2SO_4 and concentrated *in vacuo*.

E III.4.1.1 (S)-4-Methyloxepan-2-one ((S)-4-Methylcaprolactone, **S-4f**)


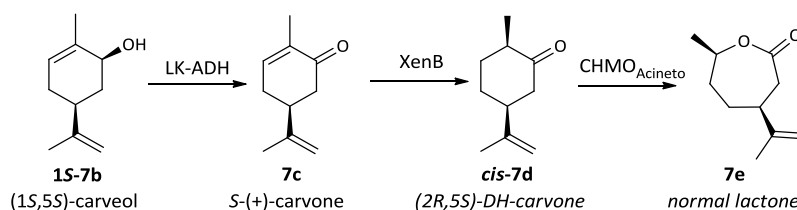
Scheme E-15

Yield 54 mg (47%; 78% over three steps)
Sum formula, m.w. C₇H₁₂O₂, 128.17
¹H-NMR (200 MHz, CDCl₃) δ = 1.05 (d, 3H, J=6.6Hz), 1.26-1.64 (m, 2H), 1.68-1.95 (m, 3H), 2.51-2.75 (m, 2H), 4.11-4.39 (m, 2H) ppm.
¹³C-NMR (50 MHz, CDCl₃) δ = 21.8, 30.5, 33.0, 35.1, 37.0, 67.9, 175.8 ppm.

 E III.4.1.2 (3R,6S)-3-Methyl-6-(prop-1-en-2-yl)oxepan-2-one ((3R,6S)-abn-carvolactone, **6e**)


Scheme E-16

Yield 69 mg (62%; 85% over three steps)
Sum formula, m.w. C₁₀H₁₆O₂, 168.23
¹H-NMR (200 MHz, CDCl₃) δ = 1.22 (d, 3H, J = 7 Hz), 1.58-2.03 (m, 4H), 1.82 (s, 3H), 2.27-2.30 (m, 1H), 2.71-2.81 (m, 1H), 4.15-4.18 (m, 2H), 4.72-4.83 (m, 2H) ppm.
¹³C-NMR (50 MHz, CDCl₃) δ = 18.4, 21.8, 31.8, 34.2, 37.2, 46.4, 71.6, 111.1, 145.7, 177.7 ppm.

 E III.4.1.3 (4S,7R)-7-Methyl-4-(prop-1-en-2-yl)oxepan-2-one ((4S,7R)-carvolactone, **7e**)


Scheme E-17

Yield 65 mg (59%; 84% over three steps)
Sum formula, m.w. C₁₀H₁₆O₂, 168.23
¹H-NMR (200 MHz, CDCl₃) δ = 1.37 (d, 3H, J = 6 Hz), 1.66-2.04 (m, 4H), 1.79 (s, 3H), 2.51-2.59 (m, 1H), 2.74-3.03 (m, 2H), 4.43-4.58 (m, 1H), 4.84-4.86 (m, 2H) ppm.
¹³C-NMR (50 MHz, CDCl₃) δ = 21.3, 21.8, 29.7, 33.3, 38.4, 38.6, 75.5, 111.4, 146.3, 173.8 ppm.

E IV Cyclic alkene hydroxylation

E IV.1 *Cellulosimicrobium cellulans* EB-8-4

Cellulosimicrobium cellulans EB-8-4 (*C. cellulans*) was received from the group of Prof. Zhi Li and was delivered to Vienna in a stab culture from our collaboration group of Prof. Uwe T. Bornscheuer (Greifswald). Although the strain was later identified as a mixed culture with *Rhodococcus equi* by the collaboration group (Katja Zorn, Jan Muschiol^[154]) it will here be only referred to as *C. cellulans* EB-8-4.

E IV.1.1 Cultivation

Cultivation of *C. cellulans* EB-8-4 was performed in adaptation of Wang *et al.*^[157] first on LB agar plates at 30 °C. Either single colonies or generous streaks from the agar plate were grown in 5 mL LB medium in normal round bottom cultivation tubes at 30 °C overnight. For the main cultivation M9-Sambrook medium (adapted from Sambrook^[193], Table E-15 plus trace elements), optionally supplemented with 0.4% (w/v) D-glucose, was used. Trace element solutions according to Preusting *et al.*^[202] were prepared individually in dH₂O in 1000x concentration and filter sterilized over 0.2 µm.

Table E-15. Preparation of M9 salts, trace elements and M9 medium.

M9-Sambrook salts (5x)	Trace elements (1000x)		M9-Sambrook	
2.5 g NaCl	40 g L ⁻¹	FeSO ₄ · 7 H ₂ O	M9 salts (5x, autoclaved)	20 mL
33.9 g Na ₂ HPO ₄	10 g L ⁻¹	MnSO ₄ · H ₂ O	D-Glucose (20%, filter sterilized)	2 mL (optional)
15 g KH ₂ PO ₄	4 g L ⁻¹	CoCl ₂ · 6 H ₂ O	MgSO ₄ (1 M, autoclaved)	200 µL
5 g (NH ₄) ₂ SO ₄	2 g L ⁻¹	ZnSO ₄ · 7 H ₂ O	CaCl ₂ (1 M, autoclaved)	10 µL
	2 g L ⁻¹	MoO ₄ Na ₂ · 2 H ₂ O	Trace elements (1000x, filter sterilized)	100 µL each
Concentrations on 1 L dH ₂ O, then autoclaved.	1 g L ⁻¹	CuCl ₂ · 2 H ₂ O		
	1.374 g L ⁻¹	Al ₂ (SO ₄) ₃ · 18 H ₂ O	Amounts on 100 mL sterile dH ₂ O (autoclaved)	

Prior to cultivation 15 mL falcons and their caps (if applicable) were pierced with hot cannulas (heated with a gas burner) at different positions as described in Table E-16.

Table E-16. Variations in 15 mL falcon preparation for ethyl benzene utilization.

a	falcon without cap
b	falcon with pierced cap + approx. $\varnothing = 2$ mm holes at 7-10-12 mL markings
c	falcon with pierced cap + approx. $\varnothing = 1$ mm holes at 5-6-8-10-12 mL markings
d	falcon without cap + holes at 6-7-10

These falcons were autoclaved in 250 mL ground joint Erlenmeyer flasks topped with aluminum foil. 100 mL M9 were inoculated with 3 mL LB o/n culture, either directly or resuspended in M9-Sambrook, in these Erlenmeyer flasks. 1 mL ethyl benzene was filled in the 15 mL falcons, the flask were covered differently and grown for 24 to 42 h. Cultivation with glass or plastic stoppers (quasi anaerobic) was performed in orbital shakers (InforsHT Multitron 2 Standard) at 30°C and 180 rpm. Aerobic cultivation with cellulose caps was first performed on a PSU-10i Orbital Shaking Platform (Grant Instruments, Cambridge) under the fume hood at RT and 300 rpm and later at 30 °C and 200 rpm in the orbital shaker.

Cell density was measured at $\lambda=440$ nm as OD_{440} on a WPA colourwave photometer. For the determination of cell weight 1 mL samples were filled in scaled eppis, cells separated from the medium by centrifugation and the cell wet weight (cww) scaled. After drying of these samples at 60 °C cell dry weight (cdw) was scaled.

E IV.1.2 Resting cells

Resting cells of *C. cellulans* were prepared with 50 mM Tris-HCl pH 7.5 or 50 mM K-buffer pH 7.3 prepared as in Table E-17. After cultivation the ethyl benzene falcon was removed from the culture, the cells separated from the medium by centrifugation at 5000 x g and 4 °C for 15 min and resuspended in buffer to 150 mg cww mL⁻¹.

Table E-17. Preparation of 50 mM potassium phosphate buffer (K-buffer).

K-buffer	
3.51 g	K ₂ HPO ₄ · 3 H ₂ O
1.31 g	KH ₂ PO ₄
Concentrations on 500 mL dH ₂ O, autoclaved.	

E IV.1.3 Biotransformations

Biotransformations were performed in closed glass vials at 25 °C and 200 rpm in orbital shakers with resting cells of *C. cellulans* EB-8-4 supplemented with 100 mM D-glucose and 20 mM *R*-(+)-limonene as starting material.

E IV.2 Cumene dioxygenase (CumDO) in *P. putida* S12

P. putida S12 pBTBX-2_CumDO (Table E-3) was received as stab culture from Prof. Marco W. Fraaije (Groningen) and first cultivated according to Groeneveld *et al.* [152]. The protocol was then adapted to cultivation in TB medium and longer expression time as described in Table E-8.

E IV.2.1 Resting cells

After production of CumDO in *P. putida* S12 (Table E-8) cells were harvested by centrifugation at 3600 x g at 4 °C for 15 min. The cell pellet was resuspended in 50 mM K-buffer pH 7.3 (Table E-17) or 50 mM Tris-HCl pH 7.5. Standard procedure was use of Tris-HCl buffer supplemented with 1% (w/v) D-glucose to a final OD_{590} of 20 if not noted otherwise. Cells could be stored at 4 °C for some days.

E IV.2.2 Growth in presence of ionic liquids (ILs)

All tested ILs were prepared by Anna Rössmann [176] or purchased from commercial suppliers and are listed in Table E-18. LB_{kan} medium was inoculated with overnight culture to an OD_{590} of 0.05, mixed with the ILs to obtain a concentration of either 50 mM or 100 mM and aliquoted in triplicates of 1 mL each to 96-square-deep-well plates. Growth was started at 30 °C at 200 rpm and monitored via optical density measurements. A sample of 50 μ L was taken every hour and analyzed using a plate reader (Anthos Zenyth 3100) at a wavelength $\lambda = 595$ nm.

Table E-18. Tested ILs and their suppliers.

Name	Abbreviation	Structure	Supplier
1-Ethyl-3-methylimidazolium chloride	[C ₂ mim]Cl		Iolitec (Heilbronn, Germany)
1-Ethyl-3-methylimidazolium acetate	[C ₂ mim]OAc		Iolitec (Heilbronn, Germany)
Choline formate	[chol]fom		Anna Ressmann
Choline acetate	[chol]OAc		Anna Ressmann
Choline lactate	[chol]lac		Anna Ressmann
Choline butyrate	[chol]but		Anna Ressmann
1-Butyl-3-methylimidazolium chloride	[C ₄ mim]Cl		Anna Ressmann
Choline hexanoate	[chol]hex		Anna Ressmann
1-Ethyl-3-methylimidazolium bistriflimide (bistriflimide: abbreviation for bis(trifluoromethane)sulfonimide)	[C ₂ mim]N(Tf) ₂		Anna Ressmann
1-Butyl-3-methylimidazolium bistriflimide	[C ₄ mim]N(Tf) ₂		Anna Ressmann

E IV.2.3 Biotransformations

All *P. putida* S12 expressing CumDo resting cell biotransformation reactions were performed as triplicates in 20 mL screw cap glass vials and shaken in an orbital shaker at 25 °C and 200 rpm. Extraction was performed with EtOAc supplemented with 1 mM methyl benzoate as GC standard. The phases were separated, if needed by transfer of the emulsion to an Eppendorf vial and a short centrifugation step, the organic layer dried over Na₂SO₄ and subjected to GC analysis (see E 1.9).

E IV.2.3.1 Preparative scale *R*-(+)-limonene hydroxylation

133 mL resting cells of *P. putida* S12 expressing CumDO containing 1% (w/v) D-glucose were supplemented with 108 mg *R*-(+)-limonene (6 mM) in a 1L Schottflask and shaken at 24 °C and 200 rpm. Samples for GC analysis were taken after 1 h, 5 h and 9 h and work up of the reaction was done after 21 h.

E IV.2.3.2 Cell density

Resting cells of *P. putida* S12 expressing CumDO were prepared similar to the protocol described in E IV.2.1 but resuspended in 50 mM Tris-HCl pH 7.5 to different cell densities. Biotransformation of 4 mM *R*-(+)-limonene was then performed for 12 h as described above.

E IV.2.3.3 Limonene concentration

P. putida resting cells (as prepared in E IV.2.1.) were filled in the glass vials and supplemented with 1 M ethanolic stock of *R*-(+)-limonene to concentrations of 0.5 mM, 1 mM and 4 mM in a total volume of 2 mL. Reaction was performed as described in E IV.2.3 for 12 h.

E IV.2.3.4 Limonene hydroxylation in presence of Triton X-100

Triton X-100 was diluted to 10% (v/v) solution in dH₂O and then added to the *P. putida* S12 resting cell reactions to a final concentration of 1%.

E IV.2.3.5 Limonene hydroxylation in presence of ILs

The vials were loaded with 50 mM [C₂mim]Cl, [C₂mim]OAc, [chol]fom, [chol]OAc and no IL as control, 1.999 mL of *P. putida* resting cells and 1 μL of a 1 M ethanolic stock of *R*-(+)-limonene to obtain a concentration of 0.5 mM. The reaction was shaken for 12 h.

E IV.2.3.6 IL concentration

[C₂mim]OAc was weighed into the vials to concentrations of 50 mM, 100 mM and 250 mM. *P. putida* resting cells were added, supplemented with 4 mM *R*-(+)-limonene to a volume of 2 ml and reaction performed for 12 h.

E IV.2.3.7 Hydroxylation of other cyclic alkenes

P. putida resting cells (for preparation see E IV.2.1.) were filled in glass vials and supplemented with 1 M ethanolic stock of **1a**, **2a** or **3a/4a** to a concentration of 1 mM in a total volume of 2 mL. Reaction was performed as described in E IV.2.3 for 12 h.

E IV.3 CumDO in *P. taiwanensis* VLB120ΔCΔttgV

Pseudomonas taiwanensis VLB120ΔCΔttgV^[159] was received from Jan Volmer (group of Prof. Bruno Bühler, TU Dortmund University) and transformed, according to Choi *et al.*^[203] via electroporation, with pBTBX-2_CumDO, which was extracted from *P. putida* S12 with GeneJET Plasmid Miniprep Kit. Positive transformants were selected on LB_{Sm100+kan50} agar plates at 30 °C.

Here cultivation and expression protocols are described for *P. taiwanensis* VLB120ΔCΔttgV pBTBX-2_CumDO. As control *P. taiwanensis* VLB120ΔCΔttgV was cultured accordingly without kanamycin and *P. putida* S12 pBTBX-2_CumDO without streptomycin.

E IV.3.1 Cultivation and expression of CumDO in LB

First cultivations were performed in 200 mL LB_{Sm100+kan50} which were inoculated with LB_{Sm100+kan50} o/n culture to an OD₄₄₀ of approx. 0.1. After reaching an OD₄₄₀ greater 0.7 induction of CumDO expression was started by addition of 2% (w/v) L-arabinose and cultivation continued at 30 °C and 200 rpm. Samples for a crude SDS-gel were taken at 3 h and 9 h after induction. Cells were harvested via centrifugation at 6000 x g 4 °C for 15 min.

E IV.3.2 Cultivation in M9

Preparation of M9 medium was adapted from Volmer *et al.*^[159] (Table E-19) and preparation of the used US* trace element mix is described in Table E-20.

Table E-19. Preparation of M9-medium according to Volmer *et al.*

M9 salts (5x)		M9	
2.5 g	NaCl	M9 salts (5x)	20 mL
85.5 g	Na ₂ HPO ₄ · 12H ₂ O	Carbon source	0.5% (w/v)
15 g	KH ₂ PO ₄	MgSO ₄ (1 M, autoclaved)	200 μL
5 g	NH ₄ Cl	US* trace elements (sterile, 1000x)	100 μL
Concentrations on 1 L dH ₂ O, autoclaved.		Amounts on 100 mL sterile dH ₂ O	

Table E-20. US* trace element mix 1000x concentrated.

US* trace elements mix			
HCl	1 mol (from 5 M stock solution)		
FeSO ₄ · 7 H ₂ O	4.87 g	H ₃ BO ₃	0.30 g
CaCl ₂ · 2 H ₂ O	4.12 g	Na ₂ MoO ₄ · 2 H ₂ O	0.25 g
MnCl ₂ · 4 H ₂ O	1.50 g	CuCl ₂ · 2 H ₂ O	0.15 g
ZnSO ₄ · 7 H ₂ O	1.87 g	Na ₂ EDTA · 2 H ₂ O	0.84 g
Concentrations on 1 L dH ₂ O, filter sterilized			

Single colonies of *P. taiwanensis* VLB120Δ*CΔttgV* pBTBX-2_CumDO were grown in 2 mL LB_{Sm100+kan50} for 9 h at 30 °C and 200 rpm, from this 50 mL M9_{Sm100+kan50/25} with 0.5% (w/v) glycerol as C-source were inoculated 1:100 and grown for 38 h at the same conditions. Growth was monitored via OD₄₄₀.

E IV.3.3 Expression of CumDO in M9

LB pre-cultures from single colonies were prepared as described in E IV.3.2. 50 mL M9_{Sm100+kan25} with glycerol or D-glucose as C-source were inoculated 1:100 with the pre-culture and grown at 30 °C and 200 rpm. After 20 h this culture was used to inoculate M9_{Sm100+kan25} supplemented with D-glucose or glycerol to an OD₄₄₀ of 0.2. After 4.5 h when OD₄₄₀ was approx. 0.5 CumDO expression was started via addition of 2% (w/v) L-arabinose and continued for 20 h. Samples for crude SDS-gels were taken at 6 h and 17 h after induction.

E IV.3.3.1 Resting cells and biotransformation

Resting cells of *P. taiwanensis* VLB120Δ*CΔttgV* pBTBX-2_CumDO were prepared 28 h after induction according to the protocol used for *P. putida* S12 (E IV.2.1). Biotransformations were done with 2 mM and 4 mM *R*-(+)-limonene in closed glass vials at 25 °C and 200 rpm.

E IV.4 Mixed-culture biotransformations

E IV.4.1 *P. putida* S12 expressing CumDO and *E. coli*

All reactions were performed, worked up and analyzed as described in E IV.2.3.

E IV.4.1.1 Simultaneous addition

Resting cells of *P. putida* S12 expressing CumDO (E IV.2.1) and *E. coli* BL21(DE3) expressing RR-ADH, XenB and CHMO_{Acinetobacter} (E I.7.2) were mixed in a glass vial in a 1:1 ratio and supplemented with *R*-(+)-limonene (0.5 mM) to a total volume of 2.4 mL. A sample (400 μL) was taken after 10 h and the rest worked up after 20 h reaction time.

E IV.4.1.2 Sequential addition

P. putida S12 resting cells (999 μL) were mixed with ethanolic *R*-(+)-limonene stock (1 μL, 1 M) and shaken for 10 h. After sampling (400 μL) 600 μL of *E. coli* resting cells were added and the reaction continued for 10 h until final work-up.

E V Orange peel as starting material

Orange peel was derived from food grade oranges using a swivel-blade peeler and cut into 0.2 cm² pieces shortly before using it as starting material. All reactions were performed, worked up and analyzed as described in E IV.2.3.

E V.1 *P. putida* expressing CumDO

E V.1.1 *In situ* R-(+)-limonene conversion without additives

Orange peel (50-65 mg) pieces were weighed into the glass vials and mixed with of *P. putida* S12 resting cells expressing CumDO (2 mL), to reach a biomass loading of approx. 3% (w/v). Work-up was performed after 12 h.

E V.1.2 *In situ* R-(+)-limonene conversion in presence of aqueous IL solutions

The vials were first loaded with IL (Table E-21) to a concentration of 50 mM, then orange peel (3% (w/v)) and *P. putida* S12 resting cells were added and reaction performed as described in E V.1.1.

Table E-21. ILs as additives for *in situ* R-(+)-limonene conversion.

IL	structure
[C ₂ mim]Cl	
[C ₂ mim]Oac	
[chol]fom	
[chol]Oac	

E V.1.3 Pre-dissolution of orange peel with following R-(+)-limonene conversion

Pre-treatment of orange peel (196 mg) was done with [C₂mim]Oac (500 mg) under stirring for 1.5 h at 80 °C. The solution was diluted with *P. putida* resting cells (66 mL) in a 250 mL Schott flask to reach an IL concentration of 50 mM. The reaction was run for 12 h and work-up performed as mentioned above.

E V.2 *P. putida* and *E. coli* - mixed-culture with orange peel

E V.2.1 Simultaneous addition

Approx. 100 mg orange peel (3% (w/v) biomass loading) were mixed in a glass vial with resting cells of *P. putida* expressing CumDO and *E. coli* expressing RR-ADH, XenB and CHMO_{Acineto} in a 1:1 ratio to a total volume of 2 mL. A sample (400 μL) was taken after 10 h and the rest worked up after 20 h reaction time.

E V.2.2 Sequential addition

P. putida resting cells (2 mL) were mixed with approx. 100 mg respectively 50 mg orange peel (3% / 1.5% biomass loading) and shaken for 10 h. After sampling (400 μL) 1600 μL of *E. coli* resting cells were added and the reaction continued for 10 h until final work-up.

E VI Materials and methods – molecular biology

In silico analysis of DNA sequences was performed with Geneious® version 6.1 created by Biomatters (available from <http://www.geneious.com>) and primers were generally designed in Geneious® with Primer3^[204]. Samples for sequencing were prepared according to the company's requirements and sent to LGC genomics (LGC, Middlesex, UK). DNA concentrations were measured with a NanoDrop ND 1000 spectrophotometer (Thermo Fisher).

E VI.1 Extraction of plasmid DNA

Isolation of plasmids from bacteria was performed with Promega PureYield™ Plasmid Mini- or Midiprep System or Thermo Scientific GeneJET Plasmid Miniprep Kit according to the instruction manuals.

E VI.2 Extraction of genomic DNA (gDNA)

This protocol for the extraction of genomic DNA (gDNA) from bacteria was adapted from Syn *et al.*^[205]. 3 mL of a LB o/n culture (containing the appropriate antibiotic if necessary) was centrifuged in a 15 mL Falcon at 5000 x g and 25°C for 5 min. After discarding the supernatant the pellet was resuspended in 0.75 mL 1% NaCl and centrifuged at the same conditions. The pellet was then resuspended in 0.75 mL TES (10 mM Tris-HCl, 10 mM EDTA, pH 8.0, 2% SDS) and incubated at 75 °C for 15 min. After vortexing 1 mL of phenol:chloroform:isoamylalcohol (25:24:1 v/v) was added and the mixture was centrifuged at 16000 x g at RT for 4 min. The aqueous layer was carefully pipetted into a fresh tube, 1 mL of chloroform was added and after inverting the tube was centrifuged again. Now the aqueous layer was taken off very carefully, not touching the interphase and transferred to a new tube where 100 µL 3 M NaOAc (pH 5.2) and 1 mL isopropanol were added. After inverting the tube carefully the gDNA could be spooled out (with a glass hook) to a new tube. If spooling could not be performed the mixture was alternatively centrifuged at 9200 x g and 4 °C for 1 min and the isopropanol was discarded. After addition of 500 µL of cold 70% ethanol to the gDNA it was centrifuged at above conditions. Ethanol was discarded and gDNA was dried at 40 °C or in a RVC 2-25 CD plus speedvac from Christ equipped with an Alpha 2-4 LD plus (Martin Christ Gefriertrocknungsanlagen GmbH, Osterode am Harz, Germany) before adding 150 µL TE2 (10 mM Tris-HCl, 2 mM EDTA, pH 8.0) with 1 µL 50 µg mL⁻¹ RNase and dissolving while shaking at 40 °C. Centrifugation at 16000 x g at RT for 1 min was performed to cut off undissolved parts and the supernatant transferred to a sterile Eppendorf tube.

E VI.3 PCR

PCRs (polymerase chain reaction) were performed on a MyCycler™ thermal cycler (Bio-Rad) applying temperature programs suitable for the specific DNA polymerase, the annealing temperature of the primers and the length of the product. If needed clean-up of PCR products was performed with QIAquick® PCR purification kit (Qiagen, Hilden, Germany).

E VI.3.1 Colony PCR

With a sterile toothpick a bacterial colony was picked from an agar plate and transferred to 10 µL of sterile dH₂O in a 0.2 mL PCR tube. After a short soaking time, usually after the next 5 colonies were picked, the toothpick was streaked over a small area on a new agar plate (with the same antibiotics as the original).

Through numbering the areas on the bottom of the new agar plate, recovery of individual colonies was made sure. The PCR tubes were closed, the bacteria water mixtures denatured at 95 °C for 10 min and then shortly cooled down on ice. All other reactants for the PCR reaction were combined in a master mix (MM), then aliquoted to the individual denatured bacterial colonies in water before starting the PCR program.

E VI.4 Restriction enzyme digest

Digestion of DNA with restriction enzymes was performed according to the instruction manual of the supplier, normally Promega. Purification of DNA fragments was either performed with QIAquick® PCR purification kit or the agarose gel purification method described in E VI.5.1.

E VI.5 Agarose Gel electrophoresis

Agarose Gel electrophoresis for the separation of DNA samples was performed with Sub-Cell GT® Agarose Gel electrophoresis system (Bio-Rad) according to the instruction manual. Agarose gels, prepared in concentrations ranging from 0.7% to 4% (w/v) were supplemented with ethidium bromide or SYBR® Safe DNA Gel Stain (Thermo Fisher) for the visualization of DNA. Samples were diluted with 6x loading dye (3 ml glycerol (30%), 5 ml 0.5% bromophenol blue (0.25%), with dH₂O to 10 mL or ready to use from Fermentas) prior to loading on the gel. BenchTop 1 kb DNA Ladder, BenchTop 100 bp DNA Ladder (both Promega) or Thermo Scientific GeneRuler 1 kb DNA Ladder (#SM0311) were used for the estimation of DNA size. A GelDoc2000 (UV Transilluminator, Bio-Rad) with QuantityOne software was used for gel analysis under UV-light.

E VI.5.1 Agarose gel purification

DNA to be purified was separated on a 1% (w/v) agarose gel as described in E VI.5. The DNA was visualized by exposure to UV light in preparative mode and the corresponding band was cut out with a sterile scalpel. The gel slice was transferred to a sterile 1.5 mL Eppendorf tube and frozen at -80°C for 30 min. The gel slice was thawed at 37°C and 550 rpm (Eppendorf Thermomixer Comfort) for 15 min and centrifuged at 17 000 x g and 4°C for 10 min (Sigma Laboratory Centrifuge 3k15). The supernatant was transferred into a fresh tube. The remaining gel slice was mixed with 100 µL nuclease-free water, the gel slice disturbed with a pipette tip, frozen and thawed again. It was centrifuged at 17 000 x g, 4°C for 10 min. The volume of the combined supernatants was determined and 1/10 of the volume of 3 M NaOAc (pH 5.2) and 2.5 times the resulting volume of ice cold absolute EtOH were added. The mixture was precipitated at -20 °C for at least 1 h but preferably overnight and then centrifuged at 17 000 x g, 4°C for 15 min. The supernatant was carefully discarded, the pellet was washed with 1 mL ice cold 70% EtOH and again centrifuged as before. After removal of the supernatant and drying (in the speedvac as described in E VI.2) the pellet was dissolved in 50 µL DNase-/RNase-free water and DNA concentration measured.

E VII Metabolic engineering

E VII.1 *E. coli* BL21(DE3) $\Delta nemA$

The amino acid (aa) sequence of OYE1 was subjected to a protein search in *E. coli* in BLAST® (<http://blast.ncbi.nlm.nih.gov/Blast.cgi>). With high sequence similarity the gene *nemA* coding for N-ethylmaleimide reductase (NemR)^[139] was identified as *E. coli* background.

For the construction of *E. coli* BL21(DE3) $\Delta nemA$ (*nemA* disruption strain) the TargeTron® Gene Knockout System from Sigma-Aldrich® was used according to the manufacturer’s manual. The primers for the Knockout System (IBS, EBS1d and EBS2) were designed at TargeTron® Design Site and ordered from Sigma-Aldrich. Additionally a primer to verify the knockout (KO) and primers with integrated restriction sites (BamHI and HindIII) to amplify the whole *nemA* gene (1098 bp) from *E. coli* BL21(DE3), including short upstream (us) and downstream (ds) regions, were ordered. Detailed primer names and descriptions are shown in Table E-22 and their sequences can be retrieved from the primer list in section E VIII.

Table E-22. Primers for the construction of *E. coli* BL21(DE3) $\Delta nemA$

Primer	description
784-785a_IBS	re-target primer located at start of intron (rev)
784-785a_EBS1d	re-target primer located in middle of intron (fwd)
784-785a_EBS2	re-target primer overlapping with EBS Universal (rev)
EBS Universal	re-target primer delivered with TargeTron® kit (fwd)
nemA_KO_fwd	$\Delta nemA$ verification primer (fwd)
nemA_HindIII_fwd	forward <i>nemA</i> cloning primer (rev)
nemA_BamHI_rev	reverse <i>nemA</i> cloning primer (fwd)

E VII.1.1 Verification of intron insertion via PCR

With colony PCR using either GoTaq Polymerase (Promega) or Phusion Green Hot Start II High Fidelity DNA Polymerase (Thermo Fisher Scientific) not all PCR products could be obtained. Therefore gDNA from potential *E. coli* BL21(DE3) $\Delta nemA$ strains was extracted according to E VI.2 and used as template for PCR.

Control PCR with GoTaq Polymerase, according to manufacturer’s standard protocol, was not successful for all primer combinations. Therefore the PCR for verification of the insertion of the intron was performed with Phusion Green Hot Start II High Fidelity DNA Polymerase (Thermo Fisher Scientific) according to the manufacturer’s standard protocol. PCR primer combinations, product description and sizes are shown in Table E-23.

Table E-23. Primer combinations and product sizes for the verification of *E. coli* BL21(DE3) $\Delta nemA+kan^R$.

Primer	template	PCR product	size [bp]
nemA_BamHI_rev + nemA_HindIII_fwd	<i>E. coli</i> BL21(DE3)	<i>nemA</i> (+ short us and ds regions and restriction sites)	1199
	<i>E. coli</i> BL21(DE3 $\Delta nemA+kan^R$)	<i>nemA</i> with intron	3095
nemA_KO_fwd + 784-785a_EBS2	<i>E. coli</i> BL21(DE3) $\Delta nemA+kan^R$	little piece <i>nemA</i> and nearly full intron	1841
nemA_KO_fwd + nemA_HindIII_fwd	<i>E. coli</i> BL21(DE3)	end of <i>nemA</i>	486
	<i>E. coli</i> BL21(DE3) $\Delta nemA+kan^R$	full intron and end of <i>nemA</i>	2382

E VII.1.2 Confirmation of NemR disruption via biotransformation test

CFE of *E. coli* BL21(DE3) and *E. coli* BL21(DE3) $\Delta nemA+kan^R$ were prepared following E I.6. Biotransformations were performed in triplicates with 5 mg mL⁻¹ total protein concentration, 4 mM S-(+)-carvone (**6c**) and R-(-)-carvone (**7c**), 1.2 equiv. NADP⁺ and cofactor recycling system according to the ERED requirements in Table E-14.

E VII.1.3 Removal of the kanamycin resistance

To gain the possibility to produce *E. coli* BL21(DE3) $\Delta nemA$ without kanamycin resistance (kan^R) TargeTron[®] Vector pACD4K-C-loxP was used in the TargeTron[®] Gene Knockout System. After the disruption of the *nemA* gene was verified via PCR as described before (E VII.1.1), competent cells of a positive clone were transformed with the 706-Cre plasmid (GeneBridges) and selected on LB_{tet} (5 µg mL⁻¹) plates. A positive single colony was grown in 1 mL LB at 30°C for 3 h before switching the temperature to 37 °C overnight. The culture was plated on LB agar plates and resulting colonies replica plated on LB and LB_{kan} (40 µg mL⁻¹) by picking one colony and streaking it on both plates in numbered areas. A positive *E. coli* BL21(DE3) $\Delta nemA$ without kanamycin resistance would just grow on the LB plate and was verified via PCR. Table E-24 shows the PCR product description and sizes used for the verification of *E. coli* BL21(DE3) $\Delta nemA$.

Table E-24. Primer combination and product sizes for the verification of *E. coli* BL21(DE3) $\Delta nemA$.

Primer	template	PCR product	size [bp]
nemA_KO_fwd + 784-785a_EBS2	<i>E. coli</i> BL21(DE3) $\Delta nemA+kan^R$	little piece <i>nemA</i> and nearly full intron with kan^R	1841
	<i>E. coli</i> BL21(DE3) $\Delta nemA-loxP$	little piece <i>nemA</i> and nearly full intron with kan^R flanked by loxP sites	1908
	<i>E. coli</i> BL21(DE3) $\Delta nemA$	little piece <i>nemA</i> and nearly full intron without kan^R	866

E VII.2 *E. coli* BL21(DE3) $\Delta nemA \Delta fadH$

The TargeTron[®] Gene Knockout system, as described in E VII.1, was also used for the construction of *E. coli* BL21(DE3) $\Delta nemA \Delta fadH$. After re-targeting via PCR the intron expression vector pACD4K-C-loxP was transformed in *E. coli* DH5 α and re-targeting verified via colony PCR. A positively re-targeted vector was extracted from *E. coli* DH5 α and transformed in *E. coli* BL21(DE3) $\Delta nemA$ and the protocol for *fadH* disruption was done following the instruction manual and according to E VII.1.

Table E-25. Primers used for the disruption of *fadH* and verification of *E. coli* BL21(DE3) $\Delta nemA \Delta fadH$.

Primer	description
fadH_123-124s_IBS	re-target primer located at start of intron (fwd)
fadH_123-124s_EBS1d	re-target primer located in middle of intron (rev)
fadH_123-124s_EBS2	re-target primer overlapping with EBS Universal (fwd)
EBS Universal	re-target primer delivered with TargeTron [®] kit (rev)
fadH_KO_rev	$\Delta fadH$ verification primer (rev)
fadH_NdeI_2487F	forward <i>fadH</i> cloning primer (fwd)
fadH_444R_XhoI	reverse <i>fadH</i> cloning primer (rev)

Verification of *E. coli* BL21(DE3) $\Delta nemA \Delta fadH$ was performed via PCR of extracted gDNA using the primer combinations in Table E-26. After the initial disruption of *fadH*, the kanamycin resistance was removed with Cre-recombinase as described in E VII.1.3.

Table E-26. Primer combinations and product sizes for the verification of *E. coli* BL21(DE3) $\Delta nemA \Delta fadH$.

Primer	template	PCR product	size [bp]
fadH_NdeI_2487F + fadH_KO_rev	<i>E. coli</i> BL21(DE3) $\Delta nemA$	Short piece of <i>fadH</i>	508
	<i>E. coli</i> BL21(DE3) $\Delta nemA \Delta fadH + kan^R$	Short piece of <i>fadH</i> with intron and kan^R	2471
	<i>E. coli</i> BL21(DE3) $\Delta nemA \Delta fadH$	Short piece of <i>fadH</i> with intron	1463

E VII.2.1 *E. coli* BL21(DE3) $\Delta nemA \Delta fadH-2 + kan^R$

For a second group II intron insertion in *fadH* new KO primers were ordered from Sigma-Aldrich and the TargeTron® Gene Knockout system executed on *E. coli* BL21(DE3) $\Delta nemA \Delta fadH$ as described in E VII.2. Used primers are listed in Table E-27 and the resulting KO strain was named *E. coli* BL21(DE3) $\Delta nemA \Delta fadH-2 + kan^R$.

Table E-27. Primers used for the second disruption of *fadH* and verification of *E. coli* BL21(DE3) $\Delta nemA \Delta fadH-2 + kan^R$.

Primer	description
fadH_1392-1393s_IBS	re-target primer located at start of intron (fwd)
fadH_1392-1393s_EBS1d	re-target primer located in middle of intron (rev)
fadH_1392-1393s_EBS2	re-target primer overlapping with EBS Universal (fwd)
EBS Universal	re-target primer delivered with TargeTron® kit (rev)
fadH_1392-KO	$\Delta fadH-2 + kan^R$ verification primer (fwd)
fadH_NdeI_2487F	forward <i>fadH</i> cloning primer (fwd)
fadH_444R_XhoI	reverse <i>fadH</i> cloning primer (rev)

E VII.3 Cloning of *nemA* into pET-22b(+)

To clone *nemA* from gDNA of *E. coli* BL21(DE3) the already introduced primers with restriction sites flanking the gene (*nemA*_BamHI_rev and *nemA*_HindIII_fwd) were used in a PCR reaction. The PCR product was cut with the restriction enzymes *Bam*HI and *Hind*III and purified via PCR clean-up kit. The plasmid pET-22b(+) was digested with the same restriction enzymes and cleaned up via the agarose gel purification method (E VI.5.1). Ligation of the vector and insert fragment was performed with T4 DNA Ligase (Thermo) according to the standard protocol, the ligation mix transformed into *E. coli* DH5 α and selection performed on LB_{amp} agar plates. To verify pET-22b(+)_{nemA} colony PCR with pET94F and pET417R (standard primers) and GoTaq polymerase was performed. The sequence of *nemA* and a plasmid map of pET-22b(+)_{nemA} can be found in the Appendix.

E VII.4 Expression of NemR

pET-22b(+)_{nemA} was extracted from *E. coli* DH5 α through plasmid prep (E VI.1). *E. coli* BL21(DE3) $\Delta nemA$ was transformed with pET-22b(+)_{nemA} via chemical transformation (E I.3.1) and selected on LB_{amp} plates. Three positive colonies were grown in LB_{amp} (100 $\mu\text{g mL}^{-1}$) overnight and cultivation performed as described in E I.5 in TB_{amp} (100 $\mu\text{g mL}^{-1}$). Induction was done with 0.1 mM IPTG and expression continued at 25 °C and 200 rpm. Samples for a crude SDS gels were taken after 3 h and 20 h.

E VII.5 Cloning of *fadH* and expression of DCR

Cloning *fadH* from *E. coli* BL21(DE3) was achieved via PCR of gDNA with the primers *fadH_NdeI_2487F* and *fadH_444R_XhoI*. The rest of the procedure was performed as for *nemA* cloning and described in E VII.2.1 but with the restriction enzymes *NdeI* and *XhoI*. *E. coli* DH5 α pET-22b(+)*_fadH* was verified via colony PCR with pET94F and pET417R and GoTaq polymerase.

Production of DCR from *fadH* in *E. coli* BL21(DE3) Δ *nemA* was performed according to the procedure for NemR described in E VII.4. The sequence of *fadH* and a plasmid map of pET-22b(+)*_fadH* can be found in the Appendix.

E VIII Primer list

Primers (DNA Oligonucleotides) were ordered from Sigma Aldrich, dissolved in sterile dH₂O to a concentration of 100 mM if not noted otherwise and stored at -20 °C.

Table E-28. List of primers used in this thesis.

Entry	Name	Sequence(5'-3')	Length [bp]	Tm [°C]	GC%
1	tet_lk_2260fwd	GCAGAACCAATGCATTCCCGGAAA	25	76.9	52.0
2	tet_lk_2260rev	TTCGCAACCTTCAAATCCCCTCCCG	25	77.7	56.0
3	pET 94F	CAGCCAACTCAGCTTCCTTTCGGGC	25	76.4	60.0
4	pET 417R	GCGTCCGGCGTAGAGGATCGAGATC	25	76.6	64.0
5	pBAD 107F	ACAAAGCGGGACCAAAGCCATGACA	25	76.2	52.0
6	pBAD 496R	GGCTGAAAATCTTCTCATCCGCCA	26	74.2	50.0
7	pTrcHis-TOPO 4188F	ATCTGTGTGGGCACTCGACCGAAT	25	75.8	56.0
8	pTrcHis-TOPO 159R	TTCTGAGTTCGGCATGGGGTCAGGT	25	75.8	56.0
9	nemA_KO_fwd	GTACTGGAAGTGGTCGATGCCGGGA	25	76.0	60.0
10	nemA_BamHI_rev	TTGGATCCAACATTATTGCGAGGCC	25	74.3	48.0
11	nemA_HindIII_fwd	TTTAAGCTTTACGCCGCTCGCAATGTT	27	74.0	44.4
12	784 785a-IBS	AAAAAAGCTTATAATTATCCTTATGCCGCGTTTACGTG CGCCCAGATAGGGTG	53	83.5	43.3
13	784 785a-EBS1d	CAGATTGTACAAATGTGGTGATAACAGATAAGTCGTTT ACCCTAACTTACCTTTCTTTGT	60	78.7	35.0
14	784 785a-EBS2	TGAACGCAAGTTTCTAATTTTCGGTTCGGCATCGATAGA GGAAAGTGTCT	49	83.5	42.8
15	fadH_NdeI_2487F	GGACAATCATATGAGCTACCCGTCGCTGTT	30	75.1	50.0
16	fadH_444R_XhoI	GGACTCGAGGCATCCGCGCTTAAAATA	28	77.2	53.5
17	fadH_123-124s_IBS	AAAAAAGCTTATAATTATCCTTAGAGCGCCTGGCAGTG CGCCCAGATAGGGTG	53	84.6	47.1
18	fadH_123-124s_EBS1d	CAGATTGTACAAATGTGGTGATAACAGATAAGTCCTGG CAGCTAACTTACCTTTCTTTGT	60	81.0	38.3
19	fadH_123-124s_EBS2	TGAACGCAAGTTTCTAATTTTCGATTTCGCTCTCGATAGA GGAAAGTGTCT	49	81.6	40.8
20	fadH_KO_rev	CCCTTCGGAACCCATCACCTCTACAC	26	73.5	57.6
21	fadH_1392-KO	CAGATCCCCGGCAAAGAGGAGTTTACGAA	30	76.9	50.0
22	Stop_Sall_rev	GCGTCGACTCACACGGTAACCATTTCTGCGCT	32	81.8	56.2
23	fadH_1392-1393s_IBS	AAAAAAGCTTATAATTATCCTTAATCCTCGCCAGTGTG CGCCCAGATAGGGTG	53	83.0	43.3
24	fadH_1392-1393s_EBS1d	CAGATTGTACAAATGTGGTGATAACAGATAAGTCGCCA GTGGTAACTTACCTTTCTTTGT	60	81.3	38.3
25	fadH_1392-1393s_EBS2	TGAACGCAAGTTTCTAATTTTCGATTAGGATTCGATAGA GGAAAGTGTCT	49	78.9	36.7

F Appendix

F I Sequences

```
>nemA|E. coli
ATGTCATCTGAAAAACTGTATTTCCCACTGAAAAGTGGGCGCGATCACGGCGGCAAACCGTATTTTTATGGCACCGCTGACCGCTGCGCGAGTA
TTGAACCGGGTGACATTCCTACCCCGTTGATGGCGGAATACTATCGCCAACGTGCCAGTGCCGGTTTGATTATTAGTGAAGCCACGCAAATTTTC
TGCCACAGGCAAAGGATATGCAGGTGCGCCTGGCATCCATAGTCCGGAGCAAATTTGCCGCATGGAAAAAATCACCGCTGGCGTTCATGCTGAA
AATGGTCATATGGCCGTGACGCTGTGGCACACCGGACGCATTTCTCACGCCAGCTGCAACCTGGCGGTGAGGACCGGTAGCGCCTTCAGCAC
TTAGCGCGGGAACACGTACTTCTCTGCGCGATGAAAAATGGTCAGGCGATCCGTGTTGAAACATCCATGCCGCGTGGCGTTGAACTGGAAGAGAT
TCCAGGTATCGTCAATGATTTCCGTCAGGCCATTGCTAACCGCGTGAAGCCGGTTTTGATCTGGTAGAGCTCCACTCTGCTCACGGTTATTTG
CTGCATCAGTTCCCTTTCTCTTCTTCAAACCATCGTACCGATCAGTACGGCGGCGAGCGTGGAAAAATCGCGCACGTTTGGTACTGGAAGTGGTCCG
ATGCCGGGATTGAAGAATGGGGTGGCGATCGCATTTGGCATTTCGCGTTTCGCCAATCGGTACTTCCAGAACACAGATAACGGCCCCGAATGAAGA
AGCCGATGCACGTATCTGATTGAACAACCTGGGTAACCGCGGCAATTGCTTATCTGCATATGTCAGAACCAGATTGGGCGGGGGTGAACCGTAT
ACTGATGCGTTCCGCGAAAAAGTACGCGCCCGTTTCCACGGTCCGATTATCGGCGCAGGTGCATACACAGTAGAAAAAGCTGAAACGCTGATCG
GCAAAGGGTTAATTGATGCGGTGGCATTGGTCTGACTGGATTGCGAACC CGGATCTGGTCCGCCGCTGACAGCGCAAAGCTGATCTTAACCC
ACAGCGTGCCGAAAGTTTCTACGGTGGCGGGCGGGAAGGCTATACCGATTACCCGACGTTGTAA
```

```
>fadH|E. coli
ATGAGCTACCCGTCGCTGTTTCGCCCGCTGGATTTAGGTTTTACCACGTTAAAAAACCGCGTGTGATGGGCTCAATGCACACCGGGCTGGAGG
AATACCCGGACGGTGCCGAGCGGCTGGCAGCGTTTTATGCCGACGCGCCGTCACGGCGTGGCGTTGATTGTCAGCGCGGCATTCACCCAGA
TTTAACAGGCGTTGGCATGGAAGGGGTCGAATGCTCAATGACGCCAGCCAGATCCCACACCATCGCACCATTTACCGAAGCCGTCATCAGGAA
GGCGGCAAATAGCCCTGCAAATTTGTCATACCGGGCGCTACAGCTACCAACCGCATCTGGTCCGCCGTCGCCATTGACAGGCCCCCATCAACC
GTTTCGTGCCCATGAGTTAAGCCATGAAGAGATCCTGCAACTGATCGACAATTTCCGCCGCTGCGCGCAACTGGCGCGGGAGGCAGGATACGA
CGGTGTAGAGGTGATGGGTTCCGAAGGGTATTTGATCAACGAATTTCTGACGCTGCGCAACCAATCAGCGTAGTGACCAAGTGGGGCGGCGATTAC
CGCAACCGGATGCGATTTGCCGTAGAAGTAGTGCCTGCGGTGCGCGAACGCGTGGCAACGACTTCATTATTATCTACCGACTGTCGATGCTCG
ACCTGGTCAAGACGGCGGGGACTTTTGCCGAAACGGTAGAGCTGGCGCAGGCCATTGAAGCGGGCGCGACCATTTATCAACACCGGCATTGG
CTGGCATGAAGCACGATTTCCGACCATTTGCCACGCCCGTGGCGCGGGCGCATTTAGCTGGGTACGCGCAAACGAAAGGCCACGTTCTCGCTG
CCGCTGGTAACCAACCGGATTAACGATCCGCAGGTGCGGACGATATTTCTCTCGCGCGGCGATGCCGATATGGTATCGATGGCGCGACCGT
TTCTTGCTGATGCGGAGCTGCTGTCAAAAAGCGCAATCGGGACGAGCCGATGAGATCAACACTTGTATTGGCTGCAATCAGGCCTGTCTCGATCA
AATCTTCGTTGGCAAAGTCACTCGTGCTGGTGAATCCTCGCGCCTGCCACGAAACCAAAATGCCAATCCTTCCCGCCGTGCAGAAAAAAAT
CTGGCGGTGGTGGTGGCGGACCTGTGGGCTGGCGTTTGCCATTAACCGCGGGCGCGTGGGCATCAGGTAACATTTGTTTGACGCTCATAGCG
AGATTGGCGGGCAGTTTAAATATCGCCAAACAGATCCCGGCAAAGAGGAGTTTTACGAAACGCTGCGCTATTACCGCCGATGATCGAAGTGAC
GGGCGTGACGCTAAAACCAATCACACCGTGACGGCGGATCAGTTACAGGCTTTTCGATGAAACGATCCTCGCCAGTGGGATCGTGCCGCGCACT
CCGCCCATCGACGGGATCGATATCCGAAGGTATTGAGTTATCTCGATGTAAGTGCAGCAAAAGCGCCGTTGGCAACAAAGTTGCCATCATCG
GTTGTGGCGGGATTGGTTTTGATACGGCGATGATTTAAGTACAGCCGGCGAATCCACCAGCCAGAATATCGCCGGGTTCTGTAATGAATGGGG
GATCGACAGTAGCCTACAACAGGCTGGTGGCTTAAGCCCGAGGGAATGCAGATCCCCGTAGCCACCGCAGATTGTGATGCTCCAGCGCAAA
GCCAGCAAACAGGACAGGGTTAGGCAAAACACCGGCTGGATCCATCGCACCCCTGCTCTCGCGGGGTGTGAAAAATGATCCAGGCGTAA
GTTATCAGAAGATTGACGATGACGGGCTGCATGTTGGTGTCAACGGCGAAACGAGGTATTAGCAGTGGACAATGTGGTGTCTGCGCAGGGCA
AGAGCCAAACCGCGCTGGCGCAACCGCTGATTGATAGCGGAAACGGTGCATTTAATTGGCGGCTGCGATGTGGCTATGGAGCTGGACGCA
CGACGGCAATTTCCAGGGAACACGGTGGCGCTGGAGATTTAA
```

F II Plasmid maps

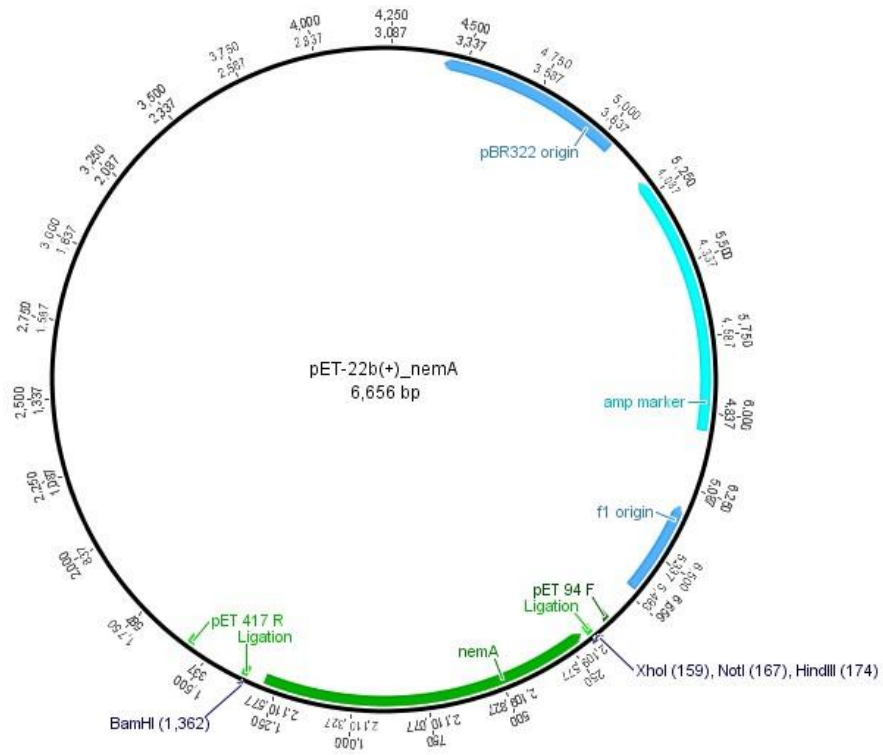


Figure F-1. Plasmid map of the constructed pET-22b(+)_nemA created with Geneious version 6.1.

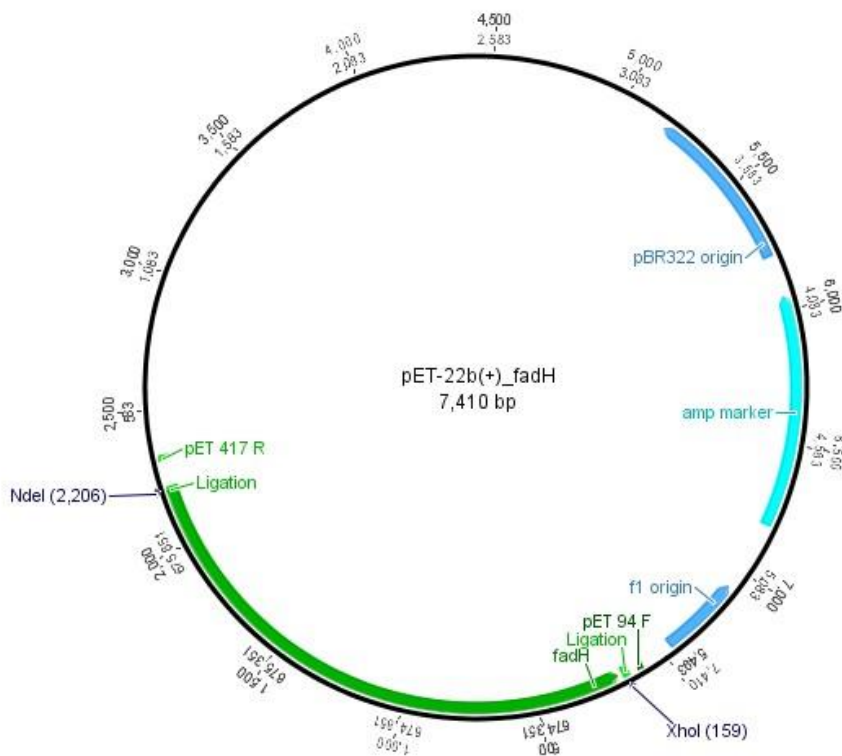


Figure F-2. Plasmid map of the constructed pET-22b(+)_fadH created with Geneious version 6.1 created by Biomatters.

Available from <http://www.geneious.com>

F III Publications resulting from this thesis

From waste to value – Direct utilization of limonene from orange peel in a biocatalytic cascade reaction towards chiral carvolactone

Oberleitner, N.*; Ressmann, A.K.*; Bica, K.; Gärtner, P.; Fraaije, M.W.; Bornscheuer, U.T.; Rudroff, F. and Mihovilovic, M.D.

Green Chemistry **2017**, DOI: 10.1039/C6GC01138A

Three Enzyme-Catalyzed redox cascade for the production of a Carvo-lactone

Oberleitner, N.; Peters, C.; Muschiol, J.; Rudroff, F.; Mihovilovic, M.D. and Bornscheuer, U.T. (2016)

in *Practical Methods for Biocatalysis and Biotransformations 3* (Eds.: Whittall, J.; Sutton, P. W. and Kroutil, W.), Wiley, **2016**, pp. 222-226.

In vitro characterization of an enzymatic redox cascade composed of an alcohol dehydrogenase, an enoate reductases and a Baeyer-Villiger monooxygenase

Oberleitner, N.; Peters, C.; Rudroff, F.; Bornscheuer, U.T.; Mihovilovic, M.D.

Journal of Biotechnology **2014**, 192(Part_B), 393-399.

An Enzymatic Toolbox for Cascade Reactions: A Showcase for an *In vivo* Redox Sequence in Asymmetric Synthesis

Oberleitner, N.*; Peters, C.*; Muschiol, J.; Kadow, M.; Sass, S.; Bayer, T.; Schaaf, P.; Iqbal, N.; Rudroff, F.; Mihovilovic, M.D.; Bornscheuer, U.T.

ChemCatChem **2013**, 5(12), 3524-3528.

* these authors contributed equally

F IV Curriculum vitae

NIKOLIN-ELISABETH OBERLEITNER

Date and place of birth: March 28, 1986
in Stockerau, Austria

Nationality: Austria



Education

- Jan 2012 to date PhD program at the Institute of Applied Synthetic Chemistry, Technische Universität Wien with Prof. Marko D. Mihovilovic and Dr. Florian Rudroff
“Biocatalytic cascade reactions towards the production of valuable fine chemicals”
- Dec 2011 Graduation *with distinction* at Technische Universität Wien (MSc)
Master thesis: “Introduction of an N-acetylneuraminic acid production pathway in *Trichoderma atroviride* (Einbringung eines N-Acetylneuraminsäure Stoffwechselweges in *Trichoderma atroviride*)”
Supervised by Prof. Robert Mach, Institute of Chemical Engineering, research division biotechnology and microbiology
- Jun, Jul 2010 IAESTE (International Association for the Exchange of Students for Technical Experience)
internship with Dr. David Weinkove,
School of Biological and Biomedical Sciences, Durham University, Durham, UK
- Oct 2004 – Dec 2011 Bachelor studies in Technical Chemistry and
Master studies in Biotechnology and Bioanalytics
at Technische Universität Wien
- Jun 2004 Graduation *with distinction* at Gymnasium Sacré-Cœur Wien,
A-Level exams and specialization thesis in chemistry: “Studies on the biocatalytic production of calorie free carbohydrates (Untersuchungen zur biokatalytischen Herstellung kalorienfreier Kohlenhydrate)”
-

Professional experience

- 2002 – 2010 Perennial internships at Octapharma, Vienna, Austria
Technology Transfer, with short stays in Strasbourg, France and Stockholm, Sweden
Quality Control
-

Awards

2015	“Biotrans Poster Award”, Biotrans2015, Vienna, Austria
2014	“Best Poster Award” Gordon Research Conference Biocatalysis, Bryant University, Smithfield, RI, USA
2004	“Max-Perutz-price for the best biochemical work” Award for graduation specialization thesis in chemistry from GÖCH (Austria’s chemical society) and VCÖ (Union of Austria’s chemistry teachers)

Language skills

German	Mother tongue
English	Fluent in written and spoken Cambridge English: First certificate (FCE)
French, Spanish	Basic knowledge

Further skills

Advanced user and administrative skills with PC hard- and software

Profound knowledge of bioinformatics and chemistry related databases and software (BLAST, Brenda, Scifinder, Reaxys, VectorNTI, Geneious, ChemDraw)

Intensive experience with diverse analytical techniques from chemistry and microbiology (GC, HPLC, MS, spectrometry, chromatography, gel electrophoresis)

Additional work experience

Jul 2015	Helping hand at Biotrans2015 conference, Vienna
2009 – 2011	Perennial work experience at VIENNALE Vienna international film festival, Press and Protocol
Jan 2003	Internship at the hospital Krankenhaus der Barmherzigen Schwestern, Vienna, in course of the caring project “Compassion” from Gymnasium Sacré-Cœur Wien
2002 – 2009	Weekly voluntary work with children at Jungschar Deutsch-Wagram, Austria

Leisure activities

Sports (running, yoga, climbing, hiking, swimming, cycling, snowboard...), music and movies, cooking

Additional publications

Cascade catalysis – strategies and challenges en route to preparative synthetic biology
Muschiol, J.; Peters, C.; Oberleitner, N.; Mihovilovic, M.D.; Bornscheuer, U.T.; Rudroff, F.
Chemical Communications **2015**, 51, 5798-5811.

Excessive folate synthesis limits lifespan in the *C. elegans*: *E. coli* aging model
Virk, B.; Correia, G.; Dixon, D. P.; Feyst, I.; Jia, J.; Oberleitner, N.; Briggs, Z.; Hodge, E.; Edwards, R.; Ward, J.; Gerns, D.; Weinkove, D.
BMC Biology **2012**, 10, 67.

Conference contributions

From waste to value – ionic liquid based extraction meets whole cell multistep biocatalysis
Oberleitner, N.*; Ressmann, A.K.*; Bica, K.; Gärtner, P.; Mihovilovic, M.D., Bornscheuer, U.T.; Rudroff, F.
Poster: Biotrans2015, July 26-30, 2015, Vienna, Austria

Enzymatic Redox Sequences in Asymmetric Synthesis – Artificial Enzyme Cascades In vitro and In vivo
Oberleitner, N.; Peters, C.; Muschiol, J.; Kadow, M.; Sass, S.; Bayer, T.; Schaaf, P.; Iqbal, N.; Rudroff, F.; Mihovilovic, M.D.; Bornscheuer, U.T.
Poster: Biocatalysis Gordon Research Conference (GRC), July 6-11, 2014, Bryant University, Smithfield, RI, USA

Enzymatic Redox Sequences in Asymmetric Synthesis – Artificial Enzyme Cascades In vitro and In vivo
Oberleitner, N.; Peters, C.; Muschiol, J.; Kadow, M.; Sass, S.; Bayer, T.; Schaaf, P.; Iqbal, N.; Rudroff, F.; Mihovilovic, M.D., Bornscheuer, U.T.
Poster and short talk: Biocatalysis Gordon Research Seminar (GRS), July 5-6, 2014, Bryant University, Smithfield, RI, USA

Enzymatic Redox Sequences in Asymmetric Synthesis – Artificial enzyme cascades in vitro and in vivo
Oberleitner, N.; Peters, C.; Muschiol, J.; Kadow, M.; Sass, S.; Bayer, T.; Schaaf, P.; Iqbal, N.; Rudroff, F.; Mihovilovic, M.D.; Bornscheuer, U.T.
Poster: 3rd Multistep Enzyme Catalyzed Processes Congress (MECP14), April 7-10, 2014, Madrid, Spain

An Enzymatic Toolbox for Cascade Reactions – A Showcase for an In vivo Redox Sequence in Asymmetric Synthesis
Oberleitner, N.; Peters, C.; Muschiol, J.; Kadow, M.; Sass, S.; Bayer, T.; Schaaf, P.; Iqbal, N.; Rudroff, F.; Mihovilovic, M.D.; Bornscheuer, U.T.
Poster: Biotrans2013, July 21-25, 2013, Manchester, UK

F V List of abbreviations

Abbreviation		Abbreviation	
ADAME	ω -aminocarboxylic acid methyl esters	HIV	human immunodeficiency virus
ADH	alcohol dehydrogenase	IL	ionic liquid
amp	ampicillin	IPTG	isopropyl- β -D-thiogalactopyranoside
amp100	amp (100 $\mu\text{g mL}^{-1}$)	kan	kanamycin
anTet	anhydrotetracycline	kan100	kan (100 $\mu\text{g mL}^{-1}$)
AOX	alcohol oxidase	LB	lysogeny broth
BEHP	bis(2-ethylhexyl)phthalate	MEV	mevalonate pathway
BVMO	Baeyer-Villiger monoxygenase	MM	master mix
BVOx	Baeyer-Villiger oxidation	MS	mass spectrometry
cdw	cell dry weight	NAD ⁺	nicotinamide adenine dinucleotide
CFE	cell free extract	NADH	nicotinamide adenine dinucleotide (reduced)
chl	chloramphenicol	NADP ⁺	nicotinamide adenine dinucleotide phosphate
chl34	chl (34 $\mu\text{g mL}^{-1}$)	NADPH	nicotinamide adenine dinucleotide phosphate (reduced)
CHMO	cyclohexanone monoxygenase	NemR	N-ethylmaleimide reductase
CumDO	cumene dioxygenase	o/n	overnight
cww	cell wet weight	OD	optical density
DAME	dodecanoic acid methyl ester	ODAME	12-oxododecanoic acid methyl ester
DCM	dichloromethane	Ox-HR	oxidative half reaction
DCR	2,4 dienoyl-CoA reductase	<i>P.</i>	<i>Pseudomonas</i>
DDAME	dodecanedioic acid monomethyl ester	PFDH	ADH from <i>Pseudomonas fluorescens</i>
de	diastereomeric excess	PKS	polyketide synthase
DH	dihydro	PMSF	phenylmethylsulfonyl fluoride
DNA	deoxyribonucleic acid	PP	polypropylene
DOPA	L-3,4-dihydroxyphenylalanine	PPP	pentose phosphate pathway
<i>E. coli</i>	<i>Escherichia coli</i>	RARE	reduced aromatic aldehyde reduction
ee	enantiomeric excess	Red-HR	reductive half reaction
ERED	enoate reductase	RNA	ribonucleic acid
FAD	flavin adenine nucleotide	rpm	rounds per minute
FAME	fatty acid methyl esters	RT	room temperature
FDH	formate dehydrogenase	sm	streptomycin
FID	flame ionization detector	sm100	sm (100 $\mu\text{g mL}^{-1}$)
FMN	flavin mononucleotide	TB	terrific broth
G6P	glucose-6-phosphate	tet	tetracycline
G6PDH	glucose-6-phosphate dehydrogenase	ThDP	thiamine diphosphate
GC	gas chromatography	TLC	thin layer chromatography
GDH	glucose dehydrogenase	Tris	tris(hydroxymethyl)aminomethane
gDNA	genomic DNA	v/v	volume per volume
HDAME	12-hydroxydodecanoic acid methyl ester	w/v	weight per volume

F VI References

- [1] F. Lopez-Gallego and C. Schmidt-Dannert, *Curr Opin Chem Biol* **2010**, *14*, 174-183.
- [2] G. M. Whitesides, *Interface Focus* **2015**, *5*.
- [3] M. Filice and J. M. Palomo, *ACS Catalysis* **2014**, *4*, 1588-1598.
- [4] W. Kroutil and M. Rueping, *ACS Catalysis* **2014**, *4*, 2086-2087.
- [5] M. J. Climent, A. Corma, S. Iborra and M. J. Sabater, *ACS Catalysis* **2014**, *4*, 870-891.
- [6] C. A. Denard, J. F. Hartwig and H. Zhao, *ACS Catalysis* **2013**, *3*, 2856-2864.
- [7] A. Bruggink, R. Schoevaart and T. Kieboom, *Org Proc Res Dev* **2003**, *7*, 622-640.
- [8] N. Ladkau, A. Schmid and B. Bühler, *Curr Opin Biotechnol* **2014**, *30*, 178-189.
- [9] T. Nakayama, *J Biochem* **1959**, *46*, 1217-1225.
- [10] U. T. Bornscheuer, G. W. Huisman, R. J. Kazlauskas, S. Lutz, J. C. Moore and K. Robins, *Nature* **2012**, *485*, 185-194.
- [11] J. W. Lee, T. Y. Kim, Y.-S. Jang, S. Choi and S. Y. Lee, *Trends Biotechnol* **2011**, *29*, 370-378.
- [12] X. Chen, M. Li, L. Zhou, W. Shen, G. Algasan, Y. Fan and Z. Wang, *Bioresour Technol* **2014**, *166*, 64-71.
- [13] V. J. J. Martin, D. J. Pitera, S. T. Withers, J. D. Newman and J. D. Keasling, *Nat Biotechnol* **2003**, *21*, 796-802.
- [14] Z. Lin, Z. Xu, Y. Li, Z. Wang, T. Chen and X. Zhao, *Microb Cell Fact* **2014**, *13*, 014-0104.
- [15] D. Na, T. Y. Kim and S. Y. Lee, *Curr Opin Microbiol* **2010**, *13*, 363-370.
- [16] T. Bayer, S. Milker, T. Wiesinger, F. Rudroff and M. D. Mihovilovic, *Adv Synth Catal* **2015**, *357*, 1587-1618.
- [17] J. Alonso-Gutierrez, R. Chan, T. S. Bathth, P. D. Adams, J. D. Keasling, C. J. Petzold and T. S. Lee, *Metab Eng* **2013**, *19*, 33-41.
- [18] K. V. Solomon, T. S. Moon, B. Ma, T. M. Sanders and K. L. Prather, *ACS Synth Biol* **2013**, *2*, 126-135.
- [19] A. M. Kunjapur, Y. Tarasova and K. L. J. Prather, *J Am Chem Soc* **2014**, *136*, 11644-11654.
- [20] Z. Dai and J. Nielsen, *Curr Opin Biotechnol* **2015**, *36*, 8-15.
- [21] Y. Chen and J. Nielsen, *Curr Opin Biotechnol* **2013**, *24*, 965-972.
- [22] C. Cho, S. Y. Choi, Z. W. Luo and S. Y. Lee, *Biotechnol Adv* **2015**, *33*, 1455-1466.
- [23] S. Y. Lee, H. M. Kim and S. Cheon, *Curr Opin Biotechnol* **2015**, *33*, 15-22.
- [24] L. d'Espaux, D. Mendez-Perez, R. Li and J. D. Keasling, *Curr Opin Chem Biol* **2015**, *29*, 58-65.
- [25] H. Chung, J. E. Yang, J. Y. Ha, T. U. Chae, J. H. Shin, M. Gustavsson and S. Y. Lee, *Curr Opin Biotechnol* **2015**, *36*, 73-84.
- [26] K. W. George, M. G. Thompson, A. Kang, E. Baidoo, G. Wang, L. J. G. Chan, P. D. Adams, C. J. Petzold, J. D. Keasling and T. Soon Lee, *Scientific Reports* **2015**, *5*, 11128.
- [27] D. Julleson, F. David, B. Pflieger and J. Nielsen, *Biotechnol Adv* **2015**, *33*, 1395-1402.
- [28] H. Gröger and W. Hummel, *Curr Opin Chem Biol* **2014**, *19*, 171-179.
- [29] A. Corma, M. E. Domine and S. Valencia, *J Catal* **2003**, *215*, 294-304.
- [30] V. Köhler, Y. M. Wilson, M. Dürrenberger, D. Ghislieri, E. Churakova, T. Quinto, L. Knörr, D. Häussinger, F. Hollmann, N. J. Turner and T. R. Ward, *Nat Chem* **2013**, *5*, 93-99.
- [31] M. Heidlindemann, G. Rulli, A. Berkessel, W. Hummel and H. Gröger, *ACS Catalysis* **2014**, *4*, 1099-1103.
- [32] I. Ardao, E. T. Hwang and A. P. Zeng, *Adv Biochem Eng Biotechnol* **2013**, *137*, 153-184.
- [33] E. Ricca, B. Brucher and J. H. Schrittwieser, *Adv Synth Catal* **2011**, *353*, 2239-2262.
- [34] I. Oroz-Guinea and E. Garcia-Junceda, *Curr Opin Chem Biol* **2013**, *17*, 236-249.
- [35] J. Muschiol, C. Peters, N. Oberleitner, M. D. Mihovilovic, U. T. Bornscheuer and F. Rudroff, *Chem Commun* **2015**, *51*, 5798-5811.
- [36] M. Fuchs, K. Tauber, J. Sattler, H. Lechner, J. Pfeffer, W. Kroutil and K. Faber, *RSC Advances* **2012**, *2*, 6262-6265.
- [37] A. Jakoblinert and D. Rother, *Green Chemistry* **2014**, *16*, 3472.
- [38] T. Sehl, H. C. Hailes, J. M. Ward, R. Wardenga, E. von Lieres, H. Offermann, R. Westphal, M. Pohl and D. Rother, *Angew Chem Int Ed Engl* **2013**, *52*, 6772-6775.
- [39] T. Sehl, H. C. Hailes, J. M. Ward, U. Menyes, M. Pohl and D. Rother, *Green Chemistry* **2014**, *16*, 3341-3348.
- [40] K. B. Otte and B. Hauer, *Curr Opin Biotechnol* **2015**, *35*, 16-22.
- [41] C. A. Tracewell and F. H. Arnold, *Curr Opin Chem Biol* **2009**, *13*, 3-9.
- [42] M. T. Reetz, *J Am Chem Soc* **2013**, *135*, 12480-12496.
- [43] W. C. DeLoache, Z. N. Russ, L. Narcross, A. M. Gonzales, V. J. J. Martin and J. E. Dueber, *Nat Chem Biol* **2015**, *11*, 465-471.
- [44] K. Yu, C. Liu, B. G. Kim and D. Y. Lee, *Biotechnol Adv* **2015**, *33*, 155-164.
- [45] I. Wheeldon, S. D. Minter, S. Banta, S. C. Barton, P. Atanassov and M. Sigman, *Nat Chem* **2016**, *8*, 299-309.
- [46] C. Peters, F. Rudroff, M. D. Mihovilovic and T. B. U, *Biol Chem* **2016**, *14*, 2016-0150.
- [47] S. Dutta, J. R. Whicher, D. A. Hansen, W. A. Hale, J. A. Chemler, G. R. Congdon, A. R. H. Narayan, K. Hakansson, D. H. Sherman, J. L. Smith and G. Skiniotis, *Nature* **2014**, *510*, 512-517.
- [48] J.-L. Lin, L. Palomec and I. Wheeldon, *ACS Catalysis* **2014**, *4*, 505-511.
- [49] H. Lee, W. C. DeLoache and J. E. Dueber, *Metab Eng* **2012**, *14*, 242-251.
- [50] D. J. Pitera, C. J. Paddon, J. D. Newman and J. D. Keasling, *Metab Eng* **2007**, *9*, 193-207.
- [51] J. E. Dueber, G. C. Wu, G. R. Malmirchegini, T. S. Moon, C. J. Petzold, A. V. Ullal, K. L. J. Prather and J. D. Keasling, *Nat Biotechnol* **2009**, *27*, 753-759.
- [52] S. Sabri, J. A. Steen, M. Bongers, L. K. Nielsen and C. E. Vickers, *Microb Cell Fact* **2013**, *12*, 60.
- [53] T. Baba, T. Ara, M. Hasegawa, Y. Takai, Y. Okumura, M. Baba, K. A. Datsenko, M. Tomita, B. L. Wanner and H. Mori, *Molecular Systems Biology* **2006**, *2*, 2006.0008-2006.0008.
- [54] I. M. Brockman and K. L. Prather, *Metab Eng* **2015**, *28*, 104-113.
- [55] B. Wörsdörfer, K. J. Woycechowsky and D. Hilvert, *Science* **2011**, *331*, 589-592.
- [56] C. Fan, S. Cheng, S. Sinha and T. A. Bobik, *Proc Natl Acad Sci U S A* **2012**, *109*, 14995-15000.
- [57] F. Sargent, F. A. Davidson, C. L. Kelly, R. Binny, N. Christodoulides, D. Gibson, E. Johansson, K. Kozyrska, L. L. Lado, J. Maccallum, R. Montague, B. Ortman, R. Owen, S. J. Coulthurst, L. Dupuy, A. R. Prescott and T. Palmer, *Microbiology* **2013**, *159*, 2427-2436.
- [58] M. K. Julsing, M. Schrewe, S. Cornelissen, I. Hermann, A. Schmid and B. Bühler, *Appl Environ Microbiol* **2012**, *78*, 5724-5733.

- [59] S. Cornelissen, M. K. Julsing, J. Volmer, O. Riechert, A. Schmid and B. Bühler, *Biotechnol Bioeng* **2013**, *110*, 1282-1292.
- [60] M. Schrewe, N. Ladkau, B. Bühler and A. Schmid, *Adv Synth Catal* **2013**, *355*, 1693-1697.
- [61] M. Schrewe, M. K. Julsing, B. Bühler and A. Schmid, *Chem Soc Rev* **2013**, *42*, 6346-6377.
- [62] M. Schrewe, M. K. Julsing, K. Lange, E. Czarnotta, A. Schmid and B. Bühler, *Biotechnol Bioeng* **2014**, *111*, 1820-1830.
- [63] M. J. Dunlop, Z. Y. Dossani, H. L. Szmids, H. C. Chu, T. S. Lee, J. D. Keasling, M. Z. Hadi and A. Mukhopadhyay, *Molecular Systems Biology* **2011**, *7*, 21.
- [64] S. Boyarskiy and D. Tullman-Ercek, *Curr Opin Chem Biol* **2015**, *28*, 15-19.
- [65] L. M. Blank, B. E. Ebert, K. Buehler and B. Bühler, *Antioxid Redox Signaling* **2010**, *13*, 349-394.
- [66] S. G. Burton, *Trends Biotechnol* **2003**, *21*, 543-549.
- [67] R. Bernhardt, *J Biotechnol* **2006**, *124*, 128-145.
- [68] V. B. Urlacher and M. Girhard, *Trends Biotechnol* **2012**, *30*, 26-36.
- [69] S. Staudt, E. Burda, C. Giese, C. A. Müller, J. Marienhagen, U. Schwaneberg, W. Hummel, K. Drauz and H. Gröger, *Angew Chem Int Ed* **2013**, *52*, 2359-2363.
- [70] H. Jörnvall, J.-O. Höög and B. Persson, *FEBS Lett* **1999**, *445*, 261-264.
- [71] K. L. Kavanagh, H. Jörnvall, B. Persson and U. Oppermann, *Cell Mol Life Sci* **2008**, *65*, 3895-3906.
- [72] H. Gröger, W. Hummel, S. Borchert and M. Kraußner, in *Enzyme Catalysis in Organic Synthesis*, Wiley-VCH Verlag GmbH & Co. KGaA, **2012**, pp. 1035-1110.
- [73] S. M. De Wildeman, T. Sonke, H. E. Schoemaker and O. May, *Acc Chem Res* **2007**, *40*, 1260-1266.
- [74] V. Prelog, *Pure Appl Chem* **1964**, *9*, 119.
- [75] K. Faber, *Biotransformations in organic chemistry. A textbook*, 6 ed., Springer-Verlag Berlin Heidelberg, **2011**.
- [76] F. Hollmann, I. W. C. E. Arends, K. Buehler, A. Schallmeyer and B. Bühler, *Green Chemistry* **2011**, *13*, 226-265.
- [77] A. Schallmeyer, P. Domínguez de María and P. Bracco, in *Stereoselective Synthesis of Drugs and Natural Products*, John Wiley & Sons, Inc., **2013**.
- [78] J. H. Sattler, M. Fuchs, K. Tauber, F. G. Mutti, K. Faber, J. Pfeffer, T. Haas and W. Kroutil, *Angew Chem Int Ed* **2012**, *51*, 9156-9159.
- [79] S. Benson and J. Shapiro, *J Bacteriol* **1976**, *126*, 794-798.
- [80] J. B. van Beilen, G. Eggink, H. Enequist, R. Bos and B. Witholt, *Mol Microbiol* **1992**, *6*, 3121-3136.
- [81] C. K. Winkler, G. Tasnádi, D. Clay, M. Hall and K. Faber, *J Biotechnol* **2012**, *162*, 381-389.
- [82] H. S. Toogood and N. S. Scrutton, *Curr Opin Chem Biol* **2014**, *19*, 107-115.
- [83] E. D. Amato and J. D. Stewart, *Biotechnol Adv* **2015**, *33*, 624-631.
- [84] T. Barna, H. L. Messiha, C. Petosa, N. C. Bruce, N. S. Scrutton and P. C. Moody, *J Biol Chem* **2002**, *277*, 30976-30983.
- [85] F. Schaller, C. Biesgen, C. Mussig, T. Altmann and E. W. Weiler, *Planta* **2000**, *210*, 979-984.
- [86] R. Stuermer, B. Hauer, M. Hall and K. Faber, *Curr Opin Chem Biol* **2007**, *11*, 203-213.
- [87] H. S. Toogood, J. M. Gardiner and N. S. Scrutton, *ChemCatChem* **2010**, *2*, 892-914.
- [88] R. E. Williams and N. C. Bruce, *Microbiology* **2002**, *148*, 1607-1614.
- [89] O. Warburg and W. Christian, *Naturwissenschaften* **1932**, *20*, 688-688.
- [90] R. M. Kohli and V. Massey, *J Biol Chem* **1998**, *273*, 32763-32770.
- [91] C. E. Paul and F. Hollmann, *Appl Microbiol Biotechnol* **2016**, *100*, 4773-4778.
- [92] C. E. Paul, S. Gargiulo, D. J. Opperman, I. Lavandera, V. Gotor-Fernández, V. Gotor, A. Taglieber, I. W. C. E. Arends and F. Hollmann, *Org Lett* **2013**, *15*, 180-183.
- [93] T. Knaus, C. E. Paul, C. W. Levy, S. de Vries, F. G. Mutti, F. Hollmann and N. S. Scrutton, *J Am Chem Soc* **2016**, *138*, 1033-1039.
- [94] M. A. Swiderska and J. D. Stewart, *Journal of Molecular Catalysis B: Enzymatic* **2006**, *42*, 52-54.
- [95] S. K. Padhi, D. J. Bougioukou and J. D. Stewart, *J Am Chem Soc* **2009**, *131*, 3271-3280.
- [96] R. Agudo and M. T. Reetz, *Chem Commun* **2013**, *49*, 10914-10916.
- [97] A. Baeyer and V. Villiger, *Berichte der deutschen chemischen Gesellschaft* **1899**, *32*, 3625-3633.
- [98] M. M. Kayser, *Tetrahedron* **2009**, *65*, 947-974.
- [99] N. A. Donoghue, D. B. Norris and P. W. Trudgill, *Eur J Biochem* **1976**, *63*, 175-192.
- [100] M. J. Taschner and D. J. Black, *J Am Chem Soc* **1988**, *110*, 6892-6893.
- [101] V. Alphand, A. Archelas and R. Furstoss, *Tetrahedron Lett* **1989**, *30*, 3663-3664.
- [102] J. D. Stewart, K. W. Reed and M. M. Kayser, *J Chem Soc, Perk Trans 1* **1996**, 755-757.
- [103] M. Kayser, G. Chen and J. Stewart, *Synlett* **1999**, *1999*, 153-158.
- [104] G. Chen, M. M. Kayser, M. D. Mihovilovic, M. E. Mrstik, C. A. Martinez and J. D. Stewart, *New Journal of Chemistry* **1999**, *23*, 827-832.
- [105] H. Leisch, K. Morley and P. C. K. Lau, *Chem Rev* **2011**, *111*, 4165-4222.
- [106] M. D. Mihovilovic, F. Rudroff, B. Grotzl, P. Kapitan, R. Snajdrova, J. Rydz and R. Mach, *Angew Chem Int Ed* **2005**, *44*, 3609-3613.
- [107] V. Alphand, G. Carrea, R. Wohlgemuth, R. Furstoss and J. M. Woodley, *Trends Biotechnol* **2003**, *21*, 318-323.
- [108] Z.-G. Zhang, L. P. Parra and M. T. Reetz, *Chem Eur J* **2012**, *18*, 10160-10172.
- [109] M. Bučko, P. Gemeiner, A. Schenkmyerová, T. Krajčovič, F. Rudroff and M. D. Mihovilovič, *Appl Microbiol Biotechnol* **2016**, 1-15.
- [110] G. J. ten Brink, I. W. C. E. Arends and R. A. Sheldon, *Chem Rev* **2004**, *104*, 4105-4124.
- [111] C. C. Ryerson, D. P. Ballou and C. Walsh, *Biochemistry* **1982**, *21*, 2644-2655.
- [112] D. Sheng, D. P. Ballou and V. Massey, *Biochemistry* **2001**, *40*, 11156-11167.
- [113] J. W. Song, E. Y. Jeon, D. H. Song, H. Y. Jang, U. T. Bornscheuer, D. K. Oh and J. B. Park, *Angew Chem Int Ed* **2013**, *52*, 2534-2537.
- [114] J.-W. Song, J.-H. Lee, U. T. Bornscheuer and J.-B. Park, *Adv Synth Catal* **2014**, *356*, 1782-1788.
- [115] K. G. Johnson and L. S. Yang, in *Modern Polyesters: Chemistry and Technology of Polyesters and Copolyesters*, John Wiley & Sons, Ltd, **2004**, pp. 697-713.
- [116] J. Liu and Z. Li, *ACS Catalysis* **2013**, *3*, 908-911.
- [117] S. Warren and P. Wyatt, *Organic Synthesis. The Disconnection Approach*, Wiley-VCH, Weinheim, **2008**.
- [118] N. J. Turner and E. O'Reilly, *Nat Chem Biol* **2013**, *9*, 285-288.
- [119] B. G. Kyte, P. Rouvière, Q. Cheng and J. D. Stewart, *J Org Chem* **2004**, *69*, 12-17.
- [120] K. Götz, A. Liese, M. Ansorge-Schumacher and L. Hilterhaus, *Appl Microbiol Biotechnol* **2013**, *97*, 3865-3873.
- [121] R. C. Simon, E. Busto, J. H. Schrittwieser, J. H. Sattler, J. Pietruszka, K. Faber and W. Kroutil, *Chem Commun* **2014**, *50*, 15669-15672.
- [122] S. Kara, D. Spickermann, J. H. Schrittwieser, A. Weckbecker, C. Leggewie, I. W. C. E. Arends and F. Hollmann, *ACS Catalysis* **2013**, *3*, 2436-2439.
- [123] A. Glieder, E. T. Farinas and F. H. Arnold, *Nat Biotechnol* **2002**, *20*, 1135-1139.

- [124] T. Reignier, V. de Berardinis, J. L. Petit, A. Mariage, K. Hamze, K. Duquesne and V. Alphand, *Chem Commun* **2014**, *50*, 7793-7796.
- [125] P. Goswami, S. S. R. Chinnadayala, M. Chakraborty, A. K. Kumar and A. Kakoti, *Appl Microbiol Biotechnol* **2013**, *97*, 4259-4275.
- [126] J. D. Stewart, K. W. Reed, J. Zhu, G. Chen and M. M. Kayser, *J Org Chem* **1996**, *61*, 7652-7653.
- [127] R. Snajdrova, PhD thesis, University of Chemistry and Technology Prague (Prague), **2007**.
- [128] M. J. Fink, D. V. Rial, P. Kapitanova, A. Lengar, J. Rehdorf, Q. Cheng, F. Rudroff and M. D. Mihovilovic, *Adv Synth Catal* **2012**, *354*, 3491-3500.
- [129] J. D. Stewart, K. W. Reed, C. A. Martinez, J. Zhu, G. Chen and M. M. Kayser, *J Org Chem* **1998**, *120*, 3541-3548.
- [130] P. Cernuchova and M. D. Mihovilovic, *Organic & Biomolecular Chemistry* **2007**, *5*, 1715-1719.
- [131] N. Oberleitner, C. Peters, J. Muschiol, M. Kadow, S. Saß, T. Bayer, P. Schaaf, N. Iqbal, F. Rudroff, M. D. Mihovilovic and U. T. Bornscheuer, *ChemCatChem* **2013**, *5*, 3524-3528.
- [132] A. Weckbecker and W. Hummel, *Biocatal Biotransform* **2006**, *24*, 380-389.
- [133] W. Stampfer, B. Kosjek, W. Kroutil and K. Faber, WO 03/078615 A1, **2003**, CAN
- [134] D. S. Blehert, B. G. Fox and G. H. Chambliss, *J Bacteriol* **1999**, *181*, 6254-6263.
- [135] C. Peters, PhD thesis, Ernst-Moritz-Arndt-Universität Greifswald (Greifswald), **2015**.
- [136] Y. C. J. Chen, O. P. Peoples and C. T. Walsh, *J Bacteriol* **1988**, *170*, 781-789.
- [137] S.-M. Lu and C. Bolm, *Angew Chem Int Ed* **2008**, *47*, 8920-8923.
- [138] W. A. van der Donk and H. Zhao, *Curr Opin Biotechnol* **2003**, *14*, 421-426.
- [139] N. J. Mueller, C. Stueckler, B. Hauer, N. Baudendistel, H. Housden, N. C. Bruce and K. Faber, *Adv Synth Catal* **2010**, *352*, 387-394.
- [140] N. Oberleitner, C. Peters, F. Rudroff, U. T. Bornscheuer and M. D. Mihovilovic, *J Biotechnol* **2014**, *192*, Part B, 393-399.
- [141] G. Fronza, G. Fogliato, C. Fuganti, S. Lanati, R. Rallo and S. Servi, *Tetrahedron Lett* **1995**, *36*, 123-124.
- [142] N. Iqbal, F. Rudroff, A. Brige, J. Van Beeumen and M. D. Mihovilovic, *Tetrahedron* **2012**, *68*, 7619-7623.
- [143] S. Z. Wang, M. M. Kayser and V. Jurkauskas, *J Org Chem* **2003**, *68*, 6222-6228.
- [144] M. Schittmayer, A. Glieder, M. K. Uhl, A. Winkler, S. Zach, J. H. Schrittwieser, W. Kroutil, P. Macheroux, K. Gruber, S. Kambourakis, J. D. Rozzell and M. Winkler, *Adv Synth Catal* **2011**, *353*, 268-274.
- [145] J. L. Bicas, A. P. Dionisio and G. M. Pastore, *Chem Rev* **2009**, *109*, 4518-4531.
- [146] P. K. Ajikumar, K. Tyo, S. Carlsen, O. Mucha, T. H. Phon and G. Stephanopoulos, *Mol Pharm* **2008**, *5*, 167-190.
- [147] W. A. Duetz, H. Bouwmeester, J. B. van Beilen and B. Witholt, *Appl Microbiol Biotechnol* **2003**, *61*, 269-277.
- [148] J. B. van Beilen, R. Holtackers, D. Lüscher, U. Bauer, B. Witholt and W. A. Duetz, *Appl Environ Microbiol* **2005**, *71*, 1737-1744.
- [149] T. Vanek, I. Valterova and T. Vaisar, *Phytochemistry* **1999**, *50*, 1347-1351.
- [150] H. J. Bouwmeester, M. C. J. M. Konings, J. Gershenzon, F. Karp and R. Croteau, *Phytochemistry* **1999**, *50*, 243-248.
- [151] W. A. Duetz, A. H. M. Fjällman, S. Ren, C. Jourdat and B. Witholt, *Appl Environ Microbiol* **2001**, *67*, 2829-2832.
- [152] M. Groeneveld, H. L. van Beek, W. A. Duetz and M. W. Fraaije, *Tetrahedron* **2016**.
- [153] C. J. Whitehouse, S. G. Bell and L. L. Wong, *Chem Soc Rev* **2012**, *41*, 1218-1260.
- [154] J. Muschiol, PhD thesis, Ernst-Moritz-Arndt-Universität Greifswald (Greifswald), **2016**.
- [155] M. Dietrich, S. Eiben, C. Asta, T. A. Do, J. Pleiss and V. B. Urlacher, *Appl Microbiol Biotechnol* **2008**, *79*, 931-940.
- [156] S. Lupien, F. Karp, M. Wildung and R. Croteau, *Arch Biochem Biophys* **1999**, *368*, 181-192.
- [157] Z. Wang, F. Lie, E. Lim, K. Li and Z. Li, *Adv Synth Catal* **2009**, *351*, 1849-1856.
- [158] A. Fernández-Mateos, P. Herrero Teijón and R. Rubio González, *Tetrahedron* **2013**, *69*, 1611-1616.
- [159] J. Volmer, C. Neumann, B. Bühler and A. Schmid, *Appl Environ Microbiol* **2014**, *80*, 6539-6548.
- [160] V. Chubukov, F. Mingardon, W. Schackwitz, E. E. Baidoo, J. Alonso-Gutierrez, Q. Hu, T. S. Lee, J. D. Keasling and A. Mukhopadhyay, *Appl Environ Microbiol* **2015**, *81*, 4690-4696.
- [161] F. J. Weber, L. P. Ooijkaas, R. M. Schemen, S. Hartmans and J. A. de Bont, *Appl Environ Microbiol* **1993**, *59*, 3502-3504.
- [162] X. Y. He, S. Y. Yang and H. Schulz, *Eur J Biochem* **1997**, *248*, 516-520.
- [163] M. Mizugaki, C. Kimura, T. Nishimaki, A. Kawaguchi, S. Okuda and H. Yamanaka, *J Biochem* **1983**, *94*, 409-413.
- [164] X. Liang, C. Thorpe and H. Schulz, *Arch Biochem Biophys* **2000**, *380*, 373-379.
- [165] X. Tu, P. A. Hubbard, J.-J. P. Kim and H. Schulz, *Biochemistry* **2008**, *47*, 1167-1175.
- [166] P. A. Hubbard, X. Liang, H. Schulz and J. J. Kim, *J Biol Chem* **2003**, *278*, 37553-37560.
- [167] J. Zhong, M. Karberg and A. M. Lambowitz, *Nucleic Acids Res* **2003**, *31*, 1656-1664.
- [168] D. Boyd, D. S. Weiss, J. C. Chen and J. Beckwith, *J Bacteriol* **2000**, *182*, 842-847.
- [169] L. A. Pfaltzgraff, M. De bruyn, E. C. Cooper, V. Budarin and J. H. Clark, *Green Chemistry* **2013**, *15*, 307-314.
- [170] R. Ciriminna, M. Lomeli-Rodriguez, P. Demma Cara, J. A. Lopez-Sanchez and M. Pagliaro, *Chem Commun* **2014**, *50*, 15288-15296.
- [171] E. Deziel, Y. Comeau and R. Villemur, *Biodegradation* **1999**, *10*, 219-233.
- [172] T. C. Brennan, C. D. Turner, J. O. Kromer and L. K. Nielsen, *Biotechnol Bioeng* **2012**, *109*, 2513-2522.
- [173] F. Rudroff, V. Alphand, R. Furstoss and M. D. Mihovilovic, *Org Proc Res Dev* **2006**, *10*, 599-604.
- [174] A. Brandt, M. J. Ray, T. Q. To, D. J. Leak, R. J. Murphy and T. Welton, *Green Chemistry* **2011**, *13*, 2489-2499.
- [175] L. L. Fan, H. J. Li and Q. H. Chen, *Int J Mol Sci* **2014**, *15*, 12196-12216.
- [176] A. K. Ressmann, PhD thesis, TU Wien (Wien), **2015**.
- [177] K. Bica, P. Gaertner and R. D. Rogers, *Green Chemistry* **2011**, *13*, 1997-1999.
- [178] N. Wood, J. L. Ferguson, H. Q. N. Gunaratne, K. R. Seddon, R. Goodacre and G. M. Stephens, *Green Chemistry* **2011**, *13*, 1843-1851.
- [179] M. Pourbafrani, G. Forgács, I. S. Horváth, C. Niklasson and M. J. Taherzadeh, *Bioresour Technol* **2010**, *101*, 4246-4250.
- [180] M. Ouellet, S. Datta, D. C. Dibble, P. R. Tamrakar, P. I. Benke, C. Li, S. Singh, K. L. Sale, P. D. Adams, J. D. Keasling, B. A. Simmons, B. M. Holmes and A. Mukhopadhyay, *Green Chemistry* **2011**, *13*, 2743-2749.
- [181] D. Weuster-Botz, *The Chemical Record* **2007**, *7*, 334-340.
- [182] R. J. Cornmell, C. L. Winder, G. J. T. Tiddy, R. Goodacre and G. Stephens, *Green Chemistry* **2008**, *10*, 836-841.
- [183] X. Turon, J. Venus, M. Arshadi, M. Koutinas, C. S. K. Lin and A. Koutinas, *BioResources* **2014**, *9*, 4.
- [184] J. H. Clark, L. A. Pfaltzgraff, V. L. Budarin, A. J. Hunt, M. Gronnow, A. S. Matharu, D. J. Macquarrie and J. R. Sherwood, *Pure Appl Chem* **2013**, *85*, 1625.
- [185] R. Ravindran and A. K. Jaiswal, *Trends Biotechnol* **2016**, *34*, 58-69.
- [186] J. R. Lowe, M. T. Martello, W. B. Tolman and M. A. Hillmyer, *Polymer Chemistry* **2011**, *2*, 702-708.

- [187] S. C. Knight, C. P. Schaller, W. B. Tolman and M. A. Hillmyer, *RSC Advances* **2013**, *3*, 20399-20404.
- [188] S. Schmidt, H. C. Büchsenhützer, C. Scherkus, A. Liese, H. Gröger and U. T. Bornscheuer, *ChemCatChem* **2015**, *7*, 3951-3955.
- [189] T. L. Ruegg, E.-M. Kim, B. A. Simmons, J. D. Keasling, S. W. Singer, T. Soon Lee and M. P. Thelen, *Nature Communications* **2014**, *5*, 3490.
- [190] M. Frederix, K. Hütter, J. Leu, T. S. Batth, W. J. Turner, T. L. Rüegg, H. W. Blanch, B. A. Simmons, P. D. Adams, J. D. Keasling, M. P. Thelen, M. J. Dunlop, C. J. Petzold and A. Mukhopadhyay, *PLoS One* **2014**, *9*, e101115.
- [191] H. Pfruender, R. Jones and D. Weuster-Botz, *J Biotechnol* **2006**, *124*, 182-190.
- [192] H. Mallin, H. Wulf and U. T. Bornscheuer, *Enz Microb Technol* **2013**, doi: *j.enzmictec.2013.01.007*.
- [193] J. Sambrook, E. F. Fritsch and T. Maniatis, *Molecular Cloning: a Laboratory Manual*, Cold Spring Harbor Lab. Press, Plainview, NY, 2nd Ed., **1989**.
- [194] A. L. Draper, H. J. Shine, W. J. Heilman, W. E. Schaefer and J. N. Shoolery, *J Org Chem* **1962**, *27*, 2727-&.
- [195] A. L. J. Beckwith and G. Phillipou, *Aust J Chem* **1976**, *29*, 1277-1294.
- [196] A. L. Gemal and J. L. Luche, *J Am Chem Soc* **1981**, *103*, 5454-5459.
- [197] F. Bertozzi, P. Crotti, B. L. Feringa, F. Macchia and M. Pineschi, *Synthesis* **2001**, 483-486.
- [198] M. F. Ansell and T. M. Kafka, *Tetrahedron* **1969**, *25*, 6025-&.
- [199] P. Cernuchova, Postdoctoral report, TU Wien (Wien), **2006**.
- [200] X. Liu, Z. Han, Z. Wang and K. Ding, *Angew Chem Int Ed Engl* **2014**, *53*, 1978-1982.
- [201] V. Alphand, R. Furstoss, S. Pedragosa-Moreau, S. M. Roberts and A. J. Willetts, *J Chem Soc, Perk Trans 1* **1996**, 1867-1872.
- [202] H. Preusting, R. van Houten, A. Hoefs, E. K. van Langenberghe, O. Favre-Bulle and B. Witholt, *Biotechnol Bioeng* **1993**, *41*, 550-556.
- [203] K.-H. Choi, A. Kumar and H. P. Schweizer, *Journal of Microbiological Methods* **2006**, *64*, 391-397.
- [204] A. Untergasser, I. Cutcutache, T. Koressaar, J. Ye, B. C. Faircloth, M. Remm and S. G. Rozen, *Nucleic Acids Res* **2012**, *40*, e115-e115.
- [205] C. K. Syn and S. Swarup, *Anal Biochem* **2000**, *278*, 86-90.